UNIVERSITY OF SOUTHAMPTON

FACULTY OF SCIENCE, ENGINEERING & MATHEMATICS

School of Chemistry

~§~

The Synthesis and Characterisation of Complexes of Tin and Germanium Fluorides with Soft Donor Ligands.

~§~

by

Martin Frank Davis

~§~

Thesis for the Degree of Doctor of Philosophy

~§~

February 2008

UNIVERSITY OF SOUTHAMPTON

ABSTRACT

FACULTY OF SCIENCE ENGINEERING & MATHEMATICS
SCHOOL OF CHEMISTRY

Doctor of Philosophy

"THE SYNTHESIS AND CHARACTERISATION OF COMPLEXES OF TIN AND GERMANIUM FLUORIDES WITH SOFT DONOR LIGANDS."

By Martin Frank Davis

The pseudooctahedral complexes $[SnF_4L_2]$ (L = THF, pyridine, OPR_3, $OAsR_3$, PR_3) and $[SnF_4\{L–L\}]$ (L–L = 2,2'-bipyridyl, 1,10-phenanthroline, $MeO(CH_2)_2OMe$, $Me_2N(CH_2)_2NMe_2$, $R_2P(O)CH_2P(O)R_2$, *o*-$C_6H_4(P(O)R_2)_2$, $R_2P(CH_2)_2PR_2$, *o*-$C_6H_4(PR_2)_2$) have been prepared from $[SnF_4\{MeCN\}_2]$ and the appropriate ligands in rigorously anhydrous CH_2Cl_2 solution. This includes the first phosphane and thioether complexes of the hard Lewis acid SnF_4 and are the first reported examples of thioether complexes with any main group metal/metalloid fluoride acceptor. Attempts to prepare tertiary arsane complexes of SnF_4 have been unsuccessful.

Similar complexes of $[GeF_4\{PR_3\}_2]$ and $[GeF_4\{L–L\}]$ (L–L = $R_2P(CH_2)_2PR_2$ and *o*-$C_6H_4(PR_2)_2$) have also been prepared from $[GeF_4\{MeCN\}_2]$ and the appropriate ligands in rigorously anhydrous CH_2Cl_2 solution. This includes the first phosphane and thioether complexes of the hard Lewis acid GeF_4. In anhydrous CH_2Cl_2 solution the complexes are slowly converted into the corresponding phosphane oxide adducts by dry O_2. The apparently contradictory literature on the reaction of $GeCl_4$ with phosphanes is clarified. The complexes *trans*-$[GeCl_4\{AsR_3\}_2]$ (R = Me or Et) are obtained from $GeCl_4$ and AsR_3 either without solvent or in CH_2Cl_2. All the complexes have been characterised by microanalysis, Raman, IR, ^1H, $^{31}P\{^1H\}$, $^{19}F\{^1H\}$ and ^{119}Sn NMR spectroscopy as appropriate.

The crystal structures of *trans*-$[SnF_4\{OPMe_3\}_2]$, *trans*-$[SnF_4\{PCy_3\}_2]$, $[SnF_4\{1,10\text{-phenanthroline}\}]$, $[SnF_4\{MeO(CH_2)_2OMe\}]$, $[SnF_4\{o\text{-}C_6H_4(P(O)Ph_2)_2\}]\cdot CH_2Cl_2\cdot H_2O$, $[SnF_4\{Et_2P(CH_2)_2PEt_2\}]$, $[SnF_4\{EtS(CH_2)_2SEt\}]$, $[SnF_4\{^iPrS(CH_2)_2S^iPr\}]$, $[SnCl_4\{Et_2P(CH_2)_2PEt_2\}]$, $[SnBr_4\{MeC(CH_2AsMe_2)_3\}]$, $[GeF_4\{Ph_2P(CH_2)_2PPh_2\}]$, $[GeF_4\{o\text{-}C_6H_4(PMe_2)_2\}]$, *trans*-$[GeCl_4(AsEt_3)_2]$ and Et_3AsCl_2 have been determined. Comparison of the structural and NMR spectroscopic data shows that SnF_4 and GeF_4 are the strongest Lewis acids in each series.

This Thesis also describes the attempted synthesis of a few tridentate arsane macrocycles as well as the synthesis and characterisation of their respective intermediaries. This included the facultative As_2O-donors $O\{(CH_2)_2AsR_2\}_2$ (R = Me, Ph). They act as bidentate chelating As_2-donors (L-L) in the distorted tetrahedral $[M(L–L)_2]BF_4$ (M = Cu or Ag). Representative crystal structures of $[Ag(O\{(CH_2)_2AsPh_2\}_2)_2]BF_4\cdot MeOH$ and $[Cu(O\{(CH_2)_2AsPh_2\}_2)_2]BF_4\cdot MeOH$ were also obtained as well as the unexpected Cu(I)–Cu(I) complex, $[Cu_2\{Me_2As(CH_2)_2OH\}_3](BF_4)_2$ of the fragmented ligand.

Acknowledgements

I would like to thank my supervisors Prof. Bill Levason and Prof. Gill Reid for all their help and advice throughout the course of my research degree, and the EPSRC for funding. I would also like to thank Dr. Mike Webster for help with certain aspects of the *X*-ray crystallography and my advisor Dr. Andreas Danopoulos for his support over the three years.

Special thanks go to my friends and colleagues in the research group and Inorganic floor, past and present, for their continued encouragement, specifically Marek Jura for proof reading this work. I would also like to thank the Mass Spectrometry, NMR Spectroscopy and *X*-ray crystallography departments for the use of instruments and the Microanalysis service at the University of Strathclyde.

Thanks also go to the members of the Canoe and Archery Clubs for fun and distractions.

To Helen, for simply putting up with me.

Finally I would like to thank my family and friends who I could not have done this without.

Abbreviations

TM	Transition Metal
CH_2Cl_2	dichloromethane
EtOH	ethanol
MeCN	acetonitrile
THF	tetrahydrofuran
Et_2O	diethyl ether
CCl_4	carbon tetrachloride
$MeNO_2$	nitromethane
δ	chemical shift
ppm	parts per million
Hz	hertz
Me	methyl
Et	ethyl
Ph	phenyl
Cy	cyclohexyl
NMR	Nuclear Magnetic Resonance
s	singlet
d	doublet
t	triplet
q_4	quartet
q^5	quintet
s^7	septet
m	multiplet
D^p	relative receptivity to ^1H
R^C	relative receptivity to ^{13}C
$\{^1H\}$	proton decoupled
J	coupling constant
IR	Infrared
s	strong
m	medium
w	weak
br	broad
ν	vibrational frequency
Å	Ångstrom (10^{-10} m)
MS	Mass Spectrometry
ES+	Electrospray positive ion
ES-	Electrospray negative ion
bipy	2,2'-bipyridyl
phen	1,10-phenanthroline

Contents Page

List of Figures

Chapter 1

Chapter 2

Chapter 3

Chapter 4

List of Tables

Chapter 1

Chapter 2

Chapter 3

Chapter 4

Chapter 5

Chapter 6

List of crystal structures and CCDC No's

Chapter 2

Chapter 3

Chapter 4

Chapter 5

Chapter 6

Chapter 1

Introduction

1.1 Aims of this Study:

The primary aim of the study was to explore the Lewis acidity of tin(IV) halides, especially SnF_4, and of germanium(IV) halides, especially GeF_4, with a range of neutral hard and soft donor ligands.

Attempts at synthesising new polydentate and macrocyclic arsane ligands and investigation of their ligating abilities with p-block Lewis acid centres from Groups 14 and 15 are also described.

This chapter will review the general background and techniques needed for this study, with more detailed discussion of specific systems presented in the later chapters.

1.2 Lewis Acidity:

A Lewis acid is an electron pair acceptor as it possesses a vacant orbital, whereas a Lewis base is an electron pair donor as it has a non-bonded or lone pair of electrons. Both Lewis acids and bases can be classified as either hard or soft. The HSAB (Hard/Soft-Acid/Base) principle[1] states that hard acids preferentially bond to (or form adducts with) hard bases (ionic bonding) and soft acids with soft bases (covalent bonding). This can be explained by the fact that hard acids have no low energy LUMO's (Lowest Unoccupied Molecular Orbital's) and do not readily form covalent bonds with bases. Hard bases have no high HOMO's (Highest Occupied Molecular Orbital) and also do not readily form covalent bonds to acids. They can however, bond to each other strongly through ionic interactions. Soft acids and bases do have low energy LUMO's and high energy HOMO's respectively, which readily form covalent bonds, the combination of which maximises the covalent interaction.[2] The hardness of an atom, ion or molecule, can be quantified in the form of η.

$$\eta = (I-A)/2 \quad (I = \text{first ionisation energy}, A = \text{first electron affinity})$$

AsR_3, PR_3 and SR_2 are all classed as soft bases but to varying amounts. The terms "ionic" and "covalent" bonding are useful descriptions but are extremes within bonds of varying polarities.

1.3 Group 14:

The elements of Group 14 exhibit, perhaps, the most diverse chemical behaviour seen for the members of any single group.[3,4] As such there is no such thing as "handle turning" in the study of these elements.[5] The reason for this statement is due to a number of factors such as, the variation in stability of oxidation states, the wide tolerance for coordination numbers, different ligand types and coordination geometries. It is also seen in the classification of the elements themselves, carbon is non-metallic, silicon and germanium are both classed as metalloids, where as tin and lead are typical metals. The findings within this Thesis have not only reinforced the above statements, but have also extended significantly some of the findings.

The Group 14 elements of most interest in this work are tin and germanium, with some of the physical properties of their halides listed in Table 1.

Table 1 General properties of Group(IV) halides MX_4.[6]

M	X	Colour	MP/°C	BP/°C	Density (T°C)/g cm^{-3}
Sn	F	White	-	~705 (subl)	4.78 (20°)
Sn	Cl	Colourless	-33.3	114	2.234 (20°)
Sn	Br	Colourless	31	205	3.340 (35°)
Sn	I	Brown	144	348	4.56 (20°)
Ge	F	Colourless	-15 (4 atm)	-36.5 (subl)	2.126 (0°)
Ge	Cl	Colourless	-49.5	83.1	1.844 (30°)
Ge	Br	Colourless	26	186	2.100 (30°)
Ge	I	Red	146	~400	4.322 (26°)

1.3.1 Tin:

One of the main aims of this work is to explore in detail the coordination chemistry of some of the main group halides with the initial objective to determine whether the Lewis acidities of Sn(IV) halides are in agreement with the generally held view (by many standard texts)[7] that SnF_4 is a stronger Lewis acid than the others $SnCl_4$>$SnBr_4$>>SnI_4. Only one example of the former with a neutral ligand, [SnF_4{2,2'bipy}], had been structurally characterised.[8] Very few

other compounds of SnF_4 had been made previously.[8,9,10,11,12,13,14] In these papers a few complexes with N or O donor ligands were reported (such as $[SnF_4\{Me_2SO\}_2]$ and $[SnF_4\{C_5H_5N\}_2]$) but only microanalysis results were given.[9] The literature also reports limited examples of IR spectra of SnF_4 complexes with THF[10] and $OAsPh_3$,[13] with all examples lacking in supporting data.[10,11,13,14] All are either N or O donating ligands and hence are considered hard bases. Reviews on tin(IV) halides tend to ignore the existence of these compounds due to their small number and the lack of spectroscopic data to accompany them.[15] The only known examples of NMR spectroscopic data for SnF_4 derivatives are the ^{19}F NMR spectra of anionic inorganic fluoro-complexes.[12]

This work will involve creating a series of Sn(IV) fluoride complexes and comparing them with the analogous halides. This study will also test the limits of SnF_4 chemistry in terms of hard/soft Lewis acidity by attempting to react with progressively softer donor ligands such as P, As and S based ligands.

Although isolation of tin in its pure form probably only dates from about 800 BC, the discovery around 3500 BC that copper smelted with tin forms bronze is considered one of the great milestones in man's technological (as well as warfare) development. Tin is even mentioned in the old testament (Numbers 31:22).

The major source of tin is from its naturally occurring tin(IV) oxide ore, Cassiterite, the name of the ore presumably comes from the name of tin, Cassiteros in the story of the Trojan war in the Iliad by Homer.

Tin has the largest number (10) of stable isotopes of any element with ^{118}Sn and ^{120}Sn being most abundant. Three of the isotopes (^{115}Sn, ^{117}Sn and ^{119}Sn) have spin = ½, all others being spin zero.

Tin(IV) is the most stable oxidation state, using all of its valence shell electrons in bonding, but tin(II) is also quite common having a non-bonding electron pair and using its p-electrons in bonding. Tin(IV) tends to be tetrahedral or octahedral but examples of 5-, 7- and 8-coordination are known (see Table 2).[16]

Table 2 Examples of tin(IV) valences and stereochemistry.[16]

Coordination No	Geometry	Examples	Reference
4	Tetrahedral	$SnCl_4$	4
		$Sn(NCPh_2)_4$	4
5	Trigonal bipyramidal	$Me_3SnCl(py)$,	16
		$SnCl_5^-$	16
6	Octahedral	$Sn(S_2CNEt_2)_4$,	16
		$SnF_4(2,2'\text{-bipy})$,	8
		SnX_6^{2-}	4
7	Pentagonal bipyramidal	$Ph_2Sn(NO_3)_2(OPPh_3)$	16
8	Dodecahedral	$Sn(NO_3)_4$	16

Sn_2S_3 is an example of a mixed valence compound with both an octahedral tin(IV) site and a trigonal pyramidal tin(II) site.[17] Sn_3F_8 or $(SnF)_2SnF_6$ has a *trans* fluorine bridged octahedral $Sn(IV)F_6$ unit linked to polymeric pyramidal Sn(II)F chains (see Figure 1).[18]

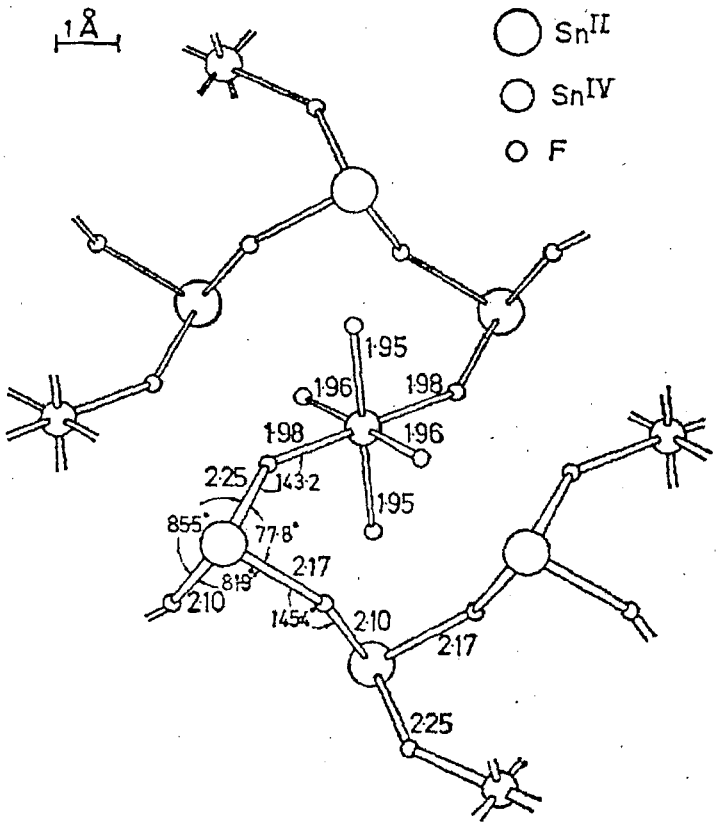

Figure 1 X-ray crystal structure of Sn_3F_8.[18]

Of particular interest to this study will be previous reports on SnX_4 and their properties which are discussed further in the relevant chapters.

Tin(IV) halides, SnX_4, like organotin(IV) halides (SnR_nX_{4-n} where n=1-3: R=alkyl, alkenyl or aryl) are tetrahedral in the vapour and liquid states, but as a solid they exhibit a preference for the formation of halogen bridged lattices.[19] As with bivalent tin, fluorotin(IV) compounds have a strong tendency for the formation of strong Sn-F-Sn bridges in the solid. Thus, SnF_4 forms a very strongly bridged two-dimensional sheet polymer with octahedrally coordinated tin (see Figure 2).[20,21]

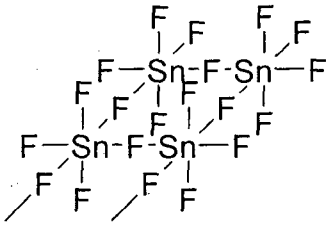

Figure 2 Structure of SnF_4.

The enthalpy of formation of SnX_4 (X = halides) becomes more negative with increasing electronegativity/decreasing size (see Table 3).

Table 3 Enthalpy of formation of SnX_4.

SnX_4	ΔH_f (kJmol^{-1})
SnI_4	-214.3[a]
$SnBr_4$	-405.9[a]
$SnCl_4$	-544.7[a]
SnF_4	-1226[b]

a. Ref 4 b. Ref 22

The tin(IV) halides and organotin(IV) halides are good Lewis acids and acceptors of halide or neutral donor molecules. Lewis acidity is said to increase with the number of halides 1 < 2 < 3 < 4 and increase with the halide I < Br < Cl < F.[4] Tetrahalides can form 1:2 or 1:1 adducts with an octahedral or trigonal bipyramidal geometry respectively. In the latter the organic groups always occupy the equatorial sites.

The spectroscopic studies of the tin compounds have been carried out by predominantly IR, and NMR spectroscopy, but methods such as mass spectrometry and X-ray crystallography are also used.

1.3.2 Germanium:

In contrast to tin, germanium's existence was predicted prior to its discovery by C. A. Winkler in 1886.[23] Originally predicted to lie between silicon and tin in the periodic table by J. A. R. Newlands in 1864,[6] and D. I. Mendeleev very accurately predicted its properties in 1871.[6] Germanium is widely distributed in trace amounts within other ores but rarely as its own germanium mineral.

Like tin, germanium is in Group 14, it has a smaller covalent radius (1.22 compared to 1.41 Å) but also has an NMR active nucleus ^{73}Ge. Unfortunately, its spin is 9/2 and even though its natural abundance (7.76%) is similar to the NMR active tin nuclei, its receptivity is also low, 0.617. As a consequence of the medium quadrupolar moment of the ^{73}Ge nucleus, its NMR spectroscopic signals are very broad if the charge distribution around the Ge is non-spherical. This coupled with its low resonance frequency means that very few ^{73}Ge NMR resonances are reported, although germanium tetrahalides are some of the exceptions.[24,25] Germanium-73 (like Sn) NMR spectroscopy also suffers from 'rolling baselines' caused by acoustic ringing, which makes the assignment of broad peaks even harder.[26,27]

Relationships between chemical shifts have been seen between Group 14 elements. Although the correlation is not exact, a knowledge of the Sn chemical shift can give a useful guide for the Ge shift in analogous compounds.[28]

In general germanium has a preference towards an oxidation state of IV i.e the tetrahedral $GeCl_4$ or forming complexes such as the octahedral *trans*-$GeCl_4(py)_2$ and $GeCl_4$(bipy).[16,29] Germanium(IV)fluoride is a strong electron acceptor and forms complexes with donor molecules, it sublimes at 236 K compared to 977 K for SnF_4.[16] Recent studies of Lewis acidity of Group 14 tetrahalides in the gas phase has concluded that the stability of complexes decreases Sn>Ge>Si and F>Cl>Br in the gas phase at least.[30,31]

This study looks at complexes of Group 14 metals with ligands containing Group 15 and 16 donors.

1.4 Group 15:

The pnictogens as they are collectively called, show marked variation in both the chemical and physical properties on descending the Group. Both phosphorus and arsenic, which are the primary pnictogens being investigated, are classed as non-metals, unlike antimony (a metalloid) or bismuth which is classed as metallic. In the +3 oxidation state (which is common) the Group 15 elements have a lone pair of electrons, this allows both phosphorus and arsenic ligands to act as σ-donors.

1.4.1 Phosphane and Arsane Ligands:

Studies of the co-ordination chemistry of arsenic ligands with transition metals have been reported from over 100 years ago and possible uses of arsenic within therapeutics and also as poisonous gases have been studied. Similar efforts were also made into the synthesis of phosphane co-ordination chemistry but originally more progress was made with arsanes due to their easier preparations, often because of their better stability in air. The advantage however, for phosphorus is that it has only one naturally occurring isotope, which has a spin of ½. The ^{31}P nucleus has a relative receptivity to proton of 6.6×10^{-2} ($R^C = 3.77 \times 10^2$) which allows additional characterisation by NMR spectroscopy.[32] These factors combine to make ^{31}P a very good NMR probe.

Arsenic-75 is 100% abundant with a relative receptivity to proton of 2.5×10^{-2} ($R^C = 1.44 \times 10^2$) but its spin is 3/2, which means that like ^{73}Ge, relatively little NMR spectroscopic characterisation has been done. The associated quadrupole would again mean broad NMR lines as well as difficulty in observing them, although two reviews do contain some As NMR spectroscopic data.[26,33]

Systematic studies of the stabilisation of high oxidation state transition metals by phosphorus[34] and arsenic donor ligands (such as *o*-$C_6H_4(EMe_2)(E'Me_2)$ (E, E' = P, As)) have been carried out, exploring what influences the stability of the oxidation states. Denticities of up to eight have been reported in phosphane and

arsane ligands.[15,35] For Sn(IV) however, most complexes form a 6 co-ordinate octahedral structure yet others have been reported such as a 5 co-ordinate trigonal bipyramidal $[(Ph_3As)SnBr_4]$ moiety associated with a second Ph_3As through a long Br-As interaction.[36] A variety of tripodal and facultative tri- and tetra-arsanes have also been reported, which were produced similarly to that of diarsanes.[15,37]

The trend of σ–donor power of Group 15 tertiary ligands has been well documented as $PR_3 > AsR_3 > SbR_3 >> BiR_3$, due to the σ-donor orbitals becoming larger and more diffuse as the atom size increases, which decreases the strength of bonds.[37]

1.5 Sulfur:

Sulfur has a naturally occurring NMR active isotope, ^{33}S, but it is far from ideal for studying (see Table 4). Group 16 neutral donors are generally considered poorer ligands compared to their Group 15 counterparts, this is due to their modest σ-donor abilities (little to no π-acceptor component) and to some extent the stereoelectric effects arising from the non-bonding pair of electrons. Steric effects are however much less important for thioethers than their phosphane and arsane equivalents, due to having one less R substituent. Group 16 neutral donors also have the ability for both lone pairs to form σ–bonds to metal centres, sometimes resulting in bridged ligands. All are considerations for thioether bonding discussed in this study.

The non-bonding pair of electrons on sulfur do however, give additional conformations due to invertomers formed, when bidentate thioethers bond to a MX_4 metal centre (see Figure 3).

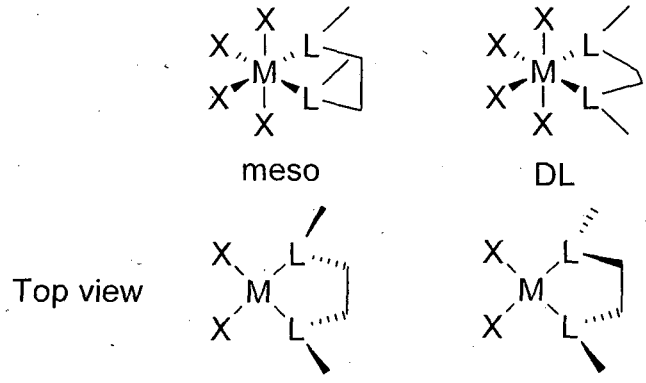

Figure 3 Examples of *meso* and *DL* conformations in $MX_4(L\text{-}L)$ where L-L is a bidentate chalcogenoether.

Switching between *DL* and *meso* forms can sometimes be seen, depending on conditions and can be accomplished by two routes, dissociation or pyramidal inversion.[38] The first is also helped by the relatively poor ligating abilities of thioethers.

Large reviews on sulfur ligand chemistry can be found in many text books[6,16] but also with respect to thioether ligands.[39]

1.6 N and O donor ligands:

Nitrogen- and oxygen-donor ligands have also been reported extensively in reviews.[6,16] Nitrogen donors such as bipy[40] and phen[41] are considered modest σ-donors and although π-backbonding does occur it is not exceptional, with the Group 14 metals discussed in this Thesis.[16] They primarily give chelate complexes similar to those produced by diphosphanes and diarsanes but are significantly harder Lewis donors. The rigidity due to the π-systems forces is, in effect, a preorganisation of the ligands, this reduces the loss of rotational and vibrational degrees of freedom upon co-ordination compared to other chelates. This is similar to the entropic contribution in macrocycles (see below).

Oxygen ether donors such as THF or DME are commonly used as solvents and can form solvates with metal halides. Like N-donors they are good σ-donors. R_3EO (E = P or As) are also studied within this Thesis and are similarly classed as

hard Lewis donors but for the phosphorus examples at least gives an additional NMR active nuclei to probe.

1.7 Spectroscopy and Structural Characterisation:

1.7.1 NMR Spectroscopy:

This Thesis contains ^{1}H, ^{13}C, ^{19}F, ^{31}P and ^{119}Sn NMR spectra with chemical shifts, coupling constants and coordination shifts reported. Examples of dynamic compounds in solutions are discussed and hence so are the variable temperature (VT) NMR spectroscopies used to study these. Table 4 lists the nuclear properties of the relevant isotopes.

Table 4 List of possible NMR nuclei with standard details.

Nucleide	Spin	Natural Abundance (%)	Receptivity R^C	Frequency Ξ (MHz)*
^{1}H	1/2	99.99	5.67×10^{3}	100
^{13}C	1/2	1.11	1.00	25.1
^{19}F	1/2	100	4.73×10^{3}	94.1
^{31}P	1/2	100	3.77×10^{2}	40.5
^{33}S	3/2	0.76	0.097	7.7
^{73}Ge	9/2	7.76	0.622	3.5
^{75}As	3/2	100	1.44×10^{2}	17.2
^{119}Sn	1/2	8.58	25.7	37.3

* Resonance frequency for the nucleus in a magnetic field such that the protons in TMS resonate at exactly 100 MHz.

The existence of Nuclear Magnetic Moments was recognised by Pauli in the 1920's.[43] In the 1930's C. J. Gorter demonstrated the phenomenon of paramagnetic relaxation and recognised that in principle NMR could be observed.[42] It was not until 1946 that the existence of NMR was first reported. This was by two separate groups at Harvard and Stanford and was the detection of protons in bulk materials.

From that point on the increase in sensitivity and higher resolution spectrometers gradually introduced other elements such as ^{19}F, $^{10}B/^{11}B$ and ^{31}P, all of which are now common experiments.

Nuclei have nuclear angular momentum which has an associated magnetic field comparable to the magnetic field produced by an electric current in a loop. A nuclear spin thus behaves as a magnetic dipole, which tends to align with an applied magnetic field.

For comparing different nuclei, the receptivity, R, is defined as the product of the natural abundance, A, of the isotope (%) and the sensitivity at constant field. This receptivity is often compared to the receptivity of ^{13}C, R^C.

$R^C = |\gamma^3|AI(I+1)/(\gamma_C{}^3 A_C 3/4)$ where γ is the magnetogyric ratio and I the spin.[43]

That way a comparison can be made between any nuclei giving its effective "sensitivity".

Another condition to take into account is that NMR signals are accumulated from a series of repeated scans. The problem is that if equilibrium has not been re-established before repetition, then usable spectra are not obtained, therefore relaxation times have to be taken into account. Also, the longer the time before repetition, the longer the time taken for a usable data collection. It was because of the long relaxation times of his specimens that C. J. Gorter failed to discover NMR in the 1930's.[44]

It has also been found that the negative magnetogyric ratios of Sn and Ge can lead to disadvantageous NOE (Nuclear Overhauser Effect) behaviour which can be avoided by the addition of certain unreactive paramagnetic reagents such as $[Cr(acac)_3]$ which is used to increase the speed of relaxation.[45] Slight imperfections in the NMR machine, particularly the applied field significantly effect the obtained spectrum and spinning the sample helps to reduce this.

Chemical shifts (δ in ppm) are given relative to a standard substance (depending on nuclei) and relate to the shielding difference between the observed compound and the standard. Coordination shift is similar but refers to the change in shielding from free ligand to the coordinated ligand.

For any spin = ½ nuclei the number of lines seen in a spectra can be given by the equation 2nI +1 where n is the number of equivalent nuclei being coupled and I is its spin.

n	I=1/2
0	1
1	1 1
2	1 2 1
3	1 3 3 1
4	1 4 6 4 1

Singlets (s), doublets (d), triplets (t) and quartets (q) are common couplings within ^{1}H NMR's, however this work also shows quintets (q^5) as well as more complex examples such as doublet of doublet of triplets (d,d,t) etc.

If spin >1/2 then the equation still holds, but the spectra become vastly more complicated.

n	I=1
0	1
1	1 1 1
2	1 2 3 2 1
3	1 3 6 7 6 3 1

When I=3/2 the n=3 line is 1 3 6 10 12 12 10 6 3 1 for example.

Dynamic processes which occur at rates of the same order as the NMR time-scale can be studied by reducing the temperature at which the experiment is taking place.

1.7.2 IR Spectroscopy of Tin Compounds:

Although tin-element stretching vibration bands are dominated by the mass effect, falling to lower frequencies as the element mass increases from *ca.* 1900 cm^{-1} for Sn-H[46] down to *ca.* 150 cm^{-1} for fourth row elements,[47] these values can be significantly affected by other elements in close proximity. The Sn-H stretch changes from 1948 to 1905 cm^{-1} in SnH_3X with X changing from Cl to I.[48] The Sn-O stretch in $[SnX_4\{OEPh_3\}_2]$ changes from 390 to 310 cm^{-1} with E changing from P to As.[13] It has also been shown that intermolecular interactions can affect the band position, particularly in organotin fluorides where fluorine bridging occurs in the solid state (ν(Sn-F) changes from *ca.* 570 in gas phase to 360 cm^{-1} in solid state).[49]

1.7.3 IR Spectroscopy of MX_4L_2 Species:

Table 5 Normal stretching modes of *cis* and *trans* $[MX_4L_2]$ geometries.[a]

	Symmetry point group	ν(M-X)	ν(M-L)
cis- MX_4L_2	C_{2v}	$2A_1 + B_1 + B_2$	$A_1 + B_1$
trans- MX_4L_2	D_{4h}	$A_{1g} + B_{1g} + E_u$	$A_{1g} + A_{2u}$

a. Infrared-active species are italicised.

This shows that for *cis*-SnX_4L_2 with C_{2v} symmetry there should be four ν(Sn-X) IR active bands whereas there is only one in *trans*- SnX_4L_2 with D_{4h} symmetry.

1.7.4 Tin NMR Spectroscopy:

A number of reviews on tin NMR have been produced with large tables of data for tin containing compounds.[50] As mentioned above, three naturally occurring tin isotopes have spin = ½ however, only ^{117}Sn and ^{119}Sn are of use. This is because ^{115}Sn is a factor of twenty less abundant as well as having a receptivity (R^C) twenty times less than the other isotopes (see Table 6). As well as obtaining Sn NMR patterns, having two spin ½ nuclei also gives readily recognisable spectra when looking at other bonded NMR active nuclei (specifically used in this work ^{19}F and ^{31}P). As tin, phosphorus and fluorine all

detailed information can be obtained about the structure of the compounds being formed by using multinuclear NMR spectroscopic techniques, which might otherwise be elusive.

Table 6 NMR spectroscopic properties of tin nuclei with spin ½.

Nucleus	^{115}Sn	^{117}Sn	^{119}Sn
Natural abundance (C/%)	0.35	7.61	8.58
Magnetogyric ratio ($\gamma/10^7$ rad $T^{-1}s^{-1}$)	-8.792	-9.578	-10.021
Receptivity R^C	0.707	19.9	25.7

Although either ^{117}Sn or ^{119}Sn can be studied by NMR, it is the latter that is generally used due to both its slightly increased abundance and relative receptivity. It has also been established that any chemical shift effect caused by studying ^{117}Sn or ^{119}Sn has an effect of less than 0.1 ppm so is irrelevant within this work due to the experimental error.[51]

Tin-119 NMR has a large, negative magnetogyric ratio. Unlike most nuclei where this ratio is positive and enhances the signal, this means the observed resonances from decoupled spectra are heavily affected by signal diminuation from the NOE.[26] Adding a non reactive paramagnetic centre such as $Cr(acac)_3$ removes the NOE by introducing a second relaxation mechanism which over-rides the nuclear dipole-dipole relaxation, greatly reducing the overall relaxation times. Tin-119 chemical shifts vary depending on a number of factors, the main ones being: electronegativity (decreases the more electronegative) of attached groups, geometric distortions and coordination number at tin (greatly shifts upfield on going from 4 to 5 to 6 coordinate tin compounds).[26,52] Group IV chemical shifts are only affected by a few ppm by changing solvents, this is of course unless there is a specific chemical interaction, and when compared to their overall ranges (and accuracy) this is also usually irrelevant.[43] Similarly changes in temperature are also relatively unimportant.[53] The major factor that does vary the chemical shifts greatly is when any chemical change is made to the system.[43] With halogen derivatives the dominating effect of the chemical shifts appears to be factors

associated with the bulk and/or polarisability of the halogen, with iodides at the lowest frequency.[54]

Coupling constants have also been shown to vary depending on the orientation to other more electronegative nuclei. The Sn-P bond situated *trans* to the more electron donating ligand is strengthened, whereas the *cis* Sn-P bond is weakened.[55]

1.7.5 Mass Spectrometry of Tin Compounds:

The natural abundances of the 10 stable isotopes of tin gives a very characteristic abundance distribution which can be easily identified. Electron impact (EI), chemical ionisation (CI) and fast atom bombardment (FAB) mass spectrometry can all be used to identify tin containing compounds and ions. In practice however, the compounds made for this study are very moisture sensitive.

1.7.6 Single Crystal X-ray Diffraction:

This work shows a substantial number of crystal structure determinations of a variety of often quite sensitive complexes. The most crucial aspect of obtaining these is growing the crystals in the first place and many fruitless hours have been spent trying to obtain structures. Even when crystals are grown they are often highly sensitive (prone to decomposition or 'melting' (re-dissolving into oils when no longer in a saturated environment)) and very moisture sensitive. In comparison once the suitable crystals are obtained and successfully mounted onto the goniometer the data collection has become almost routine and while the size, morphology and optical characteristics in plane polarised light (all of which can be assessed using a microscope with polarisers) are important to get 'usable' data, compensations can generally be made while collecting such as increasing the length of each scan.

1.8 Steric Effects:

The steric effects in complexes that involve Group 15 tertiary ligands, in particular phosphanes have been widely explained by Tolman's Cone angle model (see Figure 4).[56] In summary the larger the steric bulk of the ligand, the larger the

size of the angle (θ) and the larger the value of θ the lower the coordination number that is favoured around a given metal centre.

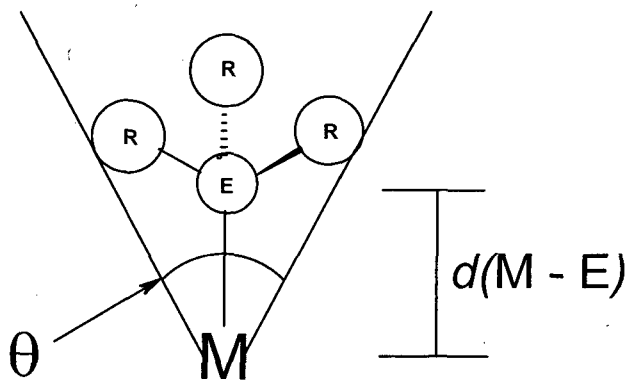

Figure 4 Tolman's Cone Angle Model.[56]

A number of factors make this model more complicated. The ligands are in fact not a uniform cone shape and allow intermeshing of substituents and the M-E bond distance will change depending on R, E, M and any substituents on M. Within this work however, the general bulk of the ligand tends to only affect the ratio of *cis* and *trans* isomers seen.

1.9 Bonding:

An octahedral SnX_4L_2 complex with phosphane or arsane ligands means that the octet rule has been exceeded for the main group atom. The model that currently explains this is either *electron rich multi-centre* bonding or *donor-acceptor* bonding (which are not mutually exclusive models) in which a primary M-X (Sn-Cl) σ bond is polarised towards the more electronegative halide as it is the lower energy atomic orbital, the corresponding antibonding orbital σ* is polarised towards the metal. If this σ* orbital lies low enough in energy it can act as an acceptor orbital on the metal through which a Lewis base (the phosphane or arsane ligand) can bond.[57,58] This means that not only is the X-M-L (L=ligand) linear but also that as M-L becomes stronger the population of σ* orbital is increased, the M-X bond is hence weaker and longer.[58]

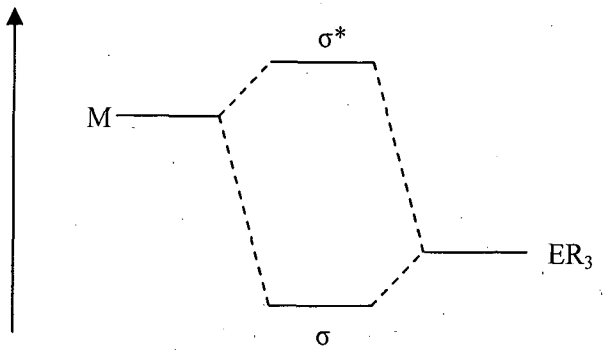

Figure 5 Schematic of the donor-acceptor bonding model.

SnX_4 Lewis acids have been widely reported and form adducts with a wide variety of neutral donor ligands (especially the strong Lewis acids X = Cl and Br) some of which (mainly the weaker acid, SnI_4) are often extensively dissociated in solution.[4,59,60] Lewis acid strength of the SnX_4 follows the usual order of Cl > Br > I.[61]

With bulky ligand groups co-ordinating octahedrally with an MX_4 (Group 14 halide) group a *trans* co-ordination would be expected especially if X = I due to the seemingly bulky nature of the base ligands. NMR spectroscopic studies of SnX_4L_2 have been carried out but both X = I or F are often ignored.[62]

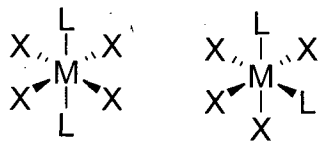

Figure 6 Examples of *trans* and *cis* conformations of octahedral MX_4L_2.

1.10 Macrocyclic Effect:

The chelate effect describes the increased stability of polydentate ligand complexes over complexes of the same metal with analogous monodentate ligands. It is known that the stability of the complexes increases as more donors are incorporated i.e. as the ligand denticity is increased. The macrocyclic effect describes the increase in stability observed for transition metal complexes when the open chain polydentate ligands are compared to the closest analogous

macrocyclic ligand. It is the macrocyclic effect that is the predominant reason for intense research efforts over recent decades focusing on the synthesis of macrocycles and their subsequent applications. It was first observed in Cu(II) aza macrocyclic species (see Figure 7) and showed that the copper complex of the macrocycle was 10^4 times more stable than its open chain intermediate.[63,64]

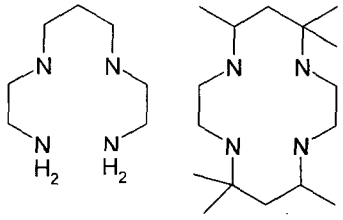

Figure 7 Diagram of the open chain and macroclic ligands for which the macrocyclic effect was discovered.

One limitation of the macrocyclic effect, however, is that it becomes less important with very large flexible rings and is only considered to be significant when the macrocyclic hole size is well matched with the metal ion radius.[65] With more conventional size rings however, both the entropic effect and enthalpic effects favour the formation of a macrocyclic complex over its open chain analogue. The enthalpy stability comes from the difference in solvation of the uncomplexed ligands (open chain more heavily solvated). The entropic contribution to the macrocyclic effect is predominantly due to the preorganisation of the macrocyclic ligand, which means that upon co-ordination there is only a small reduction in its rotational and vibrational degrees of freedom compared to the more flexible open chain polydentate ligand.[63]

1.11 Synthesis of Macrocycles:

There are two major methods to synthesise macrocycles; Metal Template Synthesis[66] and High Dilution Cyclisation synthesis.[65] The latter of which is the method primarily to be used in this project. It is worth noting that the formation of macrocycles are generally more problematic than their corresponding acyclic derivatives. The general premise for both methods is to favour the formation of the macrocycle over that of the more likely polymer which would be favoured under normal reaction conditions. The former method uses a metal ion to coordinate with the donor atoms, hence preorganising the reagents into the correct

conformation (the two ends relatively close together) for the cyclisation step. Unfortunately, once this cyclisation step has occurred an often difficult demetalation step is required to obtain the macrocyclic ligand as not all metal ions can act as templates. The latter and in our case more useful method involves dramatically reducing the concentrations of the reagents, therefore, there is a very low probability of two precursor molecules being close enough to form a polymer. Hence a single precursor reacts with itself under the imposed conditions to form the macrocycle. Unfortunately most of these reactions need to be under strictly anhydrous reaction conditions and this is often made even more difficult by the low concentrations and large time scales the reactions need. Another problem is that if stereoisomers are possible, as with the arsane macrocycle targets in Figure 8 this route will usually yield mixtures which may be very difficult to separate.

1.12 Arsane Macrocycles:

A small number of macrocyclic arsane ligands have been reported (see Chapter 6),[67] very few examples of their complexes with transition metals, and there are no reports of macrocyclic phosphane or arsane complexes with p-block metals despite the probable enhancement of the thermodynamic and kinetic stability associated with the macrocyclic effect. On the other hand it has been shown in Southampton that macrocyclic S and Se ligands produce a large range of structures with p-block metals.[57] Many of the thioether or selenoether macrocyclic structures complexed with p-block metals are not found in their acyclic analogues.[68,69] Therefore, arsane macrocycles such as those in Figure 8, could lead to structures not associated with acyclic phosphane or arsane complexes.

There has been widespread use of face-capping ligands such as Cp, Cp*, [9]aneS_3 and R_3[9]aneN_3, so the availability of strongly binding (As_3) ligands with very different electronic properties to C, N or S analogues could also be of interest in transition metal chemistry.

Macrocyclic arsane ligands and organoarsenic intermediates are less oxygen sensitive than the corresponding phosphanes. The haloarsanes are also much less moisture sensitive than the phosphane analogues and are therefore generally easier to handle. However, arsenic does not have a suitable spin active nucleus (unlike

phosphorus) making it more difficult to follow the reaction by NMR spectroscopy. Arsane macrocycles are less strongly reducing than the corresponding phosphanes, alkylphosphanes reduce many p-block halides whereas this rarely occurs with the less oxidizable arsenic analogues. Many p-block halides halogenate R_3P to R_3PX^+.

The problems in making arsane macrocycles include, the volatility and toxicity of the arsenic-containing precursors as well as the high energy barrier of inversion at arsenic (167.4 $kJmol^{-1}$),[70] which means that numerous stereoisomers[67] may be formed upon cyclisation which cannot be interconverted or easily separated.[71,72]

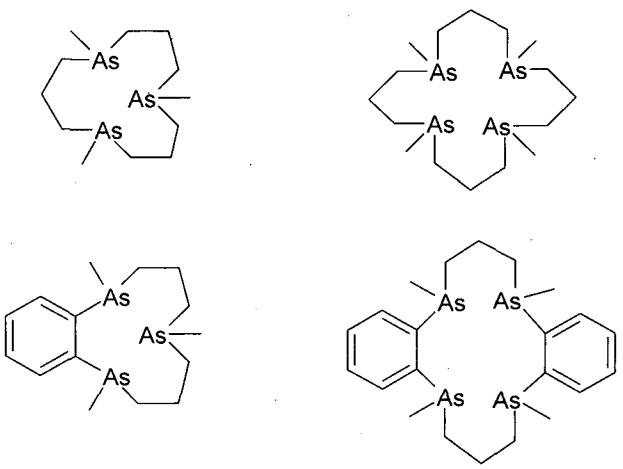

Figure 8 Possible macrocyclic arsane target molecules.

The methyl groups on the arsenic atoms (Figure 8) could also be replaced by bulky alkyl or phenyl groups.

More relevant details on the arsane macrocycle literature can be seen in Chapter 6.

1.13 References:

[1] R. G. Pearson, *Coord. Chem. Rev.*, **1990**, 100, 403-425.
[2] N. C. Norman, *Periodicity and the P block Elements*, Oxford University Press, **1995**.
[3] P. G. Harrison, *Comp. Coord. Chem.*; G. Wilkinson, R. D. Gillard, J. A. McCleverty, (Eds.), Pergamon press, Oxford, **1987**, vol. 3, ch. 26.
[4] P. G. Harrison, *The Chemistry of Tin*, Blackie & Son, London, **1989**.
[5] J. Parr, *Comp. Coord. Chem. II*, J. A. McCleverty and T. A. Meyer (Eds.), Elsevier, Oxford, **2004**, **3**, 545–608.
[6] N. N. Greenwood, A. Earnshaw, *Chemistry of the Elements*, Reed Elsevier plc, **1997**, ch. 10, 367-405.
[7] D. F. Shriver, P. W. Atkins, *Inorganic Chemistry, 3rd ed.*, Oxford University Press, Oxford, **1999**.
[8] A. D. Adley, P. H. Bird, A. R. Fraser, M. Onyszchuk, *Inorg. Chem.*, **1972**, 11, 1402-1409.
[9] E. L. Muetterties, *J. Am. Chem. Soc.*, **1960**, 82, 1082-1087.
[10] C. J. Wilkins, H. M. Haendler, *J. Chem. Soc.*, **1965**, 3174-3179.
[11] C. E. Michelson, D. S. Dyer, R. O. Ragsdale, *J. Inorg. Nucl. Chem.*, **1970**, 32, 833-838.
[12] P. A. W. Dean, D.F. Evans, *J. Chem. Soc. A.*, **1968**, 1154-1166.
[13] J. P. Clark, V. M. Langford, C. J. Wilkins, *J. Chem. Soc.* A., **1967**, 792-796.
[14] S. H. Hunter, V. M. Langford, G. A. Rodley, C. J. Wilkins, *J. Chem. Soc. A.*, **1968**, 305-308.
[15] W. Levason, C. A. McAuliffe, *Coord. Chem. Rev.*, **1976**, 19, 173-185.
[16] F. A. Cotton, G. Wilkinson, C. A. Murillo, M. Bochmann, *Advanced Inorganic Chemistry*, John Wiley & Sons, N.Y., **1999**, 6th ed.
[17] R. Kniep, D. Mootz, U. Severin, A. Wunderlich, *Acta Crystallogr.*, **1982**, 38B, 2022-2023.
[18] M. F. A. Dove, R. King, J. King, *J. Chem. Soc. Chem. Commun.*, **1973**, 24, 944-945.
[19] J. Zubieta, J. J. Zuckerman, *Progr. Inorg. Chem.*, **1978**, 24, 251-475.
[20] R. Hoppe, W. Dahne, *Naturwissenschaften*, **1962**, 49, 254-255.
[21] M. Bork, R. Hoppe, *Z. Anorg. Allgem. Chem.*, **1996**, 622, 1557–1563.
[22] G. P. Adams, J. L. Margrave, R. P. Steiger, P. W. Wilson, *J. Chem. Thermodyn.*, **1971**, 3, 297-305.
[23] M. E. Weeks, *Discovery of the Elements, 6th edn., J. Chem. Edu. Publ.* **1956**, 683-693.
[24] K. M. Mackay, R. A. Thomson, *Main Group Met. Chem.*, **1987**, 10, 83-108.
[25] A. L. Wilkins, P. Watkinson, K. M. Mackay, *J. Chem. Soc. Dalton Trans.*, **1987**, 2365-2372.
[26] R. K. Harris, J. D. Kennedy, W. McFarlane, *N.M.R. and the Periodic Table*, eds. R. K. Harris, B. E. Mann, Academic Press London, **1978**.
[27] E. Fukushima, S. B. W. Roeder, *J. Magn. Reson.*, **1979**, 33, 199-203.
[28] P. J. Watkinson, K. M. Mackay, *J. Organomet. Chem.*, **1984**, 275, 39-42.
[29] G. R. Willey, U. Somasunderam, D. R. Aris, W. Errington, *Inorg. Chim. Acta.*, **2001**, 315, 191-195.
[30] E. I. Davydova, T. N. Sevast'yanova, A. V. Suvorov, G. Frenking, *Russ. J. Gen. Chem.*, **2006**, 76, 545-553.
[31] E. I. Davydova, A. Y. Timoshkin, T. N. Sevastianova, A. V. Suvorov, G. Frenking, *J. Mol. Str. Theochem.*, **2006**, 767, 103-111.
[32] W. Levason, G. Reid, *Comp. Coord. Chem. II*, J. A. McCleverty and T. A. Meyer (Eds.), Elsevier, Oxford, **2004**, 1, 377-389.
[33] F. W. Wehrli, *Annu. Rep. NMR Spectrosc.*, **1979**, 9, 177-219.
[34] E. P. Kyba, M. C. Kerby, S. P. Rines, *Organometallics*, **1986**, 5, 1194-1197.
[35] O. Stelzer, K. P. Langhans, *The Chemistry of Organophosphorus Compounds*, F. R. Hartley (Eds.), Wiley, N.Y., **1990**, 1, ch 8.
[36] M. F. Mahon, N. L. Moldovan, K. C. Molloy, A. Muresan, I. Silaghi-Dumitrescu, L. Silaghi-Dumitrescu, *Dalton Trans.*, **2004**, 4017-4021.
[37] C. A. McAuliffe, *Phosphorus, Arsenic, Antimony and Bismuth Ligands, Comp. Coord. Chem.*, Pergamon: Oxford, **1987**, 2, ch. 14, 989-1066.
[38] E. W. Abel, R. P. Bush, F. J. Hopton, C. R. Jenkins, *J. Chem. Soc., Chem. Commun.*, **1966**, 3, 58-59.
[39] W. Levason, G. Reid, *Comp. Coord. Chem. II*, J. A. McCleverty and T. A. Meyer (Eds.), Elsevier, Oxford, **2004**, 1, 391-410.
[40] A. P. Smith, C. L. Fraser, *Comp. Coord. Chem. II*, J. A. McCleverty and T. A. Meyer (Eds.), Elsevier, Oxford, **2004**, 1, 1-23.

[41] C. R. Luman, F. N. Castellano, *Comp. Coord. Chem. II*, J. A. McCleverty and T. A. Meyer (Eds.), Elsevier, Oxford, **2004**, 1, 25-39.
[42] D. M. Grant, R. K. Harris, *Encyclopaedia of Nuclear Magnetic Resonance*, Wiley, **1996**.
[43] J. Mason, *Multinuclear NMR, Plenum, New York*, **1987**.
[44] C. J. Gorter, *Physica*, **1936**, 3, 955-998.
[45] R. Freeman, K. G. R. Pachler, G. D. LaMar, *J. Chem. Phys.*, **1971**, 55, 4586-4593.
[46] D. C. McKean, A. R. Morrison, P. W. Clark, *Spectrochim. Acta*, **1985**, 41A, 1467-1470.
[47] N. A. D. Carey, H. C. Clark, *Chem. Commun.*, **1967**, 292-293.
[48] J. M. Bellama, R. A. Gsell, *Inorg. Nucl. Chem. Lett.*, **1971**, 7, 365-368.
[49] K. Licht, H. Geissler, P. Koehler, K. Hottmann, H. Schnorr, H. Kriegsmann, *Z. Anorg. Allg. Chem.*, **1971**, 385, 271-288.
[50] B. Wrackmeyer, *Annual Reports on NMR Spectroscopy*, **1999**, 38, 203-264.
[51] H. C. E. McFarlane, W. McFarlane, C. J. Turner, *Mol. Phys.*, **1979**, 37, 1639-1642.
[52] J. Otera, *J. Organomet. Chem.*, **1981**, 221, 57-61.
[53] T. Gasparis-Ebeling, H. Nöth, B. Wrackmeyer, *J. Chem. Soc. Dalton Trans.*, **1983**, 97-100.
[54] A. A. Cheremisin, P. V. Schastnev, *J. Magn. Reson.*, **1980**, 40, 459-468.
[55] O. A Reutov, V. S. Petrosyan, N. S. Yashina, E. I. Gefel, *J. Organomet. Chem.*, **1988**, 341, C31.
[56] C. A. Tolman, *Chem. Rev.*, 1977, **77**, 313-348.
[57] W. Levason, G. Reid, *Dalton Trans.*, **2001**, 2953-2960.
[58] N. C. Norman, *Chemistry of Arsenic, Antimony and Bismuth*, Blackie Academic & Professional, London, **1998**.
[59] S. J. Ruzicka, A. E. Merbach, *Inorg. Chim. Acta.*, **1976,** 20 221-229.
[60] S. J. Ruzicka, A. E. Merbach, *Inorg. Chim. Acta.*, **1977,** 22, 191-200.
[61] A. R. J. Genge, W. Levason, G. Reid, *Inorg. Chim. Acta.*, **1999**, 288, 142-149.
[62] R. Colton, D. Dakternieks, *Inorg. Chim. Acta.*, **1983**, 71, 101-107.
[63] E. C. Constable, *Coordination Chemistry of Macrocyclic Compounds*, Oxford Primer, OUP Oxford, **1999**.
[64] D. K. Cabbiness, D. W. Margerum, *J. Am. Chem. Soc.*, **1969**, 91, 6540-6541.
[65] L. F. Lindoy, *The Chemistry of Macrocyclic Ligand Complexes*, Cambridge University Press, **1989**.
[66] D. Sellmann, L. Zapf, *Angew. Chem. Int. Ed. Engl.*, **1984**, 23, 807-808.
[67] E. P. Kyba, S. P. Chou, *J. Org. Chem.*, **1981**, 46, 860-863.
[68] A. J. Barton, N. J. Hill, W. Levason, G. Reid, *Dalton Trans.*, **2001**, 1621-1627.
[69] A. J. Barton, A. R. J. Genge, W. Levason, G. Reid, *Dalton Trans.*, **2000**, 859-865.
[70] R. C. Braechler, K. Mislow, J. P. Casey, R. J. Cook, G. H. Senkler Jr., *J. Am. Chem. Soc.*, **1972**, 94, 2859-2861.
[71] W. Levason, G. Reid, *Comp. Coord. Chem. II*, J. A. McCleverty and T. A. Meyer (Eds.), Elsevier, Oxford, **2004**, 1, 475-484.
[72] S. B. Wild, *The Chemistry of Organic Arsenic, Antimony and Bismuth Compounds*, S. Patai, Z. Rappoport (eds). Wiley, New York, **1994**, ch. 3.

Chapter 2

Complexes of SnF_4 with Hard Donor Ligands

2.1 Introduction:

Tin(IV) chloride is widely used in synthesis both as a source of tin(IV) and as a strong Lewis acid.[1,2] A very wide range of adducts of $SnCl_4$ with neutral ligands {L} are known, mostly six-coordinate $[SnCl_4\{L_2\}]$. Similar complexes are formed by $SnBr_4$ and SnI_4, although Lewis acidity decreases down the Group $SnCl_4$ > $SnBr_4$ >> SnI_4. The majority of these ligands have hard O or N donor atoms, but examples with softer P, As, S, Se or Te donors have also been characterised.[3,4,5,6,7,8,9,10,11] In marked contrast, little is known about adducts of SnF_4 with neutral ligands. Some examples were reported in the period 1950–1975, often as part of larger surveys including the heavier tin(IV) halides, but little data were provided and only a single complex, $[SnF_4\{2,2'\text{-bipy}\}]$, was structurally characterised.[12,13,14,15,16,17]

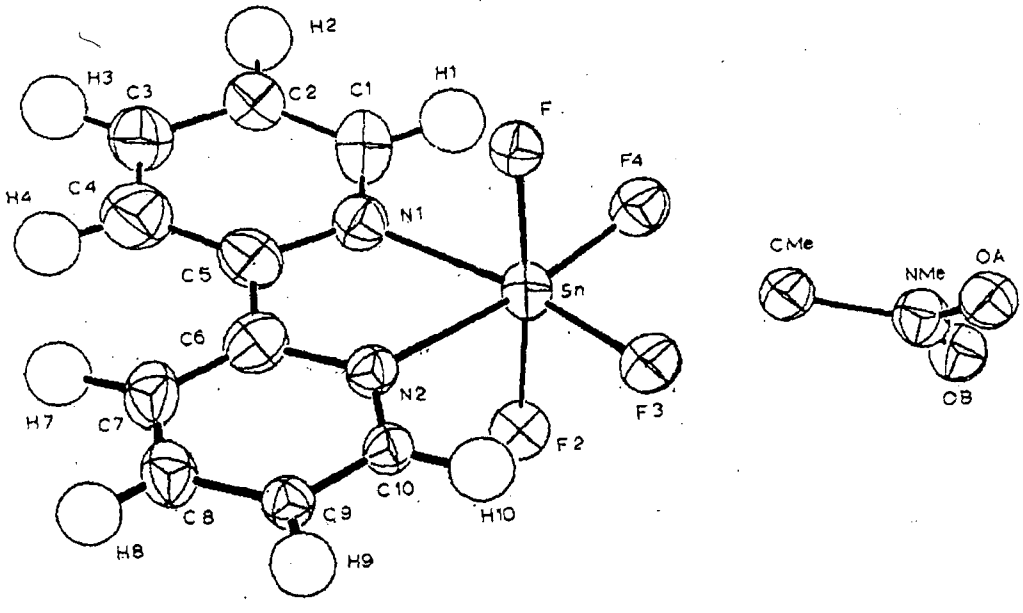

Figure 1 Molecular structure of $SnF_4C_{10}H_8N_2.CH_3NO_2$ projected down [010].[17]

There are no reports of SnF_4 complexes with softer donor ligands. This neglect in part is similar to that of other p-block fluorides, whose Lewis acidity, except towards F^- or in superacid media (for MF_5, M = As or Sb), is little explored. This also reflects the more difficult synthetic entry into the complexes. The SnX_4 (X = Cl, Br or I) are tetrahedral molecules readily soluble in weak or non-coordinating solvents such as chlorocarbons, hydrocarbons or arenes. The synthesis of $[SnX_4\{L\}_2]$ usually involves mixing the constituents in a solvent with precautions

to avoid hydrolysis. In contrast, anhydrous SnF_4 has a polymeric structure based upon vertex sharing SnF_6 octahedra,[18] and although readily hydrolysed, is otherwise rather unreactive towards neutral ligands and insoluble in weak donor solvents. A convenient entry into the chemistry is provided by Tudela and co-workers who have reported the preparation of $[SnF_4\{MeCN\}_2]$ made from SnF_2, I_2 and MeCN.[19,20]

Although standard texts state (usually without quoting supporting evidence) that Lewis acidity of the four tin(IV) halides is greatest for SnF_4, remarkably few complexes of the latter are known.[13,14,15,16,17,21] Tin(IV) chloride and bromide are strong Lewis acids forming adducts with a wide variety of neutral donor ligands, whereas tin(IV) iodide is only a weak Lewis acid forming similar, although much less stable, complexes which are often extensively dissociated in solution.[1,6,22]

The Southampton group has reported previously the syntheses, structural and spectroscopic characterisation (especially by multinuclear NMR techniques) of several series of SnX_4 (X = Cl, Br or I) adducts with soft donors including dithioethers,[7] diselenoethers,[8] ditelluroethers,[9] diphosphanes and diarsanes[10] and thiamacrocycles.[11] This work is now extended here to the investigation of the SnF_4 adducts and reported here are some examples with phosphane and arsane oxides.

Subsequent to this work and in connection with the work on GeF_4 complexes with soft donor ligands (Chapter 4) work on GeF_4 with hard N and O donor ligands was carried out within the group and comparisons with these systems are also made.[23,24]

2.2 SnF_4 Complexes of N and O Donor Ligands:

Due to the polymeric structure of SnF_4[18] $[SnF_4\{MeCN\}_2]$ was produced (from SnF_2 and I_2 in MeCN (see Figure 2))[19,20] as a starting synthon for all subsequent reactions. The subsequent conversion to $[SnF_4\{THF\}_2]$ by dissolving the MeCN adduct in THF and the removal of excess solvent was also used as a starting synthon but no apparent gains were noted.

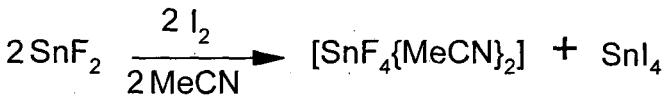

Figure 2 Reaction scheme for $[SnF_4\{MeCN\}_2]$.

A number of complexes of hard N- or O-donor ligands, previously obtained directly from SnF_4,[15] itself made by direct fluorination of tin(II) oxide in a nickel boat at between 200 and 500 °C[25] were re-prepared in this study from $[SnF_4\{MeCN\}_2]$ for comparison purposes, viz- $[SnF_4\{L–L\}]$ (L–L = 2,2'-bipyridyl, 1,10-phenanthroline, N,N,N',N'-tetramethyl-1,2-diaminoethane and 1,2-dimethoxyethane) and $[SnF_4\{L\}_2]$ (L = pyridine, THF).

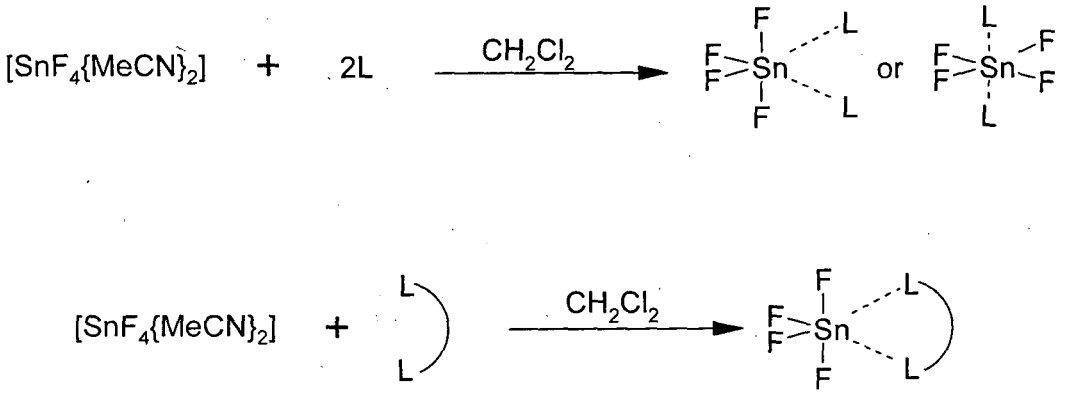

Figure 3 Formation of $SnF_4\{L\}_2$ and $SnF_4\{L\text{-}L\}$ complexes.

The complexes with N-donor ligands are unaffected by exposure to air for several hours and although moisture sensitive in solution, are much less readily decomposed than many of the other complexes in this study. The solid $[SnF_4\{L\}_2]$ (L = THF or L_2 = $MeO(CH_2)_2OMe$) rapidly hydrolyse in air. The IR and ^1H NMR spectroscopic data are given in the experimental section and were as expected from the previous literature.[15] The $^{19}F\{^1H\}$ and ^{119}Sn NMR data are

shown in Table 3. Although the ranges overlap there is a general shift to lower frequency in the ^{119}Sn NMR shifts with donor, P → N → O. The complexes with L–L = 2,2'-bipyridyl, 1,10-phenanthroline, $Me_2N(CH_2)_2NMe_2$ have the expected *cis* geometry, whilst the $[SnF_4\{pyridine\}_2]$ is the *trans* isomer. In contrast to the N-donor complexes, the ether adducts, $[SnF_4\{MeO(CH_2)_2OMe\}]$ and $[SnF_4\{THF\}_2]$, undergo rapid neutral ligand exchange in solution at ambient temperatures, only at low temperatures is it possible to observe $^{19}F\{^1H\}$ and ^{119}Sn NMR resonances. These revealed that in CH_2Cl_2 solution at 220 K the THF complex was a mixture of *cis* and *trans* isomers in approximately equal amounts. The $^{19}F\{^1H\}$ NMR spectrum of $[SnF_4\{THF\}_2]$ shows a singlet and two triplets almost identical to that shown in Figure 8. Figure 4 shows the ^{119}Sn NMR spectrum of $[SnF_4\{THF\}_2]$ and shows both the quintet of the *trans* isomer and the triplet of triplets of the *cis* isomer with coincidental chemical shifts and the coupling of the *trans* isomer being very similar to that of one of the couplings in the *cis* isomer. Figure 5 shows the predicted ^{119}Sn NMR spectrum of $[SnF_4\{THF\}_2]$ based on coupling constants from the $^{19}F\{^1H\}$ NMR spectrum of this compound (using the chemical shift observed in the ^{119}Sn NMR spectrum) in a 1:1 ratio of *cis*:*trans*.

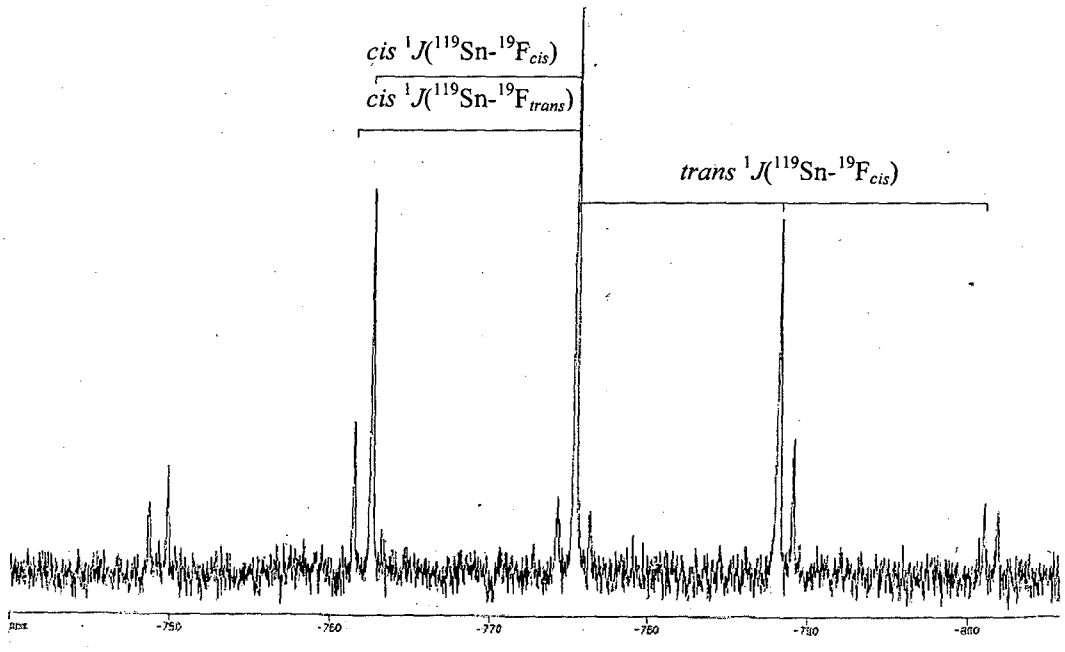

Figure 4 ^{119}Sn NMR spectrum of $[SnF_4\{THF\}_2]$ (220 K, CH_2Cl_2).

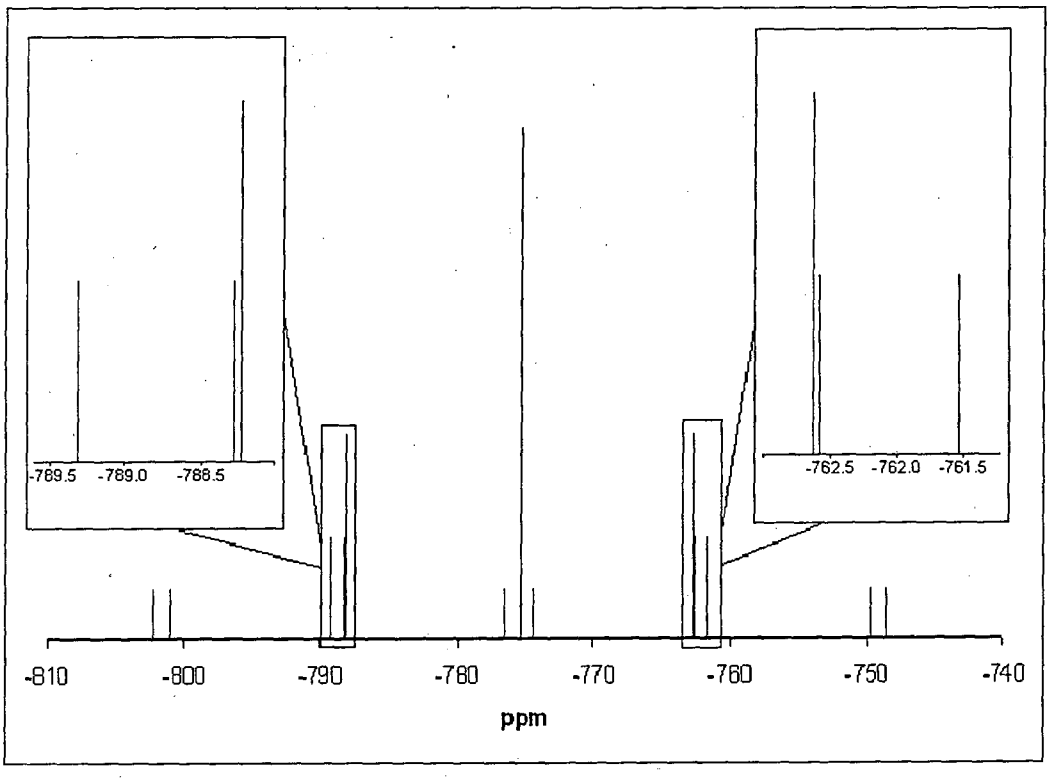

Figure 5 Predicted ^{119}Sn NMR spectrum of $[SnF_4\{THF\}_2]$.*

* Chemical shift from ^{119}Sn NMR spectrum of $[SnF_4\{THF\}_2]$.

Tudela[19] concluded that the $[SnF_4\{L\}_2]$ (L = pyridine or THF) were *trans* isomers in the solid state based upon IR and Mössbauer spectroscopic data.

Crystals of $[SnF_4\{MeO(CH_2)_2OMe\}]$ and $[SnF_4\{1,10\text{-phenanthroline}\}]$ were both grown from CH_2Cl_2/*n*-hexane. The structure of the former shows (Figure 6, Table 1) the expected *cis* geometry with Sn–O = 2.156(2), 2.144(2) Å, which are shorter than those in *trans*-$[SnCl_4\{THF\}_2]$[26] but significantly longer than the Sn–O distances in phosphane oxide adducts of SnF_4 which lie in the range 2.045(3)–2.088(5) Å (see Section 2.3). The latter complexes show no dissociation in solution indicative of stronger binding of the phosphane oxide ligands compared to the ethers. The differences in the distances $Sn–F_{transF}$ (1.926(2), 1.927(2) Å) and $Sn–F_{transO}$ (1.921(2), 1.923(2) Å) are much less than in the phosphane complex.

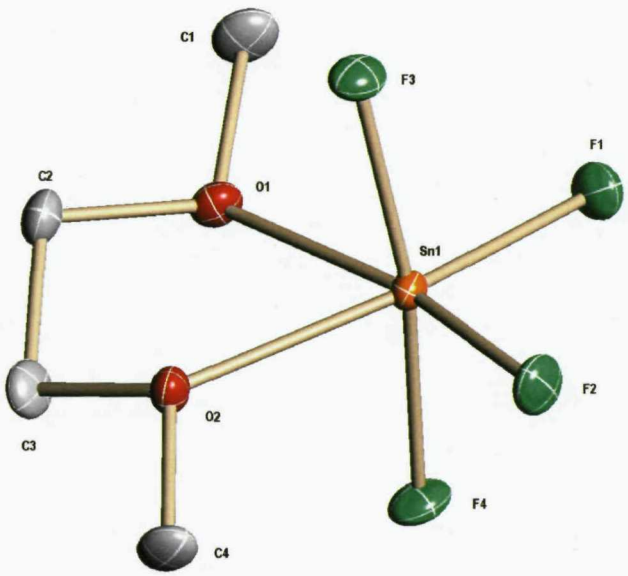

Figure 6 Structure of $[SnF_4\{MeO(CH_2)_2OMe\}]$ showing the atom numbering scheme. Ellipsoids are drawn at the 50% probability level and H atoms omitted for clarity.

Table 1 Selected bond lengths (Å) and angles (°) for [SnF_4{$MeO(CH_2)_2OMe$}].

Sn1–F3	1.9263(17)	Sn1–F4	1.9274(17)
Sn1–F1	1.9210(18)	Sn1–F2	1.9234(18)
Sn1–O1	2.1559(19)	Sn1–O2	2.144(2)
O1–C1	1.463(3)	O2–C3	1.454(3)
O1–C2	1.456(3)	O2–C4	1.463(3)
C2–C3	1.502(4)	O1···O2	2.673(3)
F1–Sn1–F2	99.27(8)	F3–Sn1–F4	170.07(7)
F–Sn1–F (the rest)	92.09(8)–93.93(8)	O2–Sn1–O1	76.88(8)
F1–Sn1–O2	169.84(8)	F2–Sn1–O1	167.62(8)
F–Sn1–O (the rest)	84.27(8)–93.07(8)		
Sn1–O1–C1	117.34(18)	Sn1–O2–C3	112.38(17)
Sn1–O1–C2	111.60(15)	Sn1–O2–C4	121.09(17)
O1–C2–C3	107.0(2)	O2–C3–C2	106.5(2)

The structure of [SnF_4{1,10-phenanthroline}] (Sn–N = 2.157(7) Å) (Figure 7, Table 2) may be compared with that of [$SnCl_4${1,10-phenanthroline}][27] which shows Sn–N = 2.234(7)–2.251(8) Å. One can also compare the literature data on [SnX_4{2,2'-bipyridyl}] for which Sn–N are X = F (2.181(3), 2.183(3) Å), X= Cl (2.247(4), 2.226(4) Å), X = Br (2.23(1), 2.23(1) Å), X = I (2.28(2) Å).[17,28,29] The 2,2'-bipyridyl series shows the longest Sn–N bonds in the iodide and the shortest in the fluoride, with the chloride and bromide less clearly discriminated, providing support for the fluoride being the strongest Lewis acid of the four halides.

Direct comparison can now be made with [GeF_4{1,10-phenanthroline}][24] for which Ge-F bond distances (1.781(2), 1.753(2)) are naturally shorter, as is the Ge-N (2.046(3) Å), due to the smaller metal acceptor.

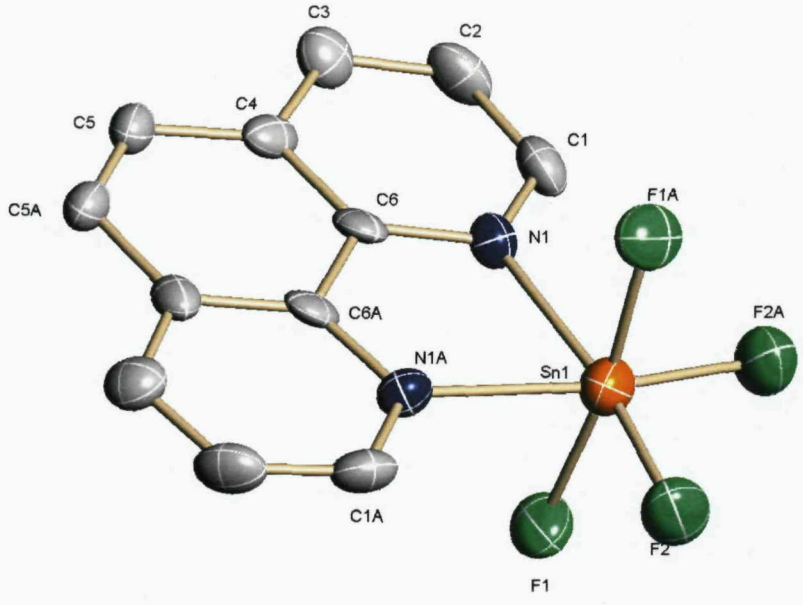

Figure 7 Structure of [SnF_4{1,10-phenanthroline}]·MeOH showing the atom numbering scheme. Ellipsoids are drawn at the 40% probability level with H atoms and solent omitted for clarity. The tin atom is on a 2-fold axis. Symmetry operation: a = 1 – x, ½ – y, z.

Table 2 Selected bond lengths (Å) and angles (°) for [SnF_4{1,10-phenanthroline}]·MeOH.

Sn1–F1	1.887(5)	Sn1–N1	2.157(7)
Sn1–F2	1.860(6)	N1–C1	1.339(11)
N1···N1a	2.670(13)	N1–C6	1.349(10)
F1–Sn1–F2	93.3(3)	F1–Sn1–F2a	91.9(3)
F2–Sn1–F2a	99.2(4)	F1–Sn1–F1a	172.0(3)
F1–Sn1–N1	88.0(3)	F2–Sn1–N1	168.4(3)
N1–Sn1–N1a	76.5(3)		
Sn1–N1–C1	126.4(5)	Sn1–N1–C6	115.1(5)

Symmetry operation: a = 1 – x, ½ – y, z.

Table 3 Selected NMR spectroscopic data for SnF_4 complexes with N or O donor ligands.[a]

Compound	δ ^{119}Sn[b]	δ $^{19}F\{^1H\}$	$^1J(^{19}F\text{-}^{119}Sn)$ (Hz)	$^2J(^{19}F\text{-}^{19}F)$ (Hz)
$[SnF_4\{2,2'\text{-bipyridyl}\}]$	-708.2(t,t)	–149.8(t) –179.8(t)	1964 1978	48
$[SnF_4\{1,10\text{-phen}\}]$	–715.1(t,t)	–149.5(t) –180.8(t)	1987 1982	50
$[SnF_4\{THF\}_2]$ *trans* isomer *cis* isomer	–775.4(q^5)[c] –775.4(t,t)[c]	–166.7(s) –166.2(t) –178.8(t)	1910 1918 2074	54
$[SnF_4\{pyridine\}_2]$ (*trans*)	–670.8(q^5)	–163.8(s)	1983	-
$[SnF_4\{Me_2N(CH_2)_2NMe_2\}]$	[d]	–167.8(t) –184.4(t)	2266 2096	50
$[SnF_4\{MeCN\}_2]$	n.o.[e]	–181.0(s)	n.o.	-
$[SnF_4\{MeO(CH_2)_2OMe\}]$ (190 K)	–753.8(t,t)	–167.1(t) –183.3(t)	2233 2189	61

[a] In CH_2Cl_2-10% $CDCl_3$. [b] ^{119}Sn Spectra were typically recorded at 250 K. [c] ^{119}Sn Spectra recorded at 220 K. [d] Insufficiently soluble to record spectrum. [e] n.o. = not observed in temperature range 295–180 K.

By comparing the NMR spectroscopic data for related Sn and Ge complexes of hard N or O donor ligands (see Table 3 and Table 4) it can be noted that δ $^{19}F\{^1H\}$ shifts to high frequency (more positive) in the Ge case consistently by between 30 and 40 ppm. Also the $^2J(^{19}F\text{-}^{19}F)$ coupling constants increase in the Ge case by 11 Hz (±1 Hz) with the N donors and 19 Hz (±1 Hz) for the O donors.

Table 4 Selected NMR spectroscopic data for GeF_4 complexes with N or O donor ligands.[24]

Compound	δ $^{19}F\{^1H\}$[a]	$^2J(^{19}F\text{-}^{19}F)$ (Hz)
$[GeF_4\{2,2'\text{-bipyridyl}\}]$	–116.2(t) –151.2(t)	58
$[GeF_4\{1,10\text{-phen}\}]$	–115.7(t) –150.1(t)	62
$[GeF_4\{THF\}_2]$ *trans* isomer *cis* isomer	–130.4(s) –128.7(t) –145.9(t)	72
$[GeF_4\{pyridine\}_2]$ (*trans*)	–125.7(s)	n.o.
$[GeF_4\{Me_2N(CH_2)_2NMe_2\}]$	–132.7(t) –150.9(t)	60
$[GeF_4\{MeCN\}_2]$ *trans* isomer *cis* isomer	–108.2(s) –101.2(t) –134.2(t)	55
$[GeF_4\{MeO(CH_2)_2OMe\}]$	–131.0(t) –151.1(t)	81

a In CH_2Cl_2-10% $CDCl_3$.

2.3 SnF_4 Complexes of $R_3P{=}O$ and $R_3As{=}O$ Donor Ligands:

The reaction of $[SnF_4\{MeCN\}_2]$ or $[SnF_4\{THF\}_2]$ with 2.0-2.1 mol. equivalents of the monodentate ligands or 1.0-1.1 mol. equivalents of the bidentate ligands in anhydrous CH_2Cl_2 resulted in the formation of white six coordinate complexes in high yields. The solids are moisture sensitive, tenaciously retain organic solvents - clearly evident in the ^1H NMR spectra, and are only modestly soluble in chlorocarbons. Solubility is not significantly better in acetone or nitromethane and stronger donor solvents were generally avoided for spectroscopic studies since they can lead to some displacement of the neutral ligands. The complexes with Ph_3PO, Ph_3AsO and Me_3PO were briefly reported in larger compilations of their metal complexes many years ago,[13,15,16] but characterisation was limited to microanalysis and partial IR spectra. Our IR spectra (Table 5) are generally in good agreement with those reported; where differences occur they can be attributed to differing amounts of *cis* and *trans* isomers present in the different samples resulting from differences in the isolation procedures and/or solvents used.[30] Comparing the IR ν(P(As)=O) bands in the Sn and Ge complexes shows negligible change, however, the metal-F vibration frequency increases by *ca.* 50 cm^{-1} in the case of germanium.[23]

Table 5 IR[a] and ^1H NMR[b] spectroscopic data for SnF_4 complexes with R_3PO and R_3AsO donor ligands.

Compound	ν(P(As)O)/cm^{-1}	ν(Sn-F)/cm^{-1}	δ(^1H)
$[SnF_4\{OPMe_3\}_2]$	1085(br)	576, 559	1.855(d) $^2J_{PH}$= 13.5 Hz 1.860(d) $^2J_{PH}$= 13.5 Hz
$[SnF_4\{OPPh_3\}_2]$	1137, 1082	580, 549, 537	7.36–7.88(m)
$[SnF_4\{OAsMe_3\}_2]$	865, 812(br)	550(br)	2.04(s), 2.05(s)
$[SnF_4\{OAsPh_3\}_2]$	877(br), 850(sh)	559(br)	7.40–7.87(m)
$[SnF_4\{o\text{-}C_6H_4(P(O)Ph_2)_2\}]$	1145, 1087(br)	585, 569, 548	7.31–7.71(m)
$[SnF_4\{Ph_2P(O)CH_2P(O)Ph_2\}]$	1145, 1092	596, 577	4.00(t) $^2J_{PH}$ = 13 Hz 7.36–7.75(m)[c]
$[SnF_4\{o\text{-}C_6H_4(P(O)Me_2)_2\}]$	1147, 1093	572(br)	1.79– 1.84 (m) 7.49–7.85(m)[d]

a Nujol mull. b In $CDCl_3$ at 300 MHz. c In CD_2Cl_2. d. In d^6-dmso

The multinuclear NMR spectroscopic data (Table 8) show the presence of both *cis* and *trans* isomers in CH_2Cl_2 solutions for the monodentate ligand complexes, the approximate isomer ratios being determined from the $^{19}F\{^1H\}$ NMR spectrum, however, in general the *trans* isomer predominates. Although resonances were observed at ambient temperatures in the ^1H, $^{31}P\{^1H\}$ and $^{19}F\{^1H\}$ spectra, the ^{119}Sn spectra showed broad and poorly resolved features and the samples were cooled to temperatures down to a minimum of 183 K to obtain the clearest resolution. The $^{31}P\{^1H\}$ NMR spectra show singlet resonances for each isomer with very similar chemical shifts, and no resolved coupling to ^{19}F, but with weak $^{119/117}Sn$ satellites. The $^2J(^{119/117}Sn\text{-}^{31}P)$ which lie in the range 20–65 Hz, appeared as single lines rather than as separate features for the two tin isotopes - no doubt the differences were lost in the line width since from the magnetogyric ratios $\gamma^{119}Sn/\gamma^{117}Sn$ (1.046) the values are expected to differ by < 2 Hz. The $^{19}F\{^1H\}$ spectra show singlet resonances for the *trans* isomers and two triplets for the *cis* (see Figure 8, Table 8), with $\delta(^{19}F)$ in the range -135 to -170, and with $^1J(^{119}Sn\text{-}^{19}F)$ 1700–1950 Hz, similar to the values in substituted fluorostannates(IV).[21] In these cases the $^1J(^{117}Sn\text{-}^{19}F)$ satellites were also clearly resolved and although not quoted in Table 8, the magnitudes were consistent with expectation, based upon $\gamma^{119}Sn/\gamma^{117}Sn$.

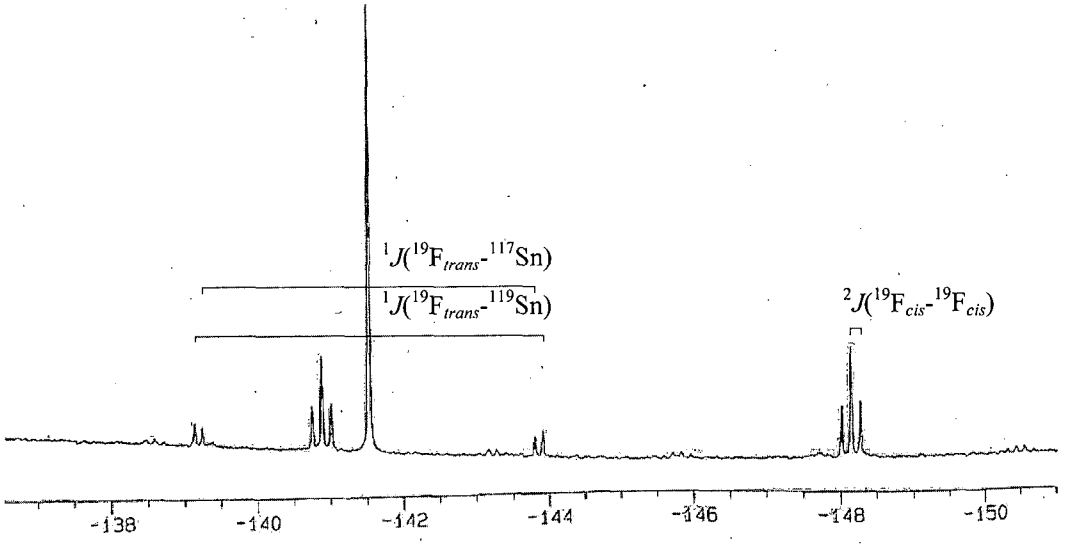

Figure 8 $^{19}F\{^1H\}$ NMR spectrum of $[SnF_4\{OAsMe_3\}_2]$ (273 K, $CDCl_3$).

Obtaining good quality ^{119}Sn NMR spectra proved difficult due to the modest receptivity of the tin (D_c = 25), poor solubilities, the presence of both isomers and also the complexity of the coupling patterns. For example, for $[SnF_4\{OPMe_3\}_2]$ the symmetrical quintet of triplets of the *trans* isomer was clearly evident centred at δ -781.8. Underlying this resonance is another weaker and more complex pattern centred on δ -769.0 attributed to the *cis* isomer. Based upon the various coupling constants obtained from the $^{19}F\{^1H\}$ and $^{31}P\{^1H\}$ spectra the major lines of the expected 27 line multiplet (t,t,t) were identified. The solubility of $[SnF_4\{OPPh_3\}_2]$ is lower, but again two multiplets can be discerned, consistent with approximately equal amounts of the two geometric isomers, although in this case the spectral quality was poor. For the $[SnF_4\{OAsR_3\}_2]$ complexes, the quintet due to the *trans* isomer was clearly identified in each case, but the resonance (t,t) of the less abundant *cis* form appeared near coincident and hence the chemical shift assignment less clear, although the more intense lines of the multiplets were found.

Comparing the NMR spectroscopic data of the Sn and Ge complexes of Me_3PO, Ph_3PO and Ph_3AsO hard donor ligands, it can be noted that δ $^{19}F\{^1H\}$ shifts to high frequency (more positive) in the Ge case consistently by around 40 ppm. It can also be seen that the $^2J(^{19}F\text{-}^{19}F)$ coupling constants increase in the Ge case by 9 Hz (±2 Hz).

Colourless crystals of $[SnF_4\{OPMe_3\}_2]$ were grown from a sample containing both isomers by vapour phase diffusion of hexane into a CH_2Cl_2 solution. These proved on structure solution to be the *trans* isomer. As can be seen from Figure 9 and Table 6, the molecule is centrosymmetric with Sn–F = 1.937(2), 1.954(2) Å, not significantly different from the values in *cis*-[SnF_4{2,2'-bipy}] 1.924(3)–1.948(3) Å.[17] Comparison of d(P–O) in the complex (1.532(3) Å) with that in Me_3PO itself (1.489(6) Å)[31] shows the bond is significantly lengthened upon co-ordination, but is the same within experimental error of $[GeF_4\{OPMe_3\}_2]$ (1.528(5) Å).[23] Differences in the IR ν(P=O) stretch are also negligible between Sn and Ge and both Ge-O and Ge-F bond distances are shorter due to the smaller metal size.

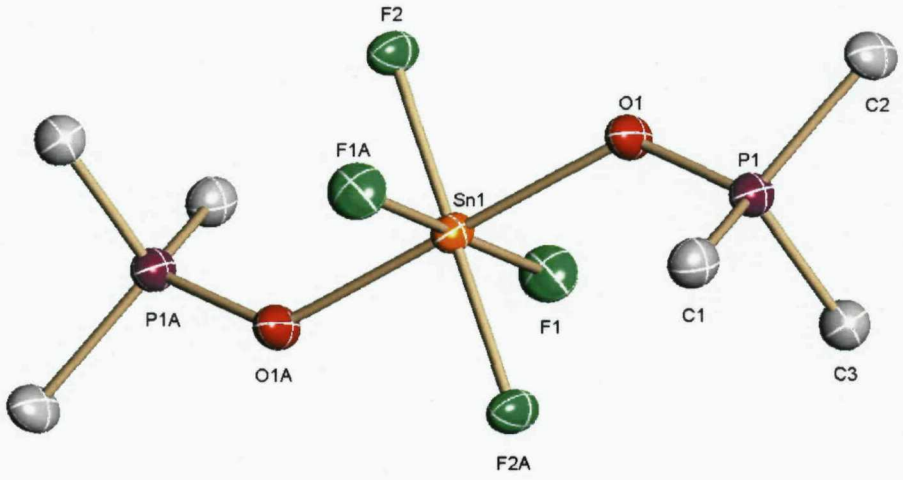

Figure 9 Structure of *trans*-$[SnF_4\{OPMe_3\}_2]$ showing the atom numbering scheme. Ellipsoids are drawn at the 50% probability level and H atoms omitted for clarity. Sn1 is positioned on a centre of symmetry. Symmetry operation: a = 0.5-x, 0.5+y, 0.5-z.

Table 6 Selected bond lengths (Å) and angles (°) for *trans*-$[SnF_4\{OPMe_3\}_2]$[a]

Sn1–F1	1.937(2)	Sn1–F2	1.954(2)
Sn1–O1	2.045(3)	P1–O1	1.532(3)
P1–C	1.774(4)–1.782(4)		
F1–Sn1–F2	89.85(10)	F1–Sn1–O1	91.13(11)
F2–Sn1–O1	89.48(10)	P1–O1–Sn1	131.50(17)
O1–P1–C	108.4(2)–111.7(2)	C–P1–C	107.2(2)–110.2(2)

a The tin atom is on a centre of symmetry.

Colourless crystals of $[SnF_4\{OPPh_3\}_2]$ were grown from a sample containing both isomers by vapour phase diffusion of hexane into CH_2Cl_2 solution as well as from the $[SnF_4\{PPh_3\}_2]$ complex left in CH_2Cl_2 solution for 1 month. These proved on structure solution to be the *trans* isomer. As can be seen from Figure 10, Table 7 the molecule is centrosymmetric with Sn–F = 1.929(3), 1.934(3) Å, again not significantly different from the trimethyl analogue above. Comparison of d(P–O) in the complex (1.520(4) Å) with that in free Ph_3PO (1.46(1) Å)[32] shows the bond is significantly lengthened upon co-ordination, but, within experimental error of $[GeF_4\{OPPh_3\}_2]$ (1.522(2) Å).[23] Differences in the IR ν(P=O) stretch are also negligible between Sn and Ge.

The bond lengths for both these crystal structures are entirely in keeping with our previous conclusions[33] that SnF_4 is the strongest Lewis acid of the four tin(IV) halides towards O-donor phosphane oxide ligands.

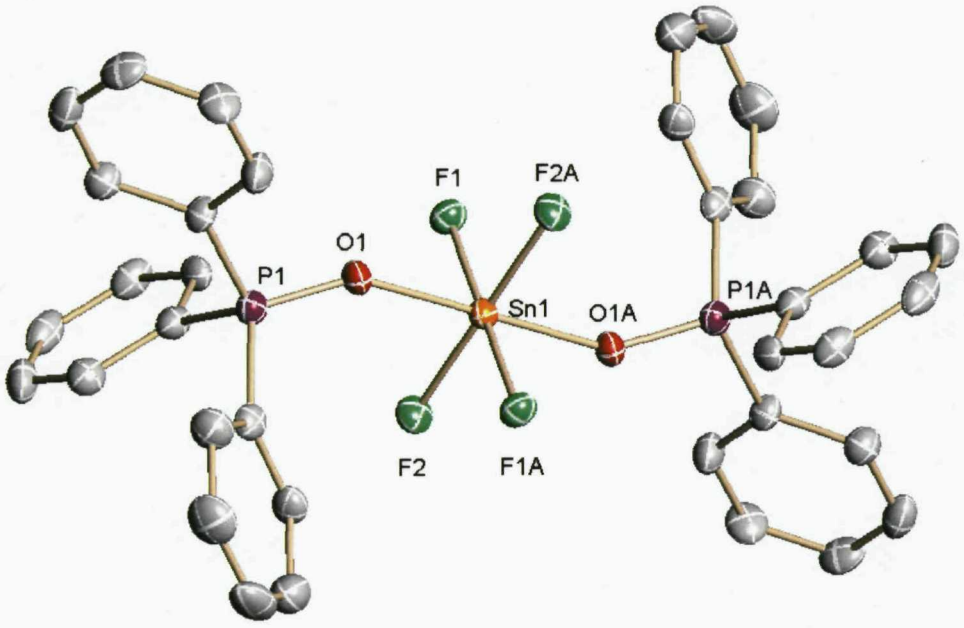

Figure 10 Structure of *trans*-$[SnF_4\{OPPh_3\}_2]$ showing the atom numbering scheme. Ellipsoids are drawn at the 50% probability level and H atoms omitted for clarity. Sn1 is positioned on a centre of symmetry. Symmetry operation: a = – x, 1 – y, 1 – z.

Table 7 Selected bond lengths (Å) and angles (°) for *trans*-$[SnF_4\{OPPh_3\}_2]\cdot 2CH_2Cl_2$.

Sn1–F1	1.928(3)	Sn1–O1	2.050(3)
Sn1–F2	1.934(3)	O1–P1	1.523(3)
P1–C1	1.792(5)	P1–C7	1.795(5)
P1–C13	1.797(6)		
F1–Sn1–F2	90.56(12)	F1–Sn1–O1	89.06(13)
F2–Sn1–O1	91.79(13)	Sn1–O1–P1	146.3(2)
O1–P1–C1	108.0(2)	O1–P1–C7	112.5(2)
O1–P1–C13	111.4(2)		

The diphosphane dioxide complexes are, as expected, *cis* isomers showing (Table 8) two triplets in the $^{19}F\{^1H\}$ NMR spectra and singlets in the $^{31}P\{^1H\}$ NMR spectra. At temperatures a little above ambient, the resonances in the $^{19}F\{^1H\}$ NMR spectra broaden, presumably due to some dynamic process, probably

chelate ring opening. On cooling the solutions the complexes precipitate which prevented low temperature studies. $[SnF_4\{o\text{-}C_6H_4(P(O)Me_2)_2\}]$ was however, insoluble in chlorinated solvents, but dissolved with some decomposition (diphosphane dioxide displacement) in anhydrous N,N-dimethylformamide. The $^{19}F\{^1H\}$ and $^{31}P\{^1H\}$ NMR spectra of the complex are given in Table 8, but the poor solubility and partial decomposition prevented a ^{119}Sn spectrum from being obtained.

Table 8 $^{31}P\{^{1}H\}$, ^{119}Sn and $^{19}F\{^{1}H\}$ NMR spectroscopic data for SnF_4 complexes with R_3PO and R_3AsO donor ligands.[a]

Compound		$\delta\ ^{31}P\{^{1}H\}$[b]	$\delta\ ^{119}Sn$[c]	$\delta\ ^{19}F\{^{1}H\}$[d]	$^{1}J(^{19}F\text{-}^{119}Sn)$ (Hz)	$^{2}J(^{19}F\text{-}^{19}F)$ (Hz)	$^{2}J(^{31}P\text{-}^{119}Sn)$ (Hz)	Isomer ratio
$[SnF_4\{OPMe_3\}_2]$	*trans*	65.9(s)	-781.8(q^5,t)	-149.2(s)	1725	-	50	3
	cis	65.4(s)	-769.0(t,t,t)	-147.2(t)	1772	51	50	1
				-158.0(t)	1850	-		
$[SnF_4\{OPPh_3\}_2]$	*trans*	42.5(s)	-770.0(q^5,t)	-149.8(s)	1704	-	20	1
	cis	42.3(s)	-775.1(t,t,t)	-146.2(t)	1730	53	22	1
				-159.8(t)	1850	-		
$[SnF_4\{OAsMe_3\}_2]$	*trans*	-	-747.7(q^5)	-141.6(s)	1804	-	-	3
	cis	-	-748.4(t,t)	-140.9(t)	1827	49	-	1
				-148.2(t)	1818	-		
$[SnF_4\{OAsPh_3\}_2]$	*trans*	-	-757.5(q^5)	-141.3(s)	1788	-	-	2
	cis	-	-758.6(t,t)	-137.8(t)	1800	51	-	1
				-151.9(t)	1860	-		
$[SnF_4\{o\text{-}C_6H_4(P(O)Ph_2)_2\}]$		45.5(s)	-790.0(t,t,t)	-142.9(br)	1730	53	63	-
				-167.2(t)	1923			
$[SnF_4\{Ph_2P(O)CH_2P(O)Ph_2\}]$		44.1(s)	-792.4(t,t,t)	-143.0(t)	1753	50	57	-
				-168.0(t)	1930			
$[SnF_4\{o\text{-}C_6H_4(P(O)Me_2)_2\}]$		62.1(s)		-143.5(t)	1740	50	57	-
				-165.4(t)	1930			

a To obtain good resolution of the complex couplings, spectra were typically recorded at 273 K. b Relative to external 85% H_3PO_4. c Relative to external neat $SnMe_4$. d Relative to external $CFCl_3$. e N,N-Dimethylformamide solution.

The crystal structures of *cis*-[SnF_4{*o*-$C_6H_4(P(O)Ph_2)_2$}] Figure 11, Table 9 and of the parent ligand, *o*-$C_6H_4(P(O)Ph_2)_2$ Figure 12, Table 10 have also been determined and the key bond lengths may be compared similarly. The d(Sn–F) are very similar to those in [SnF_4{$OPMe_3$}$_2$], and essentially independent of the nature of the *trans* ligand. The d(Sn–O) at 2.088(5) and 2.071(5) Å are rather longer than in the Me_3PO complex which probably reflects the effect of the seven-membered chelate ring. As found for the Me_3PO case, co-ordination of the diphosphane dioxide to the SnF_4 results in a significant lengthening of the P–O bond, from 1.484(2), 1.485(2) in the free ligand to 1.512(5), 1.525(5) Å in the complex.

A few poor quality crystals were also obtained from a solution of [SnF_4{*o*-$C_6H_4(PMe_2)_2$}] in CH_2Cl_2 after several weeks. X-ray examination of these established them as the compound [$SnClF_3${*o*-$C_6H_4(P(O)Me_2)_2$}]* containing a chelating diphosphane dioxide. The origin of the chlorine atom is presumably from reaction with the solvent and the oxygen in the phosphane oxide from aerial oxidation.[17]

* Crystal data for [$SnClF_3${*o*-$C_6H_4(P(O)Me_2)_2$}]·1/2CH_2Cl_2: MW = 483.77; orthorhombic, space group Pbcn (no. 60), Z = 8, T = 120 K, a = 15.290(5), b = 17.266(6), c = 13.380(3) Å, V = 3532.3(19) Å^3; 3772 unique data gave R_1 = 0.095, wR_2 = 0.173 ($I > 2\sigma(I)$) based on 186 independent parameters with S = 0.95.

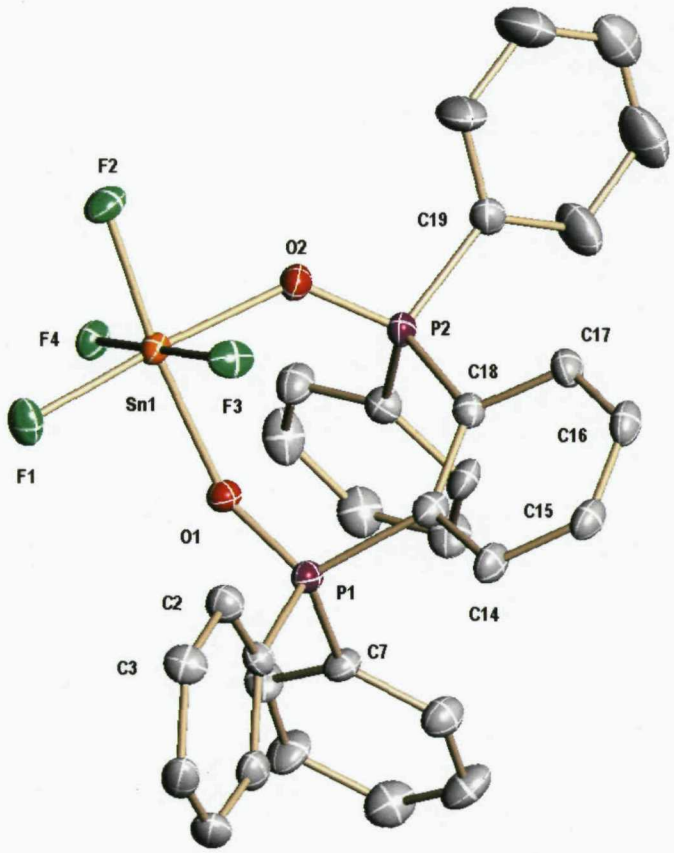

Figure 11 Structure of the tin residue in $[SnF_4\{o\text{-}C_6H_4(P(O)Ph_2)_2\}]\cdot CH_2Cl_2\cdot H_2O$ showing the atom numbering scheme. Atomic displacement ellipsoids are drawn at the 50% probability level, H atoms and solvent molecules are omitted for clarity.

Table 9 Selected bond lengths (Å) and angles (°) for $[SnF_4\{o\text{-}C_6H_4(P(O)Ph_2)_2\}]\cdot CH_2Cl_2\cdot H_2O$

Sn1–F1	1.930(4)	Sn1–F3	1.951(4)
Sn1–F2	1.940(4)	Sn1–F4	1.941(4)
Sn1–O1	2.088(5)	Sn1–O2	2.071(5)
P1–O1	1.512(5)	P2–O2	1.525(5)
P–C	1.786(7)–1.819(7)		
F3–Sn1–F4	174.39(18)	F4–Sn1–F1	91.50(18)
F3–Sn1–F1	93.20(18)	F4–Sn1–F2	91.57(17)
F3–Sn1–F2	91.00(18)	F1–Sn1–F2	95.65(19)
F3–Sn1–O1	89.18(18)	F3–Sn1–O2	87.81(18)
F4–Sn1–O1	87.67 (17)	F4–Sn1–O2	87.26(18)
F1–Sn1–O1	91.13(18)	F1–Sn1–O2	175.41(19)
F2–Sn1–O1	173.19(18)	F2–Sn1–O2	88.80(19)

O1–Sn1–O2	84.40(18)		
P1–O1–Sn1	140.5(3)	P2–O2–Sn1	133.8(3)
O–P–C	106.5(3)–112.9(3)	C–P–C	106.9(3)–109.6(3)

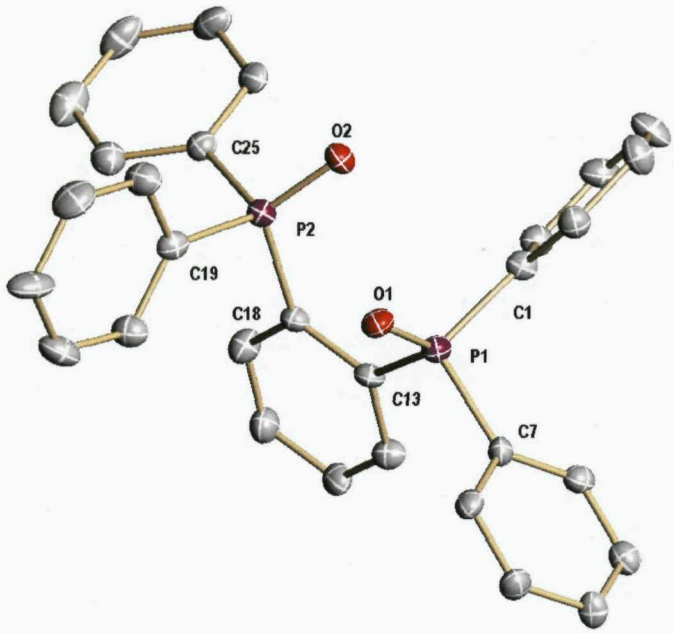

Figure 12 Structure of $[o\text{-}C_6H_4(P(O)Ph_2)_2]\cdot CH_2Cl_2$ showing the atom numbering scheme. Atomic displacement ellipsoids are drawn at the 50% probability level and H atoms and CH_2Cl_2 omitted for clarity.

Table 10 Selected bond lengths (Å) and angles (°) for $[o\text{-}C_6H_4(P(O)Ph_2)_2]\cdot CH_2Cl_2$

P1–O1	1.484(2)	P2–O2	1.485(2)
P1–C1	1.809(3)	P2–C18	1.838(3)
P1–C7	1.810(3)	P2–C19	1.800(3)
P1–C13	1.824(3)	P2–C25	1.815(3)
O1–P1–C1	115.74(13)	O2–P2–C18	114.46(12)
O1–P1–C7	110.22(12)	O2–P2–C19	116.22(13)
O1–P1–C13	112.88(13)	O2–P2–C25	109.84(12)
C1–P1–C7	105.49(13)	C18–P2–C19	105.81(13)
C1–P1–C13	105.77(13)	C18–P2–C25	104.88(13)
C7–P1–C13	106.02(13)	C19–P2–C25	104.60(13)

Most interesting is the comparison with data on other tin(IV) phosphane oxides.[30] Tudela *et al.*[30] noted that in *cis*- and *trans*-$[SnBr_4\{OPPh_3\}_2]$ the Sn–O (2.080(8), 2.101(9) Å) and P–O (1.515(8), 1.516(9)(av) Å) distances were the same within the usual criteria showing that the geometric isomer present has no effect, as might be expected for hard donor-acceptor interactions on a p-block metal. However, when one compares the key distances along the series $[SnX_4\{OPR_3\}_2]$ (Table 11) one finds that Sn–O increases with X = F < Cl < Br < I. The substantially shorter Sn–O distance in the tin(IV) fluoride is clearly consistent with stronger binding of the ligand indicative of stronger Lewis acidity of the SnF_4. This is in agreement with the conclusions from the $^{31}P\{^1H\}$ NMR data above. Moreover, studies of phosphane oxide complexes of hard early transition metals such as Y(III)[34] or Sc(III)[35] have shown that the metal-oxygen distances are independent of the R group (Me or Ph) as is so in our findings, although they do vary with the metal co-ordination number.[34,35] From Table 11 it also notable that the P–O distance in the fluoride complex is markedly longer than in the other examples, (albeit some of the comparator data are not of high precision) which also supports stronger donation from O to Sn. The trends are replicated in $[SnF_4\{o\text{-}C_6H_4(P(O)Ph_2)_2\}]$ when compared with the structural data on $[SnI_4\{o\text{-}C_6H_4(P(O)Ph_2)_2\}]$[10] (Table 11). In the iodo-complex the d(Sn–O) are much longer, consistent with the relative Lewis acidity of the tin centres.

Table 11 Selected structural data on tin(IV) phosphane oxides.

Compound	d(Sn–OPR_3)/Å	d(P–O)/Å	Ref.
trans-$[SnF_4\{OPMe_3\}_2]$[a]	2.045(3)	1.532(3)	this work
trans-$[SnF_4\{OPPh_3\}_2]$[a]	2.055(4)	1.520(4)	this work
cis-$[SnCl_4\{OPPh_3\}_2]$[b]	2.083(2)	1.510(2)	36
cis-$[SnCl_4\{OPPh_3\}_2]$[c]	2.086(2)	1.505(2)	37
trans-$[SnBr_4\{OPPh_3\}_2]$[b]	2.102(9), 2.100(8)	1.504(9), 1.527(9)	38
cis-$[SnBr_4\{OPPh_3\}_2]$[b]	2.080(8)	1.515(8)	30
cis-$[SnI_4\{OPPh_3\}_2]$[b]	2.11(2), 2.15(2)	1.47(2), 1.50(2)	39
$[SnF_4\{o\text{-}C_6H_4(P(O)Ph_2)_2\}]$[a]	2.071(5), 2.088(5)	1.512(5), 1.525(5)	this work
$[SnI_4\{o\text{-}C_6H_4(P(O)Ph_2)_2\}]$[d]	2.120(5), 2.138(5)	1.509(6), 1.513(5)	10

a 120 K. b 295 K. c 90 K. d 150 K.

2.4 $[SnX_4\{L\}_2]$ X = Cl, Br or I; L = Ph_3PO, Ph_3AsO or Me_3PO – some Spectroscopic Comparisons:

These complexes have been studied on several occasions and structures have been reported for *cis*-$[SnX_4\{OPPh_3\}_2]$[30,37,39] and *trans*-$[SnX_4\{OPPh_3\}_2]$ (X = Cl or Br).[36,38] The IR spectra have been discussed in detail[3,13,16] and our data are generally in agreement with the literature and hence not discussed further. Curiously little NMR spectroscopic data have been reported previously and complete data are presented in Table 12.

Table 12 Selected NMR data on phosphane oxide and arsane oxide comparator complexes.[10]

Compound	δ $^{31}P\{^1H\}$[a]	$^2J(^{31}P$-$^{119}Sn)$ Hz[b]	δ ^{119}Sn	Ratio of isomers
$[SnCl_4\{OPMe_3\}_2]$	+63.4 (273 K)[c]	140	-695(t) (243 K)	4
	+62.5	106	-686(t)	1
$[SnBr_4\{OPMe_3\}_2]$	+61.0 (223 K)	140	-1439(t)	
$[SnI_4\{OPMe_3\}_2]$	+58.3 (193 K)	n.o.	n.o.[d]	
$[SnCl_4\{OPPh_3\}_2]$	+40.8 (233 K)	198	-710(t) (233 K)	1
	+40.35	162	-698(t)	5
$[SnBr_4\{OPPh_3\}_2]$	+38.9 (223 K)	214	-1480(t) (223 K)	
$[SnI_4\{OPPh_3\}_2]$	+36.5 (183 K)	n.o.	n.o.	
$[SnCl_4\{OAsPh_3\}_2]$			-639(s) (243 K)	1
			-637(s)	2
$[SnBr_4\{OAsPh_3\}_2]$			-1364(s) (233 K)	
$[SnI_4\{OAsPh_3\}_2]$			n.o.	
$[SnCl_4\{o\text{-}C_6H_4(P(O)Ph_2)_2\}]$[e]	+42.4 (300 K)		n.o.	
$[SnBr_4\{o\text{-}C_6H_4(P(O)Ph_2)_2\}]$[e]	+41.6 (300 K)		n.o.	
$[SnI_4\{o\text{-}C_6H_4(P(O)Ph_2)_2\}]$[e]	+39.8 (190 K)		n.o.	

[a] In CH_2Cl_2-10% $CDCl_3$. [b] Separate resonances for ^{119}Sn and ^{117}Sn couplings not resolved in $^{31}P\{^1H\}$ NMR spectra- couplings are from ^{119}Sn spectra. [c] Ligand chemical shifts are:- Me_3PO +38, Ph_3PO +28, o-$C_6H_4(P(O)Ph_2)_2$ +31. [d] n.o. = Not observed in temperature range 295–180 K. [e] Data from Ref. 10.

The trends in the spectroscopic data were examined to see if support for the greater Lewis acidity of the SnF_4 was forthcoming which is most evident in the $^{31}P\{^1H\}$ NMR spectroscopic data (Table 8, Table 12). The chemical shift differences between the geometric isomers are small and therefore one can compare directly the changes in chemical shift simply as a function of the halide present. This shows a small but clear shift to high frequency along the series F > Cl > Br > I consistent with decreased acceptor power along this series. Although the shift to low frequency in the ^{119}Sn NMR, $[SnCl_4\{L\}_2] \rightarrow [SnF_4\{L\}_2] \rightarrow [SnBr_4\{L\}_2]$ cannot be used directly to determine acceptor power (it is affected also by elecronegativity of the substituents, ligand interactions and ligand polarisabilities[1,40]) it is however, parallel to that in the hexahalostannates(IV).[40,41,42] ^{119}Sn resonances are rarely observed for iodotin species mainly due to exchange reactions in solution resulting from the weak Lewis acidity of SnI_4.

2.5 Oxidation of Phosphanes:

It was mentioned above that the crystals of $[SnF_4\{OPPh_3\}_2]$ were obtained from both $[SnF_4\{OPPh_3\}_2]$ and $[SnF_4\{PPh_3\}_2]$ samples in CH_2Cl_2. The group has previously reported[10] that mixtures of phosphanes or diphosphanes with SnX_4 (X = Cl, Br or I) in chlorocarbon solution air-oxidise readily to the corresponding phosphane oxides, specifically that catalytic amounts of SnI_4 can be used to cleanly generate phosphane oxides from the corresponding phosphanes, using dry air or dioxygen, and whilst the mechanism remains obscure, the use of $^{18}O_2$ in these reactions showed that the source of the oxygen is O_2,[43] not water as in a halogenation/hydrolysis mechanism.[44]

The phosphane complexes of tin(IV) fluoride made in the present study also show varying degrees of oxygen sensitivity, especially in solution. The $[SnF_4\{PCy_3\}_2]$ is particularly sensitive and even brief exposure to air of a CH_2Cl_2 solution produced substantial oxidation. The $[SnF_4\{PMe_3\}_2]$ and the diphosphane complexes are less rapidly air oxidised, but modest amounts of phosphane oxides can be detected by $^{31}P\{^1H\}$ NMR in solutions exposed to air for some hours. In these systems the phosphane oxide binds strongly to the SnF_4 (see Section 2.3) and thus in contrast to the extensively dissociated SnI_4 systems[44] the formation of

phosphane oxide is stoichiometric, since the phosphane oxide removes the SnF_4 by complexation preventing further reaction. Crystals of $[SnF_4\{OPPh_3\}_2]$ were obtained over several days from a CH_2Cl_2 solution of the products from melting $[SnF_4\{MeCN\}_2]$ with excess PPh_3.

2.6 Conclusions:

A large number of SnF_4 complexes with phosphane and arsane oxide ligands (hard metal centre to hard ligand bonding) have been fully characterised, and $^{19}F\{^1H\}$, $^{31}P\{^1H\}$ and ^{119}Sn NMR spectroscopic data obtained where possible. A number of structures have also been determined using single crystal X-ray diffraction techniques.

These compounds have confirmed the greater Lewis acidity of SnF_4 compared to the other tin(IV) halides from the trends in the $^{31}P\{^1H\}$ NMR spectroscopic data. The structural data discussed in preceding sections clearly show that for a fixed hard neutral ligand the Sn–ligand bond lengths are shortest in the fluoride complexes consistent with SnF_4 being the strongest Lewis acid.

2.7 Experimental:

See Appendix for general experimental methods. $[SnF_4\{MeCN\}_2]$ and $[SnF_4\{THF\}_2]$ were made as described.[19,20] Ligands not obtained from suppliers were made by literature methods: *o*-$C_6H_4(P(O)Ph_2)_2$, *o*-$C_6H_4(P(O)Me_2)_2$, Me_3AsO, $Ph_2P(O)CH_2P(O)Ph_2$ and $Me_2P(O)(CH_2)_2P(O)Me_2$.[10,44,45] 2,2'-Bipyridyl, and 1,10-phenanthroline were dried by heating *in vacuo*, 1,2-dimethoxyethane was dried over sodium and freshly distilled. Pyridine and $Me_2N(CH_2)_2NMe_2$ were dried by distillation from BaO. Much of the spectroscopic data below is included above in this chapter, however, for ease of use it is collected under the compound.

The nitrogen and oxygen donor complexes below are known from previous work and so microanalysis was not collected.

$[SnF_4\{2,2'\text{-bipyridyl}\}]$:.$[SnF_4\{MeCN\}_2]$ (0.276 g, 1.00 mmol) was suspended in CH_2Cl_2 (10 mL) and a solution of 2,2'-bipy (0.156 g, 1.00 mmol) in CH_2Cl_2

(5 mL) added and the mixture refluxed for 2 h. The white precipitate was filtered off and dried *in vacuo*. Yield 0.365 g, 97%. ^{1}H NMR (300 MHz, CD_3NO_2, 298 K): δ = 8.49 (s, 1H), 8.99 (s, 1H), 9.15 (s, 1H), 9.41 (s, 1H) ppm. IR (Nujol): 580(s), 560, 520(sh) υ(SnF) cm^{-1}. ^{19}F{^{1}H} NMR (CH_2Cl_2/$CDCl_3$): -149.8 (t), -179.8 (t). ^{119}Sn NMR (CH_2Cl_2/$CDCl_3$): -708.2 (t,t).

[SnF_4{1,10-phenanthroline}]: Prepared similarly to the above. Yield 60%. ^{1}H NMR (300 MHz, $CDCl_3$, 298 K): δ = 8.45 (m, 4H), 9.16 (m, 2H), 9.35 (m, 2H) ppm. IR (Nujol): 587(s), 566(s) υ(SnF) cm^{-1}. ^{19}F{^{1}H} NMR (CH_2Cl_2/$CDCl_3$): -149.5 (t), -180.8 (t). ^{119}Sn NMR (CH_2Cl_2/$CDCl_3$): -715.1 (t,t).

[SnF_4{$MeO(CH_2)_2OMe$}]: 1,2-Dimethoxyethane (0.1 mL, 1.0 mmol) was added to a solution of [SnF_4{MeCN}$_2$] (0.276 g, 1.0 mmol) in CH_2Cl_2 (10 mL), and the mixture stirred at reflux for 2 h. The white precipitate was filtered off and dried *in vacuo*. Yield 77%. ^{1}H NMR (300 MHz, $CDCl_3$, 200 K): δ = 3.98 (s, 3H, Me), 4.25 (s, 2H, CH_2) ppm. IR (Nujol): 609(s), 584(s), 540(m) υ(SnF) cm^{-1}. ^{19}F{^{1}H} NMR (CH_2Cl_2/$CDCl_3$): -167.1 (t), -183.3 (t). ^{119}Sn NMR (CH_2Cl_2/$CDCl_3$): -753.8 (t,t).

[SnF_4{pyridine}$_2$]: Pyridine (0.16 g, 2.0 mmol) was added to a solution of [SnF_4{MeCN}$_2$] (0.186 g, 0.67 mmol) in CH_2Cl_2 (10 mL). This was stirred at reflux under nitrogen for 2 h. The white precipitate was filtered off and dried *in vacuo*. Yield 80%. ^{1}H NMR (300 MHz, $CDCl_3$, 298 K) δ = 7.7 (m, 2H), 8.2 (m, H), 9.00 (m, 2H) ppm. IR (Nujol): 568(s) υ(SnF) cm^{-1}. ^{19}F{^{1}H} NMR (CH_2Cl_2/$CDCl_3$): -163.8 (s). ^{119}Sn NMR (CH_2Cl_2/$CDCl_3$): -670.8 (q^5).

[SnF_4{$Me_2N(CH_2)_2NMe_2$}]: [SnF_4{MeCN}$_2$] (0.276 g, 1.0 mmol) was suspended in CH_2Cl_2 (10 mL), N,N,N'N'-tetramethyl-1,2-diaminoethane (0.15 g, 1.00 mmol) was added and the mixture stirred for 12 h. The white precipitate was filtered off and dried *in vacuo*. Yield 0.14 g, 54%. $C_6H_{16}N_2F_4Sn.1/2CH_2Cl_2$ (353.4) calcd. C 22.1, H 4.9, N 7.9; found C 22.3, H 5.1, N 8.1. ^{1}H NMR (300 MHz, $CDCl_3$, 298 K): δ = 2.89 (s, 12H, Me), 3.02 (s, 4H, CH_2) ppm. IR spectrum (υ(SnF)/cm^{-1}): 570 (s), 547 (s). ^{19}F{^{1}H} NMR (CH_2Cl_2/$CDCl_3$): -167.8 (t), -184.4 (t).

[SnF_4{THF}$_2$]: Was made as described.[19,20] ^{1}H NMR (300 MHz, $CDCl_3$, 298 K): δ = 2.10 (br, 2H, CH_2), 4.35 (br, 2H, OCH_2) ppm. IR (Nujol): 600(vbr) υ(SnF), 1013(br), 845(m) υ(COC) cm^{-1}. ^{19}F{^{1}H} NMR (CH_2Cl_2/$CDCl_3$, 243 K): -166.2 (t), -166.7 (s), -178.8 (t). ^{119}Sn NMR (CH_2Cl_2/$CDCl_3$, 223 K): -775.4 (t,t), -775.4 (q^5).

[SnF_4{$OPPh_3$}$_2$]: [SnF_4{MeCN}$_2$] (0.277 g, 1.0 mmol) was suspended in CH_2Cl_2 (20 mL) and Ph_3PO (0.612 g, 2.2 mmol) added and the mixture stirred at room temperature for 2 h. The white solid was filtered off, recrystallised from hot CH_2Cl_2 and dried *in vacuo*. Yield 0.66 g, 88%. $C_{36}H_{30}F_4O_2P_2Sn{\cdot}3CH_2Cl_2$ (1006.07) calcd. C 46.6, H 3.6; found C 47.1, H 3.7%. ^{1}H NMR (300 MHz, $CDCl_3$, 298 K): 7.36-7.88 (m). IR spectrum (υ(SnF)/cm^{-1}): 580, 549, 537, (υ(PO)/cm^{-1}): 1137, 1082. ^{19}F{^{1}H} NMR (CH_2Cl_2/$CDCl_3$, 298 K): -146.2 (t), -149.8 (s), -159.8 (t). ^{31}P{^{1}H} NMR (CH_2Cl_2/$CDCl_3$, 298 K): 42.5 (s), 42.3 (s). ^{119}Sn NMR (CH_2Cl_2/$CDCl_3$, 253 K): -770.0 (q^5,t), -775.1 (t,t,t).

[SnF_4{$OAsPh_3$}$_2$]: Prepared similarly from [SnF_4{MeCN}$_2$] (0.156 g, 0.56 mmol) and Ph_3AsO (0.40 g, 1.24 mmol). Yield 0.30 g, 64%. $C_{36}H_{30}As_2F_4O_2Sn{\cdot}2CH_2Cl_2$ (1009.03) calcd. C 45.2, H 3.4; found C 45.3, H 3.2%. ^{1}H NMR (300 MHz, $CDCl_3$, 298 K): 7.40-7.87 (m). IR spectrum (υ(SnF)/cm^{-1}): 559(br), (υ(AsO)/cm^{-1}): 877(br), 850(sh). ^{19}F{^{1}H} NMR (CH_2Cl_2/$CDCl_3$, 298 K): -137.8 (t), -141.3 (s), -151.9 (t). ^{119}Sn NMR (CH_2Cl_2/$CDCl_3$, 273 K): -757.5 (q^5), -758.6 (t,t).

[SnF_4{$OPMe_3$}$_2$]: Prepared similarly from [SnF_4{MeCN}$_2$] (0.28 g, 1.0 mmol) and Me_3PO (0.19 g, 2.05 mmol) and stirred for 8 h. Yield 0.30 g, 79%. $C_6H_{18}F_4O_2P_2Sn$ (378.84) calcd. C 19.0, H 4.8; found C 18.2, H 4.7%. ^{1}H NMR (300 MHz, $CDCl_3$, 298 K): 1.85 (d, $^2J_{PH}$ = 13.5 Hz), 1.86 (d, $^2J_{PH}$ = 13.5 Hz). IR spectrum (υ(SnF)/cm^{-1}): 576s, 559s, (υ(PO)/cm^{-1}): 1085 (br). ^{19}F{^{1}H} NMR (CH_2Cl_2/$CDCl_3$, 298 K): -147.2 (t), -149.2 (s), -158.0 (t). ^{31}P{^{1}H} NMR (CH_2Cl_2/$CDCl_3$, 298 K): 65.9 (s), 65.4 (s). ^{119}Sn NMR (CH_2Cl_2/$CDCl_3$, 243 K): -769.0 (t,t,t), -781.8 (q^5,t).

[SnF_4{$OAsMe_3$}$_2$]: Prepared similarly from [SnF_4{MeCN}$_2$] (0.32 g, 1.15 mmol) and Me_3AsO (0.34 g, 2.5 mmol). Yield 0.495 g, 92%. ^{1}H NMR (300 MHz, $CDCl_3$, 298 K): 2.04 (s, 2H), 2.05 (s, 1H). IR spectrum (υ(SnF)/cm^{-1}): 550(br), (υ(AsO)/cm^{-1}): 812(br), 865. ^{19}F{^{1}H} NMR (CH_2Cl_2/$CDCl_3$, 298 K): -140.9 (t), -141.6 (s), -148.2 (t). ^{119}Sn NMR (CH_2Cl_2/$CDCl_3$, 273 K): -747.7 (q^5), -748.4 (t,t). $C_{10}H_{24}F_4P_2Sn$ (400.95) calcd. C 29.9, H 6.0; found C 29.0, H 6.0.

[SnF_4{*o*-C_6H_4($P(O)Ph_2$)$_2$}]: [SnF_4{MeCN}$_2$] (0.138 g, 0.50 mmol) and *o*-$C_6H_4(P(O)Ph_2)_2$ (0.239 g, 0.50 mmol) were stirred together for 0.5 h in CH_2Cl_2 (20 mL). The white precipitate was filtered off and dried *in vacuo*. Yield 0.23 g, 68%. $C_{30}H_{24}F_4O_2P_2Sn{\cdot}0.5CH_2Cl_2$ (715.63) calcd. C 51.2, H 3.5; found C 51.2, H 3.3%. ^{1}H NMR (300 MHz, $CDCl_3$, 298 K): 7.31-7.71 (m). IR spectrum (υ(SnF)/cm^{-1}): 585, 569, 548, (υ(PO)/cm^{-1}): 1145, 1087(br). ^{19}F{^{1}H} NMR (CH_2Cl_2/$CDCl_3$, 303 K): -142.9 (br), -167.2 (t). ^{31}P{^{1}H} NMR (CH_2Cl_2/$CDCl_3$, 298 K): 45.5 (s). ^{119}Sn NMR (CH_2Cl_2/$CDCl_3$, 298 K): -790.0 (t,t,t).

[SnF_4{$Ph_2P(O)CH_2P(O)Ph_2$}]: Powdered $Ph_2P(O)CH_2P(O)Ph_2$ (0.22 g, 0.53 mmol) and [SnF_4{MeCN}$_2$] (0.133 g, 0.48 mmol) were dissolved in CH_2Cl_2 (10 mL) and stirred at room temperature overnight. The white precipitate was then filtered off and dried *in vacuo*. Yield 0.27 g, 92%. $C_{25}H_{22}F_4O_2P_2Sn{\cdot}0.5CH_2Cl_2$ (653.56) calcd. C 46.9, H 3.6; found C 46.5, H 3.7%. ^{1}H NMR (300 MHz, CD_2Cl_2, 298 K): 4.00 (t, 2H, CH_2, $^2J_{PH}$ = 13Hz), 7.36-7.75 (m, 20H, C_6H_5). IR spectrum (υ(SnF)/cm^{-1}): 596, 577, (υ(PO)/cm^{-1}): 1145 1092. ^{19}F{^{1}H} NMR (CH_2Cl_2/$CDCl_3$, 308 K): -143.0 (t), -168.0 (t). ^{31}P{^{1}H} NMR (CH_2Cl_2/$CDCl_3$, 298 K): 44.1 (s). ^{119}Sn NMR (CH_2Cl_2/$CDCl_3$, 298 K): -792.4 (t,t,t).

[SnF_4{*o*-C_6H_4($P(O)Me_2$)$_2$}]: [SnF_4{THF}$_2$] (0.30 g, 0.88 mmol) was dissolved in CH_2Cl_2 (5 mL), *o*-$C_6H_4(P(O)Me_2)_2$ (0.20 g, 0.87 mmol) dissolved in CH_2Cl_2 (5 mL) was added and the mixture stirred at room temperature for 2 h. The white solid was filtered off and dried *in vacuo*. Yield 0.257 g, 68%. ^{1}H NMR (300 MHz, d^6-dmso, 298 K): 1.79-1.84 (m, 12H, CH_3), 7.49-7.85 (m, 4H, C_6H_4). IR spectrum (υ(SnF)/cm^{-1}): 573(br), (υ(PO)/cm^{-1}): 1147 1093. ^{19}F{^{1}H} NMR (CH_2Cl_2/$CDCl_3$, 298 K): -143.5 (t), -165.4 (t). ^{31}P{^{1}H} NMR (CH_2Cl_2/$CDCl_3$, 273 K): 62.1 (s).

$[SnX_4\{L\}_2]$ (X = Cl, Br or I; L = Ph_3PO, Ph_3AsO or Me_3PO): These were made by reaction of the anhydrous tin(IV) halide with the ligand in anhydrous CH_2Cl_2 using literature methods.[3,16]

2.8 X-ray Experimental:

Crystals of $[SnF_4\{MeO(CH_2)_2OMe\}]$ and $[SnF_4\{1,10\text{-phenanthroline}\}]$ were grown from CH_2Cl_2 solutions layered with hexane. Colourless crystals of $[SnF_4\{OPMe_3\}_2]$ and $[SnF_4\{OPPh_3\}_2]$ were grown from samples containing both isomers by vapour phase diffusion of hexane into CH_2Cl_2 solution. Crystals of $[SnF_4\{OPPh_3\}_2]$ were also obtained over several days from a CH_2Cl_2 solution of the products of melting $[SnF_4\{MeCN\}_2]$ with excess PPh_3. Crystals of $[SnF_4\{o\text{-}C_6H_4(P(O)Ph_2)_2\}]\cdot CH_2Cl_2\cdot H_2O$ were obtained from CH_2Cl_2 solution layered with hexane.

The $[SnF_4\{1,10\text{-phenanthroline}\}]\cdot MeOH$ complex showed, after identifying the tin residue, two peaks in the difference electron-density map associated with a solvent molecule. The larger of the peaks positioned on a 2-fold axis (proposed as an O atom) with the second peak and its symmetry related peak being a disordered C atom of an adventitious MeOH solvate molecule. No attempt was made to position H atoms on this residue.

Brief details of the data collection and refinement are presented in Table 8. Several attempts were made to grow X-ray quality crystals of $[SnF_4\{OAsMe_3\}_2]$ by vapour diffusion from EtOH and Et_2O. The data from the crystals obtained did not lead to a structure possibly due to twinning.

2.9 Crystallography:

Table 13 Crystal data and structure refinement details.[a]

Compound	$[SnF_4\{MeO(CH_2)_2OMe\}]$	$[SnF_4\{1,10\text{-phenanthroline}\}]\cdot MeOH$	$[SnF_4\{OPMe_3\}_2]$	$[SnF_4\{OPPh_3\}_2]\cdot 2CH_2Cl_2$
Formula	$C_4H_{10}F_4O_2Sn$	$C_{13}H_{12}F_4N_2OSn$	$C_6H_{18}F_4O_2P_2Sn$	$C_{38}H_{34}Cl_4F_4O_2P_2Sn$
M	284.81	406.94	378.83	921.08
Crystal system	Monoclinic	Tetragonal	monoclinic	Monoclinic
Space group	$P2_1/n$ (no. 14)	$I4_1/a$ (no. 88)	$P21/n$ (no. 14)	$P2_1/n$ (no. 14)
a/Å	6.2957(15)	9.471(3)	6.190(2)	8.8697(16)
b/Å	20.987(6)	9.471(3)	11.089(4)	14.771(4)
c/Å	6.693(2)	29.964(8)	9.504(3)	14.446(4)
α/°	90	90	90	90
β/°	111.941(15)	90	94.32(3)	95.236(16)
γ/°	90	90	90	90
U/Å^3	820.2(4)	2687.8(15)	650.5(4)	1884.7(8)
Z	4	8	2	2
μ/mm^{-1}	3.137	1.948	2.24	1.101
F(000)	544	1584	372	924
Total no. of obsns (R_{int})	6388 (0.037)	9075 (0.097)	6333	21329 (0.138)
Unique obsns.	1867	1539	1486 (0.056)	4312
Min, max transmission	0.651, 1.000	0.569, 1.000	0.877, 0916	0.681, 1.000
No. of parameters, restraints	100,0	96, 1	71, 0	232, 0
Goodness-of-fit on F^2	1.14	1.04	1.048	0.98
Resid electron density /eÅ^{-3}	–0.76 to +0.48	–1.12 to +1.17	-1.05 to +0.94	–0.83 to +0.74
R1, wR2 ($I > 2\sigma(I)$)[b]	0.023, 0.054	0.072, 0.180	0.034, 0.073	0.058, 0.106
R1, wR2 (all data)	0.027, 0.056	0.128, 0.207	0.049, 0.079	0.135, 0.131

Compound	$[SnF_4\{o\text{-}C_6H_4(P(O)Ph_2)_2\}]\cdot CH_2Cl_2\cdot H_2O$	$[o\text{-}C_6H_4(P(O)Ph_2)_2]\cdot CH_2Cl_2$
Formula	$C_{31}H_{28}Cl_2F_4O_3P_2Sn$	$C_{31}H_{26}Cl_2O_2P_2$
M	776.06	563.36
Crystal system	monoclinic	monoclinic
Space group	*P*21/c (no. 14)	*P*21/c (no. 14)
a/Å	17.579(3)	10.840(2)
b/Å	10.1696(15)	14.734(3)
c/Å	18.178(4)	17.576(2)
α/°	90	90
β/°	99.160(8)	104.467(12)
γ/°	90	90
U/Å^3	3208.2(10)	2718.3(8)
Z	4	4
μ/mm^{-1}	1.12	0.38
F(000)	1552.0	1168.0
Total no. of obsns (R_{int})	35141	28169
Unique obsns.	7058 (0.055)	4775 (0.101)
Min, max transmission	0.763, 1.000	0.934, 0.963
No. of parameters, restraints	395, 5	335, 0
Goodness-of-fit on F^2	1.138	1.032
Resid electron density /eÅ^{-3}	-1.187 to +2.380	-0.343 to +0.269
R1, wR2 ($I > 2\sigma(I)$)[b]	0.070, 0.183	0.046, 0.095
R1, wR2 (all data)	0.082, 0.188	0.088, 0.112

[a] Common items: temperature = 120 K; wavelength (Mo-Kα) = 0.71073 Å; θ(max) = 27.5°.

[b] $R1 = \Sigma||F_o| - |F_c||/\Sigma|F_o|$. $wR2 = [\Sigma w(F_o^2 - F_c^2)^2/\Sigma wF_o^4]^{1/2}$.

2.10 References:

[1] P. G. Harrison (Ed), *The Chemistry of Tin*, Blackie, London, **1989**.
[2] P. G. Harrison in *Comp. Coord. Chem.*, G. Wilkinson, R. D. Gillard, J. A. McCleverty (Eds), Pergamon Press, Oxford, **1987**, vol. 3. Chap. 26.
[3] P.G. Harrison, B.C. Lane, J.J. Zuckerman, *Inorg. Chem.*, **1972**, 11, 1537-1543.
[4] E. W. Abel, S. K. Bhargava, K. G. Kite, V. Sik, *Inorg. Chim. Acta*, **1981**, 49, 25–30.
[5] S. J. Ruzicka, C. M. P. Favez, A. E. Merbach, *Inorg. Chim. Acta*, **1977**, 23, 239–247.
[6] S. J. Ruzicka, A. E. Merbach, *Inorg. Chim. Acta*, **1976**, 20, 221-229.
[7] S. E. Dann, A. R. J. Genge, W. Levason, G. Reid, *J. Chem. Soc., Dalton Trans.*, **1996**, 4471–4478.
[8] S. E. Dann, A. R. J. Genge, W. Levason, G. Reid. *J. Chem. Soc., Dalton Trans.*, **1997**, 2207–2213.
[9] A. R. J. Genge, W. Levason, G. Reid. *J. Chem. Soc., Dalton Trans.*, **1997**, 4549–4554.
[10] A. R. J. Genge, W. Levason, G. Reid., *Inorg. Chim. Acta*, **1999**, 288, 142–149.
[11] W. Levason, M. L. Matthews, R. Patel, G. Reid, M. Webster. *New. J. Chem.*, **2003**, 27, 1784–1788.
[12] A. A. Woolf, *J. Inorg. Nucl. Chem.*, **1956**, 3, 285–288.
[13] J. P. Clark, V. M. Langford, C. J. Wilkins, *J. Chem. Soc. (A)*, **1967**, 792–794.
[14] C. E. Michelson, D. S. Dyer, R. O. Ragsdale, *J. Inorg. Nucl. Chem.*, **1970**, 32, 833–838.
[15] C. J. Wilkins, H. M. Haendler, *J. Chem. Soc.*, **1965**, 3174–3178.
[16] S. H. Hunter, V. M. Langford, G. A. Rodley, C. J. Wilkins, *J. Chem. Soc. (A)*, **1968**, 305–308.
[17] A. D. Adley, P. H. Bird, A. R. Fraser, M. Onyszchuk, *Inorg. Chem.*, **1972**, 11, 1402–1409.
[18] M. Bork, R. Hoppe, *Z. Anorg. Allg. Chem.*, **1996**, 622, 1557–1563.
[19] D. Tudela, F. Rey, *Z. Anorg. Allg. Chem.*, **1989**, 575, 202-208.
[20] D. Tudela, J.A. Patron, *Inorg. Synth.*, **1997**, 31, 92-93.
[21] P. A. W. Dean, D. F. Evans, *J. Chem. Soc. (A)*, **1968**, 1154–1166.
[22] S. J. Ruzicka, A. E. Merbach, *Inorg. Chim. Acta*, **1977**, 22, 191-200.
[23] F. Cheng, M. F. Davis, A. L. Hector, W. Levason, G. Reid, M. Webster, W. Zhang, *Eur. J. Inorg. Chem.*, **2007**, 17, 2488-2495.
[24] F. Cheng, M. F. Davis, A. L. Hector, W. Levason, G. Reid, M. Webster, W. Zhang, *Eur. J. Inorg. Chem.*, **2007**, 31, 4897-4905.
[25] H. M. Haendler, S. F. Bartram, W. J. Bernard, D. Kippax, *J. Am. Chem. Soc.*, **1954**, 76, 2179-2180.
[26] G. R. Willey, T. J. Woodman, R. J. Deeth, W. Errington, *Main Group Met. Chemistry*, **1998**, 21, 583–591.
[27] V. J. Hall, E. R. T. Tiekink, *Z. Krystallogr.*, **1996**, 211, 247–250.
[28] V. N. Zakharov, A. V. Yatsenko, A. L. Kamyshnyi, L. A. Aslanov, *Koord. Khim.*, **1991**, 17, 789–794; (*Chem. Abstr.* **1991**, 115, 291749v).
[29] K. A. Paseshnichenko, L. A. Aslanov, A. V. Yatsenko, S. V. Medvedev, *Koord. Khim.* **1984**, 10, 1279–1284; (*Chem. Abstr.* **1984**, 101, 220263g).
[30] D. Tudela, J. D. Tornero, A. Monge, A. J. Sánchez-Herencia, *Inorg. Chem.*, **1993**, 32, 3928-3930.
[31] L. M. Engelhardt, C. L. Raston, C. R. Whitaker, A. H. White, *Aust. J. Chem.*, **1986**, 39, 2151-2154.
[32] G. Bandoli, G. Bortolozzo, D. A. Clemente, U. Croatto, C. Panattoni, *J. Chem. Soc. A.*, **1970**, 2778-2780.
[33] M. F. Davis, W. Levason, G. Reid, M. Webster, *Polyhedron*, **2006**, 25, 930–936.
[34] N. J. Hill, W. Levason, M. C. Popham, G. Reid, M. Webster. *Polyhedron*, **2002**, 21, 445-455.
[35] L. Deakin, W. Levason, M. C. Popham, G. Reid, M. Webster, *J. Chem. Soc., Dalton Trans.*, **2000**, 2439-2447.
[36] A. I. Tursina, L. A. Aslanov, S. V. Medvedev, A. V. Yatsenko, *Koord. Khim.*, **1985**, 11, 417-424.
[37] T. Szymanska-Buzar, T. Glowiak, I. Czelusniak, *Main Group Met. Chem.*, **2001**, 24, 821-822.
[38] A. I. Tursina, A. V. Yatsenko, S. V. Medvedev, V. V. Chernyshev, L. A. Aslanov, *Zh. Strukt. Khim.*, **1986**, 27, 157-159.
[39] A. I. Tursina, L. A. Aslanov, V. V. Chernyshev, S. V. Medvedev, A. V. Yatsenko, *Koord. Khim.*, **1986**, 12, 420-424.
[40] J. Mason, *Multinuclear NMR*, Plenum, New York, **1987**.
[41] K. B. Dillon, A. Marshall, *J. Chem. Soc., Dalton Trans.*, **1984**, 1245-1247.
[42] R. Colton, D. Dakternieks, *Inorg. Chim. Acta*, **1983**, 71, 101-107.

[43] M. F. Davis, M. Clarke, W. Levason, G. Reid, M. Webster, *Eur. J. Inorg. Chem.*, **2006**, 2773–2782.
[44] W. Levason, R. Patel, G. Reid, *J. Organomet. Chem.*, **2003**, 688, 280-282.
[45] A. Merijanian, R.A. Zingaro, *Inorg. Chem.*, **1966**, 5, 187-191.

Chapter 3

SnF_4 Complexes with Soft Group 15 Donor Ligands

3.1 Introduction:

As stated in Chapter 2 there have been very few compounds of SnF_4 reported, and all of those were with hard N or O donor ligands. As such, little introduction to this chapter can be given regarding SnF_4 that is not a repeat of Chapter 2. However, examples of SnX_4 (X = Cl, Br or I) with softer P, As, S, Se or Te donors have been characterised.[1,2,3,4,5,6,7] Many older references which contain only IR, Raman or Mössbauer studies going back as far as 1949 are also available which are referred to in the reviews of 1976 and 1995.[8,9]

Within these publications are a number of structurally characterised compounds such as $[SnCl_4\{PEt_3\}_2]$[10] (see Figure 1) and $[SnI_4\{PPr^n_3\}_2]$[11] being the first two monodentate phosphane complexes and $[SnCl_4\{Ph_2P(CH_2)_2PPh_2\}]$.[12]

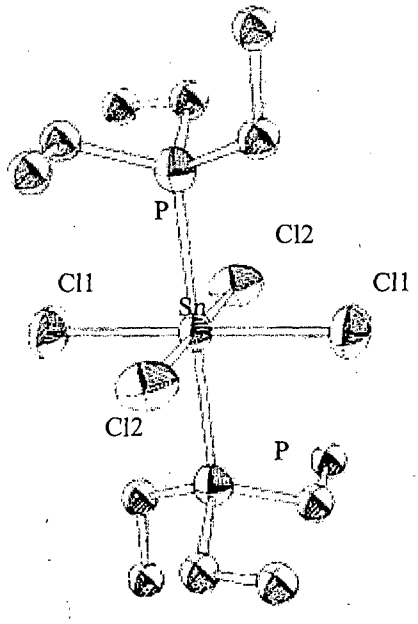

Figure 1 View of the structure of $[SnCl_4\{PEt_3\}_2]$.[10] Thermal ellipsoids are scaled to enclose 50% probability. The non labelled atoms are carbon and are shown as spheres of arbitrary radii.

The most complete compilation of P and As containing ligands complexed with SnX_4 (see Table 1 for selected NMR data) has been from our own group, and also includes the first structurally characterised SnX_4 arsane, $[SnI_4\{o\text{-}C_6H_4(AsMe_2)_2\}]$[6] (see Figure 2). Since then *trans*-$[SnCl_4\{AsPh_3\}_2]$ has also been characterised.[13]

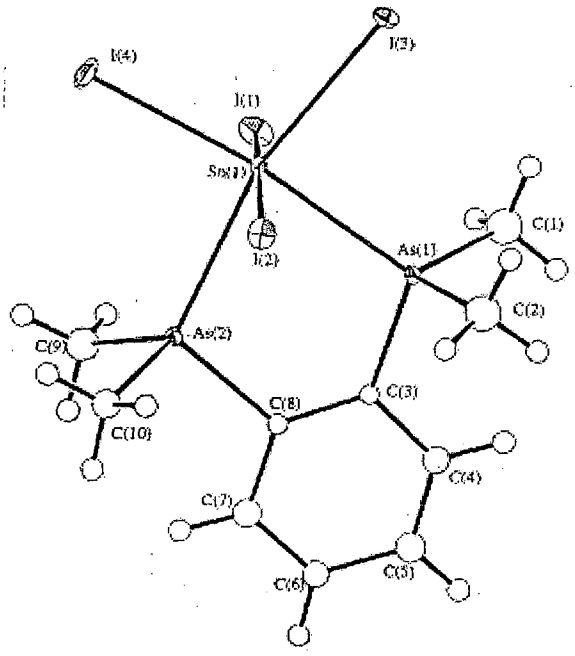

Figure 2 View of the structure of $[SnI_4\{o\text{-}C_6H_4(AsMe_2)_2\}]$ with numbering scheme adopted. Ellipsoids are drawn at 40% probability.[6]

Producing these compounds generally consists of direct reaction of the metal halide with a mono or bidentate ligand in an appropriate ratio in anhydrous solvents.

These complexes are all six coordinate, with octahedral, or distorted octahedral geometry. Distortion occurs mainly with bidentate ligands, caused by the chelating ligand. The monodentate ligand complexes are almost exclusively *trans*, the one exception to this being $[SnCl_4\{PMe_3\}_2]$[6] where both *cis* and *trans* forms were seen in $MeNO_2$. In CH_2Cl_2 however only the *trans* isomer is observed. The bidentate ligand complexes are exclusively *cis* as expected however *trans* X-Sn-X halide bonds in crystal structures always bend towards the ligand.[6,12] Reactions with potentially bidentate ligands that have a shorter backbone (i.e. $Ph_2PCH_2PPh_2$) still form six coordinate octahedral complexes but act as monodentate ligands in a 2:1 ratio (ligand:metal) and also coordinate *trans* to each other.[14]

Table 1 Selected NMR data on phosphane and arsane comparator complexes.[6]

Compound	δ $^{31}P\{^1H\}^d$	δ $^{119}Sn^e$	$^1J(^{31}P\text{-}^{119}Sn)/Hz^f$	Solvent
$[SnCl_4\{PMe_3\}_2]$	6.8 (*trans*)	n.o.	2720	CH_2Cl_2
$[SnCl_4\{PMe_3\}_2]$	3.6 (*cis*)	-630 (t)[a]	2190	$MeNO_2$
	8.0 (*trans*)	-646 (t)[a]	2768	$MeNO_2$
$[SnBr_4\{PMe_3\}_2]$	-3.0 (*trans*)	n.o.	n.o.	$MeNO_2$
$[SnI_4\{PMe_3\}_2]$	-3.7 (*trans*)	n.o.	n.o.	$MeNO_2$
$[SnCl_4\{o\text{-}C_6H_4(PPh_2)_2\}]$[a]	-13.9	-607.5 (t)	890	CH_2Cl_2
$[SnBr_4\{o\text{-}C_6H_4(PPh_2)_2\}]$[b]	-24.2	-1218 (t)	305	CH_2Cl_2
$[SnI_4\{o\text{-}C_6H_4(PPh_2)_2\}]$	-52.5	n.o.	n.o.	CH_2Cl_2
$[SnCl_4\{Ph_2P(CH_2)_2PPh_2\}]$	-18.8	-626 (t)	890	CH_2Cl_2
$[SnBr_4\{Ph_2P(CH_2)_2PPh_2\}]$[a]	-31.0	-1212 (t)	460	CH_2Cl_2
$[SnI_4\{Ph_2P(CH_2)_2PPh_2\}]$[b]	n.o.	n.o.		CH_2Cl_2
$[SnCl_4\{o\text{-}C_6H_4(AsMe_2)_2\}]$	-	-675		CH_2Cl_2
$[SnBr_4\{o\text{-}C_6H_4(AsMe_2)_2\}]$[c]	-	-1354		CH_2Cl_2
$[SnI_4\{o\text{-}C_6H_4(AsMe_2)_2\}]$[b,g]	-	-2290		CH_2Cl_2

Temperatures run at 300 K unless stated otherwise. a Temp = 250 K, b Temp = 190 K, c Temp = 270 K, d Relative to external 85% H_3PO_4, e Relative to neat external $SnMe_4$, f ± 6 Hz, g Resonances only observed in the presence of excess of the group 15 ligand. n.o. = not observed.

This Chapter attempts to correct the complete void of SnF_4 coordinating to soft donors, by attempting to do just that with the soft group 15 donor ligands, tertiary phosphanes and tertiary arsanes.

3.2 SnF_4 Complexes of Phosphanes:

The reaction of $[SnF_4\{MeCN\}_2]$ (1 mmol) (see Chapter 2) with two mol. equivalents of the monodentate ligands L (L= PMe_3 or PCy_3) yielded $[SnF_4\{L\}_2]$ in moderate to good yields. The general experimental method for these compounds as well as the bidentate ligand complexes discussed later, was to partially dissolve $[SnF_4\{MeCN\}_2]$ (1 mmol) in CH_2Cl_2 (10 mL) under inert atmosphere (N_2) and dry conditions, L/L-L (2/1 mmol) was then added and the reaction stirred for 2 h. The reaction mixture was then filtered to leave the complex as a white solid.

No evidence for fluoride (F^-) attacking the glass has been seen in either the spectroscopy or on the glass itself for any of these complexes. These complexes are both moisture and dioxygen sensitive in solution, although the dry solids only slowly decompose in air. The complexes are also much less soluble in chlorocarbons in comparison with those of the heavier tin halides and care is needed to obtain pure samples in general because neither the starting synthon nor the complexes are easily soluble and are both white solids. Reactions using $[SnF_4\{THF\}_2]$ as a starting synthon gave no advantage with solubility or ease of displacement. Reactions with L= PPh_3 did not yield a pure sample of the complex using the above route and using molten PPh_3 (90→120 °C) as a starting material showed no advantage as a complex mixture of products was observed by NMR spectroscopy. In this case some fluorination of the phosphane occurred as indicated by the triplet in the $^{31}P\{^1H\}$ NMR of Ph_3PF_2 at -54.2 ppm, $^1J_{PF}$ = 660 Hz.[15] Some crystals were also isolated from this reaction which proved to be the phosphane oxide $[SnF_4\{OPPh_3\}_2]$ (discussed in Chapter 2).

The $[SnF_4\{L\}_2]$ complexes were exclusively *trans* isomers and were identified from their $^{19}F\{^1H\}$ and $^{31}P\{^1H\}$ NMR spectra which are triplets (see Figure 3) and quintets respectively (see Figure 4) [in each case with weak satellites due to ^{119}Sn and ^{117}Sn (^{117}Sn: I = ½, 7.7%, Ξ =35.63 MHz; ^{119}Sn: I = ½, 8.6%, Ξ =37.27 MHz)] (Table 4).

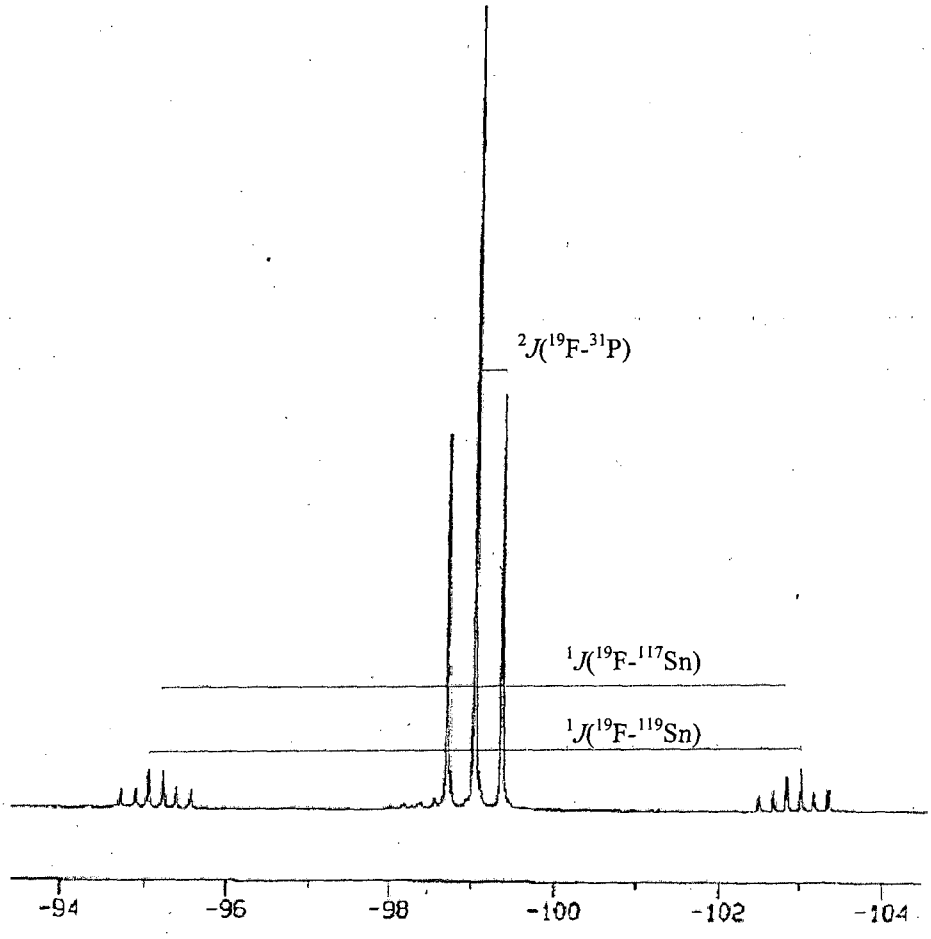

Figure 3 $^{19}F\{^1H\}$ NMR spectrum of $[SnF_4\{PCy_3\}_2]$ (298 K, CH_2Cl_2).

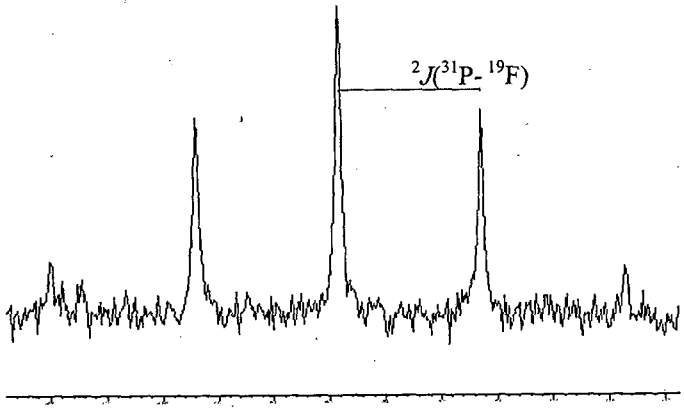

Figure 4 $^{31}P\{^1H\}$ NMR spectrum of $[SnF_4\{PMe_3\}_2]$ (298 K, CH_2Cl_2).

The IR spectrum of $[SnF_4\{PMe_3\}_2]$ showed a broad single ν(SnF) as expected with the *trans* isomer (Eu band). $[SnF_4\{PCy_3\}_2]$ shows two bands of equal intensity, this could be from the ligand itself as the free ligand has some minor peaks at around 545 cm^{-1} but is probably a solid state effect. The IR spectra along with the ^1H NMR spectra (see Table 3) are otherwise unremarkable.

It proved to be difficult to resolve the full 15 line pattern (triplet of quintets) anticipated in the ^{119}Sn NMR spectra. This is probably due to the modest receptivity of the tin (D_c = 25), poor solubilities and also the complexity of the coupling patterns. Below is the tin NMR spectrum for $[SnF_4\{PMe_3\}_2]$ (Figure 5) and appears to show only a 5 line pattern. However the coupling constants obtained from the $^{31}P\{^1H\}$ and $^{19}F\{^1H\}$ NMR spectra (2975 & 2745 Hz respectively) are quite similar and do agree with those obtained from the tin NMR spectrum. When the central peak is taken (-628 ppm) and the predicted coupling pattern is worked out (see Figure 6) the similarity becomes much more obvious.

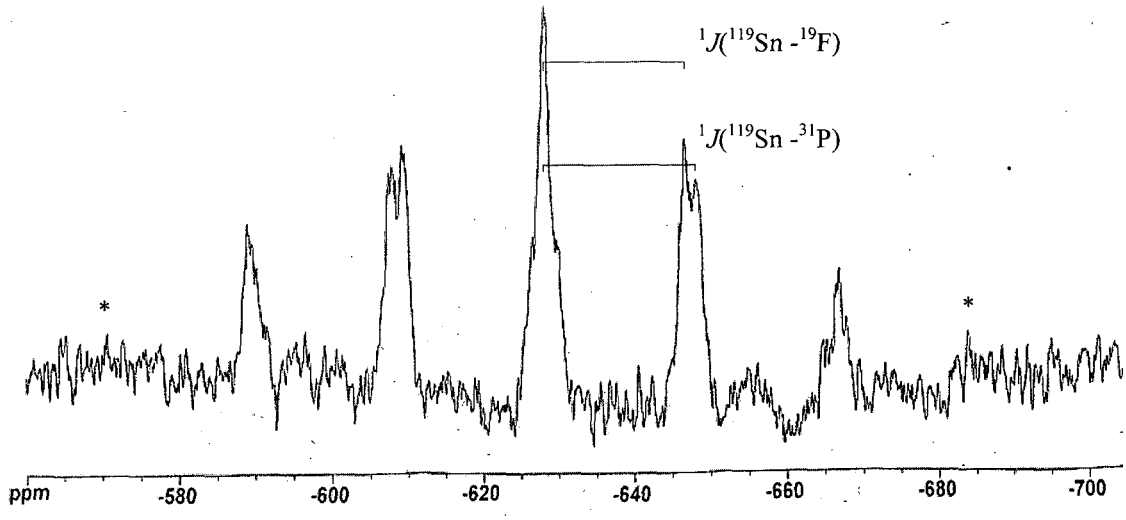

Figure 5 ^{119}Sn NMR spectrum of $[SnF_4\{PMe_3\}_2]$ (250 K, CH_2Cl_2), * mark the outer lines.

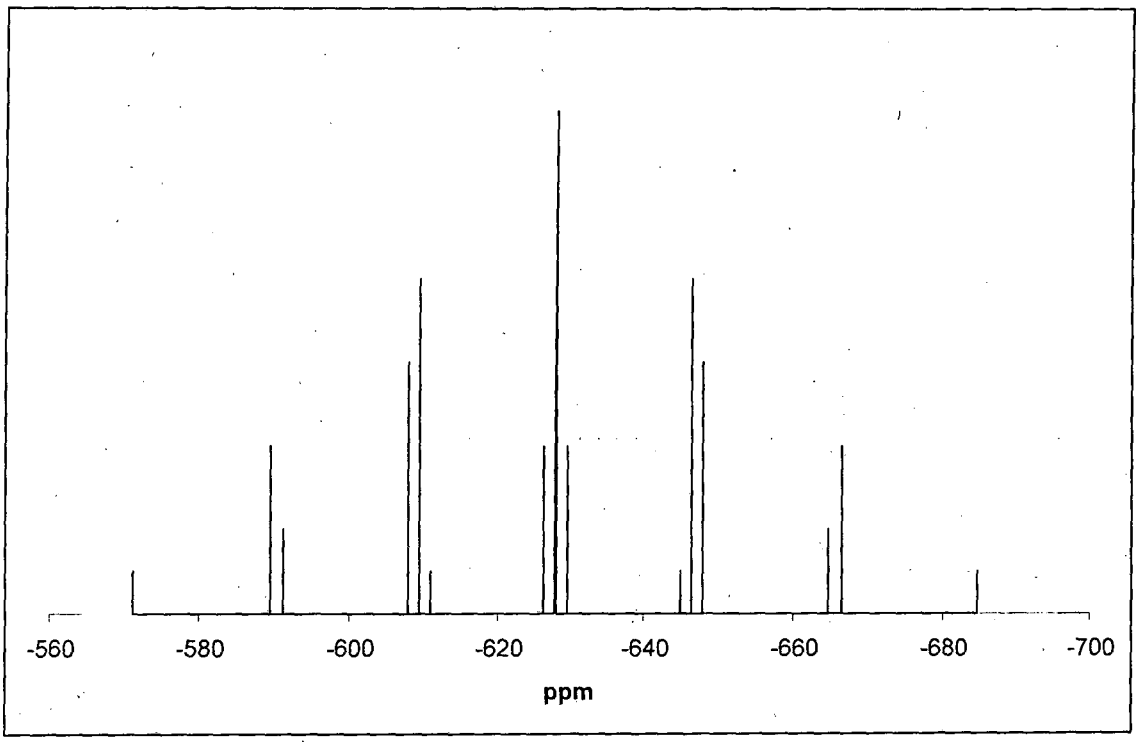

Figure 6 Predicted ^{119}Sn NMR spectrum of $[SnF_4\{PMe_3\}_2]$.

These compounds were made on more than one occasion to get clean products and to check the reproducibility of the spectra. Although on some occasions impurities were observed in both the $^{19}F\{^1H\}$ and $^{31}P\{^1H\}$ NMR spectrum no conclusive evidence could be obtained for the presence of the *cis* isomer. Expected line patterns for the *cis* isomer in the $^{19}F\{^1H\}$ NMR spectra should have shown two separate environments, one a doublet of doublet of triplets and the other a triplet of triplets. The $^{31}P\{^1H\}$ NMR spectra should also have shown a doublet of doublet of triplets.

The structure of $[SnF_4\{PCy_3\}_2]$ was determined crystallographically and shows (Figure 7, Table 2) a centrosymmetric molecule with Sn–P = 2.654(1) Å and Sn–F = 1.959(2), 1.980(2) Å. The Sn–P is longer than that in *trans*-$[SnCl_4\{PEt_3\}_2]$ (2.615(5) Å),[10] and marginally longer than in *trans*-$[SnCl_4\{\kappa^1\text{-}Ph_2PCH_2PPh_2\}_2]$ (2.649(1) Å),[14] but shorter than found in *trans*-$[SnI_4\{P^iPr_3\}_2]$ (2.69(1) Å),[11] although the differing steric requirements (specifically the large cone angle ca. 170° of PCy_3) of the three phosphanes preclude a more detailed discussion.

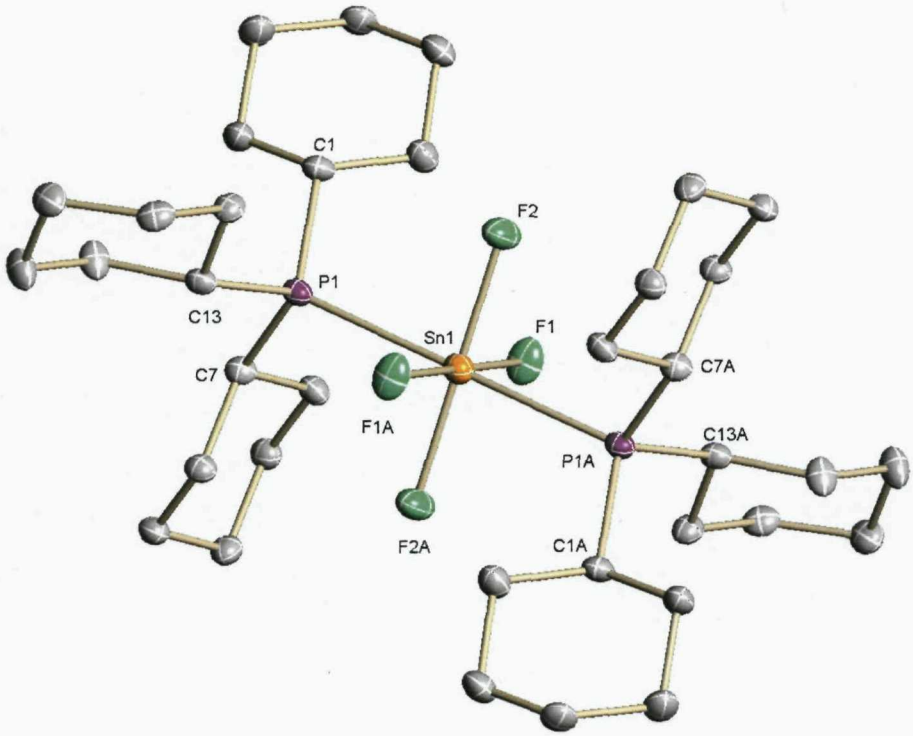

Figure 7 Structure of *trans*-$[SnF_4\{PCy_3\}_2]$ showing a partial atom numbering scheme. Cyclohexyl groups are numbered cyclically starting at the P-bonded C atom. Ellipsoids are drawn at the 50% probability level and H atoms omitted for clarity. Sn1 is positioned on a centre of symmetry. Symmetry operation: a = – x, – y, 2 – z.

Table 2 Selected bond lengths (Å) and angles (°) for *trans*-$[SnF_4\{PCy_3\}_2]$.

Sn1–F1	1.959(2)	Sn1–F2	1.980(2)
Sn1–P1	2.6538(11)	P1–C1	1.860(4)
P1–C7	1.845(4)	P1–C13	1.851(4)
F1–Sn1–F2	91.21(10)	F1–Sn1–F2a	88.79(10)
F1–Sn1–P1	89.86(7)	F2–Sn1–P1	88.24(7)
C1–P1–C7	108.09(17)	C7–P1–C13	104.81(16)
C1–P1–C13	107.96(17)	Sn1–P1–C1	112.95(12)
Sn1–P1–C7	113.77(12)	Sn1–P1–C13	108.81(12)
F1–Sn1–P1–C1	–60.0(2)	F1–Sn1–P1–C7	63.7(2)
F1–Sn1–P1–C13	–179.9(2)		

Symmetry operation: a = – x, – y, 2 – z.

The reaction of 1 mmol of $[SnF_4\{MeCN\}_2]$ with 1 mol. equivalent of the bidentate ligands L-L (L-L= $Et_2P(CH_2)_2PEt_2$, $Cy_2P(CH_2)_2PCy_2$, *o*-$C_6H_4(PPh_2)_2$, $Ph_2P(CH_2)_2PPh_2$ and *o*-$C_6H_4(PMe_2)_2$) in anhydrous CH_2Cl_2 resulted in the

formation of white six coordinate [SnF_4{L-L}] complexes in moderate to good yields. The solids are moisture sensitive, tenaciously retain organic solvents - clearly evident in the ^1H NMR spectra, and are only modestly soluble in chlorocarbons. The tendency of SnX_4 (X = Cl, Br or I) complexes with phosphanes/diphosphanes to air oxidise in chlorocarbon solutions to the phosphane oxide has also been reported and so cannot be discounted for SnF_4.[6,16] Solubility is not significantly better in acetone or nitromethane and stronger donor solvents were generally avoided for spectroscopic studies since they can lead to some displacement of the neutral ligands. No previous SnF_4 complex of a phosphane ligands has been reported so comparisons can only be made between them and with the other tin(IV) halides (see below). The IR and ^1H NMR spectra (Table 3) are as expected other than the triplets in [SnF_4{*o*-$C_6H_4(PMe_2)_2$}] for the methyl groups which are seen as a result of second order spectra, the protons are coupling to both phosphorus environments equally to give $^2J + {}^5J_{P\text{-}H} = 4$ Hz.

Table 3 IR[a] and ^1H NMR[b] spectroscopic data for SnF_4 phosphane complexes.

Compound	ν(Sn-X)/cm^{-1}	δ(^1H)
[SnF_4{PMe_3}$_2$]	546(br)	1.68 (m)
[SnF_4{PCy_3}$_2$]	557(s), 535(s)	1.29-2.34 (m)
[SnF_4{*o*-$C_6H_4(PMe_2)_2$}]	564, 534	1.87 (t) 7.75-7.81 (m)
[SnF_4{*o*-$C_6H_4(PPh_2)_2$}]	574, 557, 526	7.30-7.68 (m)
[SnF_4{$Et_2P(CH_2)_2PEt_2$}]	553(m), 526(s)	1.26-1.37 (m) 2.07-2.13 (m)
[SnF_4{$Cy_2P(CH_2)_2PCy_2$}]	560(s), 530(s)	1.26-2.21 (m)
[SnF_4{$Ph_2P(CH_2)_2PPh_2$}]	566(br)	2.09 (t) 7.26-7.95 (m)

a Nujol mull. b In $CDCl_3$ at 300 MHz.

Selected multinuclear NMR spectroscopic data for SnF_4 phosphane complexes, along with the associated coupling constants, are given in Table 4. The $^{19}F\{^1H\}$ spectra show both a 9 line pattern (triplet of triplets) for the $F_{trans\text{-}F}$ (see Figure 8) and a 12 line pattern (doublet of doublet of triplets) for the $F_{trans\text{-}P}$ (see Figure 9), (Table 4), with δ(^{19}F) in the range -110 to -165, and with $^1J(^{119}Sn\text{-}^{19}F)$ 2150–2750

Hz. Figure 10 shows the predicted $^{19}F\{^{1}H\}$ spectra of $F_{trans\text{-}P}$, illustrating why the central lines have a greater intensity due to overlap. In these cases the $^{1}J(^{117}Sn\text{-}^{19}F)$ satellites were also clearly resolved and although not quoted in Table 4, the magnitudes were consistent with expectation based upon $\gamma^{119}Sn/\gamma^{117}Sn$.

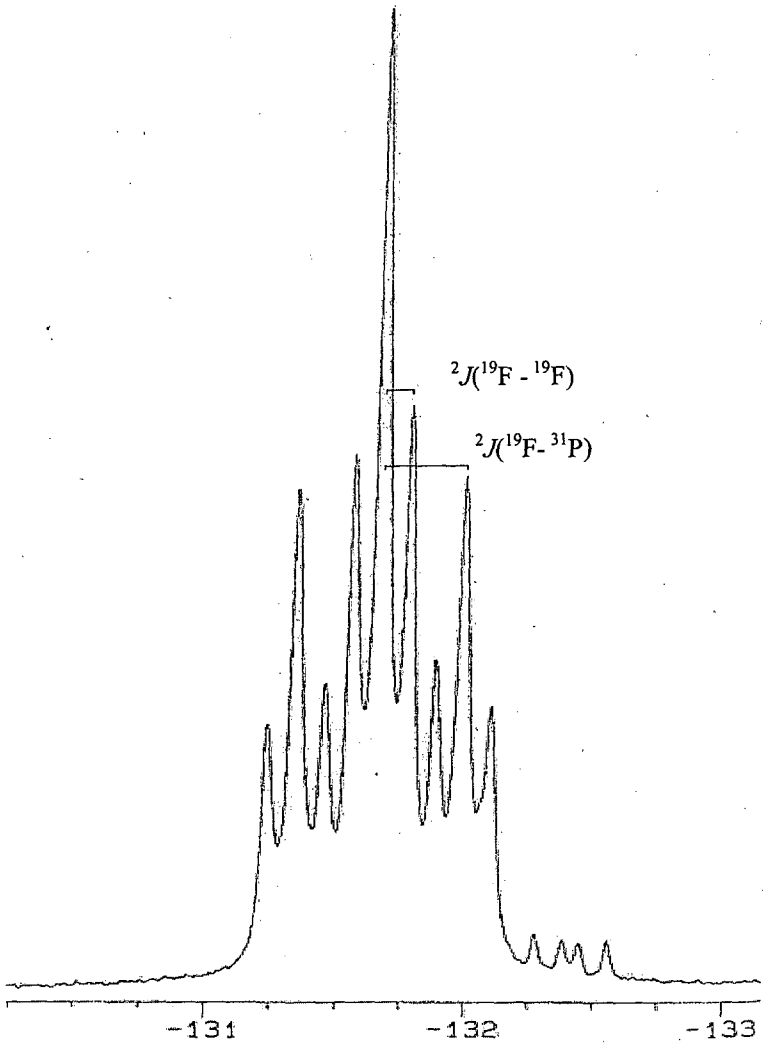

Figure 8 $^{19}F\{^{1}H\}$ NMR spectrum of the *trans* F-Sn-F environment in *cis*-$[SnF_4\{o\text{-}C_6H_4(PMe_2)_2\}]$ (243 K, CH_2Cl_2).

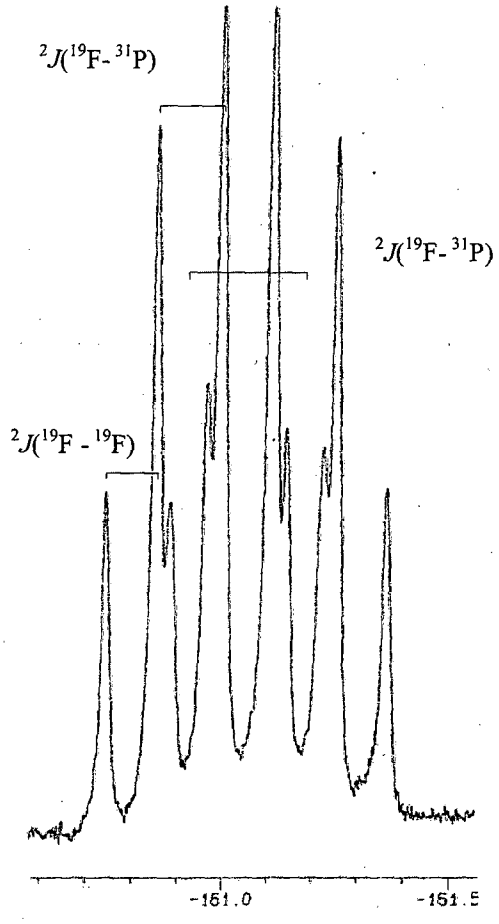

Figure 9 $^{19}F\{^1H\}$ NMR spectrum of the *trans* F-Sn-P environment in $[SnF_4\{o\text{-}C_6H_4(PMe_2)_2\}]$, (243 K, CH_2Cl_2).

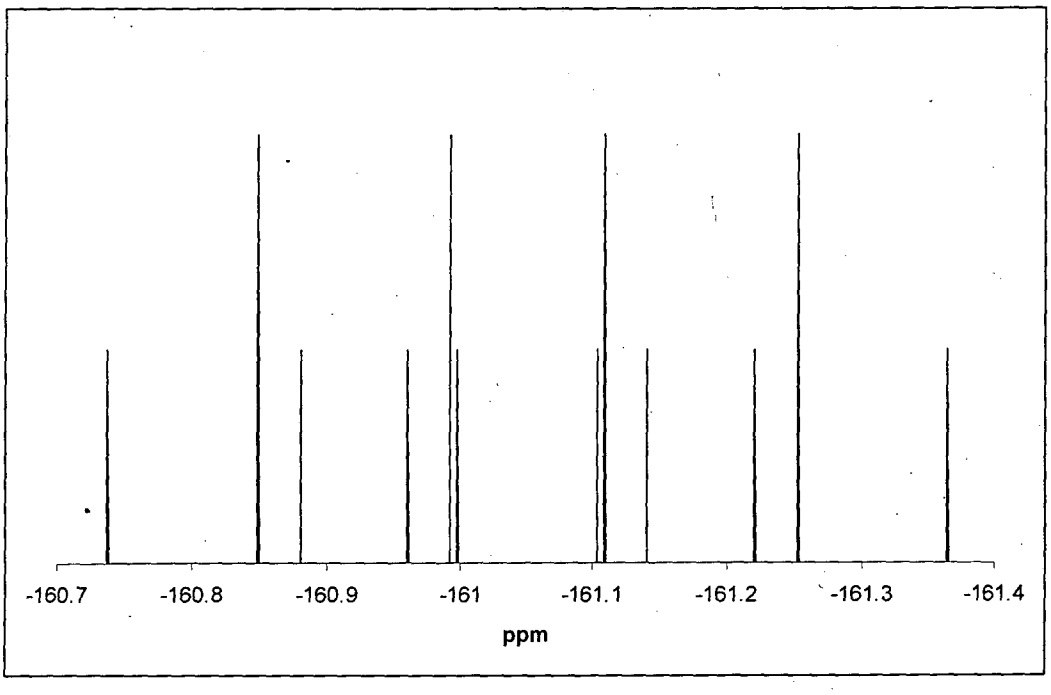

Figure 10 Predicted $^{19}F\{^1H\}$ NMR spectrum of the *trans* F-Sn-P environment in $[SnF_4\{o\text{-}C_6H_4(PMe_2)_2\}]$.

Unlike the phosphane oxides (discussed in Chapter 2) the $^{31}P\{^{1}H\}$ NMR spectra show coupling to fluorine as a doublet of doublets of triplets (see Figure 11). The resonances appear as relatively sharp spectra all with similar chemical shifts and the coupling patterns were readily recognised as first order patterns. Weak $^{119/117}Sn$ satellites can also be seen on either side but due to instrument time constraints and poor solubility the fine structure was not always resolved.

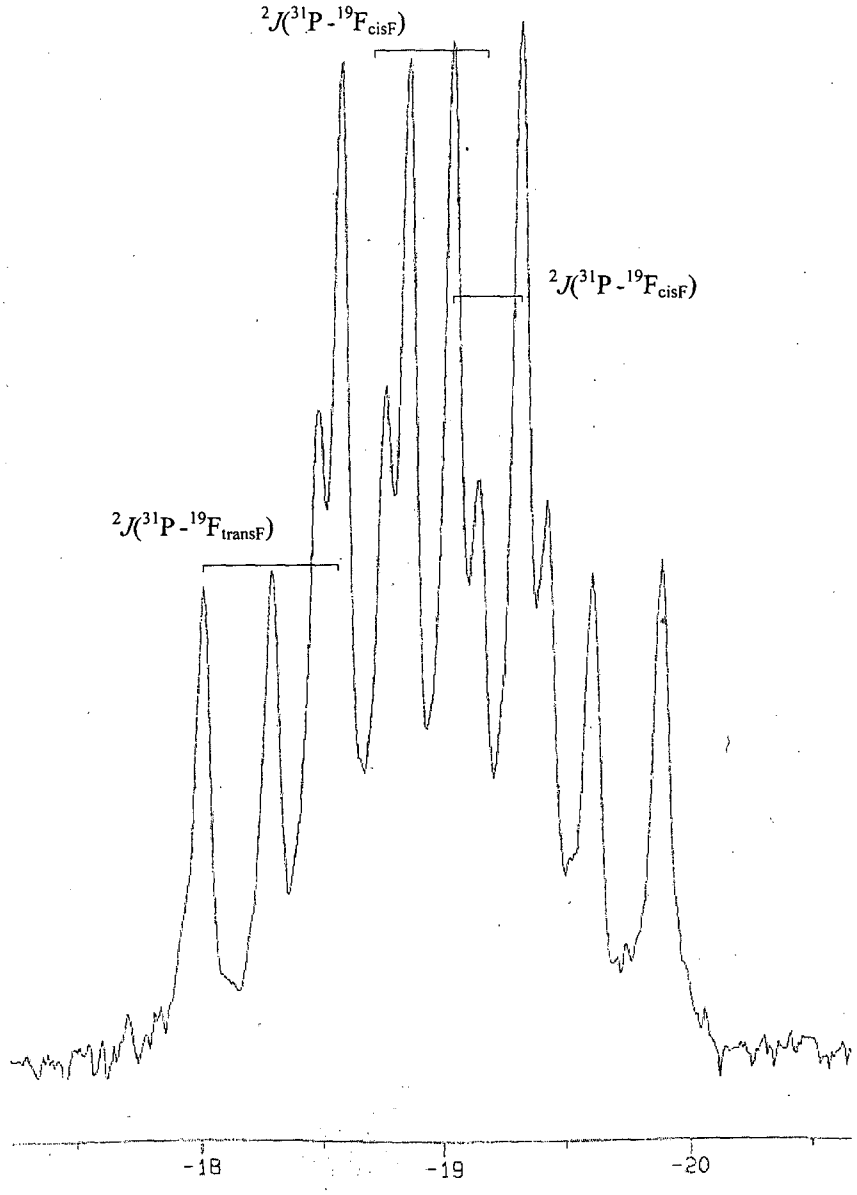

Figure 11 $^{31}P\{^{1}H\}$ NMR spectrum of $[SnF_4\{o\text{-}C_6H_4(PPh_2)_2\}]$ (193 K, CH_2Cl_2).

Although resonances were observed at ambient temperatures in the ^{1}H, $^{31}P\{^{1}H\}$ and $^{19}F\{^{1}H\}$ spectra, the ^{119}Sn spectra showed broad and poorly resolved features and the samples were cooled to temperatures of between 183 and 273 K. Good resolution was obtained typically at 250 K as a balance between maintaining solubility and reducing line broadening (due to the onset of reversible ligand dissociation) was reached. Again obtaining good quality ^{119}Sn NMR spectra proved difficult due to the modest receptivity of the tin ($D_c = 25$), poor solubilities and also the complexity of the coupling patterns. Based upon the various coupling constants obtained from the $^{19}F\{^{1}H\}$ and $^{31}P\{^{1}H\}$ spectra the major lines of the expected 27 line multiplet (t,t,t) were identified (see Figure 12).

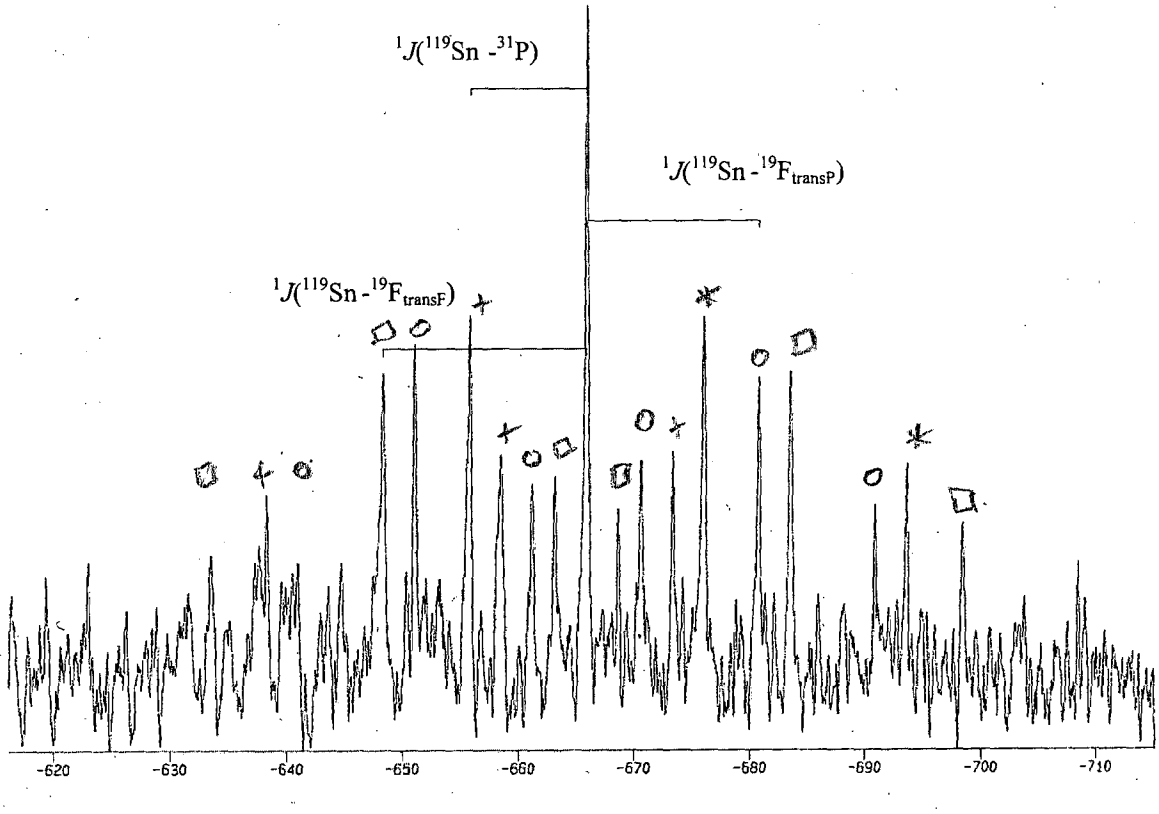

Figure 12 ^{119}Sn NMR spectrum of $[SnF_4\{o\text{-}C_6H_4(PPh_2)_2\}]$ (223 K, CH_2Cl_2).

Complexation of $[SnF_4\{MeCN\}_2]$ with $Me_2P(CH_2)_2PMe_2$ gave a white solid $[SnF_4\{Me_2P(CH_2)_2PMe_2\}]$. The complex proved to be essentially insoluble in chlorocarbons or nitromethane and was decomposed by DMSO. The IR spectra exhibited a ν(Sn-X) = 533 (br)/cm^{-1}. A $^{19}F\{^{1}H\}$ NMR spectrum obtained from a very long accumulation (ns ca. 45,000) at 273 K in CD_2Cl_2 gave two plausible

resonances at -153.7 and -132.2 ppm but other solution NMR data was not obtained. Although this is an exceptional case it highlights the difficulties involved in obtaining good quality spectra of minimally soluble complexes.

Table 4 Selected NMR data for SnF_4 phosphane complexes.[a]

Compound	δ $^{31}P\{^1H\}$[b]	ΔP[c]	δ ^{119}Sn[d]	δ $^{19}F\{^1H\}$	$^1J(^{19}F\text{-}^{119}Sn)$	$^2J(^{31}P\text{-}^{19}F)$	$^2J(^{19}F\text{-}^{19}F)$	$^1J(^{31}P\text{-}^{119}Sn)$
$[SnF_4\{PMe_3\}_2]$ *trans*	-19.1(q^5)	43	-628.0(t,q^5)	-132.8(t)	2745	155	-	2975
$[SnF_4\{PCy_3\}_2]$ *trans*	+22.2(q^5)	11	-628.5(t,q^5)	-98.9(t)	2993	124	-	2530
$[SnF_4\{o\text{-}C_6H_4(PMe_2)_2\}]$	-37.8(t,d,d)	17	-657.6(t,t,t)	-131.7(t,t)	2470	117,98,54	42	1520
				-161.1(d,d,t)	2160			
$[SnF_4\{o\text{-}C_6H_4(PPh_2)_2\}]$	-18.9(t,d,d)	-6	-665.9(t,t,t)	-123.8(t,t)	2627	93,73,48	52	1512
				-155.5(d,d,t)	2207			
$[SnF_4\{Et_2P(CH_2)_2PEt_2\}]$	-11.6(t,d,d)	6	-649.4(t,t,t)	-123.8(t,t)	2552	110,95,46	40	1628
				-150.2(d,d,t)	2183			
$[SnF_4\{Cy_2P(CH_2)_2PCy_2\}]$	-9.9(t,d,d)	-12	-639.1(t,t,t)	-113.7(t,t)	2644	98,88,46	46	1528
				-139.5(d,d,t)	2205			
$[SnF_4\{Ph_2P(CH_2)_2PPh_2\}]$	-17.8(t,d,d)	-4	-688.1(t,t,t)	-112.4(t,t)	2650	118,87,44	46	1630
				-147.1(d,d,t)	2212			

[a] In CH_2Cl_2-10% $CDCl_3$. [b] Ligand chemical shifts are: *o*-$C_6H_4(PMe_2)_2$ −55; *o*-$C_6H_4(PPh_2)_2$ −13; $Ph_2P(CH_2)_2PPh_2$ −13; $Et_2P(CH_2)_2PEt_2$ −18; $Cy_2P(CH_2)_2PCy_2$ +2; PMe_3 −62; PCy_3 +11.5. [c] Coordination shift ($\delta_{complex} - \delta_{ligand}$). [d] ^{119}Sn Spectra were typically recorded at 250 K.

Crystals found to be $[SnF_4\{Et_2P(CH_2)_2PEt_2\}]$ were obtained from a solution of the complex in CH_2Cl_2 that was layered with hexane and left to stand for 2 weeks. The structure confirms the *cis* geometry deduced from the NMR spectroscopic studies (Figure 13, Table 5). The Sn–P distance is 2.606(1) Å, shorter than in the *trans*-$[SnF_4\{PCy_3\}_2]$ (2.654(1) Å), and also shorter than the value in *cis*-$[SnCl_4\{Et_2P(CH_2)_2PEt_2\}]$ (2.648(2) Å) described below. The Sn–F_{transF} 1.986(2) Å is significantly longer than Sn–F_{transP} 1.953(2) Å, a pattern which is found in most adducts of SnX_4 (X = Cl, Br or I) with soft donor ligands.[3,4,5,6,7]

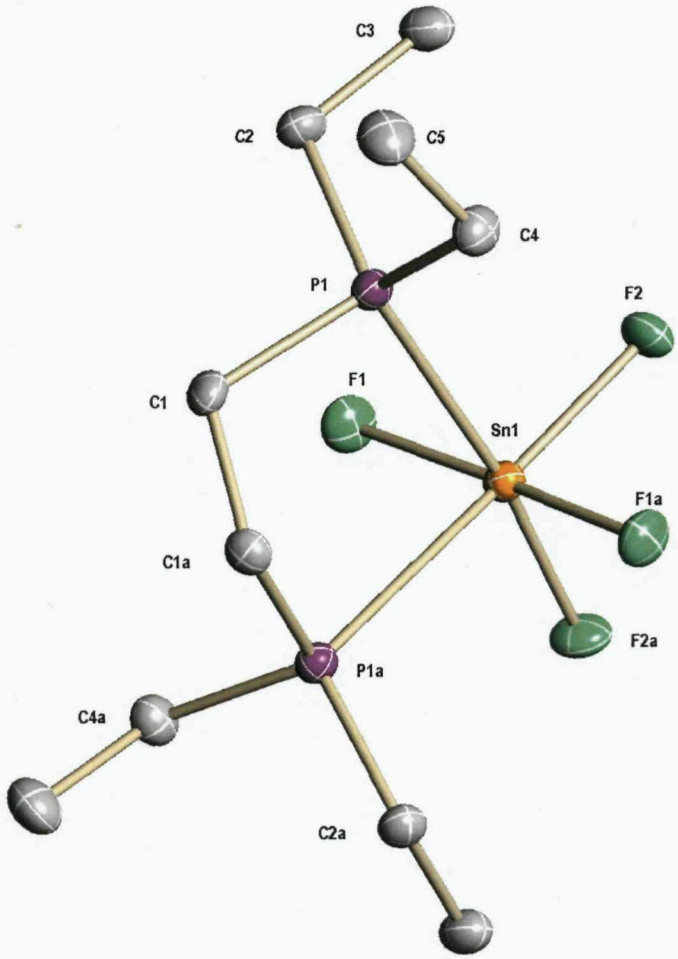

Figure 13 Structure of $[SnF_4\{Et_2P(CH_2)_2PEt_2\}]$ showing the atom numbering scheme. Ellipsoids are drawn at the 50% probability level and H atoms omitted for clarity. A 2-fold axis passes through Sn1 and the centre of the C1–C1a bond. Symmetry operation: a = – x, y, 1/2 – z.

Table 5 Selected bond lengths (Å) and angles (°) for $[SnF_4\{Et_2P(CH_2)_2PEt_2\}]$.

Sn1–F1	1.9863(17)	P1–C1	1.821(3)
Sn1–F2	1.9532(16)	P1–C2	1.815(3)
Sn1–P1	2.6058(9)	P1–C4	1.814(3)
P1···P1a	3.409(2)		
F1–Sn1–F2	92.60(7)	P1–Sn1–F1	84.66(5)
F1–Sn1–F2a	91.36(7)	P1–Sn1–F2	93.14(6)
F1–Sn1–F1a	174.29(10)	P1–Sn1–F1a	91.02(5)
F2–Sn1–F2a	92.29(10)	P1–Sn1–F2a	173.40(5)
P1–Sn1–P1a	81.70(4)	Sn1–P1–C1	102.52(9)
Sn1–P1–C2	114.54(10)	Sn1–P1–C4	116.34(10)

Symmetry operation: a = – x, y, 1/2 – z.

An attempt at obtaining a crystal of $[SnF_4\{o\text{-}C_6H_4(PPh_2)_2\}]$ from a solution in CH_2Cl_2 however only yielded crystals of the free ligand $o\text{-}C_6H_4(PPh_2)_2$.

3.3 Comparisons of the Phosphanes Complexed with Other Tin(IV) Halides:

For a list of literature comparator data see Table 1. For comparison several new complexes of SnX_4 (X = Cl, Br or I) with phosphane ligands were prepared. These included those of the diphosphane ligand $o\text{-}C_6H_4(PMe_2)_2$ with all three tin(IV) halides which surprisingly had not been previously reported (despite both the direct arsane equivalent and the similar $o\text{-}C_6H_4(PPh_2)_2$ both being reported)[6] and the $SnCl_4$ with $Et_2P(CH_2)_2PEt_2$. These reactions were all done by direct reaction with the appropriate molar ratios of ligand in anhydrous dichloromethane. The spectroscopic data obtained (Table 8) were as expected, and followed the same pattern as those of $[SnX_4\{o\text{-}C_6H_4(PPh_2)_2\}]$ and $[SnX_4\{o\text{-}C_6H_4(AsMe_2)_2\}]$ (X=Cl, Br,I).[6] Like other complexes of this type they are very moisture sensitive and also dioxygen sensitive to varying degrees in solution,[6,16] but much more soluble in chlorocarbons than their tin(IV) fluoride analogues.

The trends in the spectroscopic data were examined to see if support for the greater Lewis acidity of the SnF_4 was forthcoming. However, this is unlikely to be as conclusive because it is no longer a 'hard' metal centre (SnF_4) complexing with a 'hard' ligand (the oxide) (discussed in Chapter 2). The phosphane ligands are

much softer and therefore less likely to want to coordinate to hard acceptors. This is confirmed with the $^{31}P\{^{1}H\}$ NMR spectra of the [SnX_4({*o*-$C_6H_4(PMe_2)_2$}/{*o*-$C_6H_4(PPh_2)_2$}/{$Ph_2P(CH_2)_2PPh_2$})] series where there is no longer a consistent pattern of F > Cl > Br > I but instead the shift to high frequency along the series as far as Cl > Br > F > I as opposed to the analogous phosphane oxide series. For the series of compounds [SnX_4{PMe_3}$_2$] a similar comparison cannot be made due to differing solvents ($MeNO_2$[6] compared to CH_2Cl_2).

The ^{119}Sn NMR chemical shifts are surprisingly similar for corresponding complexes of SnF_4 and $SnCl_4$, but those of $SnBr_4$ and SnI_4 show much more deshielded resonances (Table 8) however a consistent low frequency shift with X: Cl > F > Br > I. This is the same as observed in the halostannates(IV),[17,18] evidence that electronegativity is not the dominant factor.[19] Factors that affect ^{119}Sn chemical shifts include electronegativity, Lewis acidity and bond overlap and in these cases none appear to be dominant. The $^{1}J(^{119}Sn\text{-}^{31}P)$ coupling constants fall with halogen F > Cl > Br > I and are much larger for *trans* P-Sn-P than *cis* P-Sn-P (see Table 4).

The structure of *cis*-[$SnCl_4${$Et_2P(CH_2)_2PEt_2$}] was determined (Figure 14, Table 6) and provides a direct comparison with the isostructural fluoride discussed above. Again there is a marked difference between $Sn\text{–}Cl_{transCl}$ (2.453(1) Å) and $Sn\text{–}Cl_{transP}$ (2.408(1) Å) with Sn–P = 2.648(2) Å. The longer bond distance of Sn-P in the chloro species compared to that of the fluoro species indicates that SnF_4 is the stronger Lewis acid and will coordinate with the soft phosphane more strongly than $SnCl_4$ because of this. Other structurally characterised phosphane complexes of $SnCl_4$ are *trans*-[$SnCl_4${PEt_3}$_2$] (Sn–P = 2.615(5) Å),[10] *trans*-[$SnCl_4${κ^1-$Ph_2PCH_2PPh_2$}$_2$] (Sn–P = 2.649(1) Å),[14] and *cis*-[$SnCl_4${$Ph_2P(CH_2)_2PPh_2$}] (Sn–P = 2.679(2), 2.653(2) Å, Sn–Cl = 2.402(2), 2.406(2), 2.408(2), 2.447(2) Å).[12]

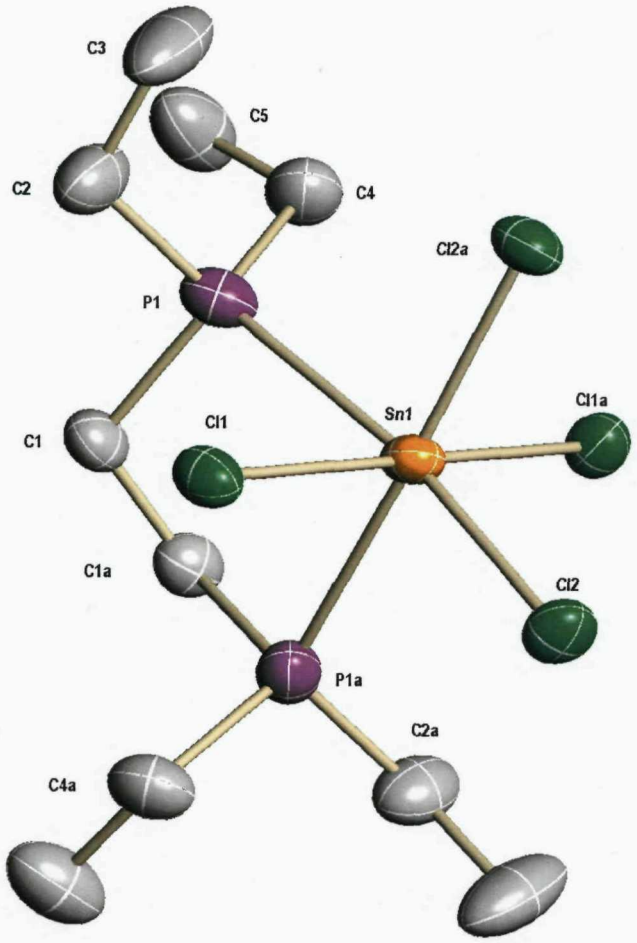

Figure 14 Structure of $[SnCl_4\{Et_2P(CH_2)_2PEt_2\}]$ showing the atom numbering scheme. Ellipsoids are drawn at the 40% probability level and H atoms omitted for clarity. The tin atom is on a 2-fold axis. Symmetry operation: a = 1 – x, y, ½ – z.

Table 6 Selected bond lengths (Å) and angles (°) for $[SnCl_4\{Et_2P(CH_2)_2PEt_2\}]$

Sn1–Cl1	2.4529(14)	Sn1–P1	2.6481(17)
Sn1–Cl2	2.4084(14)	P1–C2	1.821(6)
P1–C4	1.824(6)	P1–C1	1.825(5)
P1···P1a	3.422(3)		
Cl1–Sn1–Cl2	90.16(5)	Cl1–Sn1–Cl2a	93.97(5)
Cl1–Sn1–Cl1a	174.00(7)	Cl2–Sn1–Cl2a	92.99(7)
Cl1–Sn1–P1	84.19(5)	Cl2–Sn1–P1	171.65(5)
P1–Sn1–P1a	80.49(7)	Sn1–P1–C2	117.0(2)
Sn1–P1–C4	114.0(2)	Sn1–P1–C1	102.09(18)
P1–C1–C1a–P1a	67.7(6)		

Symmetry operation: a = 1 – x, y, ½ – z.

3.4 SnF_4 Complexes of Arsanes:

The reaction of $[SnF_4\{MeCN\}_2]$ with tertiary arsanes, including $AsMe_3$, *o*-$C_6H_4(AsMe_2)_2$ and $MeC(CH_2AsMe_2)_3$ were unsuccessful in producing pure samples of the SnF_4 complexes. The general experimental conditions for these compounds were the same as for the phosphanes, but reactions of both $[SnF_4\{MeCN\}_2]$ and $[SnF_4\{THF\}_2]$ in CH_2Cl_2 or toluene were attempted with the arsane ligands. Reactions with *o*-$C_6H_4(AsMe_2)_2$, which is a very strongly coordinating ligand towards many d-block metals,[20] resulted in white solids of variable composition which appeared to be mixtures of the starting complex, possibly $[SnF_4\{o\text{-}C_6H_4(AsMe_2)_2\}]$ and SnF_4. The IR spectra showed the presence of the diarsane, a broad υ(SnF) *ca.* 570 cm^{-1}, and usually some MeCN or THF. The ^1H NMR spectra of these products in CD_2Cl_2 solution showed only MeCN or THF and "free" *o*-$C_6H_4(AsMe_2)_2$ (since *o*-$C_6H_4(AsMe_2)_2$ is a liquid, this is supporting evidence for coordination of the diarsane to tin in the solids). The $^{19}F\{^1H\}$ NMR spectra showed no resonances at room temperature, but below *ca.* 210 K, two new broad resonances at δ –138 and –152 were observed, which seem reasonable for $[SnF_4\{o\text{-}C_6H_4(AsMe_2)_2\}]$, but no F–F coupling was resolved even at 190 K. The data suggest that $[SnF_4\{o\text{-}C_6H_4(AsMe_2)_2\}]$ forms in the reaction, but that it is extensively dissociated in solution (see Figure 15) and reforms the polymeric SnF_4.[21] Even if a substantial excess of diarsane is used a pure product is not produced. In the case of $AsMe_3$ a white solid was again obtained, the IR spectrum showing the presence of the arsane, a broad υ(SnF) *ca.* 551 cm^{-1}. Complexation with $MeC(CH_2AsMe_2)_3$ also gave a white solid with the IR spectrum showing the presence of the arsane, a broad υ(SnF) *ca.* 570 cm^{-1} but no other evidence could be obtained for coordination to SnF_4. Since the very unstable $[SnF_4\{dithioether\}]$ crystals were obtained (see Chapter 4), substantial effort was put into obtaining crystalline samples of these materials, specifically $[SnF_4\{o\text{-}C_6H_4(AsMe_2)_2\}]$ including numerous different solvents, cooling as well as layering and slow evaporation but these repeated attempts proved futile.

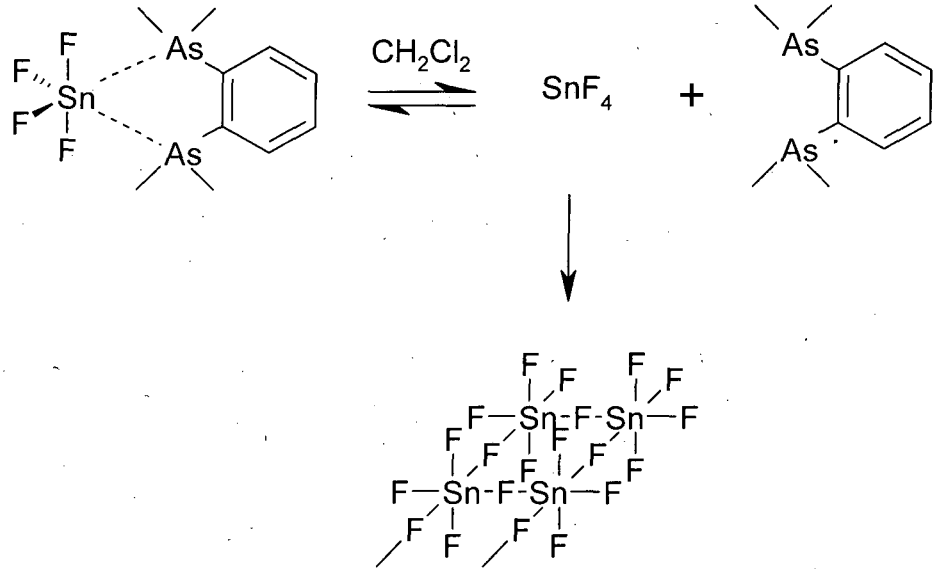

Figure 15 Believed behaviour of SnF_4-arsane complexes.

3.5 Comparisons of the Arsane Complexed with Other Tin(IV) Halides:

In contrast, arsane complexes of SnX_4 (X = Cl, Br or I) form readily,[6] and indeed $[SnI_4\{o\text{-}C_6H_4(AsMe_2)_2\}]$ is one of the very small number of structurally characterised neutral ligand adducts of SnI_4. The $[SnCl_4\{o\text{-}C_6H_4(AsMe_2)_2\}]$ was prepared to confirm this and the results were as in the previous literature.[6] The reactions of SnX_4 (X = Cl and Br) with the tripod $MeC(CH_2AsMe_2)_3$ however, had not been reported and so these were made with a 1:1 ratio of the SnX_4:tripod arsane in CH_2Cl_2. The ^1H NMR spectra show the triarsane bound as a bidentate to a six-coordinate tin centre. The ^{119}Sn NMR chemical shifts of δ -696 and -1290 (Table 8) for $[SnCl_4\{MeC(CH_2AsMe_2)_3)\}]$ and $[SnBr_4\{MeC(CH_2AsMe_2)_3)\}]$ respectively are typical of SnX_4As_2 donor sets.[6] The structures were confirmed by an X-ray study of $[SnBr_4\{MeC(CH_2AsMe_2)_3\}]$ (Figure 16, Table 7) which showed a distorted octahedral tin centre with $Sn–Br_{transBr}$ (2.5807(5), 2.6340(5) Å) longer than $Sn–Br_{transAs}$ (2.5708(6), 2.5479(5) Å), and with the axial Br–Sn–Br unit bent towards the neutral ligand (Br3–Sn1–Br4 = 170.6°), as found in tin(IV) halide structures with a variety of soft donors.[3,4,5,6] The Sn–As (2.6932(5), 2.7095(6) Å) are slightly shorter than those in the only other structurally characterised tin-arsane complexes $[SnI_4\{o\text{-}C_6H_4(AsMe_2)_2\}]$ (2.716(2), 2.752(2) Å),[6] and *trans*-$[SnCl_4\{AsPh_3\}_2]$ (2.762(1) Å).[13] The wide As–Sn–As bond angle in the present complex (86.79(2)°) reflects the six-membered chelate ring present

and compares with 78.43(7)° in [SnI_4{*o*-$C_6H_4(AsMe_2)_2$}] which contains a five-membered ring.

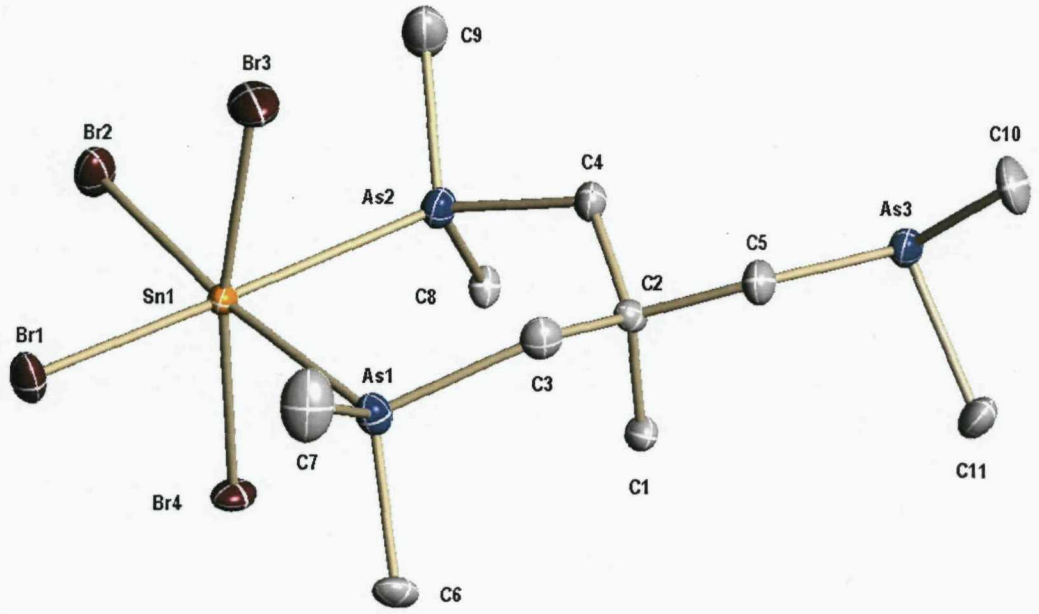

Figure 16 Structure of [$SnBr_4${$MeC(CH_2AsMe_2)_3$}] showing the atom numbering scheme. Ellipsoids are drawn at the 50% probability level and H atoms omitted for clarity.

Table 7 Selected bond lengths (Å) and angles (°) for [$SnBr_4${$MeC(CH_2AsMe_2)_3$}].

Sn1–Br1	2.5708(6)	Sn1–Br3	2.6340(5)
Sn1–Br2	2.5479(5)	Sn1–Br4	2.5807(5)
Sn1–As1	2.6932(5)	Sn1–As2	2.7095(6)
As1–C6	1.930(4)	As2–C8	1.935(3)
As1–C7	1.932(3)	As2–C9	1.928(3)
As3–C10	1.966(3)	As3–C11	1.972(3)
As1–C3	1.953(4)	As2–C4	1.954(3)
As3–C5	1.987(3)	As1···As2	3.712(1)
Br–Sn1–Br (*ca.* 90°)	91.979(2)–94.850(2)	Br3–Sn1–Br4	170.563(15)
Br–Sn1–As (*ca.* 90°)	82.905(2)–90.337(2)	Br1–Sn1–As2	173.739(14)
Br2–Sn1–As1	174.623(2)	As1–Sn1–As2	86.791(16)
C–As1–C	101.08(2)–108.21(2)	C–As2–C	99.62(2)–107.75(2)
C–As3–C	93.50(2)–98.69(2)		

Table 8 Selected NMR data for SnX_4 (X = Cl, Br or I) complexes.[a]

Compound	δ $^{31}P\{^1H\}$[b]	δ ^{119}Sn	$^1J(^{31}P-^{119}Sn)$
$[SnCl_4\{o\text{-}C_6H_4(PMe_2)_2\}]$	-28.1	-616(t)	945
$[SnBr_4\{o\text{-}C_6H_4(PMe_2)_2\}]$	-31.9	-1188(t)	581
$[SnI_4\{o\text{-}C_6H_4(PMe_2)_2\}]$	-60.4	n.o.[c]	240
$[SnCl_4\{Et_2P(CH_2)_2PEt_2\}]$	-4.9	-615(t)	1049
$[SnCl_4\{MeC(CH_2AsMe_2)\}]$	-	-696(s)	-
$[SnBr_4\{MeC(CH_2AsMe_2)\}]$	-	-1290(s)	-

[a] In CH_2Cl_2-10% $CDCl_3$. [b] Ligand chemical shifts are: $o\text{-}C_6H_4(PMe_2)_2$ -55; $Et_2P(CH_2)_2PEt_2$ –18; [c] Insufficiently soluble to record spectrum.

The explanation of this marked difference in the ability of SnF_4 to complex arsanes as opposed to phosphanes probably arises from the fact the SnF_4 is a very hard Lewis acid with contracted tin acceptor orbitals, and correspondingly has less ability to bind the large soft arsenic centre compared to the slightly smaller, slightly harder phosphane. For many transition metal systems the differences between binding corresponding phosphanes and arsanes is small, but becomes very significant with high oxidation state and/or harder metal centres of the 3d series such as Fe(IV), Ni(IV) or Mn(II) where the phosphanes result in significantly more stable complexes.[20] The results suggest that the hard Lewis acid SnF_4 similarly discriminates away from the arsanes and means that unlike the phosphanes, $SnCl_4$ is more strongly coordinating towards the arsenic ligands.

3.6 Conclusion:

This Chapter reports the first synthesis of a series of relatively stable, although highly moisture sensitive, SnF_4 adducts with soft ligands. This Chapter has proven that the hard Lewis acid, SnF_4 will form complexes with soft donor ligands. In the case of the phosphanes these complexes can vary significantly in solubility with changes of R groups and often dissociate in solution at room temperature. In the case of the arsanes, dissociation seems to be much more of a problem due to the reduced affinity of SnF_4 for As<<P. This is contrary to transition metals where the affinities of phosphanes and arsanes for a common metal centre are usually comparable.

A large amount of spectroscopic data on these compounds has been obtained and some comparisons have been made with the heavier tin(IV) halides.

Structural data on four novel complexes have been obtained, including both a monodentate and bidentate chelating phosphane ligand on SnF_4 as well as a direct comparison of the same bidentate ligand on $SnCl_4$, clearly showing that SnF_4 is the strongest Lewis acid when compared to the other tin(IV) halides for the phosphane compounds.

3.7 Experimental:

See Appendix for general experimental methods. Ligands not obtained from suppliers were made by literature methods: *o*-$C_6H_4(PPh_2)_2$, $Ph_2P(CH_2)_2PPh_2$, *o*-$C_6H_4(PMe_2)_2$, *o*-$C_6H_4(AsMe_2)_2$, $MeC(CH_2AsMe_2)_3$.[22,23,24,25] Much of the spectroscopic data below is included above in this chapter, however, for ease of use it is collected under the compound.

[SnF_4{*o*-$C_6H_4(PMe_2)_2$}]: [SnF_4{MeCN}$_2$] (0.276 g, 1.0 mmol) was suspended in CH_2Cl_2 (20 mL) and *o*-$C_6H_4(PMe_2)_2$ (0.198 g, 1.0 mmol) added and the mixture stirred overnight at ambient temperatures. The white precipitate was filtered off and dried *in vacuo*. Yield 0.205 g, 52%. $C_{10}H_{16}F_4P_2Sn{\cdot}CH_2Cl_2$ (477.8): calcd. C 27.6, H 3.8; found C 26.9, H 3.8. ^{1}H NMR (300 MHz, $CDCl_3$, 298 K) :δ = 1.87 (t, $^2J + {}^5J_{P\text{-}H}$ = 4 Hz, 12H, Me), 5.40 (CH_2Cl_2), 7.75–7.81 (m, 4H, C_6H_4) ppm. IR (Nujol): 564(s), 534(s) υ(SnF) cm^{-1}. ^{19}F{^{1}H} NMR (CH_2Cl_2/$CDCl_3$, 243 K): -131.7 (t,t), -161.1 (d,d,t). ^{31}P{^{1}H} NMR (CH_2Cl_2/$CDCl_3$, 243 K): -37.8 (t,d,d). ^{119}Sn NMR (CH_2Cl_2/$CDCl_3$, 243 K): -657.6 (t,t,t).

[SnF_4{*o*-$C_6H_4(PPh_2)_2$}]: [SnF_4{MeCN}$_2$] (0.276 g, 1.00 mmol) was suspended in CH_2Cl_2 (20 mL) and a solution of *o*-$C_6H_4(PPh_2)_2$ (0.446 g, 1.00 mmol) in CH_2Cl_2 (5 mL) added and the mixture stirred for 8 h at ambient temperatures. The white precipitate was filtered off and dried *in vacuo*. Yield 0.17 g, 27%. $C_{30}H_{24}F_4P_2Sn$ (641.2) calcd. C 56.2, H 3.8; found C, 56.9, H 4.1. ^{1}H NMR (300 MHz, $CDCl_3$, 298 K): δ = 7.70–8.01 (m, Ph) ppm. IR (Nujol): 574(s), 557(s), 526(s) υ(SnF) cm^{-1}. ^{19}F{^{1}H} NMR (CH_2Cl_2/$CDCl_3$, 193 K): -123.8 (t,t), -155.5 (d,d,t). ^{31}P{^{1}H}

NMR ($CH_2Cl_2/CDCl_3$, 243 K): -18.9 (t,d,d). ^{119}Sn NMR ($CH_2Cl_2/CDCl_3$, 223 K): -665.9 (t,t,t).

[$SnF_4\{PMe_3\}_2$]: [$SnF_4\{MeCN\}_2$] (0.277 g, 1.00 mmol) was suspended in CH_2Cl_2 (10 mL), trimethylphosphane (0.167 g, 2.20 mmol) was added and stirred at room temperature for 1 h. The solution was reduced in volume by removal of CH_2Cl_2 *in vacuo* and then dry hexane (20 mL) was added. A white solid precipitated out which was filtered off under nitrogen and dried *in vacuo*. Yield 0.250 g, 68%. $C_6H_{18}F_4P_2Sn.2CH_2Cl_2$ (516.7) calcd. C 18.6, H 4.3; found C 18.3, H 4.5. ^1H NMR (300 MHz, $CDCl_3$, 298 K): δ = 1.68 (m, Me), 5.40 (CH_2Cl_2) ppm. IR (Nujol): 546 (br) υ(SnF) cm^{-1}. $^{19}F\{^1H\}$ NMR ($CH_2Cl_2/CDCl_3$, 298 K): -132.8 (t). $^{31}P\{^1H\}$ NMR ($CH_2Cl_2/CDCl_3$, 248 K): -19.1 (q^5). ^{119}Sn NMR ($CH_2Cl_2/CDCl_3$, 248 K): -628.0 (q^5,t).

[$SnF_4\{PCy_3\}_2$]: [$SnF_4\{MeCN\}_2$] (0.277 g, 1.00 mmol) was suspended in CH_2Cl_2 (10 mL), tricyclohexylphosphane (0.588 g, 2.10 mmol) was added and stirred at room temperature for 3 h. No precipitation had occurred so the solution was reduced to *ca.* 5 mL *in vacuo* and then dry hexane (5 mL) was added. A white solid precipitated out which was filtered off under nitrogen and dried *in vacuo*. Yield 0.45 g, 60%. $C_{32}H_{66}F_4P_2Sn{\cdot}1/2CH_2Cl_2$ (750.0) calcd. C 54.9; H 8.5; found C 54.4, H 8.8. ^1H NMR (300 MHz, $CDCl_3$, 298 K): δ = 1.29–2.34 (m, Cy), 5.40 (CH_2Cl_2) ppm. IR (Nujol): 557(s), 535(s) υ(SnF) cm^{-1}. $^{19}F\{^1H\}$ NMR ($CH_2Cl_2/CDCl_3$, 298 K): -98.9 (t). $^{31}P\{^1H\}$ NMR ($CH_2Cl_2/CDCl_3$, 296 K): 22.2 (q^5). ^{119}Sn NMR ($CH_2Cl_2/CDCl_3$, 223 K): -628.5 (q^5,t).

[$SnF_4\{Cy_2P(CH_2)_2PCy_2\}$]: [$SnF_4\{MeCN\}_2$] (0.278 g, 1.00 mmol) was suspended in CH_2Cl_2 (10 mL), 1,2-*bis*(dicyclohexylphosphanyl)ethane (0.444 g, 1.05 mmol) in CH_2Cl_2 (5 mL) was added. This was stirred under nitrogen for 3 h, no precipitation had occurred so the solution was reduced to *ca.* 5 mL *in vacuo* and then dry hexane (5 mL) was added. No significant precipitate was observed so the solvent was removed and dried *in vacuo* to give a white solid. Yield 0.51 g, 83%. $C_{38}H_{70}F_4P_2Sn{\cdot}1/2CH_2Cl_2$ (826.1) calcd. C 48.6, H 8.8; found C 49.2, H 8.8. ^1H NMR (300 MHz, $CDCl_3$, 298 K): δ = 1.26–2.21 (m, CH_2 + Cy), 5.40 (CH_2Cl_2) ppm. IR (Nujol): 560(s), 530(s) υ(SnF) cm^{-1}. $^{19}F\{^1H\}$ NMR ($CH_2Cl_2/CDCl_3$, 298

K): -113.7 (t,t), -139.5 (d,d,t). $^{31}P\{^{1}H\}$ NMR ($CH_2Cl_2/CDCl_3$, 263 K): -9.9 (t,d,d). ^{119}Sn NMR ($CH_2Cl_2/CDCl_3$, 263 K): -639.1 (t,t,t).

[$SnF_4\{Ph_2P(CH_2)_2PPh_2\}$]: [$SnF_4\{MeCN\}_2$] (0.28 g, 1.0 mmol) was suspended in CH_2Cl_2 (15 mL), 1,2-*bis*(diphenylphosphanyl)ethane (0.42 g, 1.05 mmol) in CH_2Cl_2 (10 mL) was added and the mixture stirred for 3 h. Most of the solvent was removed *in vacuo* and the white precipitate was filtered off and dried *in vacuo*. Yield 0.46 g, 78%. $C_{26}H_{24}F_4P_2Sn.1/2CH_2Cl_2$ (635.6) calcd. C 50.0, H 4.0; found C 49.6, H 3.7. ^{1}H NMR (300 MHz, $CDCl_3$, 298 K): δ = 2.09 (t, 1H, CH_2), 5.40 (CH_2Cl_2), 7.45–7.89 (m, 5H, Ph) ppm. IR (Nujol): 566(br) υ(SnF) cm^{-1}. $^{19}F\{^{1}H\}$ NMR ($CH_2Cl_2/CDCl_3$, 213 K): -112.4 (t,t), -147.1 (d,d,t). $^{31}P\{^{1}H\}$ NMR ($CH_2Cl_2/CDCl_3$, 273 K): -17.8 (t,d,d). ^{119}Sn NMR ($CH_2Cl_2/CDCl_3$, 223 K): -668.1 (t,t,t).

[$SnF_4\{Et_2P(CH_2)_2PEt_2\}$]: [$SnF_4\{MeCN\}_2$] (0.278 g, 1.00 mmol) was suspended in CH_2Cl_2 (20 mL), 1,2-*bis*(diethylphosphanyl)ethane (0.28 mL, 1.20 mmol) was added dropwise and stirred for 1.5 h. The white precipitate was filtered off and dried *in vacuo*. Yield 0.32 g, 80%. $C_{10}H_{24}F_4P_2Sn$ (400.95) calcd. C 29.9, H 6.0; found C 29.0, H 6.0. ^{1}H NMR (300 MHz, $CDCl_3$, 298 K): δ = 1.26–1.37 (m, 6H, Me), 2.07–2.13 (m, 8H, CH_2) ppm. IR (Nujol): 553(m), 526(s) υ(SnF) cm^{-1}. $^{19}F\{^{1}H\}$ NMR ($CH_2Cl_2/CDCl_3$, 298 K): -123.8 (t,t), -150.2 (d,d,t). $^{31}P\{^{1}H\}$ NMR ($CH_2Cl_2/CDCl_3$, 273 K): -11.6 (t,d,d). ^{119}Sn NMR ($CH_2Cl_2/CDCl_3$, 263 K): -649.4 (t,t,t).

Attempted preparation of **[$SnF_4\{AsMe_3\}_2$]:** Trimethylarsane ($AsMe_3$) (0.26 g, 2.20 mmol) was added to a solution of [$SnF_4\{MeCN\}_2$] (0.34 g, 1.00 mmol) in CH_2Cl_2 (10 ml) and stirred under nitrogen for 2 h. This was then filtered and dried *in vacuo* to give a white solid (0.35 g, 82%). ^{1}H NMR (300 MHz, $CDCl_3$, 298 K): 2.00 (s), 2.17 (s). IR spectrum (υ(SnF)/cm^{-1}): 551 br.

Attempted preparation of **[$SnF_4\{o\text{-}C_6H_4(AsMe_2)_2\}$]:** 1,2-bis(dimethylarsanyl) benzene *o*-$C_6H_4(AsMe_2)_2$ (0.286 g, 1.00 mmol) was added to a solution of [$SnF_4\{THF\}_2$] (0.34 g, 1.00 mmol) in CH_2Cl_2 (10 ml) and stirred under nitrogen for 3 h. This was then filtered and put under vacuum to give a white solid (0.25 g,

52%). ^{1}H NMR (300 MHz, $CDCl_3$, 298 K): 1.20 (s, 12H, CH_3), 7.28-7.48 (m, 4H, C_6H_4). IR spectrum (υ(SnF)/cm^{-1}): 572 br. ^{19}F{^{1}H} NMR (CH_2Cl_2/$CDCl_3$, 188 K): -138 (s), -151.7 (s).

[$SnCl_4${*o*-$C_6H_4(PMe_2)_2$}]: A solution of $SnCl_4$ (0.12 mL, 1.0 mmol) in CH_2Cl_2 (5 mL) was added to *o*-$C_6H_4(PMe_2)_2$ (0.198 g, 1.0 mmol) in CH_2Cl_2 (20 mL) producing an immediate white precipitate. After 30 min. the solid was filtered off and dried *in vacuo*. Yield 0.427 g, 93%. $C_{10}H_{16}Cl_4P_2Sn$ (458.7) calcd. C 26.2, H 3.5; found C 25.9, H 3.2. ^{1}H NMR (300 MHz, $CDCl_3$, 298 K): δ = 1.97 (t, $^{2}J+^{5}J_{P\text{-}H}$ = 4.4 Hz, 12H, Me) 7.75–7.81 (m, 4H, C_6H_4) ppm. IR (Nujol): 307(s), 296(s) υ(SnCl) cm^{-1}. ^{31}P{^{1}H} NMR (CH_2Cl_2/$CDCl_3$, 298 K): -28.1 (s). ^{119}Sn NMR (CH_2Cl_2/$CDCl_3$, 243 K): -616 (t).

[$SnBr_4${*o*-$C_6H_4(PMe_2)_2$}]: Prepared as above yielding as a yellow solid. Yield 0.590g 93%. $C_{10}H_{16}Br_4P_2Sn$ (636.5) calcd. C 18.9, H 2.5; found C 18.7, H 2.4. ^{1}H NMR (300 MHz, $CDCl_3$, 298 K): δ = 1.95 (t, $^{2}J+^{5}J_{P\text{-}H}$ = 4.5 Hz, 12H, Me) 7.75–7.81 (m, 4H, C_6H_4) ppm. IR (Nujol): 205(sh), 202(s), 199(sh), 196(s) υ(SnBr) cm^{-1}. ^{31}P{^{1}H} NMR (CH_2Cl_2/$CDCl_3$, 243 K): -31.9 (s). ^{119}Sn NMR (CH_2Cl_2/$CDCl_3$, 243 K): -1188 (t).

[SnI_4{*o*-$C_6H_4(PMe_2)_2$}]: Prepared as above yielding as a brown powder. Yield 0.63 g, 76%. $C_{10}H_{16}I_4P_2Sn$ (824.5) calcd. C 14.6, H 2.0; found C 14.6, H 1.9. ^{1}H NMR (300 MHz, $CDCl_3$, 298 K): δ = 1.83 (t, $^{2}J+^{5}J_{P\text{-}H}$ = 4.8 Hz, 12H, Me) 7.75–7.81 (m, 4H, C_6H_4) ppm. ^{31}P{^{1}H} NMR (CH_2Cl_2/$CDCl_3$, 298 K): -60.4 (s). ^{119}Sn NMR not observed.

[$SnCl_4${$Et_2P(CH_2)_2PEt_2$}]: $SnCl_4$ (0.260 g, 1.00 mmol) was dissolved in CH_2Cl_2 (15 mL), 1,2-bis(diethylphosphanyl)ethane (0.245 mL, 1.05 mmol) was added and stirred for 2 h. Immediate precipitation occurred, and the solid was filtered off and dried *in vacuo* to give a white crystalline solid. Yield 0.45 g, 96%. $C_{10}H_{24}Cl_4P_2Sn{\cdot}CH_2Cl_2$ (551.7) calcd. C 23.9, H 4.8; found C 23.5, H 5.0. ^{1}H NMR (300 MHz, $CDCl_3$, 298 K): δ = 1.21–1.39 (m, 6H, Me), 2.11–2.12 (m, 8H, CH_2), 5.4 (CH_2Cl_2) ppm. IR (Nujol): 318(sh), 307(sh), 282(br) υ(SnCl) cm^{-1}.

$^{31}P\{^1H\}$ NMR ($CH_2Cl_2/CDCl_3$, 263 K): -4.9 (s). ^{119}Sn NMR ($CH_2Cl_2/CDCl_3$, 223 K): -615.5 (t).

[$SnCl_4\{MeC(CH_2AsMe_2)_3\}$]: $MeC(CH_2AsMe_2)_3$ (0.384 g, 1.0 mmol) was dissolved in CH_2Cl_2 (10 mL) under nitrogen. To this solution $SnCl_4$ (0.261 g, 1.0 mmol) was added and an immediate white precipitate formed. This was filtered off and dried *in vacuo* to give a white powder. Yield 0.21 g, 33%. ^1H NMR (300 MHz, $CDCl_3$, 298 K): δ = 1.03 (s, 6H, AsMe), 1.35 (s, 3H, CMe), 1.73 (s, 12H, AsMe), 1.77 (s, 2H, CH_2), 2.39 (d, ^2J = 12 Hz, 2H, CH_2), 2.54 (d, ^2J = 12 Hz, 2H, CH_2) ppm. IR Nujol: 310(sh), 302(s), 280(sh) υ(SnCl) cm^{-1}. ^{119}Sn NMR ($CH_2Cl_2/CDCl_3$, 233 K): -696 (s).

[$SnBr_4\{MeC(CH_2AsMe_2)_3\}$]: $MeC(CH_2AsMe_2)_3$ (0.384 g, 1.0 mmol) was dissolved in CH_2Cl_2 (10 mL) under nitrogen. To this solution $SnBr_4$ (0.438 g, 1.0 mmol) was added and an immediate yellow precipitate formed in a yellow solution. This was filtered and the filtrate was left to stand to give yellow crystals. Yield 0.18 g, 22%. $C_{11}H_{27}As_3Br_4Sn$ (822.4) calcd. C 16.1, H 3.3; found C 15.3, H 3.1. ^1H NMR (300 MHz, $CDCl_3$, 298 K): δ = 1.04 (s, 6H, AsMe), 1.37 (s, 3H, CMe), 1.70 (br, 12H, AsMe), 1.78 (br, 2H, CH_2), 2.32 (br, 2H, CH_2) 2.55 (br, 2H, CH_2) ppm. IR (Nujol): 215(sh), 207(s), 199(s) υ(SnBr) cm^{-1}. ^{119}Sn NMR ($CH_2Cl_2/CDCl_3$, 213 K): -1290 (s).

3.8 Crystallography:

The crystals of *trans*-$[SnF_4\{PCy_3\}_2]$, $[SnF_4\{Et_2P(CH_2)_2PEt_2\}]$, $[SnCl_4\{Et_2P(CH_2)_2PEt_2\}]$ and $[SnBr_4\{MeC(CH_2AsMe_2)_3\}]$ were grown from anhydrous CH_2Cl_2 solutions layered or by vapour diffusion with *n*-hexane under dinotrogen over several days or weeks.

Brief details of the data collection and refinement are presented in Table 9. Significant time was spent on attempts to grow X-ray quality crystals of SnF_4 phosphanes and arsanes by vapour diffusion and layering from CH_2Cl_2, Hexane, EtOH and Et_2O but only the two phosphanes were obtained.

Table 9 Crystal data and structure refinement details.[a]

Compound	$[SnF_4\{Et_2P(CH_2)_2PEt_2\}]$	$[SnF_4\{PCy_3\}_2]$	$[SnCl_4\{Et_2P(CH_2)_2PEt_2\}]$	$[SnBr_4\{MeC(CH_2AsMe_2)_3\}]$
Formula	$C_{10}H_{24}F_4P_2Sn$	$C_{36}H_{66}F_4P_2Sn$	$C_{10}H_{24}Cl_4P_2Sn$	$C_{11}H_{27}As_3Br_4Sn$
M	400.92	755.52	466.72	822.42
Crystal system	Monoclinic	Triclinic	Monoclinic	Monoclinic
Space group	$C2/c$ (no. 15)	$P\text{-}1$ (no. 2)	$C2/c$ (no. 15)	$P2_1/c$ (no. 14)
a/Å	8.8994(12)	8.251(2)	9.708(3)	11.371(2)
b/Å	11.663(3)	9.868(3)	12.177(2)	12.839(2)
c/Å	14.774(4)	11.832(4)	16.301(5)	15.227(2)
α/°	90	77.192(15)	90	90
β/°	104.257(12)	85.601(10)	107.108(12)	91.731(10)
γ/°	90	69.240(15)	90	90
U/Å^3	1486.2(5)	878.3(4)	1841.7(9)	2221.9(6)
Z	4	1	4	4
μ/mm^{-1}	1.956	0.864	2.122	12.766
$F(000)$	800	398	928	1528
Total no. of obsns (R_{int})	9486 (0.053)	18769 (0.088)	8628 (0.049)	22702 (0.064)
Unique obsns.	1708	4030	2100	5084
Min, max transmission	0.726, 1.000	0.778, 1.000	0.722, 1.000	0.767, 1.000
No. of parameters, restraints	78, 0	196, 0	80, 0	179, 0
Goodness-of-fit on F^2	1.07	1.05	1.05	1.03
Resid electron density /eÅ^{-3}	–0.64 to +0.69	–0.69 to +0.97	–0.88 to +1.65	–0.91 to +0.84
R1, wR2 ($I > 2\sigma(I)$)[b]	0.030, 0.053	0.051, 0.101	0.054, 0.112	0.026, 0.050
R1, wR2 (all data)	0.042, 0.056	0.070, 0.108	0.092, 0.126	0.045, 0.053

[a] Common items: temperature = 120 K; wavelength (Mo-Kα) = 0.71073 Å; θ(max) = 27.5°.

[b] $R1 = \Sigma||F_o| - |F_c||/\Sigma|F_o|$. $wR2 = [\Sigma w(F_o^2 - F_c^2)^2/\Sigma wF_o^4]^{1/2}$.

3.9 References:

[1] E. W. Abel, S. K. Bhargava, K. G. Kite, V. Sik, *Inorg. Chim. Acta,* **1981**, 49, 25-30.
[2] a) S. J. Ruzicka, A. E. Merbach, *Inorg. Chim. Acta,* **1976**, 20, 221-229; b) S. J. Ruzicka, C. M. P. Favez, A. E. Merbach, *Inorg. Chim. Acta,* **1977**, 23, 239-247.
[3] S. E. Dann, A. R. J. Genge, W. Levason, G. Reid, *J. Chem. Soc., Dalton Trans.,* **1996**, 4471-4478.
[4] S. E. Dann, A. R. J. Genge, W. Levason, G. Reid. *J. Chem. Soc., Dalton Trans.,* **1997**, 2207-2213.
[5] A. R. J. Genge, W. Levason, G. Reid. *J. Chem. Soc., Dalton Trans.,* **1997**, 4549-4554.
[6] A. R. J. Genge, W. Levason, G. Reid., *Inorg. Chim. Acta,* **1999**, 288, 142-149.
[7] W. Levason, M. L. Matthews, R. Patel, G. Reid, M. Webster. *New. J. Chem.*, **2003**, 27, 1784-1788.
[8] W. Levason, C. A. McAuliffe, *Coord. Chem. Rev.*, **1976**, 19, 173-185.
[9] N. C. Norman, N. L. Pickett, *Coord. Chem. Rev.*, **1995**, 145, 27-54.
[10] G. G. Mather, G. M. McLaughlin, A. Pidcock, *J. Chem. Soc., Dalton Trans.*, **1973**, 1823–1827.
[11] N. Bricklebank, S. M. Godfrey, C. A. McAuliffe, R. G. Pritchard, *Chem. Commun.*, **1994**, 695–696.
[12] F. Kunkel, K. Dehnicke, *Z. Naturforsch. Teil B.*, **1995**, 50, 848–850.
[13] M. F. Mahon, N. L. Moldovan, K. C. Molloy, A. Muresan, I. Silaghi-Dumitrescu, L. Silaghi-Dumitrescu, *Dalton Trans.*, **2004,** 4017–4021.
[14] D. Dakternieks, H. Zhu, E. R. T. Tiekink, *Main Group Met. Chem.*, **1994,** 17, 519–535.
[15] K. M. Doxsee, E. M. Hanawalt, T. J. R. Weakley,. *Inorg. Chem.,* **1992**, 31, 4420-4421.
[16] W. Levason, R. Patel, G. Reid, *J. Organomet. Chem.*, **2003**, 688, 280-282.
[17] P. A. W. Dean, D. F. Evans, *J. Chem. Soc. (A),* **1968**, 1154-1166.
[18] K. B. Dillon, A. Marshall, *J. Chem. Soc., Dalton Trans.*, **1984**, 1245-1247.
[19] J. Mason (Ed), *Multinuclear NMR*, Plenum, NY, 1987.
[20] a) L. F. Warren, M. A. Bennett, *Inorg. Chem.,* **1976**, 15, 3126–3140; b) W. Levason, *Comments Inorg. Chem.,* **1990**, 9, 331–361.
[21] R. Hoppe and W. Dähne, *Naturwissenschaften*, **1962**, 49, 254-255.
[22] R. D. Feltham, R. S. Nyholm, A. Kasenally, *J. Organomet. Chem.,* **1967**, 7, 285-288.
[23] H. C. E. McFarlane, W. McFarlane, *Polyhedron,* **1983**, 2, 303-304.
[24] A. M. Aguiar, J. Beisler, *J. Org. Chem.,* **1964**, 29, 1660-1662.
[25] E. P. Kyba, S. T. Liu, R. L. Harris, *Organometallics*, **1983,** 2, 1877-1879.

Chapter 4

GeF_4 Complexes with Soft Group 15 Donor Ligands

4.1 Introduction:

Recent work within the group on hard O- or N-donor ligands such as phosphane oxides, amines and diimines, with GeF_4, shows the small, hard GeF_4 unit has a significantly greater affinity for these ligands than the other GeX_4 (X = Cl, Br or I) analogues.[1,2] As an extension to this work, this Chapter will look at the complexes formed with GeF_4 and soft donor ligands such as those used in Chapter 3, providing direct comparisons with the Sn(IV) analogues.

Before the recent work within the Group a few isolated studies on GeF_4 with hard N and O donor ligands had been carried out, resulting in the structural data for $[GeF_4\{bipy\}]$[3] (including its SiF_4 and SnF_4 analogues) and $[GeF_4\{OEt_2\}_2]$[4] (see Figure 1).

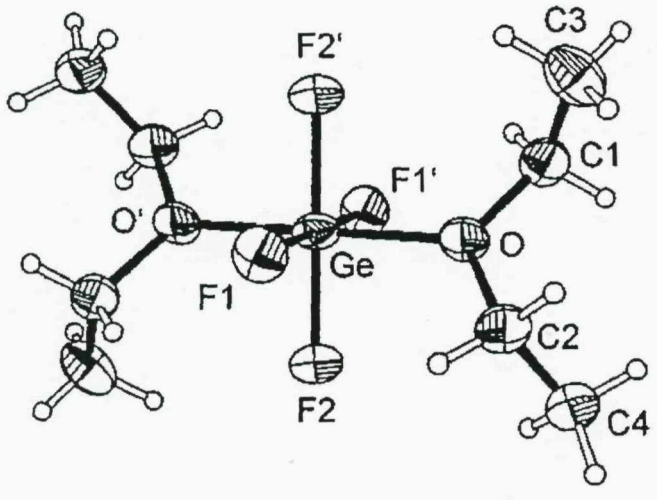

Figure 1 Molecular structure of $[GeF_4\{OEt_2\}_2]$ in the crystal as determined by low-temperature X-ray crystallography.[4]

A series of phosphane oxide and other oxygen donor complexes with GeF_4 was then reported along with full spectroscopic data and structural data on $[GeF_4\{OPR_3\}_2]$ where R = Me, Et and Ph.[1] Another series of complexes with nitrogen donor ligands and GeF_4 including macrocyclic ligands again giving full spectroscopic data and structural data on $[GeF_4\{py\}_2]$, $[GeF_4\{1,10\text{-phenanthroline}\}]$, $[GeF_4\{Me_2N(CH_2)_2NMe_2\}]$ and $[GeF_4\{Me_4\text{-cyclam}\}]$ was also reported.

Both papers also described similar reactions with the other Ge(IV) halides and supported the expected Lewis acidity trend of GeF_4 being the strongest Lewis acid of any Ge(IV) halide and the lower acceptor power for Ge compared with Sn.

In marked contrast to the very extensive chemistry with d-block metals, complexes of the p-block metals and metalloids with soft neutral ligands such as phosphanes or arsanes are rare. Whilst a variety of phosphane complexes are known for the heavier halides of Ga^{III}, In^{III}, Bi^{III} and Sn^{IV}, little is known about other Lewis acids in this block.[5,6,7,8,9,10,11] Complexes of the p-block fluorides with phosphanes are extremely rare, and apart from some very early work on SiF_4,[5] the only examples are from our study of SnF_4 adducts (Chapter 3),[12] which provided detailed spectroscopic and structural data on a range of complexes including $[SnF_4\{diphosphane\}]$ (diphosphane = *o*-$C_6H_4(PR_2)_2$, R = Me or Ph; $R_2P(CH_2)_2PR_2$, R = Me, Et, Cy or Ph) and *trans*-$[SnF_4\{PR_3\}_2]$ (R = Me or Cy). There are no reports of tertiary phosphane complexes of GeF_4, and with $GeCl_4$ the reports are few and appear contradictory. Beattie[13] and Ozin[14] reported the formation of *trans*-$[GeCl_4\{PMe_3\}_2]$ and $[GeX_4\{PMe_3\}]$ (X = Cl or Br) respectively, by reaction of GeX_4 and PMe_3 in the absence of a solvent, and used detailed IR and Raman spectroscopic studies to identify the products. In contrast, the reactions of PR_3 (R = ^{t}Bu or ^{i}Pr) with GeX_4 in benzene gave the redox products $[PR_3X][Ge^{II}X_3]$.[15,16,17] In a recent study by Godfrey *et al.*,[18] the reaction of $GeCl_4$ with a wide range of tertiary phosphanes (PR_3, R = Me, Et, ^{n}Pr, ^{n}Bu, Cy etc) in diethyl ether solution was found to give exclusively $[PR_3Cl][Ge^{II}Cl_3]$, identified by microanalysis, $^{31}P\{^1H\}$ NMR spectroscopy and by the crystal structure of $[P^nBu_3Cl][GeCl_3]$. Similar redox reactions occur with primary and secondary phosphanes, although the initial products often undergo further reaction with elimination of HX to form species such as R_2PGeX_3 or $RHPGeX_3$.[19] However, Godfrey *et al.*[18] were able to prepare and structurally characterise the first Ge(IV) arsane, *trans*-$[GeCl_4\{AsMe_3\}_2]$ (see Figure 2).

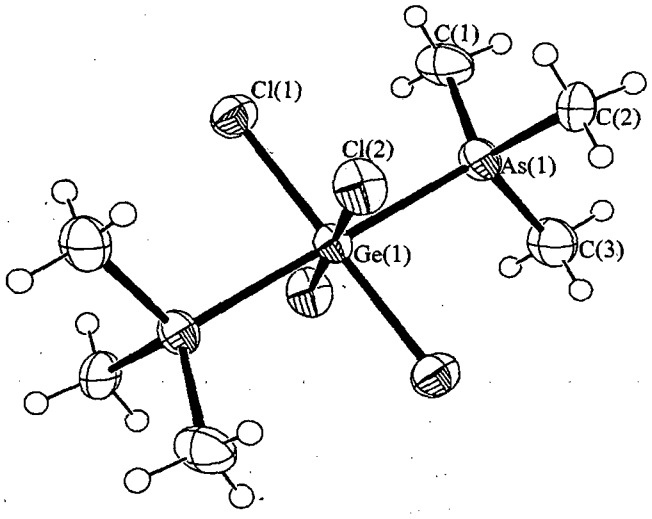

Figure 2 The crystal structure of the molecular germanium(IV) complex $[GeCl_4\{AsMe_3\}_2]$.[18]

The redox chemistry in the GeX_4/PR_3 reactions (at least under some conditions) contrasts with that of the SnX_4 systems where simple adduct formation occurs with the majority of phosphanes and diphosphanes.[8-14] It should be noted that P^tBu_3 and SnX_4 produce $[P^tBu_3X][SnX_3]$.[15-17]

This Chapter reports the synthesis, structural and spectroscopic characterisation of a series of phosphane complexes of GeF_4, further studies into the $GeCl_4$ and $GeBr_4$ reactions, and also studies of complexes of GeX_4 with arsane ligands.

4.2 GeF_4 Complexes of Monodentate Phosphanes:

Despite being able to use GeF_4 (a gas that sublimes at 236 K) directly in the syntheses, a solid precursor would be more convenient to handle. One possibility is $[GeF_4\{Et_2O\}_2]$,[20] but this sublimes and dissociates at near ambient temperatures and can only be handled under an atmosphere of Et_2O. The adduct $[GeF_4\{MeCN\}_2]$[21] is a more convenient precursor. The $[GeF_4\{MeCN\}_2]$ is made by bubbling GeF_4 into excess MeCN at room temperature when it separates as a white solid, which can be kept indefinitely in a glove box, although it vaporises slowly in a dynamic vacuum.

$$GeF_4 \xrightarrow{MeCN} [GeF_4\{MeCN\}_2]$$

Figure 3 Reaction scheme of $[GeF_4\{MeCN\}_2]$.

The IR spectrum shows three υ(CN) at 2333, 2295 and 2252 cm^{-1} and broad overlapping features assignable as υ(GeF) at 688, 657 and 639 cm^{-1}, suggesting a mixture of *cis* and *trans* isomers and too complicated for a 1:1 adduct only. In CD_2Cl_2 solution at ambient temperatures both the ^1H and $^{19}F\{^1H\}$ NMR spectra are single lines, but at 180 K the $^{19}F\{^1H\}$ NMR spectrum shows a singlet at –108.2 and two rather broad triplets δ = –101.2 and –134.2 ($^2J_{FF}$ ~55 Hz) attributable to *trans* and *cis* isomers respectively in approximate ratio 1:10, showing the complex is dynamic in solution down to quite low temperatures. The analogous complex $[GeF_4\{THF\}_2]$[22] was also produced for comparison and the $^{19}F\{^1H\}$ NMR spectrum is more clearly defined even at 223 K (see Figure 4). The ^1H NMR spectrum (243 K) of $[GeF_4\{THF\}_2]$ shows a broad multiplet at 2.0-2.1 ppm for the CH_2 backbone of the bonded THF but two broad peaks (probably triplets) at 4.20 and 4.31 ppm believed to be the OCH_2 resonances for the *cis* and *trans* isomers. The bidentate ether complex $[GeF_4\{MeO(CH_2)_2OMe\}]$ was also produced and gave the expected spectroscopic results and therefore, is not discussed further.[1]

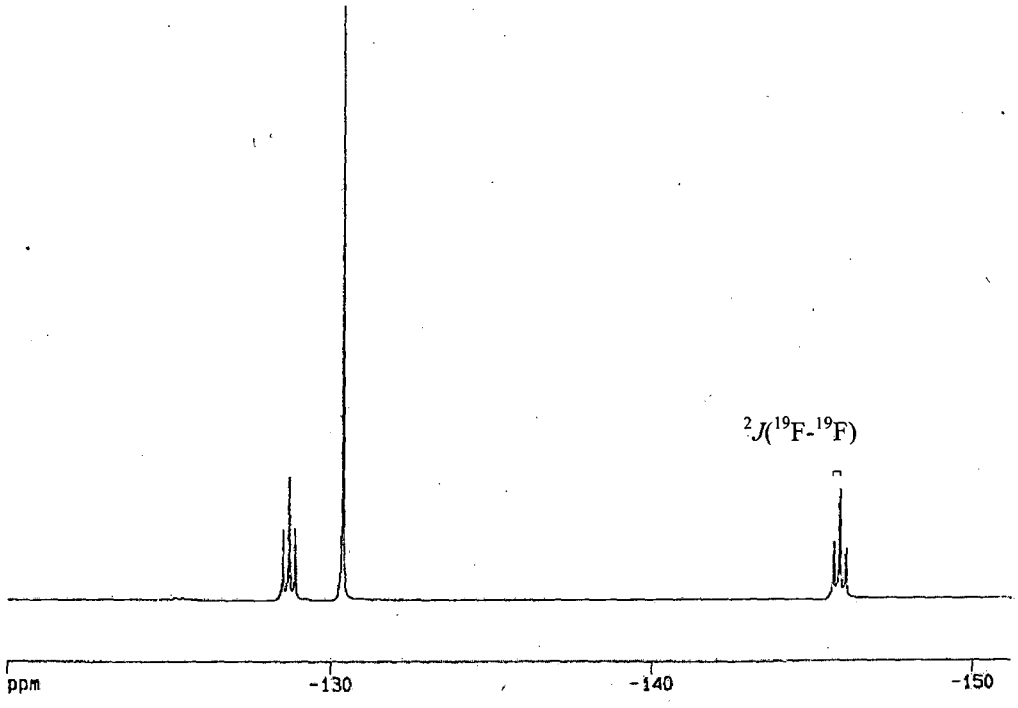

Figure 4 $^{19}F\{^1H\}$ NMR spectrum of $[GeF_4\{THF\}_2]$ (223 K, CH_2Cl_2).

The reaction of $[GeF_4\{MeCN\}_2]$[1] with two mol. equivalents of PMe_3 in anhydrous CH_2Cl_2 gave $[GeF_4\{PMe_3\}_2]$ as a white, moisture sensitive powder, only slightly soluble in chlorocarbons. The IR spectrum of $[GeF_4\{PMe_3\}_2]$ showed a broad absorption ν(GeF) at 575 cm^{-1} as expected with the *trans* isomer (Eu).

The ^1H NMR spectrum in CD_2Cl_2 solution contained a single doublet at δ = 1.46, $^2J_{PH}$ = 12 Hz, the $^{19}F\{^1H\}$ NMR spectrum is a 1:2:1 triplet at 273 K (see Figure 5) (singlet at 298 K), and was unchanged on cooling, showing only the *trans* isomer was present in detectable amounts.

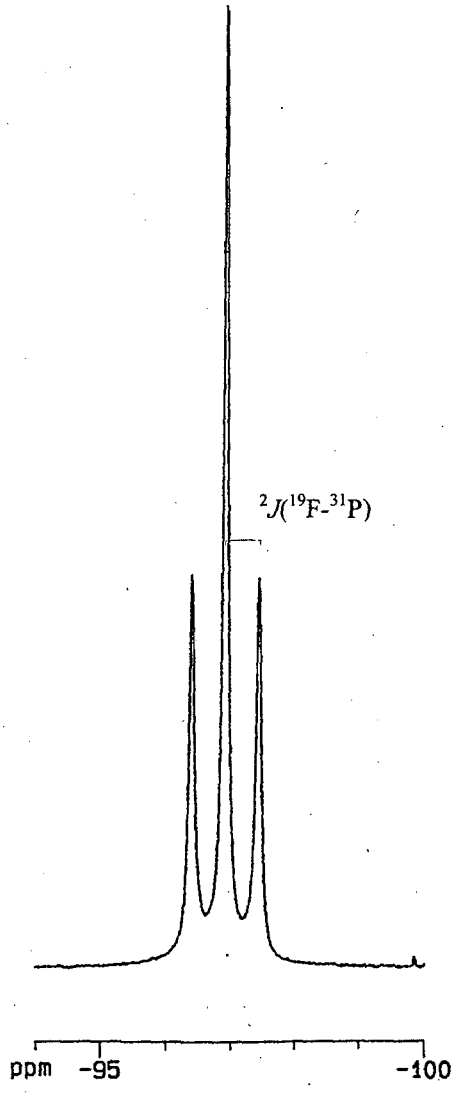

Figure 5 $^{19}F\{^1H\}$ NMR spectrum of $[GeF_4\{PMe_3\}_2]$ (273 K, $CDCl_3$).

As expected, the $^{31}P\{^{1}H\}$ NMR spectrum is a quintet at $\delta = -12.4$ ($^{2}J_{PF} = 196$ Hz) (Figure 6). The corresponding reaction using PPh_3 gave a white solid, *trans*-$[GeF_4\{PPh_3\}_2]$ which was easily soluble in chlorocarbons, but extensively dissociated at room temperature in solution. The IR spectrum again showed a broad absorption ν(GeF) at 607 cm^{-1} slightly shifted from the PMe_3 analogue. The $^{19}F\{^{1}H\}$ and $^{31}P\{^{1}H\}$ NMR data were recorded at 210 K and show the expected multiplets (similar to $[GeF_4\{PMe_3\}_2]$), but on warming >240 K the resonances are lost.

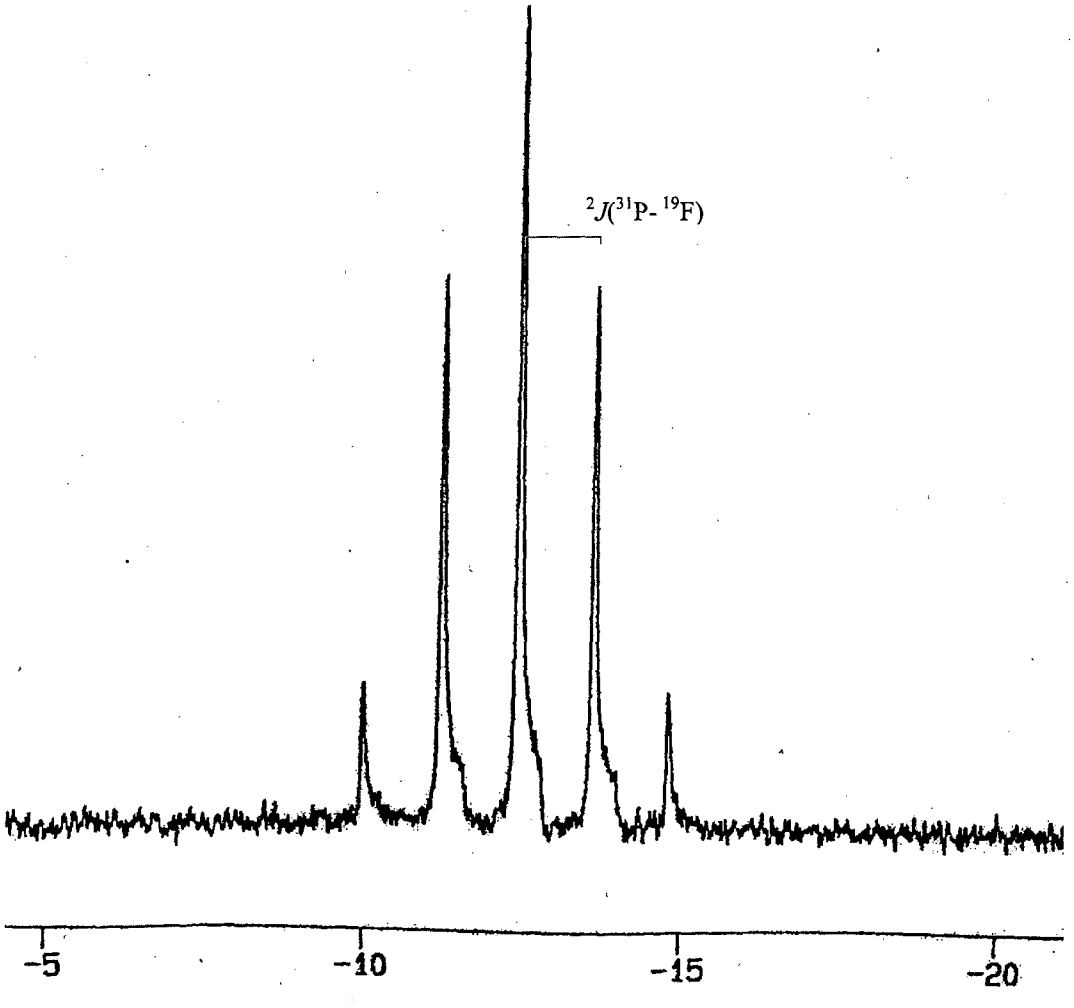

Figure 6 $^{31}P\{^{1}H\}$ NMR spectrum of $[GeF_4\{PMe_3\}_2]$ (268 K, CH_2Cl_2).

Attempts to isolate *trans*-$[GeF_4\{PCy_3\}_2]$ were unsuccessful, the products obtained were extremely moisture sensitive and NMR spectroscopic studies suggested a mixture of species was present.

In view of the easy chlorination of phosphanes by $GeCl_4$ (*vide infra*), the reaction of $[GeF_4\{MeCN\}_2]$ with excess molten PPh_3 was also carried out, which constitutes more forcing conditions. Examination of the products by $^{31}P\{^1H\}$ and $^{19}F\{^1H\}$ NMR spectroscopy revealed only *trans*-$[GeF_4\{PPh_3\}_2]$, traces of $[GeF_4\{OPPh_3\}_2]$[1] and excess PPh_3, and there is no evidence for fluorination of the ligand (to Ph_3PF_2).

4.3 Oxidation of GeF_4 Phosphanes:

Crystal growing attempts on $[GeF_4\{PR_3\}_2]$ (R = Me and Ph) produced single crystals which analysed by X-ray diffraction proved to be the corresponding phosphane oxide analogues $[GeF_4\{OPR_3\}_2]$ (R = Me and Ph). The structure of $[GeF_4\{OPMe_3\}_2]$ (Figure 7, Table 1) was obtained from a solution of $[GeF_4\{PMe_3\}_2]$ in $CH_2Cl_2/CDCl_3$. At the same time work on Ge(IV) halides with phosphane oxides and related oxygen donor ligands produced single crystals of X-ray quality.[1] These were obtained from the direct reaction of $[GeF_4\{MeCN\}_2]$ with 2 mol equiv. of $OPMe_3$ which proved to have the same parameters in the unit cell as those obtained serendipitously from the phosphane.

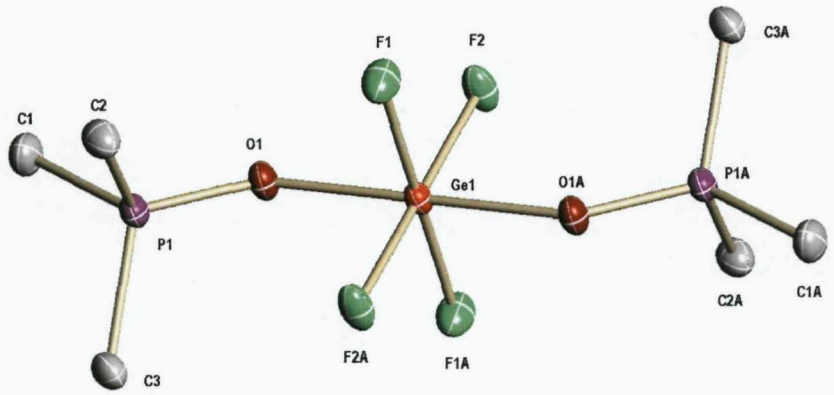

Figure 7 View of the molecule of $[GeF_4\{OPMe_3\}_2]$ with the atom numbering scheme adopted. Ellipsoids are drawn at the 50% probability level and H atoms are omitted for clarity. Symmetry operation: a = – x, – y, 1 – z.

Table 1 Selected bond lengths [Å] and angles [°] for $[GeF_4\{OPMe_3\}_2]$.[1]

Ge1–F1	1.777(2)	Ge1–F2	1.782(2)
Ge1–O1	1.903(2)	P1–O1	1.531(2)
F1–Ge1–F2	90.9 (1)	F1–Ge1–O1	90.8(1)
F1–Ge1–F2a	89.8(1)	F2–Ge1–O1	89.0(1)
Ge1–O1–P1	130.4(1)	O1–P1–C	108.2(1)–112.2(1)

Symmetry operation: a = – x, – y, 1 – z.

A solution of $[GeF_4\{PPh_3\}_2]$ in CH_2Cl_2 exposed to dry air also deposited crystals identified by an X-ray structure to be *trans*-$[GeF_4\{OPPh_3\}_2]$ (see Figure 8, Table 2),[1] and since PPh_3 is air stable in solution, this demonstrates that the reaction was promoted by the germanium complex. In view of the generation of $[PR_3X][GeX_3]$ in the cases of X = Cl or Br, which could hydrolyse to OPR_3, it was important to establish the source of the oxygen atoms incorporated. Exposure of a solution of $[GeF_4\{Ph_2P(CH_2)_2PPh_2\}]$ in CH_2Cl_2 to dry $^{18}O_2$ ($^{18}O_2$ not 100% enriched ~ 50:50 $^{18}O_2$:$^{16}O_2$) resulted in the slow formation of the diphosphane dioxide complex (monitored *in situ* by $^{31}P\{^1H\}$ NMR spectroscopy). After the reaction appeared complete the complex was decomposed by treatment with aqueous NaOH, and separation of the organic layer, drying and evaporation produced a white solid. The EI mass spectrum of this solid showed a base peak at *m/z* = 433 and 357 corresponding to $[Ph_2P(^{18}O)(CH_2)_2P(^{18}O)PPh_2–H]^+$ and $[Ph_2P(^{18}O)(CH_2)_2P(^{18}O)PPh_2–Ph]^+$, the IR spectrum showed υ(PO) at 1153 cm^{-1}. The EI mass spectrum also showed peaks at *m/z* = 431 and 429 corresponding to $[Ph_2P(^{18}O)(CH_2)_2P(^{16}O)PPh_2–H]^+$ and $[Ph_2P(^{16}O)(CH_2)_2P(^{16}O)PPh_2–H]^+$ as well as 355 and 353 which is $[Ph_2P(^{18}O)(CH_2)_2P(^{16}O)PPh_2–Ph]^+$ and $[Ph_2P(^{16}O)(CH_2)_2P(^{16}O)PPh_2–Ph]^+$. The $Ph_2P(^{16}O)(CH_2)_2P(^{16}O)PPh_2$ exhibits υ(PO) at 1177 cm^{-1}, and the simple diatomic oscillator (see below) model predicts the effect of ^{18}O substitution will lower this vibration to 1133 cm^{-1}.

By considering the P=O as a spring, the frequency of absorbance, ν can be calculated:

$$\nu = \frac{1}{2\pi}\sqrt{\frac{k}{\mu}}$$

where k is the force constant for the bond, and μ is the reduced mass of the P=O system:

$$\mu = \frac{m_P m_O}{m_P + m_O}$$

(m_i is the mass of atom i).

If $\nu(^{31}P=^{16}O)$ = 1177 then k can be worked out using $\mu(^{31}P=^{16}O)$. Using $\mu(^{31}P=^{18}O)$ and k then gives the value of $\nu(^{31}P=^{18}O)$ = 1133.

Coupling with the υ(PC) mode at ~1120cm^{-1} probably causes the higher frequency observed experimentally.[23] Thus, like SnX_4,[12,23] GeF_4 promotes air/dioxygen oxidation of phosphanes (as seen in both cases), although the reaction is considerably slower with germanium.

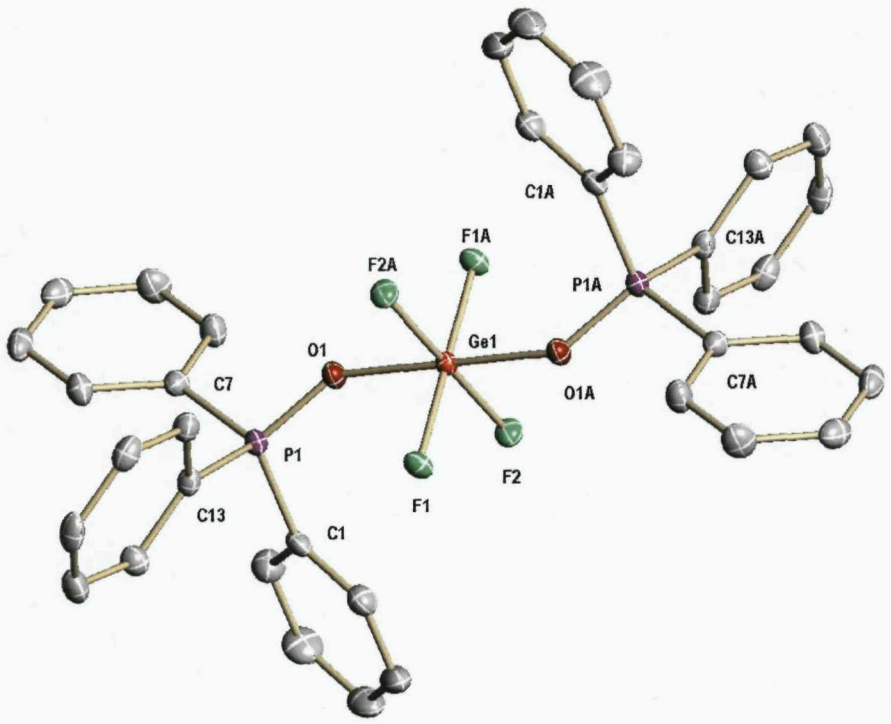

Figure 8 View of the molecule of for $[GeF_4\{OPPh_3\}_2]$ with the atom numbering scheme adopted. Ellipsoids are drawn at the 50% probability level and H atoms are omitted for clarity. Symmetry operation: a = 1 – x, 1 – y, 1 – z.

Table 2 Selected bond lengths [Å] and angles [°] for $[GeF_4\{OPPh_3\}_2]\cdot 2CH_2Cl_2$.

Ge–F1	1.774(1)	Ge–F2	1.772(1)
Ge–O1	1.925(2)	P1–O1	1.522(2)
F1–Ge–F2	89.53(6)	F1–Ge1–O1	91.76(6)
F2–Ge1–O1	90.82(6)	Ge1–O1–P1	142.5(1)
O1–P1–C	107.4(1)–113.51		

4.4 GeF_4 Complexes of Bidentate Phosphanes:

The reactions of $[GeF_4\{MeCN\}_2]$ with the diphosphanes $R_2P(CH_2)_2PR_2$ (R = Me, Et, Ph or Cy) and *o*-$C_6H_4(PR_2)_2$ (R = Me or Ph) in anhydrous CH_2Cl_2 readily gave the *cis*-$[GeF_4\{diphosphane\}]$ as white powders, which can be handled briefly in air with no detectable decomposition. Like the tin analogues (Chapter 3) the solids tenaciously retain chlorinated solvents (evident in the ^1H NMR spectra).

The complexes exhibit several strong, overlapping υ(Ge–F) vibrations in their IR spectra in the range 620–560 cm^{-1} (Table 3).

Table 3 IR[a] spectroscopic data of the GeF_4 bidentate phosphanes

Compound	ν(Ge-F)/cm^{-1}
$[GeF_4\{o\text{-}C_6H_4(PMe_2)_2\}]$	607(br), 580(sh), 567(br)
$[GeF_4\{o\text{-}C_6H_4(PPh_2)_2\}]$	619(s), 607(vs, br)
$[GeF_4\{Et_2P(CH_2)_2PEt_2\}]$	605(sh), 577(vbr), 560(sh)
$[GeF_4\{Me_2P(CH_2)_2PMe_2\}]$	565(vbr)
$[GeF_4\{Ph_2P(CH_2)_2PPh_2\}]$	603(s), 586(br)
$[GeF_4\{Cy_2P(CH_2)_2PCy_2\}]$	592(s,vbr)

a Nujol mull.

The $[GeF_4\{Me_2P(CH_2)_2PMe_2\}]$ is only slightly soluble in CH_2Cl_2 but the other complexes dissolve easily in chlorocarbons. The ^1H NMR spectra in CD_2Cl_2 or $CDCl_3$ solution at 295 K are simple, showing only coordinated diphosphane ligands present. At ambient temperatures both the $^{19}F\{^1H\}$ and $^{31}P\{^1H\}$ NMR spectra are broad lines with ill-defined or unresolved couplings, indicative of reversible dissociation or chelate ring-opening on the appropriate NMR time-scales. On moderate cooling of the solutions (273–217 K depending on the ligand present), the resonances sharpen and show the coupling patterns expected for *cis*-octahedral complexes (Table 4).[12]

Table 4 Selected NMR data for GeF_4 complexes with phospane ligands.[a]

Compound	$\delta\ ^{31}P\{^1H\}$[b]	Δ[c]	$\delta\ ^{19}F\{^1H\}$	$^2J(^{31}P-^{19}F)$	$^2J(^{19}F-^{19}F)$
$[GeF_4\{o\text{-}C_6H_4(PMe_2)_2\}]$	−31.7(t,d,d)	23	−97.2(t,t),−126.0(d,d,t)	77, 135, 155(t)	54
$[GeF_4\{o\text{-}C_6H_4(PPh_2)_2\}]$	−17.1(t,d,d)	−4	−81.9(t,t),−121.9(d,d,t)	64, 110, 129(t)	65
$[GeF_4\{Et_2P(CH_2)_2PEt_2\}]$	−9.2(t,d,d)	9	−91.9(t,t),−113.6(d,d,t)	66, 131, 136(t)	55
$[GeF_4\{Me_2P(CH_2)_2PMe_2\}]$	−24.6(t,d,d)	23	−96.2(t,t),−121.2(d,d,t)	80, 135, 149(t)	55
$[GeF_4\{Ph_2P(CH_2)_2PPh_2\}]$	−17.1(t,d,d)	−4	−73.7(t,t),−110.3(d,d,t)	64, 119, 151(t)	61
$[GeF_4\{Cy_2P(CH_2)_2PCy_2\}]$	−8.7(t,d,d)	−11	−81.2(t,t),−103.1(d,d,t)	60, 121, 122(t)	57
trans-$[GeF_4\{PMe_3\}_2]$	$-12.4(q^5)$	50	−96.9(t)	196	
trans-$[GeF_4\{PPh_3\}_2]$[d]	$2.8(q^5)$	8	−70.6(t)	180	

[a] In CH_2Cl_2-10% $CDCl_3$. Spectra were typically recorded at 240 K to resolve couplings (see text). [b] Ligand chemical shifts are: *o*-$C_6H_4(PMe_2)_2$ −55; *o*-$C_6H_4(PPh_2)_2$ −13; $Ph_2P(CH_2)_2PPh_2$ −13; $Et_2P(CH_2)_2PEt_2$ −18; $Me_2P(CH_2)_2PMe_2$ −48; $Cy_2P(CH_2)_2PCy_2$ +2; PMe_3 −62; PPh_3 −6. [c] Coordination shift ($\delta_{complex} - \delta_{ligand}$). [d] At 190 K. Resonances disappear >240 K.

The $^{31}P\{^{1}H\}$ spectra are 12 line patterns (d,d,t) although some overlap is seen depending on the coupling constants (see Figure 9).

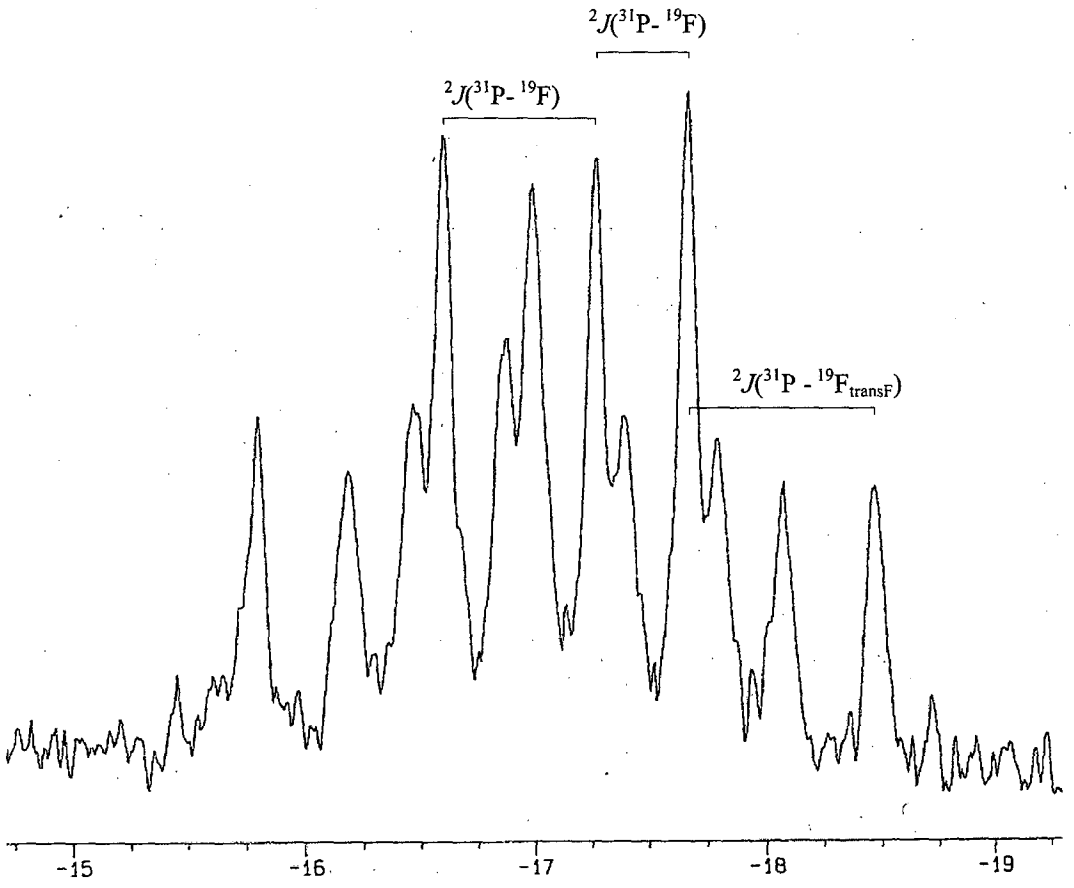

Figure 9 $^{31}P\{^{1}H\}$ NMR spectrum of $[GeF_4\{o\text{-}C_6H_4(PPh_2)_2\}]$ (223 K, $CDCl_3$).

The $^{19}F\{^{1}H\}$ NMR spectra show two resonances; a t,t (see Figure 10) for the two axial fluorines and a d,d,t for the fluorines *trans* to phosphorus (similar in pattern to that seen in Figure 9). The chemical shifts and coupling constants are shown in Table 4. Notably the spectra show no other species present in significant amounts and are unchanged after the solutions have been allowed to stand for several hours.

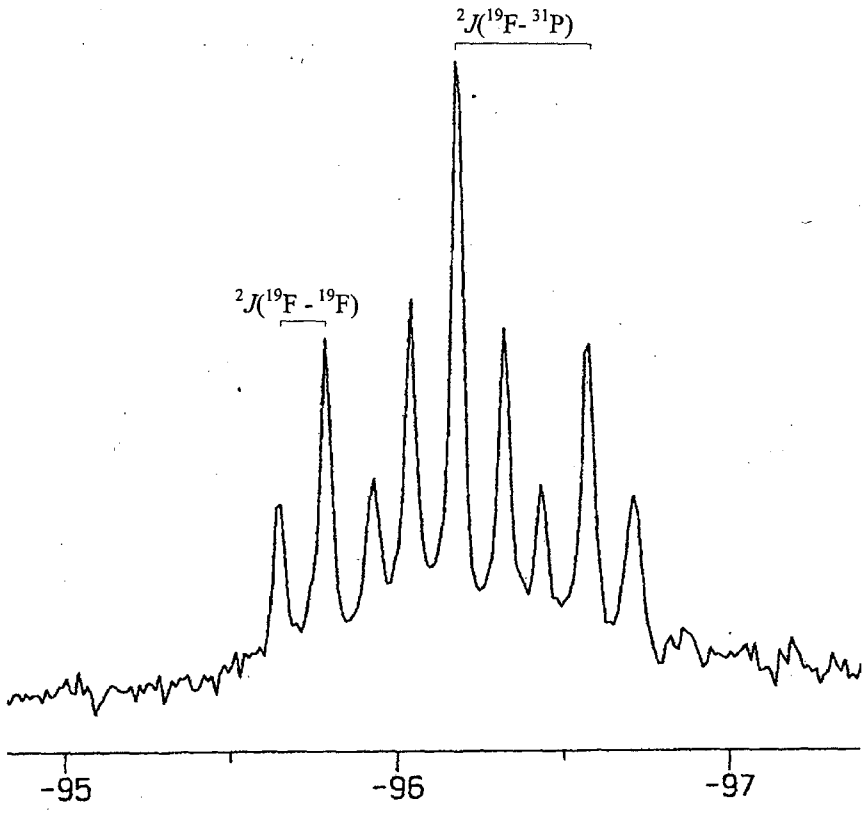

Figure 10 Partial $^{19}F\{^1H\}$ NMR spectrum of the *trans* F-Ge-F environment in $[GeF_4\{Me_2P(CH_2)_2PMe_2\}]$ (228 K, CD_2Cl_2).

The $^{31}P\{^1H\}$ chemical shifts are very similar to those observed in the analogous $[SnF_4\{diphosphane\}]$ complexes,[12] and as in those cases the coordination shifts Δ ($\Delta = \delta_{complex} - \delta_{ligand}$) are irregular, although generally the stronger σ-donor ligands produce high frequency coordination shifts and the weaker donor aryl-diphosphanes low frequency shifts. Only the $[GeF_4\{Cy_2P(CH_2)_2PCy_2\}]$ does not conform to this pattern, exhibiting a coordination shift of –11, despite being a strong σ-donor. It is likely that steric factors from this bulky ligand on the small germanium centre are a major contributor here. These erratic coordination shifts are seen in phosphane complexes of Sn^{IV} [8,12] and Ga^{III},[24,25] but the cause is presently unclear. The $^{19}F\{^1H\}$ chemical shifts are to high frequency of those observed in the $[SnF_4\{diphosphane\}]$ analogues[12] and the $^2J_{FF}$ and $^2J_{PF}$ couplings are larger in the germanium systems. Similar $^2J_{FF}$ values (50–60 Hz) are found in *cis*-$[GeF_4\{OPR_3\}_2]$[1] and in $[GeF_4\{L–L\}]$ (L–L = 2,2'-bipyridyl, 1,10-phenanthroline, $Me_2N(CH_2)_2NMe_2$),[2] although rather larger values (70–80 Hz) are seen in $[GeF_4\{RS(CH_2)_2SR\}]$ (see Chapter 5).[26]

Confirmation of the [GeF_4{diphosphane}] constitution was provided by the X-ray crystal structure of [$GeF_4\{o\text{-}C_6H_4(PMe_2)_2\}$] (Figure 11, Table 5). The germanium environment is approximately octahedral with the angles F–Ge–F slightly greater than 90°, F–Ge–P slightly less than 90°, and P–Ge–P 85.61(4)°. As observed in GeF_4 complexes with N- or O-donor ligands,[1,2] $Ge–F_{transF}$ (1.809(2), 1.815(2) Å) are longer than $Ge–F_{transP}$ (1.765(2), 1.772(2) Å).

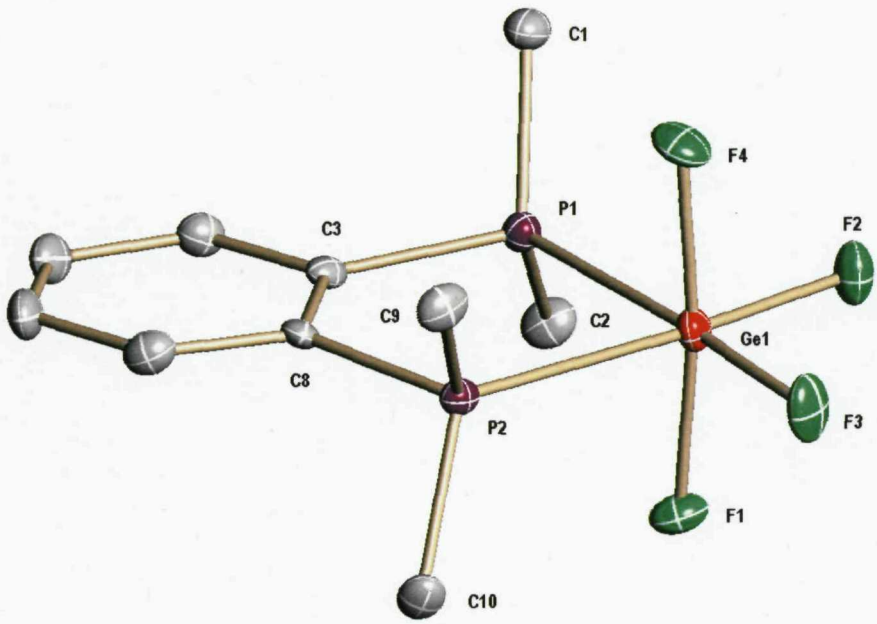

Figure 11 Structure of [$GeF_4\{o\text{-}C_6H_4(PMe_2)_2\}$] with the atom numbering scheme adopted. H atoms are omitted for clarity and displacement ellipsoids are shown at the 50% probability level.

Table 5 Selected bond lengths (Å) and angles (°) for [$GeF_4\{o\text{-}C_6H_4(PMe_2)_2\}$]

Ge1–F1	1.815(2)	Ge1–F3	1.772(2)
Ge1–F2	1.765(2)	Ge1–F4	1.809(2)
Ge1–P1	2.4273(12)	Ge1–P2	2.4271(11)
F2–Ge1–F3	93.91(10)	F2–Ge1–F4	92.49(12)
F3–Ge1–F4	93.18(12)	F2–Ge1–F1	92.76(12)
F3–Ge1–F1	91.56(12)	F2–Ge1–P1	89.80(8)
F4–Ge1–P1	87.65(9)	F1–Ge1–P1	87.26(8)
F3–Ge1– P2	90.70(9)	F4–Ge1–P2	86.77(9)
F1–Ge1–P2	87.59(8)	P1–Ge1–P2	85.61(4)

An X-ray crystal structure of $[GeF_4\{Ph_2P(CH_2)_2PPh_2\}]$ (Figure 12, Table 6) was also obtained with similar patterns of bond lengths and angles found although the Ge–P bonds are slightly longer in the complex of the aryl-diphosphane, possibly due to its weaker σ-donation.

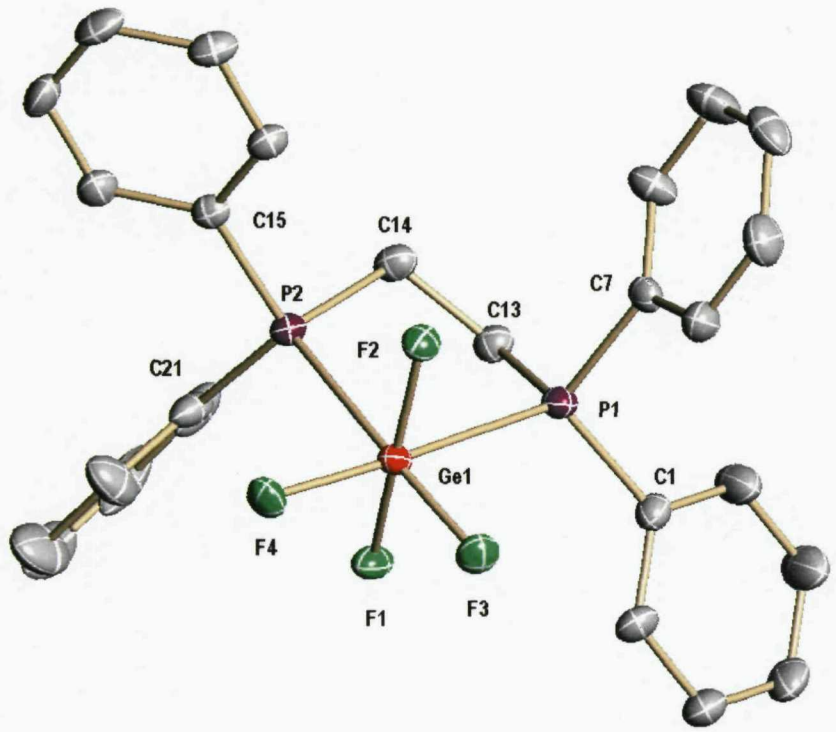

Figure 12 Structure of $[GeF_4\{Ph_2P(CH_2)_2PPh_2\}]$ with the atom numbering scheme adopted. H atoms are omitted for clarity and displacement ellipsoids are shown at the 50% probability level. Only the ipso C atom labels are shown and C atoms are numbered cyclically round the ring starting at the label shown.

Table 6 Selected bond lengths (Å) and angles (°) for $[GeF_4\{Ph_2P(CH_2)_2PPh_2\}]$

Ge1–F1	1.7987(14)	Ge1–F3	1.7731(14)
Ge1–F2	1.7829(13)	Ge1–F4	1.7692(14)
Ge1–P1	2.4636(7)	Ge1–P2	2.4822(7)
F4–Ge1–F3	93.21(7)	F4–Ge1–F2	93.44(6)
F3–Ge1–F2	93.44(7)	F2–Ge1–F1	93.02(7)
F4–Ge1–F1	92.71(7)	F2–Ge1–P1	89.28(4)
F4–Ge1–P2	90.18(5)	F1–Ge1–P1	83.94(5)

F2–Ge1–P2	88.08(5)	F1–Ge1–P2	85.08(5)
F3–Ge1–P1	92.44(5)	P1–Ge1–P2	84.08(2)

4.5 GeF_4 Complexes of Arsanes:

The reaction of $[GeF_4\{MeCN\}_2]$ with *o*-$C_6H_4(AsMe_2)_2$ in CH_2Cl_2 affords a white solid believed to be $[GeF_4\{o\text{-}C_6H_4(AsMe_2)_2\}]$. The ^1H NMR spectrum in CD_2Cl_2 shows the δ(Me) resonance is shifted to high frequency from that in the ligand, but the solution does not exhibit any $^{19}F\{^1H\}$ NMR resonances >220 K. Below this temperature two triplets are present (only sharpening at 178K) (δ = −77.7, −118.1, $^2J_{FF}$ = 66 Hz) with similar values to those in the $[GeF_4\{diphosphane\}]$ complexes (Table 4) all pointing to typical "*cis*"-GeF_4 units. Repeated attempts to obtain a microanalysis however, consistently yielded low values of both C and H. There appeared to be no complex formation between GeF_4 and the weaker σ-donor $Ph_2As(CH_2CH_2)AsPh_2$. Reaction with the tridentate arsane $MeC(CH_2AsMe_2)_3$ gave a cream/white solid with IR bands at appropriate positions for Ge-F and no MeCN, however, the ^1H NMR spectrum showed only free ligand and $^{19}F\{^1H\}$ NMR showed only a singlet (-132.1 ppm) at 179 K. Microanalysis again yielded low values of both C and H.

The reaction of $AsMe_3$ or $AsEt_3$ with $[GeF_4\{MeCN\}_2]$ in CH_2Cl_2 afforded white solids of variable composition which were not identified, probably due to incomplete displacement of the nitrile. Bubbling GeF_4 into a solution of $AsMe_3$ in *n*-hexane was more successful, producing a white, very moisture sensitive solid. In solution in CD_2Cl_2 the ^1H NMR spectrum at 243 K shows a singlet at δ = 1.26 and some free $AsMe_3$ (δ = 0.87), whilst the corresponding $^{19}F\{^1H\}$ NMR spectrum (243 K) contains two broad features at δ = −127 and −149. On further cooling of the solution these two resonances resolve into triplets of equal intensity, leading to a tentative assignment of the species present as *cis*-$[GeF_4\{AsMe_3\}_2]$ (curiously no evidence for the *trans* isomer was seen). In the solid state the IR spectrum shows υ(Ge–F) at 646, 635 and 600(sh) cm^{-1}, the Raman has corresponding bands at 642 and 597 cm^{-1} which are also consistent with a *cis* isomer. Notably there are no Raman features in the region of ~500 cm^{-1} where the a_{1g} mode of the *trans* isomer is expected (*cf* the tertiary phosphane

complexes above). Microanalytical data on the GeF_4/AsR_3 systems gave results that reproducibly approximate to 1:1 compounds and notably the spectroscopic data (see Experimental Section) would be consistent with either a *cis* disubstituted octahedron or an equatorially substituted trigonal bipyramid (Figure 13). Efforts to obtain crystals of the complex have been unsuccessful and so their precise nature remains unclear.

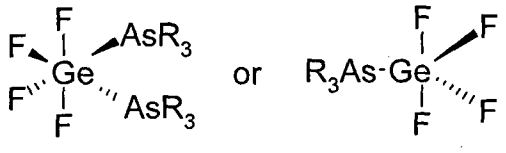

Figure 13 Possible complexes formed.

Thus, although GeF_4 forms adducts with some arsane ligands, these appear extensively dissociated in solution and far less stable than the phosphane analogues – a pattern also observed in the SnF_4 systems.[12] However, while isolation of pure complexes in the tin systems is complicated by the "SnF_4" formed on dissociation, precipitating as polymeric $[SnF_4]_n$, in the germanium systems dissociation simply forms GeF_4 monomer, and the instability is therefore a direct result of the low affinity of the hard germanium Lewis acid for the soft arsenic centre.

4.6 GeX_4 Complexes of Monodentate Phosphanes and Arsanes:

Following the successful characterisation of the phosphane adducts of GeF_4, the $GeCl_4/PMe_3$ reaction was then re-examined in an attempt to elucidate the apparently contradictory literature,[13,18] and found that the reports of Beattie[13] and Godfrey[18] are both valid, and that the species formed are extremely dependent upon the conditions. Distillation of $GeCl_4$ onto neat PMe_3 at 77K followed by slow thawing gave a vigorous reaction on melting which was moderated by judicious cooling, resulting in formation of a white powder. The Raman spectrum of this product (Figure 14a) was in excellent agreement with that reported by Beattié with a *very strong* feature at 267 cm^{-1} assigned as the a_{1g} vibration of *trans*-$[GeCl_4\{PMe_3\}_2]$ (lit.[13] 268 cm^{-1}). The values of the corresponding vibration in the crystallographically characterised *trans*-$[GeCl_4\{AsR_3\}_2]$ (see below) are also in this region. The sample was then

dissolved in rigorously dry CH_2Cl_2 and the mixture immediately pumped to dryness. The Raman spectrum of this sample showed the features of the initial spectrum and some new bands in the region below 350 cm^{-1}. The sample was redissolved in CH_2Cl_2, allowed to stand for 3h and then taken to dryness. The Raman spectrum of this sample (Figure 14b) showed loss of the 267 cm^{-1} feature, but new medium intensity bands at 314 and 260 cm^{-1} (and 2 others from the cation) which correspond to $[GeCl_3]^-$, ($[NBu_4][GeCl_3]$ has features at 320, 255 cm^{-1}).[27] From the comparison of the intensities of ν(CH) modes (not shown) it is clear the band in 14a is significantly more intense than those of 14b.

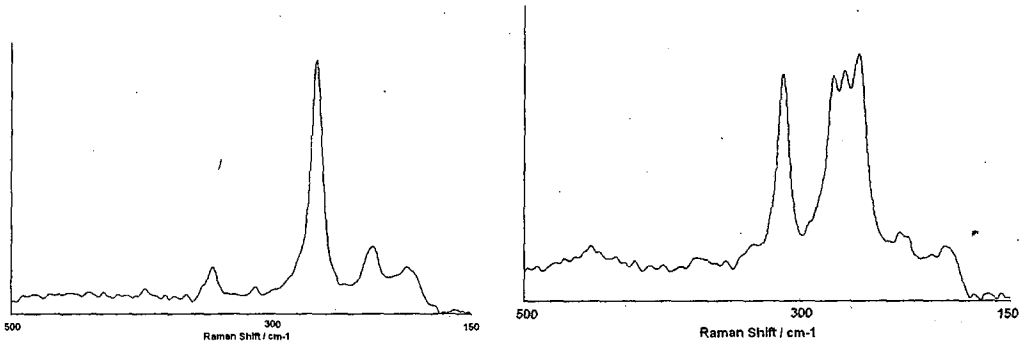

Figure 14 Raman spectra of $[GeCl_4\{PMe_3\}_2]$ (left 14a) and $[GeCl_3][PMe_3Cl]$ (right 14b).

The reactions can also be monitored by NMR spectroscopy. The initial solid, was dissolved in CH_2Cl_2 at 273 K and then immediately cooled to 200 K, does not show a $^{31}P\{^1H\}$ NMR resonance from the initial complex, but on standing a new feature at δ = +92 attributable*[28] to $[PMe_3Cl]^+$ appeared. The absence of a phosphorus resonance for the Ge(IV) complex is consistent with extensive dissociation/fast exchange even at low temperatures. This explanation is supported by the ^1H NMR spectrum of *trans*-$[GeCl_4\{PMe_3\}_2]$ obtained immediately after dissolution in $CDCl_3$ which shows a doublet at δ = 2.75, $^2J_{PH}$ = 13.5 Hz (assigned to $[PMe_3Cl]^+$) and a doublet at δ = 1.8, $^2J_{PH}$ = 13 Hz for the Ge(IV) complex. Trace hydrolysis of the solution also produces $[PMe_3H][GeCl_3]$ δ(^{31}P) = −4.9, and from such an hydrolysed sample we obtained crystals identified by their unit cell as $[PMe_3H][GeCl_3]$.[29]

* The observed ^{31}P chemical shift of "$[PMe_3Cl]^+$" seems to vary with solvent, concentration and anion, probably due to the subtle speciation involving $[PMe_3Cl]^+$, Me_3PCl_2 and Me_3PCl^-Cl forms (see Ref. 28 and refs therein).

Hence, as described by Beattie,[13] the reaction of $GeCl_4$ with PMe_3 in the absence of a solvent does indeed give *trans*-$[GeCl_4\{PMe_3\}_2]$, but this rapidly rearranges in solution in chlorocarbons or ethers to $[PMe_3Cl][GeCl_3]$, and the latter is obtained when the reaction is performed in solution.[15-18] The recrystallisation of $[GeCl_4\{PMe_3\}_2]$ from hot $GeCl_4$ was reported to give $[GeCl_4\{PMe_3\}]$ believed to be an axially substituted trigonal bypyramidal molecule,[14] however the reported Raman spectrum is very similar to that of $[PMe_3Cl][GeCl_3]$ and suggests the latter is the correct formulation. $GeBr_4$ and PMe_3 was also reacted in the absence of solvent and a cream powder was obtained with a Raman spectrum identical to that reported for $[GeBr_4\{PMe_3\}]$.[14] In this case also, the strongest features in the low energy region correspond to $[GeBr_3]^-$, and on dissolution in dry CH_2Cl_2 the $^{31}P\{^1H\}$ NMR resonance is found at $\delta = +68$, corresponding to $[PMe_3Br]^+$.

Re-examination of other tertiary phosphanes was not carried out, but it seems likely that similar reactions would occur with initial formation of a tetrachlorogermanium(IV) adduct which then (especially in solution) undergoes a redox reaction to form $[PR_3Cl][GeCl_3]$ – in some cases the rearrangement may be so rapid that the Ge(IV) species is only a transient intermediate. The $GeBr_4/PMe_3$ reaction appears to give $[PMe_3Br][GeBr_3]$ without any evidence that a Ge(IV) complex is isolable. The Raman spectrum of the cream powder produced is identical to that reported[14] for $[GeBr_4\{PMe_3\}]$ but this also corresponds to $[GeBr_3]^-$. On dissolution in dry CH_2Cl_2 the $^{31}P\{^1H\}$ NMR resonance is found at $\delta = +68$, probably corresponding to $[PMe_3Br]^+$. In contrast, the silicon(IV) and tin(IV) complexes are stable (although very moisture sensitive) and *trans*-$[SiCl_4\{PMe_3\}_2]$[30] and several SnX_4-phosphane complexes[8,12] have been authenticated by X-ray crystal structures.

In the hope of obtaining more stable Ge(IV) complexes, the reaction of the bidentate $Me_2P(CH_2)_2PMe_2$ with $GeCl_4$ was examined under a variety of reaction conditions (mixed in the absence of solvent, in solution in CH_2Cl_2 or Et_2O, at room or low temperatures) and monitored reactions by *in situ* $^{31}P\{^1H\}$ NMR spectroscopy. The reactions are very sensitive to the conditions and resonances due to mono- and di-chlorinated as well as protonated phosphane groups could be identified, the relative amounts varying with conditions and reaction times,

and with trace hydrolysis in some samples. Resonances due to $[GeCl_4\{Me_2P(CH_2)_2PMe_2\}]$ were not unequivocally identified in the ^1H or $^{31}P\{^1H\}$ NMR spectra, although this may be due to fast dissociative ligand exchange even at low temperature. The only species identified crystallographically were $[GeCl_3]^-$ salts with $[Me_2PH(CH_2)_2PHMe_2]^{2+}$ or $[Me_2P(O)(CH_2)_2P(O)Me_2H]^+$ deposited over several days or weeks (Figure 15, Figure 16, Table 7 and Table 8). It is concluded that the reactions of the diphosphane with $GeCl_4$ are similar to those with PMe_3, with the trichlorogermanate(II) as the final product.

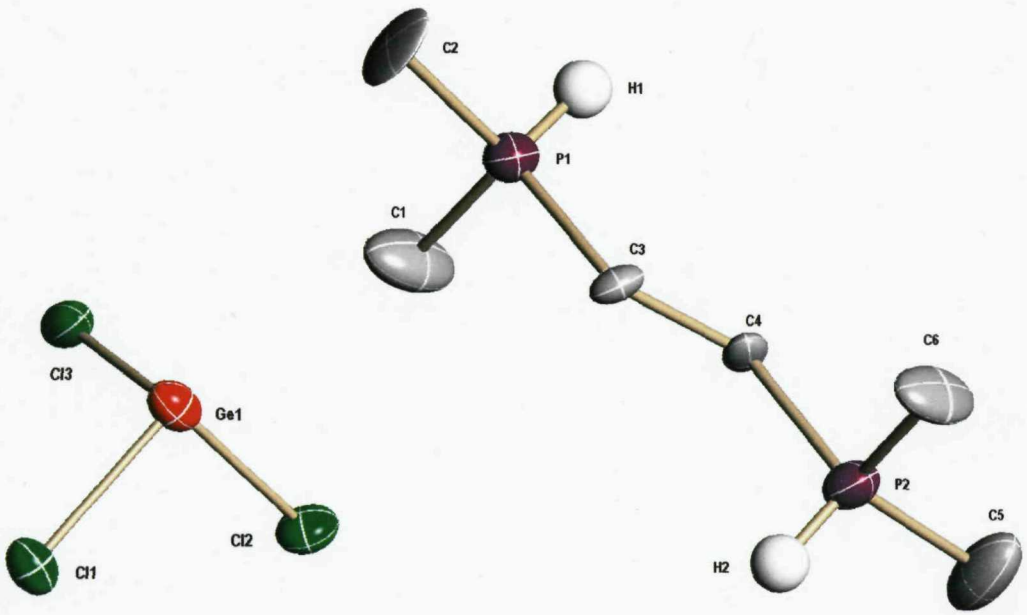

Figure 15 Structure of one of the two cations and one of the four anions of $[Me_2P(H)(CH_2)_2P(H)Me_2][GeCl_3]_2$ with the atom numbering scheme adopted. H atoms are omitted for clarity and displacement ellipsoids are shown at the 50% probability level.

Table 7 Selected bond lengths (Å) and angles (°) for $[Me_2P(H)(CH_2)_2P(H)Me_2][GeCl_3]_2$

Ge1–Cl1	2.3000(8)	Ge3–Cl7	2.318(3)
Ge1–Cl2	2.3087(8)	Ge3–Cl8	2.310(3)
Ge1–Cl3	2.3059(7)	Ge3–Cl9	2.324(3)
Ge2–Cl4	2.300(3)	Ge4–Cl10	2.299(4)
Ge2–Cl5	2.303(4)	Ge4–Cl11	2.311(4)

Ge2–Cl6	2.283(4)	Ge4–Cl12	2.285(3)
P–C(Me)	1.759(11)–1.788(13)		
Cl–Ge1–Cl	93.24(13)–95.08(12)	Cl–Ge3–Cl	93.78(12)–95.34(13)
Cl–Ge2–Cl	95.75(13)–96.10(14)	Cl–Ge4–Cl	94.71(13)– 96.10(13)

The cation H atoms bonded to P were not convincingly located in later difference electron-density maps and were introduced in calculated positions. The other cation and anions are very similar.

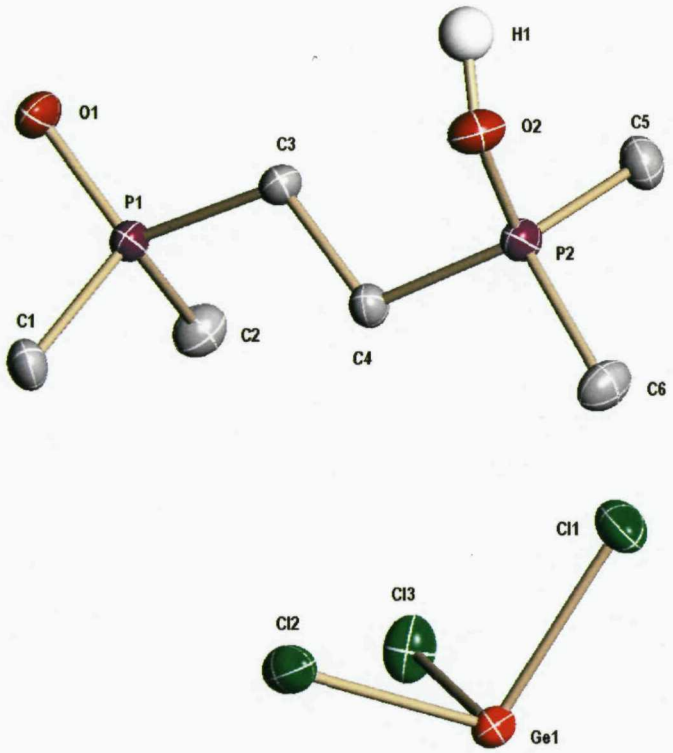

Figure 16 Structure of $[Me_2P(O)(CH_2)_2P(O)Me_2H][GeCl_3]$ with the atom numbering scheme adopted. H atoms are omitted for clarity and displacement ellipsoids are shown at the 50% probability level. H1 was identified in later electron-density maps but not refined. H1 is involved in H-bonding O2–H1···O1' where O1' is from an adjacent molecule. Note that P2–O2 is only a little longer than P1–O1 (see Table 8).

Table 8 Selected bond lengths (Å) and angles (°) for $[Me_2P(O)(CH_2)_2P(O)Me_2H][GeCl_3]$

Ge1–Cl1	2.3000(8)	Ge1–Cl2	2.3087(8)
Ge1–Cl3	2.3059(7)	P1–O1	1.5147(17)
P2–O2	1.5409(17)	P–C(Me)	1.773(2)–1.784(2)
Cl1–Ge1–Cl2	96.76(3)	Cl1–Ge1–Cl3	96.66(3)
Cl2–Ge1–Cl3	95.00(3)		

The ease of reduction of GeX_4 (X = Cl or Br) by phosphanes compared with SnX_4 or SiX_4, (or the relative instability of the $[GeX_4\{PR_3\}_2]$), may be an example in germanium chemistry of the lower stability of the element of Period 4 in the group oxidation state compared with analogues in Periods 3 or 5. This effect is well known for As^V, Se^{VI} and Br^{VII} and is usually rationalised as the result of increased nuclear charge from the 3d transition metals not completely balanced by screening from the 3d electrons.[31]

The reaction of $GeCl_4$ with $AsMe_3$ in CH_2Cl_2 or Et_2O at ambient temperatures, produced colourless crystals of *trans*-$[GeCl_4\{AsMe_3\}_2]$ which were identified by comparison of their unit cell with the literature data (see also Figure 2).[18] A similar reaction using $AsEt_3$ in CH_2Cl_2 followed by rapid isolation of the product gave white *trans*-$[GeCl_4\{AsEt_3\}_2]$ and crystals obtained from CH_2Cl_2 showed a similar structure (Figure 17, Table 9).

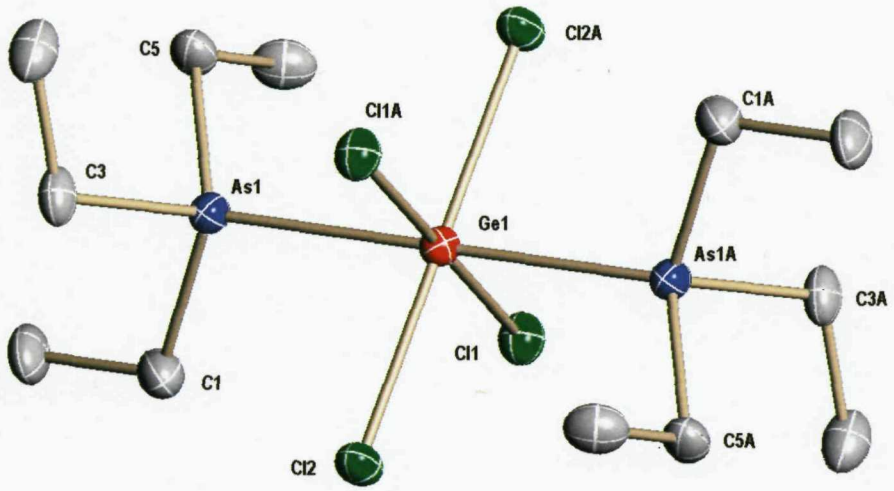

Figure 17 Structure of the centrosymmetric *trans*-[$GeCl_4\{AsEt_3\}_2$] with the atom numbering scheme adopted. H atoms are omitted for clarity and displacement ellipsoids are shown at the 50% probability level. Symmetry operation: a = –x, –y, –z.

Table 9 Selected bond lengths (Å) and angles (°) for *trans*-[$GeCl_4\{AsEt_3\}_2$]

Ge1–Cl1	2.3296(19)	Ge1–Cl2	2.3233(19)
Ge1–As1	2.4904(9)	As1–C	1.930(8)–1.944(8)
Cl2–Ge1–Cl1	90.67(7)	Ge1–As1–C	110.9(2)–116.0(2)
Cl2–Ge1–As1	87.03(5)	As1–C–C	105.1(4)–106.4(4)
Cl1–Ge1–As1	88.29(5)		

The centrosymmetric molecule has Ge–As = 2.490(1) Å slightly longer than that in *trans*-[$GeCl_4\{AsMe_3\}_2$] (2.472(1) Å). If the solution was allowed to stand for a few days very pale yellow crystals were deposited which were identified by their IR and Raman spectra as Et_3AsCl_2.[32]

The identity was confirmed by the crystal structure (Figure 18, Table 10) which showed the expected trigonal bypyramidal geometry with similar As–Cl and As–C bond lengths to those in related compounds such as Me_3AsCl_2 and Cy_3AsCl_2.[33,34] The larger than usual ellipsoids of C2 reflects some disorder within the structure.

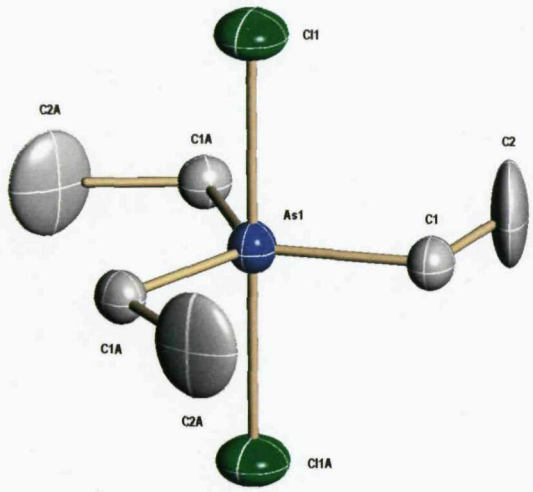

Figure 18 Structure of Et_3AsCl_2 with the atom numbering scheme adopted. H atoms are omitted for clarity and displacement ellipsoids are shown at the 50% probability level. Symmetry operations: a = 1 – y, x – y, z; b = 1 – x + y, 1 – x, z; c= x, y, –z.

Table 10 Selected bond lengths (Å) and angles (°) for Et_3AsCl_2

As1–Cl1	2.382(4)	As1–C1	1.927(6)
C1–C2	1.604(13)		
C–As1–C	120.0	C–As1–Cl	90.0
As1–C1–C2	105.4(5)		

The *trans*-$[GeCl_4\{AsR_3\}_2]$ were also made by reaction of $GeCl_4$ with the ligands in the absence of a solvent (*cf.* the $GeCl_4/PMe_3$ reactions *vide supra*) and had identical Raman spectra to samples obtained using CH_2Cl_2 as solvent.

The Raman spectra obtained from solid *trans*-$[GeCl_4\{AsR_3\}_2]$ (R = Me or Et) show very strong bands at 266 cm^{-1} (Me) or 259 cm^{-1} (Et) which are assigned as the a_{1g} modes, but in Nujol mulls (the solids dissolve in the Nujol), the strongest band in each far-IR spectrum is at 456 cm^{-1} which corresponds to the t_2 mode of tetrahedral $GeCl_4$,[35] showing that they are substantially dissociated even in this medium. The ^1H NMR spectra of both complexes are little different to those of the ligands and do not change even on cooling to 190 K, again consistent with extensive dissociation. Upon standing, the solution of *trans*-$[GeCl_4\{AsEt_3\}_2]$ in CD_2Cl_2 develops new features at 1.60 (t, $^3J_{HH}$ = 7.5 Hz) and 3.06 (q), which

correspond to Et_3AsCl_2,[32] confirming the slow decomposition. The previous report that no reaction occurs between $GeCl_4$ and $AsPh_3$ in either CH_2Cl_2 or Et_2O at ambient temperatures was confirmed.[18] No reaction occurred with $GeCl_4$ and the diarsane $Ph_2AsCH_2CH_2AsPh_2$, or (very surprisingly) with *o*-$C_6H_4(AsMe_2)_2$, which suggests that the stereochemistry at germanium also plays a role (i.e. *cis* isomers are even less favoured than the *trans* and the normally expected greater stability of chelate complexes is not found here). The reaction of $GeBr_4$ and $AsEt_3$ in the absence of solvent gave a clear viscous yellow liquid with strong bands in the Raman spectrum at 311, 267, 240 and 205 cm^{-1} which do not correspond with tetrahedral $GeBr_4$ (328, 234 cm^{-1}) or to Et_3AsBr_2[32] and when dissolved in CD_2Cl_2 the ^1H NMR spectrum shows two broad peaks (at low temperatures) to high frequency of Et_3As indicating dissociation. On standing peaks due to Et_3AsBr_2 also appear.[32] This suggests that the oil may be *trans*-$[GeBr_4\{AsEt_3\}_2]$, again extensively dissociated in solution (extrapolation from the chloride suggests the Raman active a_{1g} Ge–Br vibration will be ~180 cm^{-1}, below the limit of the instrument).

These results show that weak adducts form between $GeCl_4$ and AsR_3 (R = alkyl) but these are highly dissociated in solution, and slowly convert into R_3AsCl_2. The slower reduction by AsR_3 than by PR_3 reflects the relatively weaker reducing power of the arsanes.

4.7 Conclusions:

The Chapter has described the characterisation of the first mono- and bi-dentate phosphane adducts of GeF_4 and has shown that while $GeCl_4$ forms (unstable) complexes with some arsanes (but not others), these slowly convert into R_3AsCl_2. A large amount of spectroscopic data on these compounds has been obtained and comparisons have been made with the previously mentioned tin(IV) fluorides.

Structural data on two novel bidentate $[GeF_4\{L\text{-}L\}]$ complexes have been obtained as well as two monodentate $[GeF_4\{OPR_3\}_2]$ obtained from the phosphane complexes. Further structural data has been obtained proving the formation of $[GeCl_4\{AsEt_3\}_2]$ and subsequent decomposition to Et_3AsCl_2.

The previously contradictory reports by Beattie[13] and Godfrey[18] on the formation of *trans*-$[GeCl_4\{PMe_3\}_2]$ and $[Me_3PCl][GeX_3]$ (X = Cl or Br) have been resolved, proving that both are formed depending on conditions and that the latter can be formed from the former in solution over a period of time.

Like its Sn equivalent GeF_4 is clearly shown to be the strongest Lewis acid when compared to the other Ge(IV) halides for the phosphane compounds.

With phosphanes the reduction to Ge(II) is usually rapid and $[GeCl_4\{PR_3\}_2]$ complexes can only be obtained in the absence of solvents. The stability of Lewis acid-base complexes depends upon two major factors – the strength of the donor-acceptor bond and the energy needed to reorganise the tetrahedral GeX_4 unit into the four-coordinate fragment of the octahedron. The latter is constant for fixed X, and thus the relative affinity for PR_3 *vs.* AsR_3 (which is $GeF_4 > GeCl_4$ for the phosphanes, but appears to be reversed for the arsane compounds), must mainly reflect the difference in orbital energies and donor atom 'softness' between P and As. The reduction of Ge(IV) to Ge(II) is not evident in the fluoride systems, but is favoured for the $GeCl_4$ (and $GeBr_4$) reactions. This contrasts with the chemistry of SnX_4 (X = F, Cl, Br or I) all of which form phosphane adducts, although again the affinity of SnF_4 for arsanes is much less than for phosphanes. The chemistry observed with GeX_4 also seems to differ from the limited data reported for the SiX_4 systems.

4.8 Experimental:

See Appendix for general experimental methods. GeF_4 was obtained from Aldrich and used as received. $GeCl_4$ (Aldrich) was distilled from a mixture of $CaCl_2/Na_2CO_3$, which removes traces of water and HCl. Ligands not obtained from suppliers were made by literature methods: *o*-$C_6H_4(PPh_2)_2$, $Ph_2P(CH_2)_2PPh_2$, *o*-$C_6H_4(PMe_2)_2$, *o*-$C_6H_4(AsMe_2)_2$ and $MeC(CH_2AsMe_2)_3$.[36,37,38,39] 1,2-dimethoxyethane was dried over sodium and freshly distilled. Much of the spectroscopic data below is included above (see Table 3 and Table 4) in this chapter, however, for ease of use it is collected under the compound.

$[GeF_4\{MeCN\}_2]$:[21] GeF_4 was bubbled through a stirred solution of MeCN (30 mL) for 2 min. The solution was then stirred for 1 h before being left to settle. The solvent was decanted off and the solid dried *in vacuo*. ^1H NMR (300 MHz, $CDCl_3$, 298 K): δ = 1.99 (s). IR (Nujol): 688(br), 657(br), 639(br) υ(GeF) cm^{-1}. Raman: 620(s), υ(GeF) cm^{-1}. $^{19}F\{^1H\}$ NMR (CD_2Cl_2, 183K): δ = -101.2 (t, $^2J_{FF}$ ~ 55 Hz), -108.2 (s), -134.2(t).

$[GeF_4\{THF\}_2]$: $[GeF_4\{MeCN\}_2]$ (0.62 g, 2.67 mmol) was stirred in THF (20 ml) for 3 h. The solvent was then removed *in vacuo* to leave a white solid. Yield 0.75 g, 96%. ^1H NMR (300 MHz, $CDCl_3$, 243 K): 2.01-2.05 (m, 4H, CH_2), 4.20-4.31 (m, 4H, OCH_2). IR (Nujol): 1017(s, br), 852(s, br) υ(COC), 650(vbr) υ(GeF) cm^{-1}. $^{19}F\{^1H\}$ (CH_2Cl_2, 243 K): -128.7 (t, $^2J_{FF}$ = 72 Hz), -130.4(s), -145.9(t).

$[GeF_4\{MeO(CH_2)_2OMe\}]$: $[GeF_4\{MeCN\}_2]$ (0.55 g, 2.38 mmol) was dissolved in CH_2Cl_2 (10 mL) and 1,2-dimethoxyethane (0.22 g, 2.38 mmol) added dropwise; the mixture was stirred for 3 h at ambient temperatures. Half of the solvent was removed *in vacuo* and hexane (15 mL) added, stirred for a further 0.5 h. The white/cream solid produced was filtered off and dried *in vacuo*. Yield 0.25 g, 44%. ^1H NMR (300 MHz, $CDCl_3$, 243 K): 4.00 (s, 4H, CH_2), 4.22 (s, 6H, CH_3). IR (Nujol): 671(br), 639 (br) υ(GeF) cm^{-1}. $^{19}F\{^1H\}$ (CH_2Cl_2, 223K): -131.0 (t, $^2J_{FF}$ = 81 Hz), -151.1 (t, $^2J_{FF}$ = 81 Hz).

***trans*-$[GeF_4\{PMe_3\}_2]$:** Trimethylphosphane (0.15 g, 2.0 mmol) was added dropwise to a solution of $[GeF_4\{MeCN\}_2]$ (0.23 g, 1.0 mmol) in CH_2Cl_2 (10 mL); the mixture was stirred for 2 h. The solvent was reduced to low volume *in vacuo* and then filtered to give a white powder which was dried *in vacuo*. Yield 0.15 g, 48%. Required for $C_6H_{18}F_4GeP_2 \cdot 1/2CH_2Cl_2$ (343.5): C, 22.7; H, 5.5. Found: C, 22.7; H, 5.6%. ^1H NMR (300 MHz, $CDCl_3$, 298 K): δ = 1.46 (d, $^2J_{PH}$ = 12 Hz). IR (Nujol): 575(s, vbr). Raman: 508(ms) υ(GeF) cm^{-1}. $^{19}F\{^1H\}$ NMR (CD_2Cl_2, 273 K): δ = -96.9 (t). $^{31}P\{^1H\}$ NMR (CD_2Cl_2, 253 K): δ = -12.4 (q^5, $^2J_{PF}$ = 196Hz).

***trans*-[$GeF_4\{PPh_3\}_2$]:** A solution of triphenylphosphane (0.52 g, 2.0 mmol) in CH_2Cl_2 (5 mL) was added dropwise to a solution of [$GeF_4\{MeCN\}_2$] (0.23 g, 1.0 mmol) in CH_2Cl_2 (10 mL); the mixture was stirred for 3 h. A white precipitate was filtered and dried *in vacuo*. Yield 0.60 g, 89%. Required for $C_{36}H_{30}F_4GeP_2 \cdot 1/4CH_2Cl_2$ (694.4): C, 62.7; H, 4.4. Found: C, 63.0; H, 4.4%. ^1H NMR (300 MHz, $CDCl_3$, 298 K): δ = 7.26–7.63 (m). IR (Nujol): 607(s, vbr) υ(GeF) cm^{-1}. $^{19}F\{^1H\}$ NMR (CD_2Cl_2, 223 K): δ = -70.6 (t, $^2J_{PF}$ = 180Hz). $^{31}P\{^1H\}$ NMR (CD_2Cl_2, 210 K): δ = +2.8 (q^5).

Oxidation reactions of germanium coordinated phosphanes: A sample of [$GeF_4\{Ph_2P(CH_2)_2PPh_2\}$] (0.3 g, 0.51 mmol) was dissolved in degassed anhydrous CH_2Cl_2 under dinitrogen in a small Schlenk tube and the solution frozen solid at 77 K. The system was evacuated and then filled with $^{18}O_2$ to 1 atm and allowed to warm to room temperature. After 2 weeks a sample was removed for ^{31}P NMR study, the remaining solution was stirred with 1M aqueous NaOH for 30 min. The organic layer was separated, dried with molecular sieve, and then the solution decanted off and pumped dry to give a white solid. IR (Nujol): 1153(m) υ(PO) cm^{-1}. $^{31}P\{^1H\}$ NMR ($CDCl_3$, 298 K): δ = +34.0 (s) (nothing at -13 or -17 ppm, free ligand and coordinated to GeF_4 respectively). EIMS: m/z = 433 $[Ph_2P(^{18}O)(CH_2)_2P(^{18}O)PPh_2–H]^+$, 357 $[Ph_2P(^{18}O)(CH_2)_2P(^{18}O)PPh_2–Ph]^+$.

[$GeF_4\{o\text{-}C_6H_4(PMe_2)_2\}$]: [$GeF_4\{MeCN\}_2$] (0.23 g, 1.0 mmol) was dissolved in CH_2Cl_2 (10 mL) and *o*-$C_6H_4(PMe_2)_2$ (0.20 g, 1.0 mmol) added dropwise; the mixture was stirred for 4 h at ambient temperatures. Most of the solvent was removed *in vacuo* and the white powder produced, filtered off and dried *in vacuo*. Yield 0.32 g, 92%. Required for $C_{10}H_{16}F_4GeP_2$ (346.8): C, 34.6; H, 4.7. Found: C, 34.9; H, 4.9%. ^1H NMR (300 MHz, $CDCl_3$, 298 K): δ = 1.81 (t, ^2J + $^5J_{P\text{-}H}$ = 4.5 Hz, 12H, Me), 7.73–7.83 (m, 4H, C_6H_4). IR (Nujol): 607(br), 580(sh), 567(br) υ(GeF) cm^{-1}. $^{19}F\{^1H\}$ NMR (CD_2Cl_2, 273 K): δ = -97.2 (t,t), -126.0 (d,d,t). $^{31}P\{^1H\}$ NMR (CD_2Cl_2, 273 K): δ = -31.7 (t,d,d).

[$GeF_4\{Ph_2P(CH_2)_2PPh_2\}$]: [$GeF_4\{MeCN\}_2$] (0.23 g, 1.0 mmol) was suspended in CH_2Cl_2 (10 mL), $Ph_2P(CH_2)_2PPh_2$ (0.40 g, 1.0 mmol) in CH_2Cl_2 (5 mL) was added and the mixture stirred for 3 h. Most of the solvent was removed *in vacuo*

and the white precipitate was washed with hexane (10 mL), filtered off and dried *in vacuo*. Yield 0.37 g, 68%. Required for $C_{26}H_{24}F_4GeP_2$ (547.0): C, 57.1; H, 4.4. Found: C, 56.2; H, 4.5%. ^{1}H NMR (300 MHz, $CDCl_3$, 298 K): δ = 2.71 (s, br, H, CH_2), 7.38–7.79 (m, 5H, Ph). IR (Nujol): 603(s), 586(br) υ(GeF) cm^{-1}. ^{19}F{^{1}H} NMR (CD_2Cl_2, 233 K): δ = -73.7 (t,t), -110.3 (d,d,t). ^{31}P{^{1}H} NMR (CD_2Cl_2, 223 K): δ = -17.1 (t,d,d).

[GeF_4{*o*-$C_6H_4(PPh_2)_2$}]: [GeF_4{MeCN}$_2$] (0.23 g, 1.0 mmol) and *o*-$C_6H_4(PPh_2)_2$ (0.45 g, 1.0 mmol) were dissolved in CH_2Cl_2 (10 mL) and the solution was stirred for 4 h, during which the solution began to turn cloudy and a white precipitate formed. The precipitate was filtered off and dried *in vacuo*. Yield 0.25 g, 42%. Required for $C_{30}H_{24}F_4GeP_2 \cdot 1/3CH_2Cl_2$ (623.4): C, 58.5; H, 4.0. Found: C, 58.7; H, 3.8%. ^{1}H NMR (300 MHz, $CDCl_3$, 298 K): δ = 7.20–7.65 (m, Ph). IR (Nujol): 619(s), 607(vs,br) υ(GeF) cm^{-1}. ^{19}F{^{1}H} NMR (CD_2Cl_2, 253 K): δ = -81.9 (t,t), -121.9 (d,d,t). ^{31}P{^{1}H} NMR (CD_2Cl_2, 223 K): δ = -17.1 (t,d,d).

[GeF_4{$Me_2P(CH_2)_2PMe_2$}]: $Me_2P(CH_2)_2PMe_2$ (0.15 g, 1.0 mmol) was added dropwise to a solution of [GeF_4{MeCN}$_2$] (0.23 g, 1.0 mmol) in CH_2Cl_2 (10 mL); the mixture was stirred overnight at room temperature. A white precipitate was filtered off and dried *in vacuo*. Yield 0.29 g, 97%. Required for $C_6H_{16}F_4GeP_2 \cdot 1/2CH_2Cl_2$ (341.2): C, 22.9; H, 5.0. Found: C, 22.6; H, 5.2%. ^{1}H NMR (300 MHz, $CDCl_3$, 298 K): δ = 1.39 (m, 12H, Me), 2.05 (m, 4H, CH_2). IR (Nujol): 565(vbr) υ(GeF) cm^{-1}. ^{19}F{^{1}H} NMR (CD_2Cl_2, 217 K): δ = -96.2 (t,t), -121.2 (d,d,t). ^{31}P{^{1}H} NMR (CD_2Cl_2, 223 K): δ = -24.6 (t,d,d).

[GeF_4{$Et_2P(CH_2)_2PEt_2$}]: $Et_2P(CH_2)_2PEt_2$ (0.21 g, 1.0 mmol) was added dropwise to a solution of [GeF_4{MeCN}$_2$] (0.23 g, 1.0 mmol) in CH_2Cl_2 (10 mL); the mixture was stirred for 4 h. Most of the solvent was removed *in vacuo*, the solid filtered off and dried *in vacuo*. Yield 0.29 g, 82%. Required for $C_{10}H_{24}F_4GeP_2 \cdot 1/2CH_2Cl_2$ (397.3): C, 31.7; H, 6.3. Found: C, 31.2; H, 7.0%. ^{1}H NMR (400 MHz, $CDCl_3$, 223 K): δ = 1.22-1.27 (m, 12H, Me), 1.97 (s (br), 4H, CH_2), 2.06 (s (br), 8H, CH_2). IR (Nujol): 605(sh), 577(vbr), 560(sh) υ(GeF) cm^{-1}. ^{19}F{^{1}H} NMR (CD_2Cl_2, 263 K): δ = -91.9 (t,t), -113.6 (d,d,t). ^{31}P{^{1}H} NMR (CD_2Cl_2, 223 K): δ = -9.2 (t,d,d).

[GeF_4{$Cy_2P(CH_2)_2PCy_2$}]: 1,2-bis(dicyclohexylphosphano)ethane (0.47 g, 1.1 mmol) in CH_2Cl_2 (5 mL) was added to a stirred solution of [GeF_4{MeCN}$_2$] (0.28 g, 1.2 mmol) in CH_2Cl_2 (10 mL) and was stirred for 2 h. The solvent was removed *in vacuo* to give a white solid which was washed with hexane (10 mL), filtered off and dried *in vacuo*. Yield 0.43 g, 68%. Required for $C_{26}H_{48}F_4GeP_2 \cdot 1/2CH_2Cl_2$ (613.5): C, 51.8; H, 8.3. Found: C, 52.0; H, 8.5%. ^{1}H NMR (300 MHz, $CDCl_3$, 298 K): δ = 1.28–2.22 (m, CH_2). IR (Nujol): 592(s, vbr) υ(GeF) cm^{-1}. ^{19}F{^{1}H} NMR (CD_2Cl_2, 253 K): δ = -81.2 (t,t), -103.1 (d,d,t). ^{31}P{^{1}H} NMR (CD_2Cl_2, 223 K): δ = -8.7 (t,d,d).

Reaction of GeF_4 with *o*-$C_6H_4(AsMe_2)_2$: *o*-$C_6H_4(AsMe_2)_2$ (0.29 g, 1.0 mmol) was added dropwise to a solution of [GeF_4{MeCN}$_2$] (0.23 g, 1.0 mmol) in CH_2Cl_2 (10 mL). The mixture was stirred for 2 h. The white precipitate was filtered off and dried *in vacuo*. Yield 0.15 g, 35%. Required for $C_{10}H_{16}F_4GeAs_2$ (434.7): C, 27.6; H, 3.7. Found: C, 21.7-21.2; H, 3.6-3.1% See text. ^{1}H NMR (300 MHz, CD_2Cl_2, 298 K): δ = 1.45 (s, 12H, Me), 7.43–7.56 (m, 4H, C_6H_4). IR (Nujol): 657(s), 629(m), 613(m), 595 (m) υ(GeF) cm^{-1}. Raman: 664(w), 630(s, br), 602(s, br), υ(GeF) cm^{-1}. ^{19}F{^{1}H} NMR (CD_2Cl_2, 178 K): δ = -77.7 (t), -118.1 (t, $^2J_{FF}$ = 66Hz).

Reaction of GeF_4 with $MeC(CH_2AsMe_2)_3$: $MeC(CH_2AsMe_2)_3$ (0.38 g, 1.0 mmol) was added dropwise to a solution of [GeF_4{MeCN}$_2$] (0.23 g, 1.0 mmol) in CH_2Cl_2 (10 mL). An immediate precipitate formed but the mixture was stirred for 2 h. The white precipitate was filtered off and dried *in vacuo*. Yield 0.26 g, 49%. Required for $C_{11}H_{27}F_4GeAs_3$ (532.7): C, 24.8; H, 5.1. Found: C, 19.9; H, 4.7% See text. ^{1}H NMR (300 MHz, CD_2Cl_2, 298 K): δ = 0.95 (s, 18H, $AsMe_2$), 1.08 (s, 3H, CMe), 1.73 (s, 6H, CH_2). IR (Nujol): 650(s), 623(s), 578(s) υ(GeF) cm^{-1}. ^{19}F{^{1}H} NMR (CD_2Cl_2, 179K): δ = -132.13 (s).

Reaction of GeF_4 with $AsMe_3$: GeF_4 was bubbled through a stirred solution of trimethylarsane (0.30 g, 2.5 mmol) in hexane (10 mL). A white solid precipitated which was filtered and dried *in vacuo*. Required for $C_6H_{18}F_4GeAs_2$ (388.6): C, 18.5; H, 4.7. Found: C, 11.1-11.0; H, 3.2-2.8% See text. ^{1}H NMR (300 MHz, $CDCl_3$, 298 K): δ = 1.16 (s, Me). IR (Nujol): 646(s), 635(s), 600(sh) υ(GeF) cm^{-}

[1]. Raman: 642(s), 596(s, br), υ(GeF) cm^{-1}. $^{19}F\{^1H\}$ NMR (CD_2Cl_2, 220K): δ = -127.3 (t), -149.8 (t, $^2J_{FF}$ = 80Hz). The same product was isolated from reaction of $AsMe_3$ with $[GeF_4(MeCN)_2]$ in CH_2Cl_2 solution.

Reaction of $GeCl_4$ with PMe_3: In a small Schlenk tube, $GeCl_4$ (~0.15 g) was distilled *in vacuo* onto PMe_3 (0.105 g, 1.38 mmol) at 77 K. The mixture was cautiously allowed to warm and on melting immediately transformed into a white solid. The Schlenk was briefly evacuated to remove any excess reagent and then filled with dry nitrogen; the Raman spectrum of the solid was recorded without removing it from the Schlenk. Raman: 267(s) υ(GeCl) cm^{-1}.

The solid was then dissolved in CH_2Cl_2 (20 mL) and the solution allowed to stand for 3 h and then pumped dry. The solid was identified as $[PMe_3Cl][GeCl_3]$. Raman: 314(m), 260(m) (278(m) & 270(m) see text) υ(GeCl) cm^{-1}. $^{31}P\{^1H\}$ NMR (CD_2Cl_2, 298 K): δ = +92.4 (s).

Reaction of $GeBr_4$ with PMe_3: Trimethlyphosphane (0.15 g, 2.0 mmol) was added to $GeBr_4$ (0.39 g, 1.0 mmol) in the absence of a solvent and the two colourless liquids immediately became a white solid on contact. The Raman spectrum of the solid was recorded without removing it from the Schlenk tube. Raman: 235(s) υ(GeBr) cm^{-1}. $^{31}P\{^1H\}$ NMR (CD_2Cl_2, 253 K): δ = +68.2 (s).

***trans*-[$GeCl_4\{AsMe_3\}_2$]:** Trimethylarsane (0.341 mL, 3.19 mmol) was added to a stirred solution of germanium(IV) chloride (0.343 g, 1.59 mmol) in diethyl ether (10 mL). This was stirred for 2 d before 5 mL of solvent was removed *in vacuo* and a white solid precipitated out. The solid was filtered off and the filtrate was put in a freezer for 5 d. Colourless crystals formed which were identified by a unit cell determination as *trans*-$[GeCl_4\{AsMe_3\}_2]$.[18] The crystals and bulk powder were identical spectroscopically. IR (Nujol): 456(s) $\upsilon_3(GeCl_4)$ cm^{-1}. Raman: 266(vs) a_{1g} ($GeCl_4$) cm^{-1}.

***trans*-[$GeCl_4\{AsEt_3\}_2$]:** Triethylarsane (0.388 mL, 2.76 mmol) was added to a stirred solution of germanium(IV) chloride (0.296 g, 1.38 mmol) in diethyl ether (5 mL). The solvent was immediately removed *in vacuo* to give a white solid

which was refridgerated. Required for $C_{12}H_{30}As_2Cl_4Ge$ (538.6): C, 26.8; H, 5.6. Found: C, 24.3, H 5.5%. ^{1}H NMR (300 MHz, $CDCl_3$, 298 K): δ 1.15 (t, 3H CH_3), 1.42 (q, 2H, CH_2). IR (Nujol): 456(s) $\upsilon_3(GeCl_4)$ cm^{-1}. Raman: 259(vs) a_{1g} (GeCl) cm^{-1}.

When dissolved in CH_2Cl_2 or Et_2O and left in a freezer for 5 days before the solvent was removed *in vacuo* gave colourless crystals identified as Et_3AsCl_2 from an X-ray structure determination. ^{1}H NMR (300 MHz, $CDCl_3$, 298 K): δ = 1.60 (t, $^3J_{HH}$ = 7.5 Hz, 9H, CH_3), 3.06 (q, 6H, CH_2). Raman: 611(m), 527(vs), 413(m), 338(m), 254(vs) cm^{-1}.

Reaction of $GeBr_4$ with $AsEt_3$: Addition of $GeBr_4$ (0.39 g, 1.0 mmol) into triethylarsane (0.32, 2.0 mmol) without solvent produced a clear viscous yellow oil. ^{1}H NMR (300 MHz, $CDCl_3$, 223 K): δ 1.26 (br, 3H CH_3), 2.14 (br, 2H, CH_2). Raman: 311 (m), 267 (w), 240 (s) and 205 (m) cm^{-1}.

4.9 Crystallography:

The crystals discussed in this Chapter unless otherwise stated were grown from anhydrous CH_2Cl_2 solutions layered or by vapour diffusion with *n*-hexane under dinotrogen over several days or weeks often cooled in freezer.

The data for Et_3AsCl_2 was collected as a monoclinic C lattice using the automated software with β close to 90°, however inspection of the data with Layer[40] gave an orthorhombic system as being probable. No satisfactory solution emerged in any of the possible orthorhombic space groups with the initial promising molecules failing to refine. The strategy of trying to solve the structure in P1 was explored and the transformation matrix by good fortune produced a cell that looked remarkably hexagonal. A solution with Z = 2 in P1 readily followed (R1 = 0.042), but with severe correlation problems during refinement. The triclinic coordinates were finally transformed to the correct hexagonal system. The systematic absences for the transformed data gave 0001 = 2n, but it was likely from the As positions that this was not arising from relationships between symmetry related molecules, but rather from the difference in the z

coordinates of these two atoms (and the other atoms). The only hexagonal space group that would accommodate the molecular symmetry found in the triclinic model was P-6 (no. 174). This model converged to R1 = 0.034 with 36 refined parameters compared with 164 parameters in the triclinic model. Chemically the two models are the same, but in crystallographic terms the higher symmetry is preferred.

Brief details of the data collection and refinement are presented in Table 11.

Table 11 Crystal data and structure refinement details.[a]

Compound	$[GeF_4\{o\text{-}C_6H_4(PMe_2)_2\}]$	$[GeF_4\{Ph_2P(CH_2)_2PPh_2\}]$	$[GeCl_4\{AsEt_3\}_2]$	Et_3AsCl_2
Formula	$C_{10}H_{16}F_4GeP_2$	$C_{26}H_{24}F_4GeP_2$	$C_{12}H_{30}As_2Cl_4Ge$	$C_6H_{15}AsCl_2$
M	346.76	546.98	538.59	233.00
Crystal system	Orthorhombic	Monoclinic	Monoclinic	Hexagonal
Space group	Pna21 (33)	Cc (9)	P21/n (14)	P-6 (174)
a/Å	12.307(3)	10.6765(12)	7.849(2)	8.354(2)
b/Å	10.1285(10)	16.466(2)	13.643(4)	8.354(2)
c/Å	10.749(3)	14.2710(16)	9.537(3)	8.629(2)
α/°	90	90	90	90
β/°	90	105.003(8)	93.721(15)	90
γ/°	90	90	90	120
U/Å^3	1339.9(4)	2423.3(5)	1019.1(5)	521.5(2)
Z	4	4	2	2
μ/mm^{-1}	2.547	1.439	5.238	3.702
F(000)	696	1112	536	236
Total no. of obsns (R_{int})	8863 (0.057)	12784 (0.024)	9942 (0.079)	7342 (0.050)
Unique obsns.	2871	4506	2340	861
Min, max transmission	0.742, 1.000	0.886, 1.000	0.713, 1.000	0.721, 1.000
No. of parameters, restraints	158, 1	298, 2	91, 0	36, 2
Goodness-of-fit on F^2	1.04	1.05	1.21	1.02
Resid electron density /eÅ^{-3}	–0.53 to +0.46	–0.26 to +0.29	–0.81 to +1.00	–0.47 to +0.60
R1, wR2 ($I > 2\sigma(I)$)[b]	0.039, 0.070	0.022, 0.054	0.067, 0.109	0.034, 0.088
R1, wR2 (all data)	0.051, 0.074	0.023, 0.054	0.114, 0.126	0.044, 0.093

Compound	$[GeF_4\{OPMe_3\}_2]$	$[GeF_4\{OPPh_3\}_2]\cdot 2CH_2Cl_2$	$[Me_2P(O)(CH_2)_2P(O)Me_2H][GeCl_3]$	$[Me_2P(H)(CH_2)_2P(H)Me_2][GeCl_3]_2$
Formula	$C_6H_{18}F_4GeO_2P_2$	$C_{36}H_{30}Cl_4F_4GeO_2P_2$	$C_6H_{17}Cl_3GeO_2P_2$	$C_6H_{18}Cl_6Ge_2P_2$
M	332.74	874.98	362.08	510.02
Crystal system	Monoclinic	Monoclinic	Triclinic	Orthorhombic
Space group	$P2_1/n$ (no. 14)	$P2_1/n$ (no. 14)	P-1 (no. 2)	$Pca2_1$ (no. 29)
a/Å	6.319(5)	8.840(2)	9.098(2)	18.0377(13)
b/Å	9.574(5)	14.769(3)	9.260(2)	12.5498(9)
c/Å	10.408(5)	14.174(3)	11.171(2)	16.6597(7)
α/°	90	90	66.397(10)	90
β/°	96.384(5)	94.824(10)	89.283(10)	90
γ/°	90	90	60.695(10)	90
U/Å^3	625.8(7)	1844.0(6)	731.9(2)	3771.2(4)
Z	2	2	2	8
μ/mm^{-1}	2.733	1.263	2.836	4.185
$F(000)$	336.0	888.0	364.0	2000
Total no. of obsns (R_{int})	7381 (0.026)	16281 (0.048)	11628 (0.030)	29683 (0.202)
Unique obsns.	1438	4227	3353	8233
Min, max transmission	0.918, 1.000	0.7981, 1.000	0.842, 1.000	0.676, 1.000
No. of parameters, restraints	73, 0	232, 0	132, 0	289, 1
Goodness-of-fit on F^2	1.08	1.03	1.09	0.96
Resid electron density /eÅ^{-3}	–0.31 to +0.37	-0.56 to +0.63	–0.37 to +0.37	–0.88 to +0.81
R1, wR2 ($I > 2\sigma(I)$)[b]	0.021, 0.046	0.036, 0.074	0.028, 0.056	0.072, 0.111
R1, wR2 (all data)	0.025, 0.048	0.051, 0.080	0.036, 0.059	0.208, 0.144

[a] Common items: temperature = 120 K; wavelength (Mo-Kα) = 0.71073 Å; θ(max) = 27.5°.

[b] $R_1 = \Sigma||F_o| - |F_c||/\Sigma|F_o|$. $wR_2 = [\Sigma w(F_o^2 - F_c^2)^2/\Sigma wF_o^4]^{1/2}$.

4.10 References:

[1] F. Cheng, M. F. Davis, A. L. Hector, W. Levason, G. Reid, M. Webster, W. Zhang, *Eur. J. Inorg. Chem.*, **2007**, 2488–2495.
[2] F. Cheng, M. F. Davis, A. L. Hector, W. Levason, G. Reid, M. Webster, W. Zhang, *Eur. J. Inorg. Chem.*, **2007**, 4897-4905.
[3] A. D. Adley, P. H. Bird, A. R. Fraser, M. Onyszchuk, *Inorg. Chem.*, **1972**, 11, 1402–1409.
[4] N. W. Mitzel, U. Losehand, K. Vojinovic, *Inorg. Chem.*, **2001**, 40, 5302–5303.
[5] W. Levason, C. A. McAuliffe, *Coord. Chem. Rev.*, 1976, **19**, 173–185.
[6] N. C. Norman, N. L. Pickett, *Coord. Chem. Rev.*, 1995, **145**, 27–54.
[7] J. A. McCleverty, T. J. Meyer (eds), *Comprehensive Coordination Chemistry II*, Elsevier, Oxford, **2004**, Vol. 3.
[8] A. R. J. Genge, W. Levason, G. Reid., *Inorg. Chim. Acta,* **1999**, 288, 142–149.
[9] N. Bricklebank, S. M. Godfrey, C. A. McAuliffe, R. G. Pritchard, *Chem. Commun.*, **1994**, 695–696.
[10] D. Dakternieks, H. Zhu, E. R. T. Tiekink, *Main Group Met. Chem.*, **1994,** 17, 519–535.
[11] F. Kunnkel, K. Dehnicke, *Z. Naturforsch. Teil B*, **1995**, 50, 848–850.
[12] M. F. Davis, M. Clarke, W. Levason, G. Reid, M. Webster, *Eur. J. Inorg. Chem.*, **2006**, 2773–2782.
[13] I. R. Beattie, G. A. Ozin, *J. Chem. Soc. (A),* **1970**, 370–377.
[14] D. K. Freison, G. A. Ozin, *Can. J. Chem.*, **1973**, 51, 2685–2696; *ibid*, 2697–2709.
[15] W.-W. Du Mont, H.-J. Kroth, H. Schumann, *Chem. Ber.*, **1976**, 109, 3017–3024.
[16] W.-W. Du Mont, *Z. Anorg. Allg. Chem.*, **1979**, 458, 85–88.
[17] F. Ruthe, W.-W. Du Mont, P. G. Jones, *Chem. Commun.*, **1997**, 1947–1948.
[18] S. M. Godfrey, I. Mushtaq, R. G. Pritchard, *J. Chem. Soc., Dalton Trans.*, **1999**, 1319–1323.
[19] L. Apostolico, M. F. Mahon, K. C. Molloy, R. Binions, C. S. Blackman, C. J. Carmalt, I. P. Parkin, *Dalton Trans.*, **2004**, 470–475.
[20] N. W. Mitzel, U. Losehand, K. Vojinovic, *Inorg. Chem.*, **2001**, 40, 5302–5303.
[21] E. L. Muetterties, *J. Am. Chem. Soc.*, **1960**, 82, 1082–1087.
[22] R. C. Aggarwal, M. Onyszchuk, *Proc. Chem. Soc.*, **1962**, 20.
[23] W. Levason, R. Patel, G. Reid, *J. Organomet. Chem.*, 2003, **688**, 280–282.
[24] H. M. Sigl, A. Schier, H. Schmidbauer, *Eur. J. Inorg. Chem.*, 1998, 203–210.
[25] F. Cheng, A. L. Hector, W. Levason, G. Reid, M. Webster, W. Zhang, *Inorg. Chem.*, **2007**, 46, 7215–7223.
[26] M. F. Davis, W. Levason, G. Reid, M. Webster, W. Zhang, *J. Chem. Soc., Dalton Trans.*, **2008**, 4, 533-538.
[27] W. Zhang, *personal communication.*
[28] S. M. Godfrey, A. Hinchcliffe, *J. Mol. Struct.*, **2006**, 761, 1–5 and refs therein.
[29] G. Kociouk-Kőhn, J. G. Winter, A. C. Filippou, *Acta Crystallogr. Sect. C*, **1999**, 55, 351–353.
[30] H. E. Blayden, M. Webster, *Inorg. Nucl. Chem. Letts.*, **1970**, 6, 703–705.
[31] N. N. Greenwood and A. Earnshaw, *Chemistry of the Elements*, Butterworth, Oxford, 2nd ed **1997**; W. E. Dasent, *Non-existent Compounds*, Dekker, NY, **1965**.
[32] L Verdonck, G. P. Van der Kelen, *Spectrochim. Acta A*, **1977**, 13, 601–606.
[33] M. B. Hursthouse, I. A. Steer, *J. Organomet. Chem.*, **1971**, 27, C11–12.
[34] S. Pascu, L. Silaghi-Dumitrescu, A. J. Blake, W.-S. Li, I. Haiduc, D. B. Sowerby, *Acta Crystallogr. Sect C,* **1998**, C54, 219–221.
[35] K. Nakamoto, *Infrared Spectra of Inorganic and Coordination Compounds*, Wiley NY, 2nd ed., **1970**.
[36] R. D. Feltham, R. S. Nyholm, A. Kasenally, *J. Organomet. Chem.*, **1967**, 7, 285.
[37] H. C. E. McFarlane, W. McFarlane, *Polyhedron*, **1983**, 2, 203.
[38] A. M. Aguiar, J. Beisler, *J. Org. Chem.*, **1964**, 29, 1660.
[39] E. P. Kyba, S. T. Liu, R. L. Harris, *Organometallics*, **1983,** 2, 1877.
[40] L. J. Barbour, *J. Appl. Crystallogr.*, **1999**, 32, 351.

Chapter 5

Complexes of SnF_4 and GeF_4 with Thioether Ligands

5.1 Introduction:

Tin(IV) halide complexes of thioethers were first reported in the 1960/70's but were rarely characterised in detail.[1,2] However, a series of complexes including selenoether, thioether as well as N and O donor ligands with tin(IV) halides were observed using NMR solution methods. In the case of monodentate ligands both the *cis* and *trans* isomers were observed but with a more rapid ligand/complex exchange noted for the *cis* isomer.[3,4,5] Further experimentation into determining the *DL* and *meso* forms of selected thio- and seleno-ethers found that at low temperatures ~-95 °C the cessation of the pyramidal atomic inversion could be seen.[6] The paper states that the chelate complex of tin(IV) chloride with 2,5-dithiahexane to be either very insoluble, or unstable in all solvents suitable for NMR spectroscopic measurements.

A number of SnX_4 thioethers have been structurally characterised.[7,8,9,10,11,12] Godfrey *et al*[13] produced the first solid state structure containing both *cis* and *trans* isomers in the unit cell. The crystal structure contained both *cis* and *trans* $[SnBr_4\{SMe_2\}_2]$ in a 2:1 ratio (see Figure 1) synthesised by oxidising tin metal powder with two mol. equivs. of Me_2SBr_2 in this novel synthetic route. Previously only one isomer was observed and was found to be dependent on the sterics of the ligand, *cis* coming from sterically small ligands and *trans* from more bulky substituents.

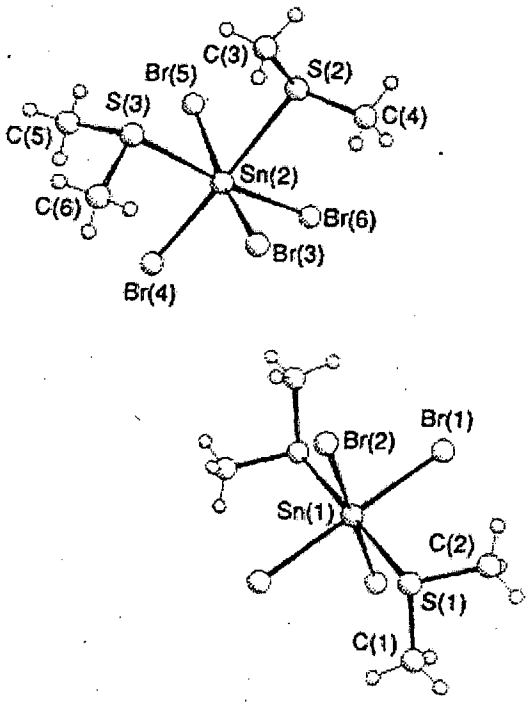

Figure 1 Structure of $[SnBr_4\{SMe_2\}_2]$ showing both *cis* and *trans* isomers.[13]

Examples of bidentate chelation have also been achieved,[14,15,16,17] including the normally bridging ligand $MeSCH_2SMe$[18] acting as a chelate. The *DL* and *meso* forms of this complex are only observed as two separate signals in the ^{119}Sn NMR spectra at temperatures of 180 K or below. In all of these SnX_4 bidentate thioether complexes trends of the $Sn\text{-}Cl_{transCl}$ bond distances are observed to be longer than the $Sn\text{-}Cl_{transS}$ distance, which is mirrored in other Sn(IV) halides complexes.

Macrocyclic thioether ligands have been shown to co-ordinate with SnX_4 in various binding modes, i.e *trans*-$[SnCl_4\{\kappa^1\text{-}1,5\text{-dithiacyclooctane}\}_2]$,[9] $[SnCl_3\{\kappa^3[9]aneS_3\}]_2[SnCl_6]$[19] and $[(SnCl_4)_2\{\kappa^2\kappa^2[18]aneS_6\}]$[19].

Chapter 3 describes the first examples of donor-acceptor adducts of SnF_4 with soft ligands and this was repeated in Chapter 4 with GeF_4. There are no examples of SnF_4 with thioether ligands in the literature.

Recent work within the group on hard O- or N-donor ligands such as phosphane oxides, amines and diimines, with GeF_4, shows the small, hard GeF_4 unit has a

greater affinity for these groups than the other GeX_4 (X = Cl, Br or I) analogues.[20,21,22,23] This, as well as the complexes mentioned in the previous Chapter, has led to attempt further studies of GeF_4 and SnF_4 with thioether ligands.

This was despite earlier work focusing on complexes of SnX_4 (X = Cl, Br, I) with neutral Group 16 donor ligands, in which it was noted that neither $GeCl_4$ or $SiCl_4$ showed any interaction with Me_2S or $MeS(CH_2)_2SMe$ in CH_2Cl_2 solution by VT NMR spectroscopy.[17] $GeCl_4$ is also reported to be reduced to Ge(II) by tertiary phosphanes, giving $[R_3PCl][GeCl_3]$.[24,25] (see Chapter 4)

Furthermore, there are no documented examples of thioether adducts with any main group metal/metalloid fluoride.

Reported below are the synthesis, spectroscopic characterisation and crystal structures of the first examples of Sn(IV) and Ge(IV) fluoride complexes with soft thioether coordination.

5.2 SnF_4 Complexes Containing Thioether Ligands:

The reaction of $[SnF_4\{MeCN\}_2]$ (1 mmol) with one mol. equivalent of the dithioethers $RS(CH_2)_2SR$ (R = Me, Et and ^{i}Pr) in anhydrous CH_2Cl_2, under inert atmosphere (N_2) and strictly anhydrous conditions yielded $[SnF_4\{L\text{-}L\}]$ complexes in moderate yields.

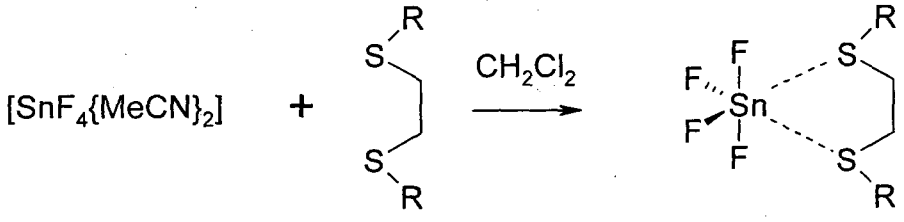

Figure 2 General reaction scheme for $[SnF_4\{L\text{-}L\}]$.

For R = Et and ^{i}Pr the reaction produced a white solid precipitate which did not contain significant amounts of dithioether, and appears to be largely $[SnF_4]_n$ polymer from its IR spectrum (in contrast to the other tin(IV) halides which are

tetrahedral molecules, in the solid state the structure of SnF_4 is based upon vertex sharing octahedra).[26] However, careful concentration of the mother liquor and cooling to *ca.* −18°C led to formation of colourless crystals of $[SnF_4\{RS(CH_2)_2SR\}]$. Using $MeS(CH_2)_2SMe$ and $[SnF_4\{MeCN\}_2]$ gives $[SnF_4\{Me(CH_2)_2SMe\}]$ as a white powder, which is less soluble in chlorocarbons than the R = Et and ^{i}Pr analogues. The NMR spectroscopic evidence described below shows that the $[SnF_4\{RS(CH_2)_2SR\}]$ are extensively dissociated in solution at room temperature, and it suggests that some of the "SnF_4" formed in this dissociation, then oligomerises to $[SnF_4]_n$. IR spectroscopic data shows features in the range 560–600 cm^{-1} (see Table 1) due to the *cis*-SnF_4 fragment as expected for these complexes,[27] and together with microanalyses confirm the formulations $[SnF_4\{RS(CH_2)_2SR\}]$.

Table 1 IR[a] spectroscopic data for thioether ligands coordinated to SnF_4 and GeF_4.

Compound	ν(Sn/Ge-F)/cm^{-1}
$[SnF_4\{MeS(CH_2)_2SMe\}]$	588(sh), 567(s, br), 556(sh)
$[SnF_4\{EtS(CH_2)_2SEt\}]$	579, 564(br)
$[SnF_4\{^iPrS(CH_2)_2S^iPr\}]$	571(s, vbr)
$[GeF_4\{MeS(CH_2)_2SMe\}]$	645(sh), 629, 614, 590(sh)
$[GeF_4\{EtS(CH_2)_2SEt\}]$	649, 635, 620, 605(sh)

a Nujol mull.

The solubility of the complexes (R = Me or Et) in anhydrous chlorocarbons is modest, hence the VT NMR spectroscopic studies were focused upon the much more soluble ^{i}Pr complex. The ^{1}H NMR spectrum of this complex in CD_2Cl_2 at 25°C is simple showing single resonances for CH_2, CH and Me protons only slightly shifted to high frequency from those in the ligand, and consistent with fast exchange/dissociation. On cooling the exchange between free and coordinated ligand slows and at −50°C in addition to resonances of the "free" ligand, two doublet δ(Me) resonances ($^3J_{HH}$ *ca.* 8 Hz) of approximately equal intensities and associated overlapping CH_2 and CH multiplets are seen due to *DL* and *meso* forms of the coordinated dithioether (see Experimental Section). No $^{19}F\{^1H\}$ NMR spectrum of this complex in CD_2Cl_2 was observed at ambient

temperatures, but on cooling two broad resonances appear and at −50°C these have resolved into two triplets $^{2}J_{FF}$ = 52 Hz with associated ^{119}Sn and ^{117}Sn satellites as two overlapping triplets either side of the central resonance (-129.1 ppm) (see Figure 3, Table 2 and Experimental Section). The $^{119/117}$Sn–^{19}F coupling constants are rather larger for the Sn–F_{transF} than Sn–F_{transS}, are similar in magnitude to those observed in tin(IV) fluoride complexes with diphosphane ligands, and larger than those in complexes of diamines, ethers or phosphane oxides (see previous chapters).

Table 2 Selected NMR spectroscopic data for SnF_4 and GeF_4 thioether donor complexes.[a]

Compound	δ ^{19}F{^{1}H}[b]	^{1}J(^{19}F-^{119}Sn) (Hz)	^{2}J(^{19}F-^{19}F) (Hz)
[SnF_4{$MeS(CH_2)_2SMe$}]	−133.1(t)	2662	53
	−159.5(t)	2221	
[SnF_4{$EtS(CH_2)_2SEt$}]	−131.6(t)	2652	53
	−154.2(t)	2239	
[SnF_4{$^{i}PrS(CH_2)_2S^{i}Pr$}]	−129.1(t)	2648	52
	−150.4(t)	2246	
[GeF_4{$MeS(CH_2)_2SMe$}]	−87.0(t)	n/a	77
	−123.0(t)		
[GeF_4{$EtS(CH_2)_2SEt$}]	−85.6(t)	n/a	74
	−117.9(t)		

[a] In CH_2Cl_2-10% $CDCl_3$. [b] See experimental for temperatures.

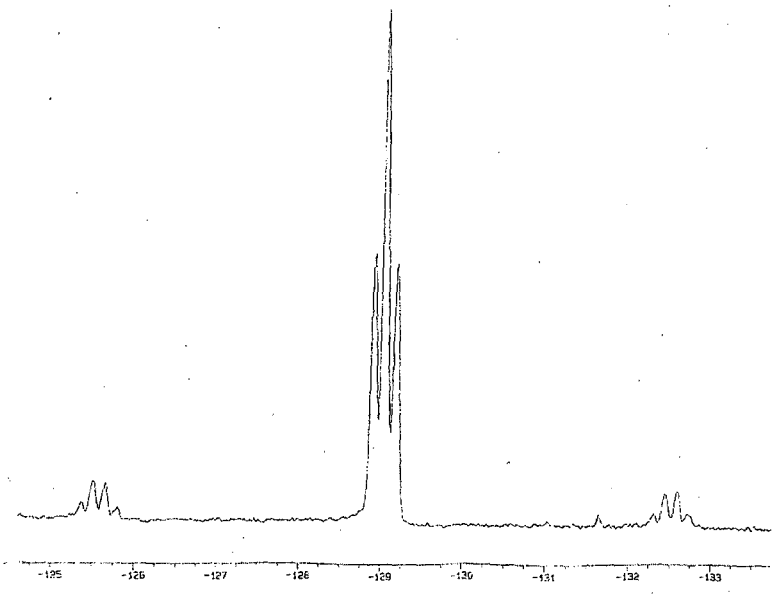

Figure 3 Partial $^{19}F\{^{1}H\}$ NMR spectrum of $[SnF_4\{^{i}PrS(CH_2)_2S^{i}Pr\}]$ (223 K, CH_2Cl_2).

Attempts to observe a ^{119}Sn NMR spectrum of this complex even at low temperatures were unsuccessful; it may be that the complex is still undergoing some dynamic processes on the tin NMR timescale, but it seems more likely the failure is due to a combination of the modest sensitivity of the ^{119}Sn nucleus (R^c = 25), the multiplet splitting expected (*t,t*) and the rather poor solubility of the complex at low temperatures.

The ^{1}H and $^{19}F\{^{1}H\}$ NMR spectra of $[SnF_4\{RS(CH_2)_2SR\}]$ (R = Me or Et) were analogous to those of $[SnF_4\{^{i}PrS(CH_2)_2S^{i}Pr\}]$, but the poor solubility hindered low temperature studies, and the invertomers were not identified.

Confirmation of the formulations follows from X-ray crystal structure determinations for $[SnF_4\{RS(CH_2)_2SR\}]$ (R = Et and ^{i}Pr). The $[SnF_4\{EtS(CH_2)_2SEt\}]$ structure (Figure 4, Table 3) shows a distorted octahedral coordination environment at Sn, giving the *DL* isomer with d(Sn–S) 2.5849(6) and 2.6026(6) Å, this is slightly shorter than the Sn–P distance of 2.606(1) Å in $[SnF_4\{Et_2P(CH_2)_2PEt_2\}]$. The Sn-F bond distances are also shorter in this compound than the phosphorus analogue being 1.9298(13) – 1.9540(12) Å compared with 1.953(2) – 1.986(2) Å and the trend of $Sn–F_{transF}$ being

significantly longer than Sn–F_{transS} is also maintained. The S–Sn–S chelate angle is 84.73(2)°.

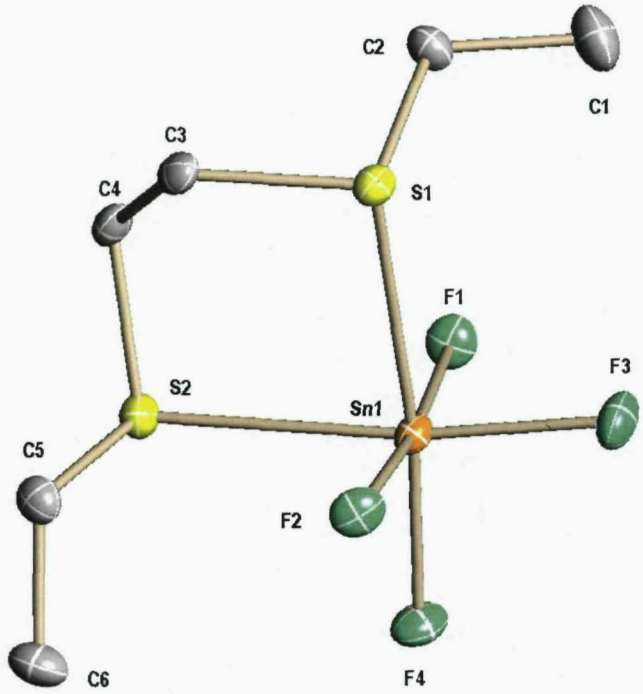

Figure 4 Structure of [SnF_4{$EtS(CH_2)_2SEt$}] showing the atom numbering scheme. Ellipsoids are drawn at the 50% probability level and H atoms omitted for clarity.

Table 3 Selected bond lengths (Å) and angles (°) for [SnF_4{$EtS(CH_2)_2SEt$}]

Sn1–F1	1.9540(12)	Sn1–F2	1.9490(12)
Sn1–F3	1.9298(13)	Sn1–F4	1.9352(12)
Sn1–S1	2.5849(6)	Sn1–S2	2.6028(6)
S1–Sn1–S2	84.732(19)	F1–Sn1–F2	173.62(5)
F3–Sn1–F4	97.48(6)		

The structure of [SnF_4{$^iPrS(CH_2)_2S^iPr$}] (Figure 5, Table 4) is similar, with d(Sn–S) = 2.5844(7) Å and the S–Sn–S chelate angle is 86.37(3)° which is now closer to 90°.

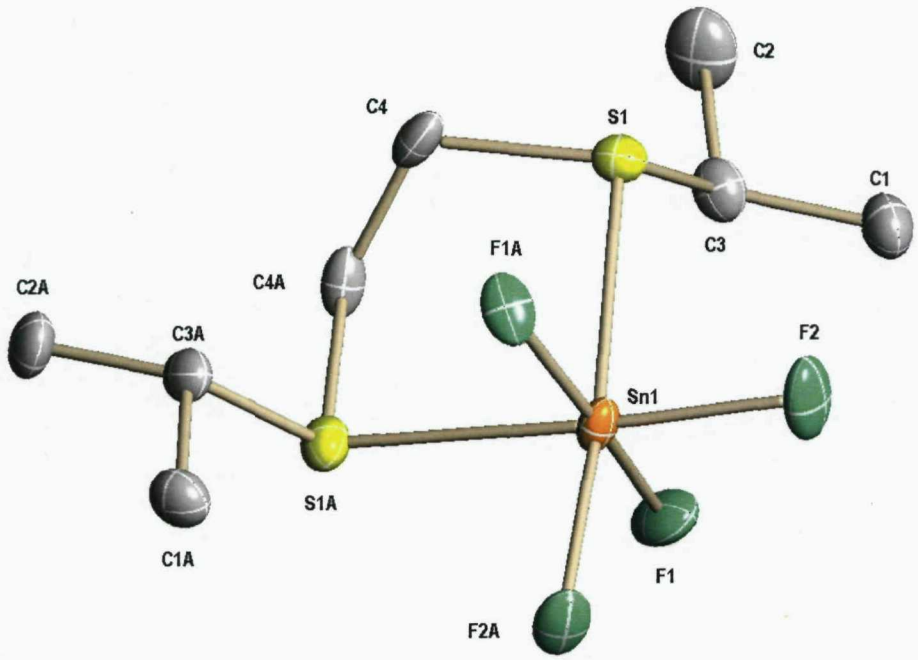

Figure 5 Structure of $[SnF_4\{^iPrS(CH_2)_2S^iPr\}]$ showing the atom numbering scheme. Ellipsoids are drawn at the 50% probability level and H atoms omitted for clarity.

Table 4 Selected bond lengths (Å) and angles (°) for $[SnF_4\{^iPrS(CH_2)_2S^iPr\}]$

Sn1–F2	1.9341(13)	Sn1–F1	1.9464(13)
Sn1–S1	2.5844(7)	S1–Sn1–S1a	86.37(3)
F1–Sn1–F1a	169.63(8)		

Symmetry operation: a = – x, y, 3/2 – z.

Attempts to prepare a complex of [9]aneS$_3$ with tin(IV) fluoride were unsuccessful. A solution of $[SnF_4\{MeCN\}_2]$ in CH_2Cl_2 treated with [9]aneS$_3$, initially precipitated "$[SnF_4]_n$", and on concentration of the mother liquor, [9]aneS$_3$ crystallised out. No convincing $^{19}F\{^1H\}$ resonances were seen from the mother liquor even at low temperatures. This behaviour contrasts with that of $SnCl_4$ which forms the structurally characterised $[SnCl_3\{[9]aneS_3\}]_2SnCl_6$.[28] [9]aneS$_3$ wants to bond facially κ^3 but unlike $SnCl_4$ its is unable to break an Sn-F bond to achieve this and κ^2 is not stable enough which allows [9]ansS$_3$ to crystallise out.

The addition of excess Me_2S to a solution of $[SnF_4\{MeCN\}_2]$ in CH_2Cl_2 gave a clear solution which did not exhibit a $^{19}F\{^1H\}$ NMR spectrum at room temperature, but at 0°C three broad singlets appeared, and on further cooling to −60°C these resolved into two triplets and a singlet, each with $^{119/117}Sn$ satellites [δ = −138.5 (*t*, $^2J(^{19}F\text{-}^{19}F)$ = 55 Hz, $^1J(^{119}Sn\text{-}^{19}F)$ = 2703, $^1J(^{117}Sn\text{-}^{19}F)$ = 2583 Hz; δ = −174.3 (*t*, $^1J(^{119}Sn\text{-}^{19}F)$ = 2263, $^1J(^{117}Sn\text{-}^{19}F)$ = 2162 Hz; δ = −145.8 (*s*, $^1J(^{119}Sn\text{-}^{19}F)$ = 2547, $^1J(^{117}Sn\text{-}^{19}F)$ = 2437 Hz] consistent with $[SnF_4\{SMe_2\}_2]$, with an approximate *cis:trans* ratio of 6:1. Evaporation of this solution under reduced pressure resulted in precipitation of a white, largely ligand-free, solid, and the complex has not been isolated. This contrasts with $[SnX_4\{SMe_2\}_2]$ (X = Cl or Br) which are readily isolated and are fully characterised both structurally and spectroscopically.[15,29,30] This could be explained by SnF_4 being harder than the Cl or Br equivalents and therefore it bonds very weakly with the soft ligand and significant dissociation occurs in solution so that under vacuum the ligand is pumped away.

A range of thioether adducts of $SnCl_4$ and $SnBr_4$ are known[15,29,30] (the only isolated SnI_4 example is the purple insoluble $[SnI_4\{[9]aneS_3\}]$, although $[SnI_4\{MeS(CH_2)_nSMe\}]$ have been detected in solution at low temperatures by ^{119}Sn NMR spectroscopy).[15,31] Comparison of X-ray structural data on $[SnX_4\{RS(CH_2)_nSR\}]$ (X = F, Cl or Br; n = 2 or 3) shows a small increase in d(Sn–S) as the halogen changes F (2.584(1)–2.603(1) Å) → Cl (2.619(2)–2.677(2) Å) → Br (2.700(7) Å), the same trend seen in complexes with hard N- or O-donor ligands and softer phosphane ligands described in previous chapters, consistent with the fluoride being the strongest Lewis acid towards the dithioethers. Comparing the solution NMR spectroscopic data is less definitive mainly due to the tendency of the fluoride adducts to deposit SnF_4 polymer. It is clear that the $[SnX_4\{RS(CH_2)_nSR\}]$ (X = Cl or Br) are also undergoing rapid exchange in solution at ambient temperatures and on cooling the resonances sharpen and split as exchange slows and invertomers are seen.[15] However, in these cases dissociation produces the tetrahedral molecular SnX_4 which remains in solution. The VT NMR results suggest that the binding of the dithioethers in solution is $SnF_4 \sim SnCl_4 > SnBr_4 >> SnI_4$.

5.3 GeF_4 Complexes of Thioethers:*

As mentioned in Chapter 4 $[GeF_4\{MeCN\}_2]$ is a convenient synthon for Ge(IV) chemistry and so the reaction of $[GeF_4\{MeCN\}_2]$ (1 mmol) (see Chapter 4) with 1 mol. equivalent of the dithioethers $RS(CH_2)_2SR$ (R = Me and Et) in anhydrous CH_2Cl_2, under inert atmosphere (N_2) and rigorously anhydrous conditions yielded $[GeF_4\{L\text{-}L\}]$ complexes in moderate yields. The products are *extremely* moisture sensitive and hence all measurements used freshly prepared crystalline samples handled in a dry-box under N_2. It was also noted that pumping the reaction mixtures or isolated solids *in vacuo* led to complete evaporation of the products. $[GeF_4\{MeS(CH_2)_2SMe\}]$ seams particularly unstable and on standing, (under N_2) gains a grayish/pink tinge from the expected colourless/white crystals.

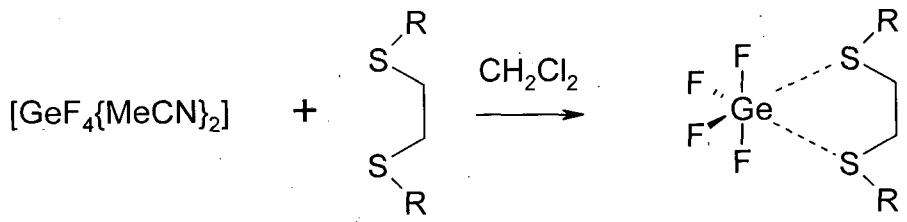

Figure 6 General reaction scheme for $[GeF_4\{L\text{-}L\}]$.

The IR spectra of these complexes show features in the range 600–650 cm^{-1} (see Table 1) assigned to the *cis*-GeF_4 fragment (slightly higher ν than in *cis*-SnF_4) as expected for these complexes, (see Chapter 4) and together with microanalyses confirm the formulations $[GeF_4\{RS(CH_2)_2SR\}]$.

Variable temperature ^1H NMR spectra of these compounds in rigorously dry CD_2Cl_2 showed extensive ligand dissociation at 25°C, although cooling led initially to broadening of the spectra and then (*ca.* −50°C) to individual resonances corresponding to the 'free' and coordinated dithioether (even at −90°C only one form of coordinated ligand is observed – either the compounds are still undergoing rapid pyramidal inversion, hence individual resonances for the *meso* and *DL* diastereoisomers are not apparent, or only one form is present

* Work in section 5.3 done in collaboration with Dr W. Zhang with the synthesis being done exclusively by Dr. W. Zhang.

in observable amounts). At 25°C the $^{19}F\{^1H\}$ NMR resonances are not observed but on cooling the solutions, ill-defined, broad resonances appear, which sharpen and split on cooling further to give two well-defined triplets. The $^{19}F\{^1H\}$ NMR shifts are to high frequency of those for GeF_4 complexes with O- or N-donor ligands such as phosphane oxides, ethers or amines,[6,7] reflecting the more deshielded nature of the GeF_4 unit coordinated to the weaker σ-donor thioether. We also note that the F–F coupling constants in the GeF_4 thioether complexes are larger than those in the phosphane oxide, diamine or diimine complexes (*ca.* 55–65 Hz) and those of the equivalent SnF_4 complexes.

The identities of the products as $[GeF_4\{RS(CH_2)_2SR\}]$ (R = Me or Et) have been authenticated by crystal structure determinations (Figure 7, Figure 8, Table 5 and Table 6) each of which reveals a distorted octahedral environment at Ge through coordination to four fluoride ligands and two sulfur atoms from a chelating dithioether. Both complexes adopt the *DL* configuration with one R group above and one below the GeF_2S_2 coordination plane. The Ge–S bond distances lie in the region 2.43–2.49 Å, the rather long distances indicating weak association of the thioether donor atoms. The S–Ge–S chelate angles are 87.26(2) and 86.55(3)° respectively. There is a disparity between the $Ge–F_{transF}$ and $Ge–F_{transS}$ bond distances, with the former *ca.* 0.02 Å longer, consistent with the order of *trans* influence of F > S in these species. Comparison of the Ge–F bond lengths with those in O- or N-donor ligand complexes shows little difference, confirming the Ge–F as the dominant interactions with much weaker secondary bonding of the sulfur.

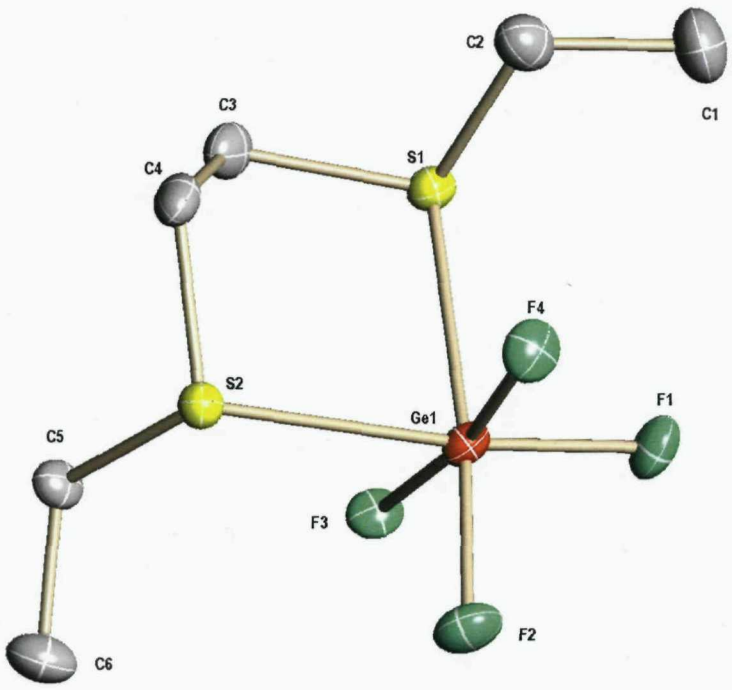

Figure 7 Structure of $[GeF_4\{EtS(CH_2)_2SEt\}]$ showing the atom numbering scheme. Ellipsoids are drawn at the 50% probability level and H atoms omitted for clarity.

Table 5 Selected bond lengths (Å) and angles (°) for $[GeF_4\{EtS(CH_2)_2SEt\}]$

Ge1–F2	1.7507(16)	Ge1–F3	1.7561(16)
Ge1–F1	1.7714(15)	Ge1–F4	1.7761(15)
Ge1–S1	2.4611(8)	Ge1–S2	2.4903(8)
F2–Ge1–F3	97.76(8)	F2–Ge1–F1	94.23(7)
F3–Ge1–F1	93.40(8)	F2–Ge1–F4	92.52(7)
F3–Ge1–F4	92.40(8)	F1–Ge1–F4	170.42(7)
F2–Ge1–S1	87.88(6)	F3–Ge1–S1	173.77(6)
F1–Ge1–S1	83.49(6)	F4–Ge1–S1	89.98(6)
F2–Ge1–S2	173.37(6)	F3–Ge1–S2	87.98(6)
F1–Ge1–S2	88.71(5)	F4–Ge1–S2	83.88(5)
S1–Ge1–S2	86.55(3)		

The crystal structure of $[GeF_4\{EtS(CH_2)_2SEt\}]$ is isomorphous with its Sn analogue (*vide supra*) and shows (Figure 7, Table 5) a distorted octahedral coordination environment at Ge, giving the *DL* isomer, with similar trends in bond distances and angles, and d(Ge–S) *ca.* 0.15 Å shorter than d(Sn–S), consistent with the decreased radius of Ge(IV) over Sn(IV), and the S–Ge–S chelate angle is 86.55(3)°.

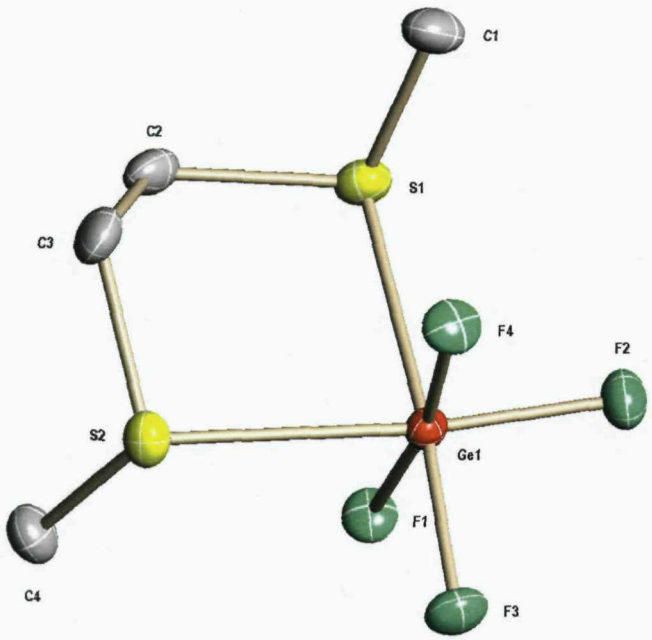

Figure 8 Structure of $[GeF_4\{MeS(CH_2)_2SMe\}]$ showing the atom numbering scheme. Ellipsoids are drawn at the 50% probability level and H atoms omitted for clarity.

Table 6 Selected bond lengths (Å) and angles (°) for $[GeF_4\{MeS(CH_2)_2SMe\}]$

Ge1–F3	1.7487(14)	Ge1–F2	1.7592(15)
Ge1–F4	1.7734(14)	Ge1–F1	1.7764(14)
Ge1–S1	2.4334(7)	Ge1–S2	2.4728(7)
F3–Ge1–F2	95.87(7)	F3–Ge1–F4	92.89(7)
F2–Ge1–F4	93.65(7)	F3–Ge1–F1	92.07(7)
F2–Ge1–F1	93.70(7)	F4–Ge1–F1	170.67(6)
F3–Ge1–S1	175.15(5)	F2–Ge1–S1	87.93(5)

F4–Ge1–S1	89.87(5)	F1–Ge1–S1	84.66(5)
F3–Ge1–S2	89.12(5)	F2–Ge1–S2	174.15(5)
F4–Ge1–S2	83.01(5)	F1–Ge1–S2	89.17(5)
S1–Ge1–S2	87.26(2)		

The structure of $[GeF_4\{MeS(CH_2)_2SMe\}]$ (Figure 8, Table 6) is similar with the S–Ge–S chelate angle is 87.26(2)°.

5.4 Conclusions:

Despite these complexes being extremely moisture sensitive and requiring very low temperatures to observe their NMR spectra, described here are the first authenticated examples of main group metal/metalloid fluoride complexes containing soft thioether ligands and also the first thioether adducts of Ge.

The results demonstrate, as in previous chapters, that molecular $[SnF_4\{MeCN\}_2]$ and $[GeF_4\{MeCN\}_2]$ are useful synthons to allow entry into these extremely unusual soft/hard donor/acceptor adducts. The absence of any evidence for adduct formation using $GeCl_4$ with similar thioether ligands[24,25] shows that GeF_4 is a significantly better Lewis acid even towards soft donor ligands, and might provide a starting point for development of a substantial new coordination chemistry for germanium(IV).

5.5 Experimental:

See Appendix for general experimental methods. GeF_4 and SnF_2 was obtained from Aldrich and converted into $[GeF_4\{MeCN\}_2]$ (see Chapter 4) and $[SnF_4\{MeCN\}_2]$ (see Chapter 2). Me_2S (Aldrich) was dried over molecular sieves. The dithioethers were made as described[33] and stored over molecular sieves. Much of the spectroscopic data below is included above (see Table 1 and Table 2) in this chapter, however, for ease of use it is collected under the compound.

$[SnF_4\{MeS(CH_2)_2SMe\}]$: $MeS(CH_2)_2SMe$ (0.12 g, 1.00 mmol) was added dropwise to a solution of $[SnF_4\{MeCN\}_2]$ (0.278 g, 1.00 mmol) in CH_2Cl_2 (10

mL) and stirred for 0.5 h. Some white precipitate formed; the solution was decanted off, and was left in the freezer for one week, when it deposited a white powder, which was collected by filtration and dried *in vacuo*. Yield 0.22 g, 69%. $C_4H_{10}F_4S_2Sn$ (316.94): calcd. C 15.2, H 3.2; found C 14.9, H 2.4. ^{1}H NMR (300 MHz, $CDCl_3$, 298 K): δ = 2.11 (s, 6H, Me), 2.69 (s, 4H, CH_2); no change at reduced temperatures. IR (Nujol): 588(sh), 567(s, br), 556(sh) υ(SnF) cm^{-1}. ^{19}F{^{1}H} NMR (CH_2Cl_2/CD_2Cl_2, 193 K): δ = −133.1 (t, ^1J(^{119}Sn-^{19}F) = 2662, ^1J(^{117}Sn-^{19}F) = 2542 Hz), −159.5 (t, ^1J(^{119}Sn-^{19}F) = 2221, ^1J(^{117}Sn-^{19}F) = ~2070, ^{2}J(^{19}F-^{19}F) = 53 Hz).

[SnF_4{$EtS(CH_2)_2SEt$}]: [SnF_4{MeCN}$_2$] (0.278 g, 1.00 mmol) was added to a solution of $EtS(CH_2)_2SEt$ (0.34 g, 2.30 mmol) in CH_2Cl_2 (10 mL) and stirred for 1 h. A small amount of white precipitate was produced and the reaction mixture was left in the freezer for 2 weeks where a few colourless crystals grew on the walls of the Schlenk tube which were removed for crystal structure analysis. The solution was then decanted off and the solvent was concentrated *in vacuo* to give a white solid which was collected by filtration and dried *in vacuo*. Yield 0.18 g, 52%. $C_6H_{14}F_4S_2Sn$ (344.99): calcd. C 20.9, H 4.1; found C 20.1, H 4.5. ^{1}H NMR (400 MHz, $CDCl_3$, 298 K): δ = 1.21 (t, 6H, Me), 2.53 (q, 4H, CH_2), 2.68 (s, 4H, CH_2); (CD_2Cl_2, 183 K): δ = 1.17 (t, Me, free L–L), 1.38 (t, Me, coordinated L–L), 2.50 (q, CH_2, free L–L), 2.64 (s, CH_2, free L–L), 2.78-3.01 (m, CH_2 and CH_2, coordinated L–L). IR (Nujol): 579, 564(br) υ(SnF) cm^{-1}. ^{19}F{^{1}H} NMR (CD_2Cl_2, 203 K): δ = −131.6 (t, ^1J(^{119}Sn-^{19}F) = 2652, ^1J(^{117}Sn-^{19}F) = 2533 Hz), −154.2 (t, ^1J(^{119}Sn-^{19}F) = 2239, ^1J(^{117}Sn-^{19}F) = 2143, ^2J(^{19}F-^{19}F) = 53 Hz).

[SnF_4{$^iPrS(CH_2)_2S^iPr$}]: ^{i}PrS(CH$_2$)$_2$S^{i}Pr (0.16 g, 0.90 mmol) was added dropwise to a solution of [SnF_4{MeCN}$_2$] (0.25 g, 0.90 mmol) in CH_2Cl_2 (10 mL) and stirred for 0.5 h. A small amount of white precipitate was present; the solution was left in the freezer for 1 week. Some crystals grew on the walls of the Schlenk tube (collected for structure determination). The solution was then decanted off and reduced *in vacuo* to give a white solid. Yield 0.22 g, 64%. $C_8H_{18}F_4S_2Sn{\cdot}2CH_2Cl_2$ (542.94): calcd. C 22.1, H 4.1; found C 21.6, H 4.3. ^{1}H NMR (400 MHz, $CDCl_3$, 298 K): δ = 1.24 (d, 12H, Me), 2.69 (s, 4H, CH_2), 2.93

(s^7, 2H, CH); (CD_2Cl_2, 203 K): δ = 1.25 (d, Me, free L–L), 1.36 (d, Me, coordinated L–L), 1.49 (d, Me, coordinated L–L), 2.63 (s, CH_2, free L–L), 2.83-2.94 (m, CH_2, coordinated L–L), 2.88-2.99 (m, CH, free L–L), 3.52–3.70 (m, CH, coordinated L–L). IR (Nujol): 571(s, vbr) υ(SnF) cm^{-1}. Raman: 608, 576 cm^{-1}. $^{19}F\{^1H\}$ NMR (CD_2Cl_2, 223 K): δ = −129.1 (t, $^1J(^{119}Sn\text{-}^{19}F)$ = 2648, $^1J(^{117}Sn\text{-}^{19}F)$ = 2564 Hz), −150.4 (t, $^1J(^{119}Sn\text{-}^{19}F)$ = 2246, $^1J(^{117}Sn\text{-}^{19}F)$ = 2148, $^2J(^{19}F\text{-}^{19}F)$ = 52 Hz).

[GeF_4{$EtS(CH_2)_2SEt$}]: The ligand $EtS(CH_2)_2SEt$ (0.018 g, 0.12 mmol) was added to a solution of [GeF_4{$MeCN$}$_2$] (0.023 g, 0.10 mmol) in CH_2Cl_2 (15 mL) at room temperature with stirring. After stirring for 10 min, the volatiles were evaporated slowly from the static solution which gave colourless crystalline solid. Yield 0.033 g, 86%. $C_6H_{14}F_4GeS_2{\cdot}CH_2Cl_2$ (383.84): calcd. C 21.9, H 4.2; found C 22.4, H 4.5. ^1H NMR (400 MHz, CD_2Cl_2, 298 K): δ = 1.35 (t, 6H, Me), 2.77 (q, 4H, CH_2), 2.98 (s, 4H, CH_2); (203 K): δ = 1.16 (t, Me, uncoordinated L–L), 1.34 (t, Me, coordinated L–L), 2.52 (q, CH_2, uncoordinated L–L), 2.64 (s, CH_2, uncoordinated L–L), 2.94 (q, CH_2, coordinated L–L), 3.29-3.41 (m, CH_2, coordinated L–L). IR (Nujol): 649, 635, 620, 605(sh) υ(GeF) cm^{-1}. Raman: 652, 633, 620, 598 υ(GeF) cm^{-1}. $^{19}F\{^1H\}$ NMR (CD_2Cl_2, 223 K): δ = −85.6 (t), −117.9 (t, $^2J_{FF}$ = 74 Hz).

[GeF_4{$MeS(CH_2)_2SMe$}]: Was made analogously to the $EtS(CH_2)_2SEt$ complex above, but using more CH_2Cl_2 (25 mL) due to the lower solubility of the target complex. 2,5-Dithiahexane (0.015 g, 0.12 mmol) was added to a solution of [GeF_4{$MeCN$}$_2$] (0.023 g, 0.10 mmol) in CH_2Cl_2 (40 mL) at room temperature with stirring. After stirring for 10 min, the volatiles were evaporated slowly from the static solution to give a colourless crystalline solid. Yield 0.018 g, 66%. ^1H NMR (400 MHz, CD_2Cl_2, 298 K): δ = 2.15 (s, 6H, Me), 2.72 (s, 4H, CH_2); no change at reduced temperatures. IR (Nujol): 645(sh), 629, 614, 590(sh) υ(GeF) cm^{-1}. Raman: 651, 642, 615, 589 υ(GeF) cm^{-1}. $^{19}F\{^1H\}$ NMR (CD_2Cl_2, 223 K): δ = −87.0 (t), −123.0 (t, $^2J_{FF}$ = 77 Hz).

5.6 Crystallography.

The crystals of $[SnF_4\{EtS(CH_2)_2SEt\}]$, $[SnF_4\{^iPrS(CH_2)_2S^iPr\}]$, $[GeF_4\{EtS(CH_2)_2SEt\}]$ and $[GeF_4\{MeS(CH_2)_2SMe\}]$ were grown from anhydrous CH_2Cl_2 solutions vapour diffusion with *n*-hexane under dinotrogen or slow evaporation over several days or weeks.

Brief details of the data collection and refinement are presented in Table 7.

Table 7 Crystal data and structure refinement details.[a]

Compound	$[SnF_4\{EtS(CH_2)_2SEt\}]$	$[SnF_4\{^iPrS(CH_2)_2S^iPr\}]$	$[GeF_4\{EtS(CH_2)_2SEt\}]$	$[GeF_4\{MeS(CH_2)_2SMe\}]$
Formula	$C_6H_{14}F_4S_2Sn$	$C_8H_{18}F_4S_2Sn$	$C_6H_{14}F_4GeS_2$	$C_4H_{10}F_4GeS_2$
M	344.98	373.03	298.88	270.83
Crystal system	Monoclinic	Monoclinic	Monoclinic	Monoclinic
Space group	$P2_1/c$ (no. 14)	$C2/c$ (no. 15)	$P2_1/c$ (no. 14)	$P2_1/n$ (no. 14)
a/Å	11.093(2)	10.540(3)	10.9011(15)	7.1148(10)
b/Å	8.4148(15)	7.573(2)	8.5151(15)	11.1822(15)
c/Å	12.276(2)	17.642(5)	11.935(3)	10.9875(15)
α/°	90°	90	90	90
β/°	100.627(7)	97.456(10)	101.202(10)	98.884(10)
γ/°	90°	90	90	90
U/Å^3	1126.2(3)	1396.2(6)	1086.7(3)	863.7(2)
Z	4	4	4	4
μ/mm^{-1}	2.649	2.144	3.212	4.030
F(000)	672.0	736.0	600.0	536.0
Total no. of obsns (R_{int})	11875 (0.024)	7267 (0.025)	13998 (0.053)	10496 (0.027)
Unique obsns.	2579	1598	2474	1981
Min, max transmission	0.897, 1.000	0.804, 1.000	0.750, 1.000	0.891, 1.000
No. of parameters, restraints	120, 0	69, 0	118, 0	100, 0
Goodness-of-fit on F^2	1.066	1.121	1.026	1.093
Resid electron density /eÅ^{-3}	-0.397 to +0.433	-0.397 to +0.377	-0.657 to +0.512	-0.458 to +0.376
R1, wR2 ($I > 2\sigma(I)$)[b]	0.018, 0.036	0.019, 0.038	0.031, 0.077	0.026, 0.065
R1, wR2 (all data)	0.020, 0.038	0.022, 0.039	0.041, 0.082	0.031, 0.069

[a] Common items: temperature = 120 K; wavelength (Mo-Kα) = 0.71073 Å; θ(max) = 27.5°. [b] $R1 = \Sigma||F_o| - |F_c||/\Sigma|F_o|$. $wR2 = [\Sigma w(F_o^2 - F_c^2)^2/\Sigma wF_o^4]^{1/2}$.

5.7 References:

[1] I. R. Beattie, L. Rule, *J. Chem. Soc.*, **1964**, 3267-3273.
[2] J. M. Dumas, M. Gomel, *Bull. Soc. Chim. France*, **1974**, 10, 1885-1890.
[3] S. J. Rusika, A. E. Merbach, *Inorg. Chim. Acta,* **1976**, 20, 221–229.
[4] S. J. Rusika, A. E. Merbach, *Inorg. Chim. Acta,* **1977**, 22, 191–200.
[5] S. J. Rusika, C. M. P. Favez, A. E. Merbach, *Inorg. Chim. Acta,* **1977,** 23, 239–247.
[6] E. W Abel, S. K. Bhargava, K. G. Orrell, V. Sik, *Inorg. Chim. Acta,* **1981,** 49, 25–30.
[7] I. R. Beattie, R. Hulme, L. Rule, *J. Chem. Soc.*, **1965**, 1581-1583.
[8] S. Calogero, U. Russo, G. Valle, P. W. C. Barnard, J. D. Donaldson, *Inorg. Chim. Acta*, **1982**, 59, 111-116.
[9] M. M. Olmstead, K. A. Williams, W. K. Musker, *J. Am. Chem. Soc.*, **1982**, 104, 5567-5568.
[10] M. G. B. Drew, J. M. Kisenya, R. G. Wiley, *J. Chem. Soc., Dalton Trans.*, **1984**, 8, 1723-1726.
[11] D. Tudela, M. A. Khan, J. J. Zuckerman, *J. Chem. Soc., Dalton Trans.*, **1991**, 4, 999-1002.
[12] I. R. Beattie, *Quart. Rev.*, **1963**, 17, 382-405.
[13] N. Bricklebank, S. M. Godfrey, C. A. McAuliffe, R. G. Pritchard, *Chem. Commun.,* **1994**, 695–696.
[14] C. T. G. Knight, A. E. Merbach, *Inorg. Chem.,* **1985**, 24, 576–581.
[15] S. E. Dann, A. R. J. Genge, W. Levason, G. Reid, *J. Chem. Soc., Dalton Trans.,* **1996**, 4471–4478.
[16] S. E. Dann, A. R. J. Genge, W. Levason, G. Reid, *J. Chem. Soc., Dalton Trans.,* **1997**, 2207–2213.
[17] A. R. J. Genge, W. Levason, G. Reid. *J. Chem. Soc., Dalton Trans.*, **1997**, 4549–4554.
[18] A. R. J. Genge, W. Levason, G. Reid. *J. Chem. Soc., Dalton Trans.*, **1997**, 4479–4480.
[19] G. R. Willey, A. Jarvis, J. Palin, W. Errington, *J. Chem. Soc., Dalton Trans.*, **1994**, 255–258.
[20] F. Cheng, M. F. Davis, A. L. Hector, W. Levason, G. Reid, M. Webster, W. Zhang, *Eur. J. Inorg. Chem.,* **2007**, 2488–2495.
[21] F. Cheng, M. F. Davis, A. L. Hector, W. Levason, G. Reid, M. Webster, W. Zhang, *Eur. J. Inorg. Chem.,* **2007**, 4897-4905.
[22] A. D. Adley, P. H. Bird, A. R. Fraser, M. Onyszchuk, *Inorg. Chem.,* **1972**, 11, 1402–1409.
[23] N. W. Mitzel, U. Losehand, K. Vojinovic, *Inorg. Chem.,* **2001**, 40, 5302–5303.
[24] S. M. Godfrey, I. Mushtaq, R. G. Pritchard, *J. Chem. Soc., Dalton Trans.,* **1999**, 1319–1323.
[25] W. W. du Mont, H. J. Kroth, H. Schumann, *Chem. Ber.*, 1976, **109**, 3017–3024.
[26] M. Bork, R. Hoppe, *Z. Anorg. Allgem. Chem.*, **1996**, 622, 1557–1563.
[27] M. F. Davis, M. Clarke, W. Levason, G. Reid, M. Webster, *Eur. J. Inorg. Chem.,* **2006**, 2773–2782.
[28] G. R. Willey, A. Jarvis, J. Palin, W. Errington, *J. Chem. Soc., Dalton Trans.*, **1994**, 255–258.
[29] S. J. Rusika, A. E. Merbach, *Inorg. Chim. Acta,* **1976, 20**, 221–229.
[30] N. Bricklebank, S. M. Godfrey, C. A. McAuliffe, R. G. Pritchard, *Chem. Commun.,* **1994**, 695–696.
[31] W. Levason, M. L. Matthews, R. Patel, G. Reid, M. Webster, *New. J. Chem.,* **2003**, 27, 1784–1788.
[32] F. R. Hartley, S. G. Murray, W. Levason, H. E. Soutter, C. A. McAuliffe, *Inorg. Chim. Acta*, **1979**, 35, 265–277.

Chapter 6

Synthesis of Acyclic As_2O ligands and Attempted Synthesis of Arsane Macrocycles

6.1 Introduction:

As has been stated in Chapter 1, the macrocyclic effect describes the increase in stability when you go from complexes of open chain polydentate ligands to the closest analogous macrocyclic ligand complexes. This Thesis has only covered some high dilution cyclisation reactions but equally template synthesis could also work but is not discussed further. The formation of macrocycles is generally more problematic than their corresponding acyclic derivatives and arsenic macrocycles even more so, due to synthetic difficulties encountered in arsane ligand synthesis.[1]

The idea behind high dilution methods is that by dramatically reducing the concentrations of the reagents, there is a very low probability of multiple precursor molecules being close enough to form a polymer, hence favouring the cyclisation reactions.

Background-prior knowledge

A small number of reviews have covered macrocyclic arsanes along with the more common phosphane equivalents,[2,3] the most recent of which came from W. Levason and G. Reid.[4] These contained reports on a small number of macrocyclic ligands mainly from the work of Kyba *et al.*[5,6,7] (Figure 1) and a very useful paper in respect to this Chapter on making a small number of arsane macrocycles from different starting synthons.[8] An earlier report on rings containing two arsane donors also exists.[9] These works contain no reports of macrocyclic arsane complexes with p-block metals or with phosphane macrocycles for that matter, but do contain a few examples of their complexes with transition metals (that were only used to deduce the stereochemistries of the ligands.[6]

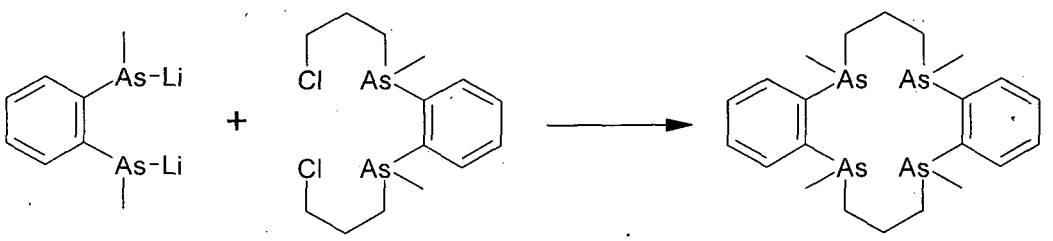

Figure 1 Synthesis of a 14-member tetradentate ring.[7]

An interesting paper describes the synthesis and separation of the racemic and *meso* isomers of linear tetradentate arsanes,[10] a number of which are the analogues of the macrocycles prepared by Kyba[7] and these analogous ligands would be ideal in testing the macrocyclic effect of arsanes.

The problems in making arsane macrocycles include, the volatility and toxicity of the arsenic-containing precursors, as well as the high energy barrier to inversion at arsenic (167.4 $kJmol^{-1}$),[11] which means that numerous stereoisomers[5] may be formed upon cyclisation, which cannot be interconverted or easily separated.[2,4] Perhaps highlighting the difficulties involved in synthesising As macrocycles is the fact that there are still no known examples of the other Group 15 element donors (stibane or bismuthane) incorporated within macrocyclic ligands.

There are also a number of literature reports on synthesising a range of arsane containing ligands that have been used within this Chapter. These were used to produce the starting materials and intermediates required before the cyclisation step could be attempted. A number of these intermediates can be seen in Figure 2.

There are also various cyclic polyarsanes with As-As bonds, references to which are contained within Ref. 12 along with a review of the arsenic-arsenic bond distances. During this work a crystalline solid was obtained, but proved to be the previously been reported cyclo-$(AsPh)_6$ and is not discussed further.[12]

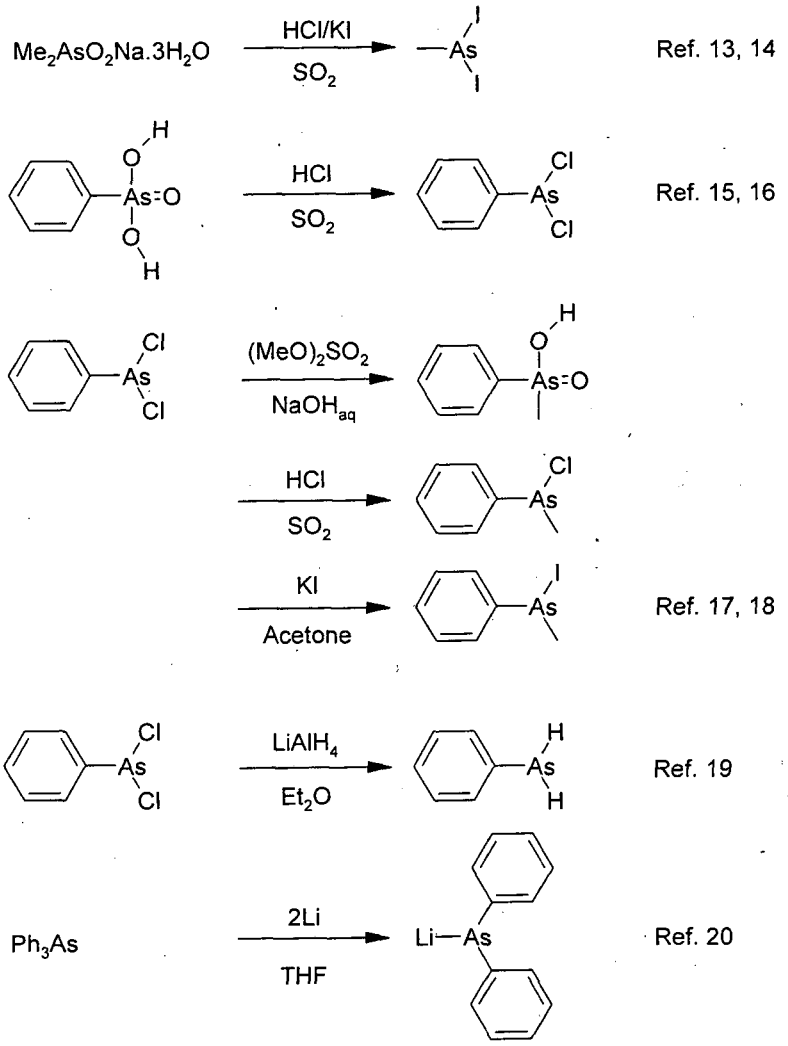

Figure 2 Production of $MeAsI_2$, $PhAsCl_2$, $PhMeAsO_2H$, MePhAsI, $LiAsPh_2$ and $PhAsH_2$ (see experimental).[13,14,15,16,17,18,19,20]

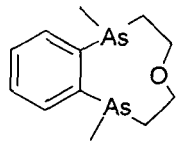

Benzo-Me_2-[9]-ane-As_2O

1,7-dimethyl-1,2,3,5,6,7-hexahydro-4,1,7-benzoxadiarsonine

[*o*-$C_6H_4(AsMe(CH_2)_2\text{-})_2O$]

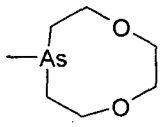

Me-[9]-ane-AsO_2

1-methyl-1-arsa-4,7-dioxacyclononane

$MeAs[\text{-}(CH_2)_2O(CH_2)_2O(CH_2)_2\text{-}]$

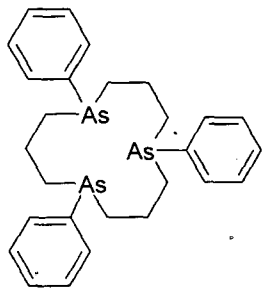

Ph_3-[12]-ane-As_3

1,5,9-Triphenyl-1,5,9-triarsacyclododecane

$[\text{-}As(Ph)(CH_2)_3\text{-}]_3$

Figure 3 Guide to nomenclature of the target arsane macrocycles.

6.2 Synthesis of Precursor Ligands and attempted Preparation of Arsane Macrocycles:

Within this work a number of essential precursor ligands, including Me_2AsI and *o*-$C_6H_4(AsMe_2)_2$, were synthesised, both of which are literature procedures and are discussed in the appendix.[21] A number of other possible precursors for making tri- and tetra-dentate arsane macrocycles (see Figure 2) were prepared according to previous works and the spectroscopic results agreed with the literature.[13,14,15,16,17,18,19,20] These precursors include $MeAsI_2$, $PhAsCl_2$, $PhMeAsO_2H$, MePhAsI, $LiAsPh_2$ and $PhAsH_2$ and also appear briefly in the experimental. A number of other intermediates and proof of concept reactions, towards the target macrocycles, (Figure 3) were also carried out and are discussed below.

Di(benzyl)methylarsane, $MeAs(CH_2Ph)_2$:

Reaction of $MeAsI_2$ in a solution of $NH_{3(liq.)}$ and excess sodium with benzyl chloride, followed by work up and distillation, gave the title compound in good yield as a colourless oil (see Figure 4). This was used as a test reaction for the possibility of introducing a MeAs unit into an open chain or macrocyclic

compound, and to establish how clean cleavage of the As-I bonds would be. The yield was 69% and the product was identified by ^{1}H and $^{13}C\{^{1}H\}$ NMR spectroscopy. The reaction in acetone with methyl iodide gave the corresponding methiodide, identified by ES+ mass spectrometry.

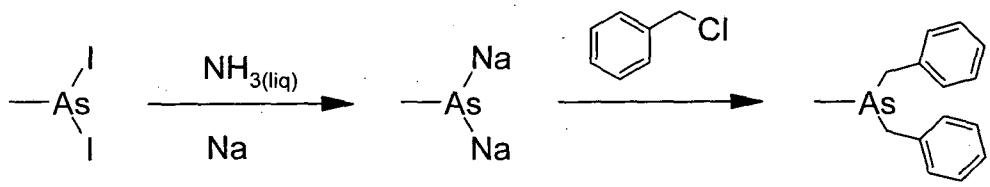

Figure 4 Formation of Di(benzyl)methylarsane, $MeAs(CH_2Ph)_2$.

1,3-Bis(methylphenylarsano)propane, $MePhAs(CH_2)_3AsPhMe$:

$MePhAs(CH_2)_3AsPhMe$ was previously reported from the reaction of sodium methylphenylarsenide Na(AsMePh) and 1,3-dichloropropane by Wild *et al.*[22] Its epimeric *meso* and racemic diastereoisomers differentiated by the methyl peaks in ^{1}H NMR and assigned as $\delta = 1.00$ ppm (rac-) and $\delta = 1.01$ ppm (*meso*-).[23] This compound was made in this study by reaction of PhMeAsI with Na in THF followed by the addition of 1,3 dibromopropane (see Figure 5). Again the title compound was obtained in good yield, on a reasonably large scale and was characterised by NMR spectroscopy and as a methiodide derivative.

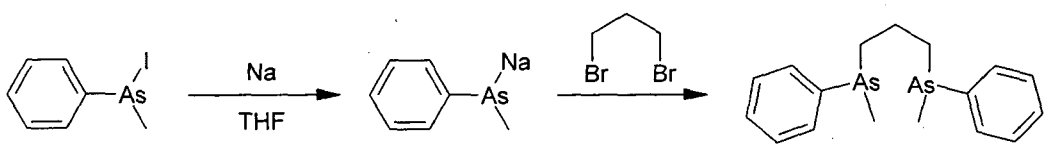

Figure 5 Formation of 1,3-Bis(methylphenylarsano)propane, $MePhAs(CH_2)_3AsPhMe$

***o*-Phenylenebis(bromomethylarsane), [*o*-$C_6H_4(AsMeBr)_2$]:**

The title compound was obtained as a dark red oil if not purified, or as a light yellow oil if distilled, in good yield by literature procedures and was characterised by ^{1}H NMR spectroscopy.[18]

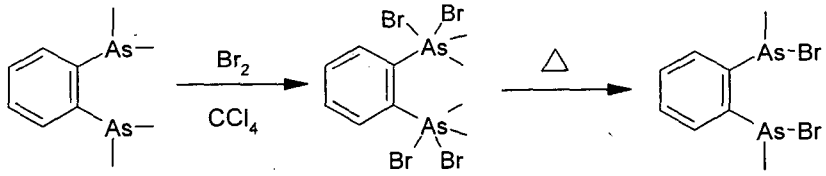

Figure 6 Synthetic route to *o*-Phenylenebis(bromomethylarsane), [*o*-$C_6H_4(AsMeBr)_2$].

o-Phenylenebis(methylarsane), [o-$C_6H_4(AsMeH)_2$]:

Attempts to obtain this product in good yields by reaction of [o-$C_6H_4(AsMeBr)_2$] with $Li(AlH_4)$ in benzene (see Figure 7) or diethyl ether gave the title product in relatively small yields *ca.* 17%. In retrospect perhaps following either the literature methods of Wild *et al*[18] or Cook *et al*[24] both from the diprimary arsane but using different starting materials would have given better yields. The route followed does appear in Wild's paper, however, detailed conditions were not given (see Figure 7).

Benzo-Me_2-[9]-ane-As_2O, As_2O macrocycle, [o-$C_6H_4(AsMe(CH_2)_2)_2O$]:

Similar to the production of the 11-membered macrocyclic rings using the $(CH_2)_3$ connecting units by Kyba *et al*[5,6] an attempt was made using the $(CH_2)_2$ as a linking unit. o-Phenylenebis(methylarsane), [o-$C_6H_4(AsMeH)_2$] was reacted with ^nBuLi and subsequent addition of either bis(2-chloroethyl)ether or bis(2-bromoethyl)ether using similar method to Kyba *et al* (see Figure 7).

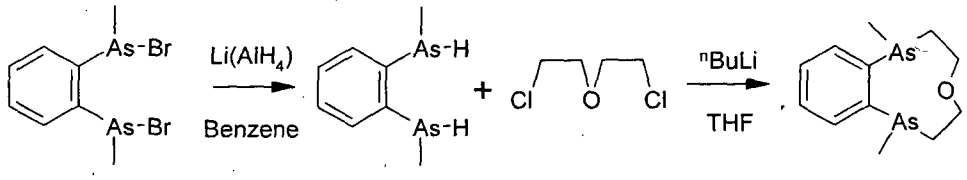

Figure 7 Synthetic route to Benzo-Me_2-[9]-ane-As_2O.[5,6,18,24]

In both cases the ^1H NMR spectra were consistent with the formation of the macrocycle (see Experimental Section), but the yields were very poor and did not permit exploration of the coordination chemistry. Substantial amounts of the starting ether were also recovered in distillation even when using the bromo ether. EI mass spectrometry from distilled ligands and ES+ from the derived methiodide reveals significant ions consistent with the presence of the expected functional groups, but do not clearly rule out acyclic products (see Experimental Section).

1,2-Bis(2-bromoethoxy)ethane, ($Br(CH_2)_2O(CH_2)_2O(CH_2)_2Br$):

The title compound was made from triethylene glycol as per the literature procedure for making the chloro species from tetraethylene glycol.[25] This was prepared from a refluxing solution of the glycol in pyridine with the addition of

$SOBr_2$. Its ^1H NMR spectroscopic data were also confirmed from Keana *et al*'s work.[26]

Me-[9]-ane-AsO_2, AsO_2 Macrocycle, (MeAs[-$(CH_2)_2O(CH_2)_2O(CH_2)_2$-]):
Using a modified method of that used to produce $MeAs(CH_2Ph)_2$, $MeAsI_2$ was reacted with sodium before $Br(CH_2)_2O(CH_2)_2O(CH_2)_2Br$ was added at low temperature in a dilute solution (see Figure 8). Although the yields of the desired product were very low, the ^1H and $^{13}C\{^1H\}$ NMR spectra appeared to show the correct product as well as some minor impurities and THF (see Experimental Section). After distillation although the THF had been removed the impurities became much more evident, possibility indicating decomposition in the distillation. Reactions of samples with MeI both before and after distillation showed $[M+Me]^+$ in the ES+ mass spectrum.

A further complication with this reaction is that it might form a larger [2 + 2] ring (see Figure 8) which would be very difficult to tell apart from the smaller ring. There is no sign of this product in the mass spectrometry data although the peak at 221 could be a fragment in both. Again due to the very poor yields and instability the synthesis was not pursued.

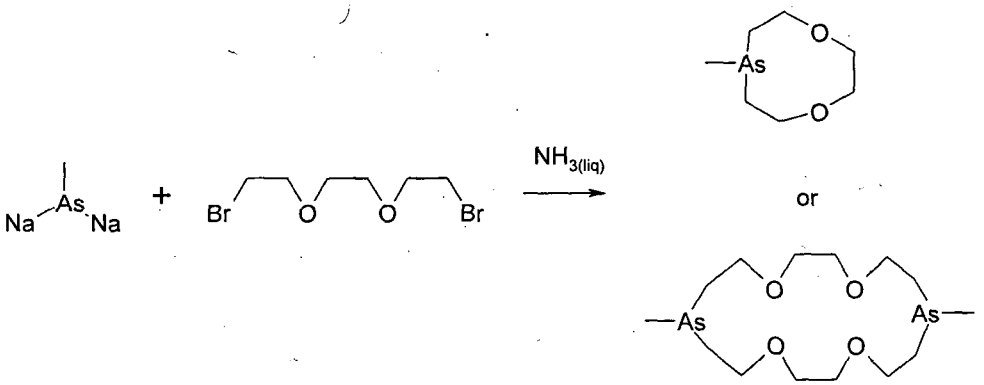

Figure 8 Synthetic route to Me-[9]-ane-AsO_2 or 1,10-dimethyl-[18]-ane-As_2O_4 macrocyle.

1,3-Bis(phenylarsano)propane, PhAs(H)$(CH_2)_3$As(H)Ph:
PhAs(H)$(CH_2)_3$As(H)Ph was produced by reacting two equivalents of PhAsLiH from $PhAsH_2$, with 1,3-dibromopropane using minor modifications of known literature.[9] Unusually the central backbones proton's all occurred at the same shift producing a broad singlet, this was confirmed by ^{13}C-^1H COSY spectrum.

After standing for several days the AsH proton resonances were lost, probably showing decomposition of the sample on storage. This was used as a precursor for further reactions.

1,3-Bis(phenylisopropylarsano)propane, $Ph^{i}PrAs(CH_2)_3As^{i}PrPh$:

As a further test to the previous reactions success, $PhAs(H)(CH_2)_3As(H)Ph$ was reacted with MeLi and 2-bromopropane to give the title ligand in a relatively high yield. Reaction with MeI gave a relatively clean ES+ MS of the $[M+Me]^+$ and expected fragments. This showed that additional substituents could be added to the $PhAs(CH_2)_3AsPh$ unit at the arsane, possibly allowing use in forming macrocycles.

Bis(3-chloropropyl)phenylarsane, $PhAs((CH_2)_3Cl)_2$:

$PhAs((CH_2)_3Cl)_2$ was produced by the reaction of $PhAsLi_2$ from $PhAsH_2$ with two equivalents of 1-bromo-3-chloropropane at reduced temperatures in good yield. The spectroscopic data were in good agreement with the literature.[8] Initially an impurity of the starting material 1-bromo-3-chloropropane was seen in the proton NMR spectrum but this was removed by pumping the oil in *vacuo*.

Ph_3-[12]-ane-As_3, As_3 Macrocycle, $[-As(Ph)(CH_2)_3-]_3$:

The reaction of equi-molar amounts of $PhAs(Li)(CH_2)_3As(Li)Ph$ and $PhAs((CH_2)_3Cl)_2$ in THF (see Figure 9) was carried out in very high dilution over a prolonged period of time as reported in the literature.[8] The resultant oil appeared to show the expected resonances within the ^1H and $^{13}C\{^1H\}$ NMR spectra, along with a number of unknown impurities. Distillation of the oil gave little improvement in purity although a few minor impurities were removed. TLC of the compound with silica gel plates gave some signs of separation using CH_2Cl_2:hexane (1:1). A large scale column using CH_2Cl_2:hexane (1:10) was attempted and gradual increase in polarity to CH_2Cl_2:hexane (1:1) gave a significant number of fractions. TLC of these showed a number of identical fractions which were combined however, after an initial impurity the remaining fractions do not seem to separate as such. $^1H/^{13}C\{^1H\}$ NMR spectra of these fractions are very similar but all still have some impurities. Direct injection

EI/MS were carried out as were reactions with MeI and subsequent ES+ MS none of which unequivocally confirmed the presence of the title compound.

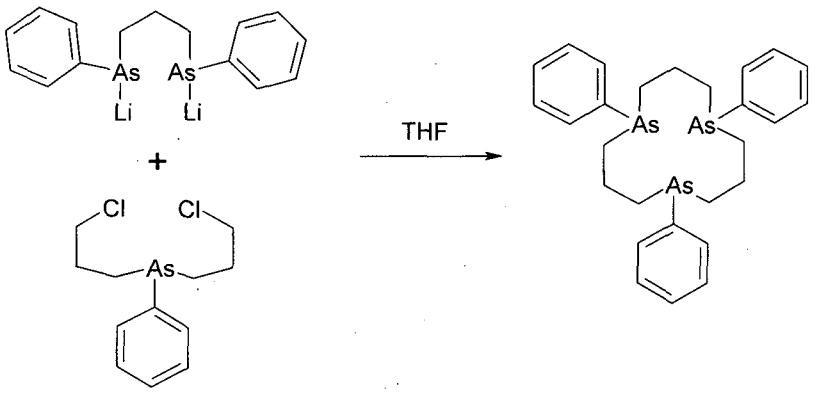

Figure 9 Synthetic route for the Ph_3-[12]-ane-As_3 macrocycle [-As(Ph)$(CH_2)_3$-]$_3$.

It was intended to return to a number of these macrocyclic routes but due to the success of other aspects of the work in this thesis, further study and identification was not undertaken.

An alternative route to making the methyl analogue of the above macrocycle can be seen in Figure 10 but this was not attempted (due to lack of time).

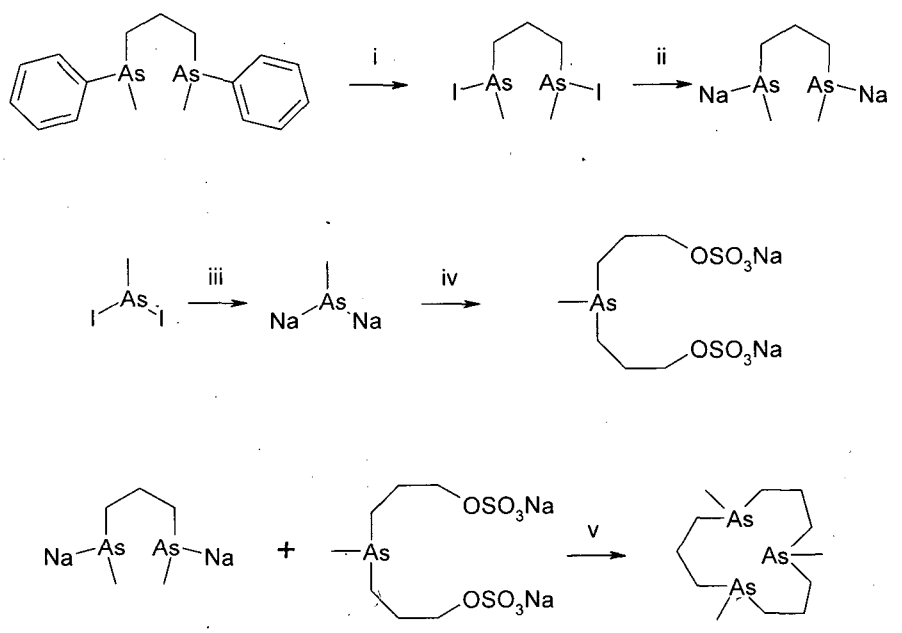

Figure 10 Synthetic route to the Me_3-[12]-ane-As_3 macrocyclic analogue [-As(Me)$(CH_2)_3$-]$_3$. i. $HI_{(g)}$, ii.Na/THF, iii.Na/THF, iv. Na/$NH_{3(liq)}$/1,3-Propanediol cyclic sulphate, v. High dilution.

6.3 Facultative As_2O Open Chain Ligands:

In the course of this study towards the development of synthetically viable routes to macrocyclic arsanes, investigations into the potentially tridentate arsane–ether ligands, $O\{(CH_2)_2AsR_2\}_2$ (R = Me and Ph) were carried out. There is an early report of the Ph compound, but it was only characterised as its NiI_2 complex.[27]

The As_2O–donor ligands were obtained from $O(CH_2CH_2Br)_2$ and $LiAsPh_2$ or $NaAsMe_2$ (see Figure 11). The α,ω-dibromo precursor is necessary to allow complete substitution (the corresponding $O(CH_2CH_2Cl)_2$ leads only to partial substitution, especially by less nucleophilic reagents, e.g. Ph_2Sb^-).[28]

While the $O\{(CH_2)_2AsPh_2\}_2$ appears to be stable, $O\{(CH_2)_2AsMe_2\}_2$ is much less so and undergoes significant degradation upon standing even under N_2 in the dry box and during distillation and reaction with transition metal salts. ^1H and $^{13}C\{^1H\}$ NMR spectroscopic data for $O\{(CH_2)_2AsR_2\}_2$ are fully in accord with the formulation, revealing the two triplets expected for the linking CH_2 groups, and for R = Me, the $AsMe_2$ groups significantly shielded as expected.

The preparation of $O\{(CH_2)_2AsMe_2\}_2$ however, gave variable yields – in some cases the ^1H and $^{13}C\{^1H\}$ NMR spectra showed the $O\{(CH_2)_2AsMe_2\}_2$ compound to be the only significant product, whereas in others additional resonances were evident. During distillation from this crude mixture a second, less volatile fraction (74°C, 0.05 mmHg) was collected in addition to the $O\{(CH_2)_2AsMe_2\}_2$ compound (58°C, 0.05 mmHg). The NMR features of both fractions show $AsMe_2$, CH_2As and CH_2O resonances, with relative integrals of 3:2:2, and while the Me and $AsCH_2$ resonances are nearly superimposed, that for CH_2O is some 0.2 ppm to low frequency of the CH_2O resonance in $O\{(CH_2)_2AsMe_2\}_2$. GCEI MS of the by-product shows peaks at m/z = 150, consistent with $Me_2As(CH_2)_2OH$, apparently formed via C–O bond fission (see Figure 11).

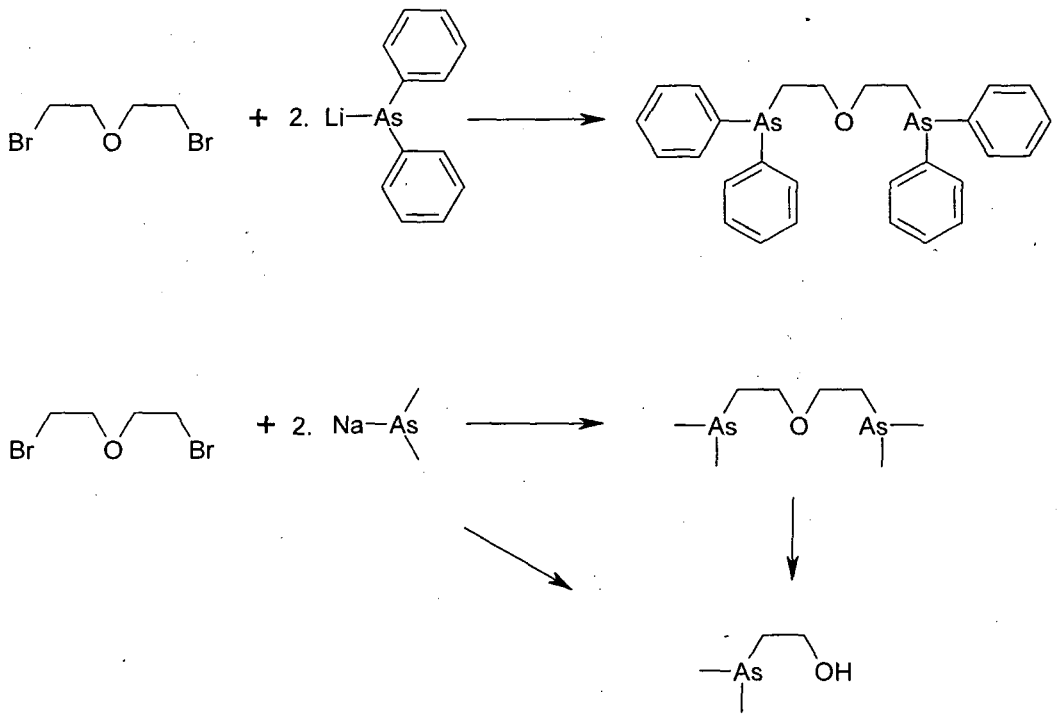

Figure 11 Synthetic route to the facultative As_2O open chain ligands.

Dimethylene linkages are well known to be unstable with respect to elimination of ethene,[29,30] however, it is a little surprising that the methyl compound appears to be markedly less stable than its phenyl equivalent (or the Sb analogues, see later) ligand in this chapter which also incorporate dimethylene linkage. It is notable that $Ph_2As(CH_2)_2AsPh_2$ is a well known stable compound, whereas $Me_2As(CH_2)_2AsMe_2$ has only been obtained in very low yield and has very little associated chemistry.[31] The compound $Me_2As(CH_2)_2OH$ has been reported as a fragmentation product from $Me_2Si(OCH_2CH_2AsMe_2)_2$ with transition metal compounds and its reaction chemistry with Group 6 carbonyls has been described, although no characterisation data on the arsanoethanol itself have been reported.[32]

A number of complexes of both ligands was investigated with transition metal ions of Ag(I), Cu(I) and the main group metals GaX_3 and BiX_3, to probe the coordination modes and to establish whether both the ether O and the As donor atoms can coordinate simultaneously. Reaction of the $O\{(CH_2)_2AsPh_2\}_2$ ligand (L–L) with $[Cu(MeCN)_4]BF_4$ in MeOH using either a 1:1 or 1:2 Cu:L–L ratio yields only the bis-ligand species $[Cu(L–L)_2]BF_4$ which was isolated as a colourless crystalline solid. Confirmation of the 1:2 Cu:L–L ratio follows from the ^{63}Cu NMR

spectroscopic measurements and microanalyses. $\delta(^{63}Cu)$ = −139 ppm for the complex. This is also demonstrated by the X-ray crystal structure (see Figure 12). Copper-63 is quadrupolar with I = 3/2 (69%) and as a result of its moderately high quadrupole moment ($Q = -0.211 \times 10^{-28}$ m^2) resonances are typically only observed for high symmetry Cu environments – in the compounds studied here the chemical shifts are consistent with approximately tetrahedral As_4 donor environments (*cf.* $[Cu\{o\text{-}C_6H_4(AsMe_2)_2\}_2]^+$ $\delta(^{63}Cu) = -63$).[33] The electrospray MS data however, reveal the main species to be $[Cu(L\text{–}L)]^+$ *m/z* = 593 and $[Cu(L\text{–}L)(MeCN)]^+$ *m/z* = 634, but the loss of ligands from a labile metal centre is not unexpected.

A similar reaction of the $O\{(CH_2)_2AsMe_2\}_2$ ligand with $[Cu(MeCN)_4]BF_4$ in MeOH solution did not yield $[Cu(O\{(CH_2)_2AsMe_2\}_2)_2]BF_4$, $[Cu(L\text{–}L)_2]BF_4$ cleanly, the solution changing from colourless to green and back to colourless during work-up. Electrospray MS (MeCN) on the colourless solid isolated showed peaks at m/z = 627, 386 and 345, consistent with $[Cu(L\text{–}L)_2]^+$, $[Cu(L\text{–}L)(MeCN)]^+$ and $[Cu(L\text{–}L)]^+$. The ^{63}Cu NMR spectrum shows a broad resonance associated with the pseudo-tetrahedral Cu(I) cation, $[Cu(L\text{–}L)_2]^+$ at −16 ppm, confirming the presence of this species in solution. However, the NMR solution also changed to pale green during data acquisition, consistent with some sample degradation, and a structure determination on crystals obtained upon slow evaporation from a solution of the product in $MeOH/Et_2O$ revealed an unexpected dinuclear Cu(I)–Cu(I) complex incorporating the fragmented ligand $Me_2As(CH_2)_2OH$ – see below.

The geometry at the metal in the Cu(I) complexes, $[Cu(L\text{–}L)_2]BF_4$, is confirmed from the crystal structure of $[Cu(O\{(CH_2)_2AsPh_2\}_2)_2]BF_4 \cdot MeOH$ (Figure 12, Table 1) which shows a distorted tetrahedral coordination environment at Cu(I), with the ligands behaving as bidentate As_2–donors and with the ether O atoms not interacting with the metal. The Cu–As bond distances lie in the range 2.4202(9)–2.4652(9) Å respectively, while the As–Cu–As angles within the chelate rings are 106.36(3) and 107.09(3)°. The bond distances are shorter than those in $[Cu(AsPh_3)_4]ClO_4$ 2.493(2)–2.533(1) Å), but significantly longer (by *ca.* 0.08 Å) than those in $[Cu(Ph_2AsCH{=}CHAsPh_2)_2]^+$ d(Cu–As) =

2.348(3)–2.358(3) Å, revealing a correlation between increasing ligand steric demands and increased bond lengths.[33,34] The lattice MeOH in $[Cu(O\{(CH_2)_2AsPh_2\}_2)_2]BF_4 \cdot MeOH$ is involved in weak H-bonding interactions with the $[BF_4]^-$ anion, O3···F2 = 2.97 Å.

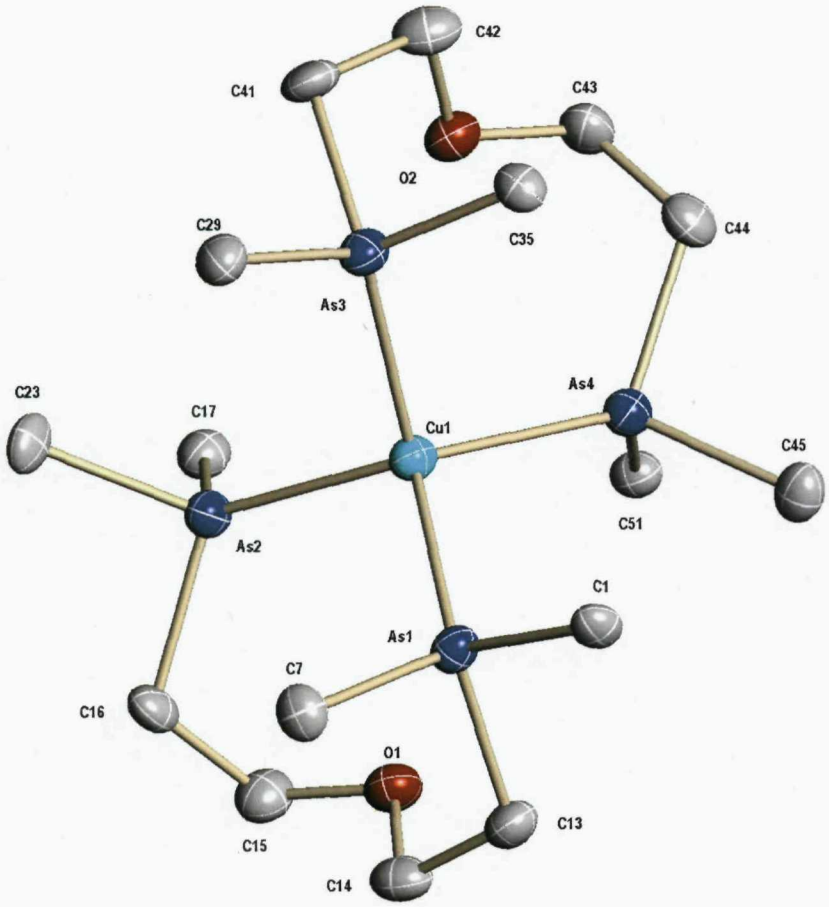

Figure 12 View of the structure of $[Cu(O\{(CH_2)_2AsPh_2\}_2)_2]^+$ with numbering scheme adopted. Ellipsoids are drawn at the 50% probability level. H atoms and the phenyl rings (except the ipso C atoms) are omitted for clarity.

Table 1 Selected bond lengths (Å) and angles (°) for $[Cu(O\{(CH_2)_2AsPh_2\}_2)_2]BF_4 \cdot MeOH$.

Cu1–As1	2.4212(9)	Cu1–As2	2.4223(9)
Cu1–As3	2.4202(9)	Cu1–As4	2.4652(9)
As3–Cu1–As1	110.64(3)	As3–Cu1–As2	107.65(3)
As1–Cu1–As2	107.09(3)	As3–Cu1–As4	106.36(3)
As1–Cu1–As4	108.09(3)	As2–Cu1–As4	117.00(3)

Similar coordination is seen for the corresponding light sensitive Ag(I) species $[Ag(L–L)_2]BF_4$ for the $(O\{(CH_2)_2AsPh_2\}_2)$, (L-L), ligand (obtained from direct reaction of $AgBF_4$ with L–L in MeOH in a foil-wrapped flask to exclude light). Like the Cu(I) complex of the $(O\{(CH_2)_2AsMe_2\}_2)$ ligand above, reaction with $AgBF_4$ did not yield a tractable, pure sample of $[Ag(O\{(CH_2)_2AsMe_2\}_2)_2]^+$. Spectroscopic data confirm the presence of this product, however it is unstable, darkening on standing even in the dark, possibly also due to some C–O bond fission. The crystal structure of $[Ag(O\{(CH_2)_2AsPh_2\}_2)_2]BF_4{\cdot}MeOH$ (Figure 13, Table 2) show discrete monomeric cations with distorted tetrahedral As_4 coordination at Ag(I) via two bidentate L–L units, and with Ag–As bond distances in the ranges of 2.6143(9)–2.6376(9) Å. This compares very well with d(Ag–As) of 2.649(2), 2.650(2) Å in $[Ag(AsPh_3)_4]ClO_4$.[34] The MeOH solvent molecule in $[Ag(O\{(CH_2)_2AsMe_2\}_2)_2]BF_4{\cdot}MeOH$ is also H-bonded to the BF_4^- anion, O3···F1 = 2.80 Å.

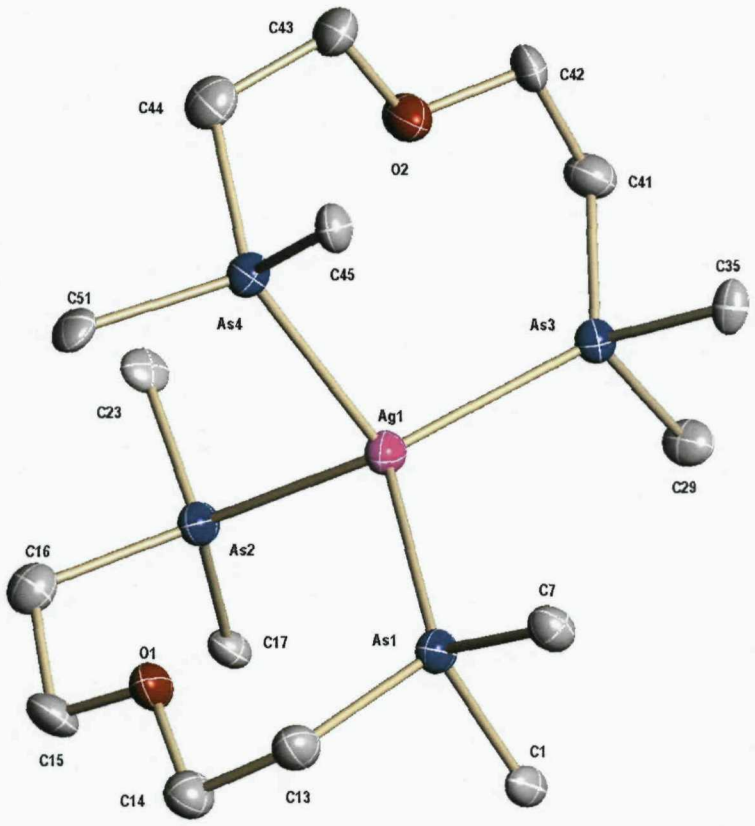

Figure 13 View of the structure of $[Ag(O\{(CH_2)_2AsPh_2\}_2)_2]^+$ with numbering scheme adopted. Ellipsoids are drawn at the 50% probability level. H atoms and the phenyl rings (except the ipso C atoms) are omitted for clarity.

Table 2 Selected bond lengths (Å) and angles (°) for $[Ag(O\{(CH_2)_2AsPh_2\}_2)_2]BF_4 \cdot MeOH$.

Ag1–As1	2.6376(9)	Ag1–As2	2.6143(9)
Ag1–As3	2.6317(9)	Ag1–As4	2.6296(9)
As2–Ag1–As4	95.67(3)	As2–Ag1–As3	118.83(3)
As4–Ag1–As3	108.09(3)	As2–Ag1–As1	107.60(3)
As4–Ag1–As1	111.63(3)	As3–Ag1–As1	113.65(3)

Colourless crystals of $[Cu_2\{Me_2As(CH_2)_2OH\}_3](BF_4)_2$ were obtained as a result of ligand fragmentation in the reaction of $[Cu(MeCN)_4]BF_4$ with two mol. equivs. of $O\{(CH_2)_2AsMe_2\}_2$ as described above. The structure of the cation shows (Figure 14, Table 3) a Cu(I)···Cu(I) dimer with the three dimethylarsanoethanol ligands bridging the metal centres, leading to distorted pyramidal coordination at each Cu

atom, with two As and one OH group bonded to Cu1 and with one As and two OH groups bonded to Cu2. The short dimethylene ligand backbone places the Cu atoms only 2.497(1) Å apart. This is towards the short end of the range typically seen for Cu(I)–Cu(I) dimers with bridging ligands.[35] We also note that As2, which is 2.283(1) Å from Cu2, appears to shows a long range interaction (2.934(1) Å) with Cu1. The Cu1–Cu2–As2 angle of 75.58(4)° also suggests that As2 is leaning towards Cu1.

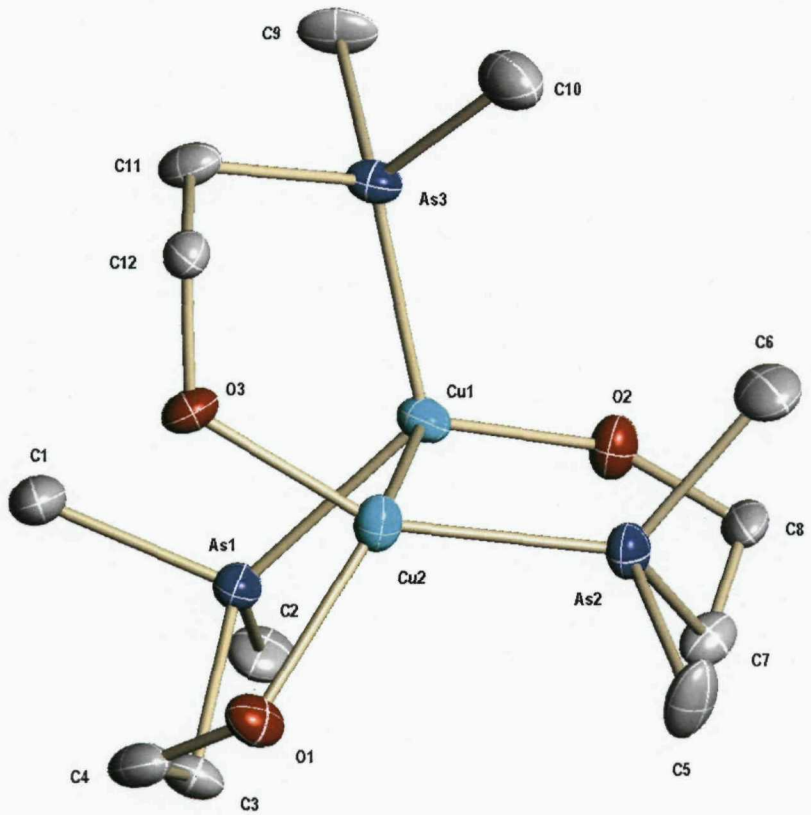

Figure 14 View of the structure of $[Cu_2\{Me_2As(CH_2)_2OH\}_3]^{2+}$ with numbering scheme adopted. Ellipsoids are drawn at the 50% probability level. H atoms are omitted for clarity.

Table 3 Selected bond lengths (Å) and angles (°) for $[Cu_2\{Me_2As(CH_2)_2OH\}_3](BF_4)_2$.

Cu1–O2	2.058(6)	Cu2–O3	2.021(5)
Cu1–As3	2.326(1)	Cu2–O1	2.116(6)
Cu1–As1	2.343(1)	Cu2–As2	2.283(1)
Cu1··· Cu2	2.497(1)	Cu1···As2	2.934(1)

O2–Cu1–As3	116.77(18)	O2–Cu1–As1	110.87(19)
As3–Cu1–As1	123.12(5)	O2–Cu1···Cu2	126.19(17)
As3–Cu1···Cu2	91.58(5)	As1–Cu1···Cu2	83.99(5)
O2–Cu1···As2	78.38(16)	As3–Cu1···As2	106.81(5)
As1–Cu1···As2	111.67(5)	O3–Cu2–O1	87.8(2)
O3–Cu2–As2	155.21(18)	O1–Cu2–As2	116.05(16)
O3–Cu2···Cu1	98.21(16)	O1–Cu2···Cu1	122.14(17)
As2–Cu2···Cu1	75.58(4)		

The dimethylarsanoethanol ligands clearly result from C–O bond fission in the $O\{(CH_2)_2AsMe_2\}_2$ ligand during the complexation reaction. Although the hydroxyl H atom were not located in the difference map, the O···F distances strongly suggest H-bonding between the O and F atoms, i.e. O–H···F (O···F ca. 2.7 Å) which, together with the fact the crystals were colourless, are consistent with Cu(I).

The analogous stibane–ethers $O\{(CH_2)_2SbR_2\}_2$ (R = Me, Ph) were also made within the group by Dr. M. Jura and the crystal structure of $[Ag(O\{(CH_2)_2SbPh_2\}_2)_2]BF_4{\cdot}CH_2Cl_2$ is included below (Figure 15, Table 4) for comparison purposes. Both As and Sb analogues form the pseudo-tetrahedral $[M(L\text{-}L)_2]BF_4$ complexes with Ag and Cu and for the phenyl derivatives are almost identical.

It was noted that the Sb–Ag–Sb angles within the chelates are *ca.* 4° smaller than the corresponding As–Ag–As chelate angles and the Sb-Ag bond distances slightly larger than those of As-Ag

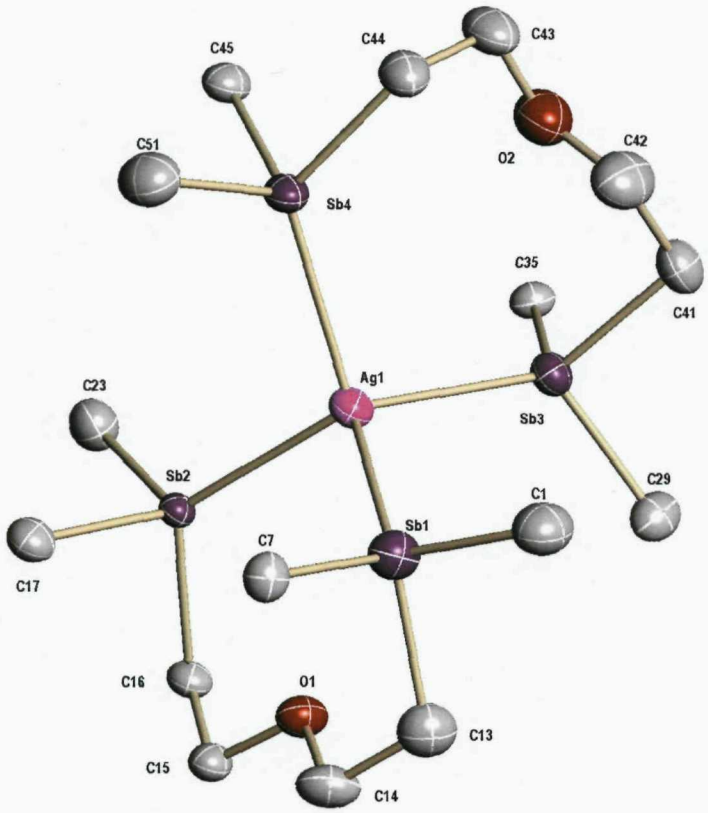

Figure 15 View of the structure of $[Ag(O\{(CH_2)_2SbPh_2\}_2)_2]^+$ with numbering scheme adopted. Ellipsoids are drawn at the 50% probability level. H atoms and the phenyl rings (except the ipso C atoms) are omitted for clarity.

Table 4 Selected bond lengths (Å) and angles (°) for $[Ag(O\{(CH_2)_2SbPh_2\}_2)_2]BF_4 \cdot CH_2Cl_2$.

Ag1–Sb1	2.7268(5)	Ag1–Sb2	2.7341(5)
Ag1–Sb3	2.7020(5)	Ag1–Sb4	2.7194(5)
Sb3–Ag1–Sb4	103.55(2)	Sb3–Ag1–Sb1	107.49(2)
Sb4–Ag1–Sb1	116.26(2)	Sb3–Ag1–Sb2	116.79(2)
Sb4–Ag1–Sb2	109.30(2)	Sb1–Ag1–Sb2	103.95(2)

The reason for using copper and silver was to produce easily characterised examples of the new ligands. The problems encountered with the $O\{(CH_2)_2AsMe_2\}_2$ ligand meant that no further study was attempted. Further study on the $O\{(CH_2)_2AsPh_2\}_2$ ligand on GaX_3 (X = Cl, Br and I) was however investigated.

Reaction of the $O\{(CH_2)_2AsPh_2\}_2$ ligand (L–L) with GaX_3 (X = Cl, Br and I) in diethyl ether in a 2:1 Ga:L–L ratio yields only the $[(GaX_3)_2(L–L)]$ species which were isolated as light yellow oily solids. Confirmation of the 2:1 Ga:L–L ratio follows from the microanalysis data. Diethyl ether was also seen in the ^1H NMR spectra, slightly shifted from free ligand but, unfortunately no crystals were obtained from any of the complexes. Several gallium(III) complexes including $[GaX_3(AsMe_3)]$ and diarsanes of type $[(GaX_3)_2(L–L)]$ have been structurally characterised[36] and contain pseudo-tetrahedral gallium centres which have typically $\delta(^{71}Ga)$ at ~264 (X = Cl), ~ 150 (X = Br) and ~ -170 (X = I). The values for the corresponding $[GaX_4]^-$ ions are $\delta(^{71}Ga)$ at ~250 (X = Cl), ~ 64 (X = Br) and ~ -455 (X = I). The ^{71}Ga NMR resonances of the gallium complexes of the $O\{(CH_2)_2AsPh_2\}_2$ ligand are (δ = 251 (X = Cl), δ = 68 (X = Br) and δ = -443 (X = I)) which are clearly indicative of $[GaX_4]^-$ ions which suggests either a $[GaX_2\{O\{(CH_2)_2AsPh_2\}_2\}][GaX_4]$ constitution or rearrangement in solution. The absence of a ^{71}Ga NMR resonance for $[GaX_2\{O\{(CH_2)_2AsPh_2\}_2\}]^+$ (if present) would be due to fast quadrupolar relaxation in the low symmetry cation.[36] In the absence of X-ray quality crystals the solid state structure remains uncertain.

Reaction of the $O\{(CH_2)_2AsPh_2\}_2$ ligand (L–L) with $BiBr_3$, in a 1:1 ratio yields only the $[(BiBr_3)(L–L)_2]$ species which was isolated as a yellow waxy solid. Confirmation of the 1:2 Bi:L–L ratio follows from the microanalysis data. The ^1H NMR spectra showed only the uncoordinated ligand due to dissociation[37] and unfortunately no crystals were obtained.

6.4 Conclusion:

A large amount of groundwork involving the synthetic steps towards producing intermediates of a number of macrocyclic arsane ligands have been successfully carried out, along with some corresponding cyclisations. In producing these macrocycles although the ^1H NMR spectra were consistent with the formation of the targeted compounds a number of complications have arisen. Decomposition while purifying through column chromatography or distillation both hampered the purification effort. From the mass spectrometry, where the molecular ions were not obtained, acyclic products could not be ruled out because many of the fragments would be common to both the acyclic and

macrocyclic products. The presence of di-cationic ions (at half mass) from the larger ring could also not be eliminated.

Generally poor yields and the success of other aspects of this thesis meant that further study, purification and unequivocal identification was not undertaken.

This Chapter also contains the development of high yielding routes to rare examples of As_2O-donor facultative ligands, $O\{(CH_2)_2AsMe_2\}_2$ and $O\{(CH_2)_2AsPh_2\}_2$ which have flexible backbones. It has been shown that they are air-sensitive oils and behave as As_2-bound bidentates towards tetrahedral, $[M(L\text{–}L)_2]BF_4$ metals where M = Cu(I) or Ag(I) on the basis of solution ^1H and ^{63}Cu NMR spectroscopic studies, mass spectrometry and microanalyses. Representative examples of the $O\{(CH_2)_2AsPh_2\}_2$ ligand with Cu(I) and Ag(I) crystal structures confirm the distorted tetrahedral As_4 coordination at the metal centres. The previously unreported $O\{(CH_2)_2AsMe_2\}_2$ ligand appears to be considerably less stable with respect to C–O bond fission under some conditions than the phenyl ligand or in comparison to its stibane analogue, $O\{(CH_2)_2SbMe_2\}_2$.

An unexpected Cu(I)–Cu(I) complex, $[Cu_2\{Me_2As(CH_2)_2OH\}_3](BF_4)_2$, has been crystallographically identified and reported as a by-product via C–O bond fission within the $O\{(CH_2)_2AsMe_2\}_2$ ligand.

Complexes of the $O\{(CH_2)_2AsPh_2\}_2$ ligand have also been produced and partially characterised with GaX_3, 1:2 and $BiBr_3$, 2:1.

6.5 Experimental:

See Appendix for general experimental methods and additional ligand synthesis.

Diiodo(methyl)arsane, $MeAsI_2$: A slow stream of sulphur dioxide was passed through a yellow solution of $MeAsO_3Na_2.6H_2O$ (35.4 g, 0.121 mol), potassium iodide (25.0 g, 0.333 mol), water (40 mL) and conc. HCl (10 mL) for 2 h. This solution immediately turned colourless and then yellow again followed by a

further change to form an orange liquid which settled at the bottom of the reaction mixture. CH_2Cl_2 (10 mL) was added aid in the separation. Once separated the orange oil/ CH_2Cl_2 layer was put into the freezer for 2 hours, filtered and washed with ice/water (3 x 10 mL) to give an yellow/orange solid which was dried in a desicator (Figure 2).[13,14] (21.9 g, 52%). ^{1}H NMR (300 MHz, $CDCl_3$, 298 K): 3.10 (s). ^{13}C NMR (300 MHz, $CDCl_3$, 298 K): 20.45.

Phenyldichloroarsane, $PhAsCl_2$: Phenyldichloroarsane (28.6 g, 99%) was produced by known literature methods (Figure 2).[14,16]

Methylphenyliodoarsane, MePhAsI: Methyphenylliodoarsane was produced by known literature methods from phenyldichloroarsane (31.5 g, 84%) (Figure 2).[17,18] ^{1}H NMR (300 MHz, $CDCl_3$, 298 K): 2.25 (s, 3H, Me), 7.37-7.77 (m, 5H, Ph).

Phenylarsane, $PhAsH_2$: The production of phenyl arsane was carried out using the phenyldichloroarsane and an excess of $LiAlH_4$ in ether at -78 °C as described in the literature (8.8 g, 48%) (Figure 2).[19]

Lithium diphenylarsanide $LiAsPh_2$: Lithium metal (0.34 g, 0.048 mol) was added to a solution of triphenylarsane (5.0 g, 0.016 mol) in THF (100 mL). The reaction mixture was refluxed for 1 h (turning the solution a dark red) and then left stirring for 8 h. ^{t}BuCl (1.4 mL, 0.013 mol) was added dropwise to remove the by-product phenylithium and stirred for 1 h. The solution lightened upon addition to an orange/red colour and was immediately used (Figure 2).[20]

Di(benzyl)methylarsane, $MeAs(CH_2Ph)_2$: $MeAsI_2$ (3.0 g, 8.7 mmol) in THF (30 mL) was added drop wise to a dark blue solution of Na (0.84 g, 0.037 mol) in liquid ammonia (200 mL) maintained at -78 °C (acetone/CO_2 slush) and left for 2 h at -78 °C. The solution was allowed to warm to room temperature before the red/orange solution was then cooled again to -78 °C. A slow orange to white/colourless colour change was observed with the addition of benzyl chloride (2.21 g, 0.017 mol). The reaction was left to stir overnight to allow evaporation of the ammonia. The solution was hydrolysed with degassed H_2O (50 mL) and

the organic layer separated. The aqueous layer was washed with diethyl ether (2 x 50 mL), and the combined organics were dried over magnesium sulphate. Following filtration the volatiles were removed under reduced pressure and distillation at 120 °C at 0.1 mm yielded a colourless oil (1.64 g, 69%). ^{1}H NMR (300 MHz, $CDCl_3$, 298 K): δ = 0.83 (s, 3H, Me), 2.71 (d ^1J=12 Hz, 2H, CHH), 2.88 (d ^1J=12 Hz, 2H, CHH), 7.42-7.08 (m, 10 H, Ph). ^{13}C NMR: δ = 7.3 (Me), 33.4 (CH_2), 125.3, 128.3, 128.5, 139.3 (Ph). A mass spectrometry sample was also prepared in acetone with methyliodide. ES+ MS (MeCN): *m/z* 287 $[Me_2As(CH_2Ph)_2]^+$.

1,3-Bis(methylphenylarsano)propane, $MePhAs(CH_2)_3AsPhMe$:
Methylphenyliodoarsane (MePhAsI) (15.1 g, 0.052 mol) was slowly added to a suspension of Na (3.0 g, 0.13 mol) in THF (200 mL). Upon heating the solution turned cloudy and NaI begun to precipitate out. The yellow/orange solution was refluxed for a further 2 h. Additional Na (0.5 g, 0.022 mol) was added and refluxed for 4 h turning the solution a deeper red. The mixture was left to cool overnight before 1,3-dibromopropane (5.15 g, 0.0255 mol) was added dropwise as a THF (15 mL) solution, into the red/green solution. Upon greying, addition of the 1,3-dibromopropane in THF was stopped and the solution was refluxed. Additional 1,3-dibromopropane in THF was added until the green colour did not return while refluxing. The NaI was removed by hydrolysing with NaCl in water (200 mL) and the organic layer separated. The aqueous layer was washed with diethyl ether (2 x 100 mL), and the combined organics were dried over magnesium sulphate. Following filtration the volatiles were removed under reduced pressure yielding a yellow/brown oil (6.65 g, 68%). ^{1}H NMR (300 MHz, $CDCl_3$, 298 K): δ = 1.15 (s, 3H, Me), 1.17 (s, 3H, Me), 1.76-1.49 (m, 6H, $(CH_2)_3$), 7.48-7.30 (m, 10 H, Ph). ^{13}C NMR: δ = 8.3 (Me), 23.7 (CH_2), 31.0 ($AsCH_2$), 128.0, 128.3, 131.9, 132.5 (Ph).

$[Me_2PhAs(CH_2)_3AsPhMe_2][I]_2$: $MePhAs(CH_2)_3AsPhMe$ (0.01g) was added to a solution of MeI (0.1 g) in acetone (5 mL). The reaction was left to stir over night under nitrogen yielding a white soild. ^{1}H NMR (300 MHz, d^6-DMSO, 298 K): δ = 1.78-1.90 (m, 2H, CH_2), 2.24 (s, 12H, Me), 2.72-2.75 (m, 4H, $AsCH_2$), 7.30-

7.84 (m, 10 H, Ph). MeI of product: ES+ MS (MeCN): *m/z* 391 $[MePhAs(CH_2)_3AsPhMe_2]^+$, 533 $[Me_2Ph(I)As(CH_2)_3AsPhMe_2]^+$.

***o*-Phenylenebis(bromomethylarsane), [*o*-C_6H_4(AsMeBr)$_2$]:** Bromine (14.07 g, 0.088 mol) was dissolved in carbon tetrachloride (CCl_4) (50 mL) and added dropwise to (*o*-$C_6H_4(AsMe_2)_2$) (6.3 g, 0.022 mol) in CCl_4 (50 mL) cooled to 0 °C and a yellow granular solid precipitated out along with a dark red viscous oil. The solid was filtered and heated under *vacuo* until the evolution of bromomethane had ceased leaving behind a dark red oil. The crude product was then distilled (150 °C, 0.1 mm) to yield [*o*-C_6H_4(AsMeBr)$_2$] as a light yellow oil (7.32 g, 80% yield).[18] ^{1}H NMR (300 MHz, $CDCl_3$, 298 K): δ = 2.14 (s, 6H, Me), 7.56-8.29 (m, 4 H, Ph). ^{13}C NMR: δ = 18.5 (Me), 130.4, 131.5, 143.5 (Ph).

***o*-Phenylenebis(methylarsane), [*o*-C_6H_4(AsMeH)$_2$]:** A solution of [*o*-C_6H_4(AsMeBr)$_2$] (8.8 g, 0.021 mol) in diethyl ether (50 mL) was added dropwise over 1 h to a suspension of $Li(AlH_4)$ (1.78 g, 0.80 mol) in diethyl ether (80 mL). The reaction was refluxed for 1 h then cooled to R.T followed by the addition of degassed H_2O (50 mL) and the organic layer separated. The aqueous layer was washed with diethyl ether (2 x 100 mL), and the combined organics were dried over magnesium sulphate. Following filtration the volatiles were removed under reduced pressure yielding a yellow oil. Distillation at 84 °C, 0.8 mm, yielded [*o*-C_6H_4(AsMeH)$_2$] (0.93 g, 17%) and a large amount of yellow oil which did not distil at 160 °C 0.8 mm and solidified on cooling, believed to be an arsane polymer. ^{1}H NMR (300 MHz, $CDCl_3$, 298 K): δ = 1.27 (m, 6H, Me), 3.52-3.66 (m, 2H, AsH), 7.20-7.47 (m, 4 H, Ph).

Benzo-Me$_2$-[9]-ane-As$_2$O, As$_2$O macrocycle, [*o*-C_6H_4(AsMe(CH$_2$)$_2$-)$_2$O]: ^{n}BuLi (0.8 mL, 1.8 mmol) was added dropwise to a stirred solution of *o*-Phenylenebis(methylarsane), [*o*-C_6H_4(AsMeH)$_2$] (0.207 g, 0.80 mmol) in THF (100 mL) maintained at -78 °C (acetone/CO_2 slush). This was allowed to warm to RT and stirred for 1 h. The solution was then cooled to -40 °C followed by the dropwise addition of bis(2-chloroethyl)ether (0.114 g, 0.80 mmol) as a THF solution (100 mL) and then stirred for 1 h at -40 °C before allowing to warm to RT

over night. Aqueous NaCl (100 mL) was added dropwise and stirred for 0.5 h before the organic layer was separated. The aqueous layer was washed with THF (2 x 30 mL), and the combined organics were dried over magnesium sulphate. Following filtration the volatiles were removed under reduced pressure yielding a yellow oil. Distillation at 100 °C, 0.08 mm, yielded a colourless oil (0.05 g, 19%) as well as the starting ether at 60 °C 0.10 mm. ^{1}H NMR (300 MHz, $CDCl_3$, 298 K): δ = 1.18 (s, 6H, Me), 1.78-1.90 (m, 4H, $AsCH_2$), 3.60-3.79 (m, 4H, OCH_2), 7.28-7.49 (m, 4 H, Ph) (starting ether triplets at 3.76 and 3.62). ^{13}C NMR: δ = 10.8 (Me), 25.6 ($AsCH_2$), 67.9 (OCH_2), 127.8, 128.3, 131.3 (Ph). EIMS: m/z = 182 $[PhAsMe_2]^+$, 167 $[PhAsMe]^+$. Methiodide of the product: ES+ MS (MeCN): *m/z* 197 $[PhAsMe_3]^+$, 287, calculated for $[PhAs(Me)_2(CH_2)_2O(CH_2)_2Cl]$ *m/z* = 289 with the correct isotope pattern.

1,2-Bis(2-bromoethoxy)ethane, ($Br(CH_2)_2O(CH_2)_2O(CH_2)_2Br$): Triethylene glycol (8.89 mL, 0.060 mol) and pyridine (10.67 mL, 0.132 mol) were added to a flask containing benzene (70 mL), this was heated to reflux and $SOBr_2$ (10.23 mL, 0.132 mol) was added dropwise over 1 h. The solution was then refluxed for 20 h before being left to cool to RT. Aqueous HCl (20 mL) was then added dropwise before the organic layer was dried over magnesium sulphate. Following filtration the volatiles were removed reduced pressure yielding a dark solution. Distillation at 76 °C, 0.05 mm, yielded ($Br(CH_2)_2O(CH_2)_2O(CH_2)_2Br$) as a yellow oil (6.23 g, 38%).[25] ^{1}H NMR (300 MHz, $CDCl_3$, 298 K): δ = 3.48 (t, 4H, CH_2Br), 3.69 (s, 4H, $O(CH_2)_2O$), 3.83 (t, ^{3}J=6.3 Hz, 4 H, OCH_2). ^{13}C NMR: δ = 30.3 (CH_2Br), 70.5 ($O(CH_2)_2O$), 71.3 (OCH_2).[26]

Me-[9]-ane-AsO_2, AsO_2 Macrocycle, ($MeAs(-(CH_2)_2O(CH_2)_2O(CH_2)_2-)$): $MeAsI_2$ (5.0 g, 14.5 mmol) in THF (80 mL) was added drop wise over 0.2 h to a dark blue solution of Na (1.54 g, 0.067 mol) in liquid ammonia (300 mL) maintained at -78 °C (acetone/CO_2 slush) and left for 2 h at -78 °C. The solution was then allowed to warm to room temperature before the red/orange solution was then cooled again to -40 °C. A slow orange to white/colourless colour change was observed with the addition of ($Br(CH_2)_2O(CH_2)_2O(CH_2)_2Br$) (4.0 g, 14.5 mmol) in THF (100 mL) over 2 h. The reaction was left to stir overnight to

allow evaporation of the ammonia. The solution was hydrolysed with degassed H_2O (70 mL) and the organic layer separated. The aqueous layer was washed with diethyl ether (2 x 20 mL), and the combined organics were dried over magnesium sulphate. Following filtration the volatiles were removed under reduced pressure and distillation at 120 °C at 0.05 mm yielded a colourless oil (0.25 g, 8%). ^{1}H NMR (300 MHz, $CDCl_3$, 298 K): δ = 0.98 (s, 3H, Me), 1.65-1.88 (m, 4H, $AsCH_2$), 3.55-3.75 (m, 8 H, (OCH_2) and ($O(CH_2)_2O$)). ^{13}C NMR: δ = 7.6 (Me), 27.0 ($AsCH_2$), 69.5 and 69.9 ((OCH_2) and ($O(CH_2)_2O$)). A mass spectrometry sample was also prepared in acetone with methyliodide. ES+ MS (MeCN): *m/z* 221.2 $[Me_2As(-(CH_2)_2O(CH_2)_2O(CH_2)_2-)]^+$.

1,3-Bis(phenylarsano)propane, $PhAs(H)(CH_2)_3As(H)Ph$: ^{n}BuLi (2.4 M, 13.6 mL, 32.6 mmol) in diethyl ether (50 mL) was added dropwise to a stirred solution of $PhAsH_2$ (5.02 g, 32.6 mmol) in diethyl ether (150 mL) maintained at -78 °C (acetone/CO_2 slush). Upon addition the colourless solution turned through yellow to a deep orange and upon complete addition was allowed to warm to -50 °C before 1,3-dibromopropane (3.29 g, 16.3 mmol) in diethyl ether (50 mL) was added dropwise and stirred overnight to warm to RT. The solution was hydrolysed with degassed H_2O (100 mL) and the organic layer separated. The aqueous layer was washed with diethyl ether (2 x 40 mL), and the combined organic volatiles were removed at atmospheric pressure by warming to 48 °C yielding a light yellow oil $PhAs(H)(CH_2)_3As(H)Ph$ (4.56 g, 80%). ^{1}H NMR (300 MHz, $CDCl_3$, 298 K): δ = 2.3 (s (br), 6H, $(CH_2)_3$), 3.50-3.65 (m, 2H, AsH), 7.23-7.56 (m, 10 H, Ph). ^{13}C NMR: δ = 30.7 ($AsCH_2$), 31.5 (CH_2), 126.4, 127.5, 131.8, 139.0 (Ph).

1,3-Bis(phenylisopropylarsano)propane, $Ph^iPrAs(CH_2)_3As^iPrPh$: MeLi (1.5 M, 5.73 mL, 8.6 mmol) was added dropwise to a stirred solution of $PhAs(H)(CH_2)_3As(H)Ph$ (1.5 g, 4.3 mmol) in THF (100 mL) maintained at -78 °C. This was stirred for 1 h while allowing to warm to RT giving an orange solution followed by the addition of 2-bromopropane (1.06 g, 8.6 mmol) as a THF (50 mL) solution. The solution was hydrolysed with degassed H_2O (50 mL) and the organic layer separated. The aqueous layer was washed with diethyl ether

(2 x 20 mL), and the combined organics were dried over magnesium sulphate. Following filtration, the volatiles were removed under reduced pressure yielding $Ph^{i}PrAs(CH_2)_3As^{i}PrPh$ as a light yellow oil (1.21 g, 65%). ^1H NMR (300 MHz, $CDCl_3$, 298 K): δ = 1.11-1.17 (m, 12H, Me), 1.56-1.97 (m, 8H, CH and $(CH_2)_3$), 7.29-7.48 (m, 10H, Ph). ^{13}C NMR: δ = 19.0 and 19.4 (Me), 23.0 and 25.6 ($(CH_2)_3$), 26.6 (CH), 127.9, 128.2, 131.9, 139.4 (Ph). Carbon Dept 135 used.
A mass spectrometry sample was also prepared in acetone with methyliodide. ES+ MS (MeCN): *m/z* 447 $[Ph^{i}PrAs(CH_2)_3As(Me)^{i}PrPh]^+$ and 419 $[PhMeAs(CH_2)_3As(Me)^{i}PrPh]^+$.

Bis(3-chloropropyl)phenylarsane, $PhAs((CH_2)_3Cl)_2$: ^{n}BuLi (2.4M, 17.5 mL, 42.0 mmol) in diethyl ether (100 mL) was added dropwise to $PhAsH_2$ (3.23, 21.0 mmol) as a diethyl ether (100 mL) solution maintained at -60 °C turning the solution orange/yellow. The reaction was stirred for a further 0.5 h, followed by the dropwise addition of 1-bromo-3-chloropropane (4.15 mL, 42.0 mmol) as a diethyl ether (20 mL) solution maintained at -60 °C. The reaction was left to stir overnight to warm to RT. The white solution was hydrolysed with degassed H_2O (100 mL) and the organic layer separated. The aqueous layer was washed with diethyl ether (2 x 50 mL), and the combined organics were dried over magnesium sulphate. Following filtration the volatiles were removed at 40 °C, 1 atm, followed by reduced pressure for 5 min. yielding the intermediate $PhAs((CH_2)_3Cl)_2$ as a yellow oil (4.92 g, 76%). ^1H NMR (300 MHz, $CDCl_3$, 298 K): δ = 1.74-1.93 (m, 8H, $AsCH_2$ and CH_2), 3.50-3.56 (m, 4H, CH_2Cl), 7.29-7.51 (m, 5H, Ph). ^{13}C NMR: δ = 22.9 (CH_2), 28.9 ($AsCH_2$), 45.2 (CH_2Cl), 127.3, 127.6, 131.6, 137.8 (Ph).

Ph_3-[12]-ane-As_3, As_3 Macrocycle [-As(Ph)$(CH_2)_3$-]$_3$: MeLi (11.5 mL, 0.017 mol) was added dropwise to a stirred solution of $PhAs(H)(CH_2)_3As(H)Ph$ (3.0 g, 8.6 mmol) in THF (200 mL) maintained at -78 °C. The reaction was stirred for 1 h while allowing to warm to RT. The orange solution was then transferred to a dropping funnel and diluted with THF (250 mL). $PhAs((CH_2)_3Cl)_2$ (2.65 g, 8.6 mmol) in THF (450 mL) was also transferred into an identical dropping funnel where both solutions were added dropwise at the same rate into THF (300 mL)

over 7 h. The solution was hydrolysed with degassed H_2O (250 mL) and the organic layer separated and dried over magnesium sulphate. Following filtration the volatiles were removed under reduced pressure yielded a yellow oil (3.63 g, 72%). Distillation of which showed no significant separation or improvement by NMR.^{1}H NMR (300 MHz, $CDCl_3$, 298 K): δ = 1.30-1.83 (m, 18H, $(CH_2)_3$), 7.22-7.52 (m, 15H, Ph). ^{13}C NMR: δ = 22.9 (CH_2), 28.0 ($AsCH_2$), 127.1, 127.3, 131.5, 139.1 (Ph).

O{$(CH_2)_2AsPh_2$}$_2$: Lithium metal (0.34 g, 0.048 mol) was added to a solution of triphenylarsane (5.0 g, 0.016 mol) in THF (100 mL). This was refluxed for 1 h to give a dark red solution and then left stirring for 8 h. ^{t}BuCl (1.4 mL, 0.013 mol) was added dropwise to remove the PhLi bi-product and the mixture was stirred for 1 h, turning to a lighter orange/red colour. To this was added a solution of $O(CH_2CH_2Br)_2$ (0.70 mL, 5.60 mmol) in THF (10 mL) to give an off-white reaction mixture, which upon refluxing for 2 h turned to a green oil. Aqueous NH_4Cl (50 mL) was added and the organic fraction was separated. The aqueous layer was washed with THF (20 mL) and the combined organic fractions were dried over $MgSO_4$ for 8 h. The solvent was removed *in vacuo* to give the title product as a yellow waxy oil which was stored in a Schlenk tube over molecular sieves (Yield: 2.3 g, 77%). ^{1}H NMR (300 MHz, $CDCl_3$, 298 K): δ = 2.27 (t, ^3J = 7.5 Hz, 4H, CH_2As), 3.55 (t, 4H, CH_2O), 7.31–7.44 (m, 20H, Ph). ^{13}C{^{1}H} NMR ($CDCl_3$): δ = 29.0 (CH_2As), 68.9 (CH_2O), 129.0, 129.2, 133.7, 141.0 (Ph). EIMS: m/z = 530 $[M]^+$, 453 $[M - Ph]^+$.

Methiodide of O{$(CH_2)_2AsPh_2$}$_2$: O{$(CH_2)_2AsPh_2$}$_2$ (0.2 g, 0.38 mmol) in acetone (5 mL) and MeI (0.2 g, 1.42 mmol, excess) was added and the reaction mixture was stirred for 72 h. The volatiles were removed in vacuo to leave a white solid. ^{1}H NMR (300 MHz, $CDCl_3$, 298 K): δ = 2.77 (s, 6H, Me), 3.70–3.77 (m, 8H, CH_2) 7.61–7.90 (m, 20H, Ph). ^{13}C{^{1}H} NMR ($CDCl_3$): δ = 10.3 (MeAs), 27.6 (CH_2As), 65.3 (CH_2O), 122.2, 130.6, 132.2, 133.6 (Ph). Electrospray MS (MeCN): m/z = 687 $[MePh_2As(CH_2)_2O(CH_2)_2AsPh_2MeI]^+$; 280 $[MePh_2As(CH_2)_2O(CH_2)_2AsPh_2Me]^{2+}$.

$O\{(CH_2)_2AsMe_2\}_2$: Me_2AsI (8.4 g 0.036 mol) was added dropwise to a flask containing small pieces of sodium metal (2.00 g, 0.087 mol) in THF (200 mL). The reaction mixture was heated to 85 °C for 1 h, whereupon the reaction solution changed from yellow to white and then to green. It was then left stirring for 8 h. $O(CH_2CH_2Br)_2$ (4.20 g, 0.018 mol) was added dropwise, and the mixture was stirred for a further 8 h. Degassed H_2O was added until all the solids dissolved. The organic layer was separated and the aqueous washed with diethyl ether (2 x 40 mL). The combined organic phases were dried over $MgSO_4$ for 8 h. The solvent was removed *in vacuo* to give the title ligand as a yellow oil (3.38 g, 67%). ^1H NMR (300 MHz, $CDCl_3$, 298 K): δ = 0.94 (s, 12H, Me), 1.68 (t, ^3J = 7.5 Hz, 4H, CH_2As), 3.74 (t, 4H, CH_2O). $^{13}C\{^1H\}$ NMR ($CDCl_3$): δ = 9.9 (MeAs), 32.4 (CH_2As), 61.6 (CH_2O). EI MS: m/z = 267 $[M - Me]^+$.

In one case the ^1H NMR spectrum of the product isolated as above showed some additional resonances, hence purification by distillation was attempted, giving two fractions. Fraction 1: Bp. 58°C at 0.05 mmHg turned out to be the As_2O ligand, with identical spectroscopic features to those quoted above. Fraction 2: (identified as $Me_2As(CH_2)_2OH$ (see text)) Bp. 74°C at 0.05 mm Hg; ^1H NMR spectrum ($CDCl_3$): δ = 0.93 (s, 6H, Me), 1.70 (t, ^3J = 7.5 Hz, 2H, CH_2As), 3.54 (t, 2H, CH_2O). GCEI MS: m/z = 150 $[Me_2As(CH_2)_2OH]^+$.

$[Cu(O\{(CH_2)_2AsPh_2\}_2)_2]BF_4$: $O\{(CH_2)_2AsPh_2\}_2$ (0.53 g, 1.0 mmol) was added dropwise to a solution of $[Cu(MeCN)_4]BF_4$ (0.315 g, 1.0 mmol) in methanol (10 mL). The reaction mixture was stirred for 0.5 h and the light yellow solution was then concentrated to half the volume *in vacuo*. Colourless crystals were obtained by cooling this solution in the freezer over several days. These were filtered off and dried *in vacuo* to give a cream solid (0.36 g, 60%). Anal. Found: C, 51.0; H, 4.8. Calc. for $C_{56}H_{56}As_4BCuF_4O_2 \cdot 2CH_2Cl_2$: C, 50.5; H, 4.4%. ^1H NMR (300 MHz, $CDCl_3$, 298 K): δ = 2.62 (br, 4H, CH_2As), 3.84 (br, 4H, OCH_2), 7.28–7.39 (m, 20H, Ph). ^{63}Cu NMR (CH_2Cl_2): δ = −139. IR (Nujol): 1050 (BF_4^-) cm^{-1}. Electrospray MS (MeCN): m/z = 634 $[Cu(O\{(CH_2)_2AsPh_2\}_2)]^+$.

$[Ag(O\{(CH_2)_2AsPh_2\}_2)_2]BF_4$: $O\{(CH_2)_2AsPh_2\}_2$ (0.57 g, 1.1 mmol) was added dropwise to a solution of $AgBF_4$ (0.21 g, 1.1 mmol) in methanol (10 mL) in a foil-wrapped flask. The reaction mixture was stirred for 1 h, the brown solution was then filtered and colourless crystals were obtained by leaving the filtrate in the dark for one month. (Yield: 0.29 g, 43%). Anal. Found: C, 52.1; H, 4.4. Calc. for $C_{56}H_{56}AgAs_4BF_4O_2 \cdot 2MeOH$: C, 52.8; H, 4.9%. ^1H NMR (300 MHz, $CDCl_3$, 298 K): δ = 2.41 (br, 4H, CH_2As), 3.48 (br, 4H, OCH_2), 7.17–7.39 (m, 20H, Ph). $^{13}C\{^1H\}$ NMR ($CDCl_3$): δ = 29.2 (CH_2As), 66.9 (CH_2O), 129.3, 129.9, 132.7, 134.9 (Ph). IR (Nujol): 1060 (BF_4^-) cm^{-1}. Electrospray MS (MeCN): m/z = 1167 $[Ag(O\{(CH_2)_2AsPh_2\}_2)_2]^+$.

$[Cu(O\{(CH_2)_2AsMe_2\}_2)_2]BF_4$: $O\{(CH_2)_2AsMe_2\}_2$ (0.07 g, 0.25 mmol) was added dropwise to a solution of $[Cu(MeCN)_4]BF_4$ (0.156 g, 0.50 mmol) in degassed methanol (10 mL), this was stirred for 2 h before the solution was then reduced *in vacuo* to give a green paste. This dissolved partially in methanol (10 mL), the colourless mother liquor was then transferred and diethyl ether (10 mL) added to produce a green fluffy solid. This was left to stand, the solvent was decanted off and then solid was dried in vacuo. ^1H NMR (300 MHz, $CDCl_3$, 298 K): δ = 1.38 (s, 12H, CH_3), 2.08 (t, ^3J = 6.0 Hz, 4H, CH_2As), 3.99 (br, 4H, OCH_2). ^{63}Cu NMR (CH_2Cl_2): δ = −16. IR (Nujol): 1065 (BF_4^-) cm^{-1}. Electrospray MS (MeCN): m/z = 627 $[Cu(O\{(CH_2)_2AsMe_2\}_2)_2)]^+$, 386 $[Cu(O\{(CH_2)_2AsMe_2\}_2)(MeCN)]^+$, 345 $[Cu(O\{(CH_2)_2AsMe_2\}_2)]^+$.

$[Ag(O\{(CH_2)_2AsMe_2\}_2)_2]BF_4$: $O\{(CH_2)_2AsMe_2\}_2$ (0.07 g, 0.25 mmol) was added dropwise to a solution of $AgBF_4$ (0.10 g, 0.50 mmol) in degassed methanol (10 mL) in a foil-wrapped schlenk. After stirring for ca. 2 h the solvent was then removed *in vacuo* to give a light brown oily paste. ^1H NMR (300 MHz, $CDCl_3$, 298 K): δ = 1.42 (s, 12H, Me), 2.13 (t, ^3J = 6.0 Hz, 4H, CH_2As), 3.95 (t, 4H, OCH_2). $^{13}C\{^1H\}$ NMR ($CDCl_3$): δ = 8.9 (Me), 31.8 (CH_2As), 58.7 (CH_2O). IR (Nujol): 1057 (BF_4^-) cm^{-1}. Electrospray MS (MeCN): m/z = 539 $[Ag(O\{(CH_2)_2AsMe_2\}_2)(O\{(CH_2)_2AsMe_2\}_2 - CH_2CH_2AsMe_2)]^+$, 407 $[Ag(O\{(CH_2)_2AsMe_2\}_2)(H_2O)]^+$, 389 $[Ag(O\{(CH_2)_2AsMe_2\}_2)]^+$.

[$(GaCl_3)_2(O\{(CH_2)_2AsPh_2\}_2)$]: $GaCl_3$ (0.18 g, 1.0 mmol) was added as a solid to a stirred solution of $O\{(CH_2)_2AsPh_2\}_2$ (0.27 g, 0.51 mmol) in diethyl ether (10 mL). The reaction mixture was stirred for 1 h before the solvent was removed *in vacuo*. Hexane (10 mL) was then used to wash the yellow residue before being filtered to give a light yellow sticky solid. Required for $C_{28}H_{28}As_2Cl_6Ga_2O.C_4H_{10}O$ (956.7): C, 40.2; H, 4.0. Found: C, 40.8; H, 3.8%. ^1H NMR (300 MHz, $CDCl_3$, 298 K): δ = 1.26 (t, ^3J = 7.2 Hz, 6H, CH_3 (Et_2O)), 2.66 (t, ^3J = 6.5 Hz, 4H, CH_2As), 3.56 (t, ^3J = 6.5 Hz, 4H, OCH_2), 3.63 (q, ^3J = 7.2 Hz, 4H, CH_2 (Et_2O)), 7.36–7.52 (m, 20H, Ph). ^{71}Ga NMR (CH_2Cl_2): δ = +251. IR (Nujol): 365 br, 344 (GaCl) cm^{-1}. Raman: 361, 345 υ(GaCl) cm^{-1}.

[$(GaBr_3)_2(O\{(CH_2)_2AsPh_2\}_2)$]: $GaBr_3$ (0.32 g, 1.0 mmol) was added as a solid to a stirred solution of $O\{(CH_2)_2AsPh_2\}_2$ (0.27 g, 0.51 mmol) in diethyl ether (10 mL). The reaction mixture was stirred for 1 h before the solvent was removed *in vacuo*. Hexane (10 mL) was then used to wash the yellow residue before being filtered to give a light yellow sticky solid. Required for $C_{28}H_{28}As_2Br_6Ga_2O.2C_4H_{10}O$ (1297.5): C, 33.3; H, 3.7. Found: C, 33.1; H, 3.0%. ^1H NMR (300 MHz, $CDCl_3$, 298 K): δ = 1.23 (t, ^3J = 7.2 Hz, 12H, CH_3 (Et_2O)), 2.58 (br, 4H, CH_2As), 3.54 (br, 8H, CH_2 (Et_2O)), 3.66 (br, 4H, OCH_2), 7.38–7.47 (m, 20H, Ph). ^{71}Ga NMR (CH_2Cl_2): δ = +68. IR (Nujol): 296, 226 (GaBr) cm^{-1}. Raman: 296, 232 υ(GaBr) cm^{-1}.

[$(GaI_3)_2(O\{(CH_2)_2AsPh_2\}_2)$]: GaI_3 (0.46 g, 1.0 mmol) was added as a solid to a stirred solution of $O\{(CH_2)_2AsPh_2\}_2$ (0.27 g, 0.51 mmol) in diethyl ether (10 mL). The reaction mixture was stirred for 1 h before the solvent was removed *in vacuo* to give a yellow oil. Hexane (10 mL) was then added but the oil did not mix so was decanted off before again going under *vacuo* to give a light yellow paste. Required for $C_{28}H_{28}As_2Ga_2I_6O$ (1431.2): C, 23.5; H, 2.0. Found: C, 23.7; H, 2.2%. ^1H NMR (300 MHz, $CDCl_3$, 298 K): δ = 2.78 (t, ^3J = 6.8 Hz, 4H, CH_2As), 3.83 (t, ^3J = 6.9 Hz, 4H, OCH_2), 7.35–7.68 (m, 20H, Ph), trace Et_2O resonances also observed. ^{71}Ga NMR (CH_2Cl_2): δ = –443. IR (Nujol): 240 (GaI) cm^{-1} Raman: 244 υ(GaI) cm^{-1}.

[$BiBr_3(O\{(CH_2)_2AsPh_2\}_2)_2$]: $BiBr_3$ (0.16 g, 0.36 mmol) was added as a solid to a stirred solution of $O\{(CH_2)_2AsPh_2\}_2$ (0.19 g, 0.36 mmol) in CH_2Cl_2 (10 mL). The reaction mixture was stirred overnight going from a light yellow through dark yellow to a dark green solution. Filtration gave a brown precipitate and a bright yellow filtrate. The solvent was removed *in vacuo* from the filtrate to give a yellow waxy solid. Required for $C_{56}H_{56}As_4Bi_1Br_3O_2$ (1509.4): C, 44.6; H, 3.7. Found: C, 44.4; H, 3.8%.

6.6 Crystallography:

The crystals structures within this Chapter, unless otherwise reported were grown from anhydrous CH_2Cl_2 solutions layered or by vapour diffusion with *n*-hexane under dinotrogen or from the slow evaporation from a solution of MeOH over several days or weeks.

Brief details of the data collection and refinement are presented in Table 5.

Table 5 Crystal data and structure refinement details.[a]

Compound	$[Cu(O\{(CH_2)_2AsPh_2\}_2)_2]BF_4{\cdot}MeOH$	$[Ag(O\{(CH_2)_2AsPh_2\}_2)_2]BF_4{\cdot}MeOH$	$[Cu_2\{Me_2As(CH_2)_2OH\}_3](BF_4)_2$	$[Ag(O\{(CH_2)_2SbPh_2\}_2)_2]BF_4{\cdot}CH_2Cl_2$
Formula	$C_{57}H_{60}As_4BCuF_4O_3$	$C_{57}H_{60}AgAs_4BF_4O_3$	$C_{12}H_{33}As_3B_2Cu_2F_8O_3$	$C_{57}H_{58}Ag_4BCl_2F_4O_2Sb_4$
M	1243.08	1287.41	750.84	1527.61
Crystal system	Monoclinic	Triclinic	Orthorhombic	Monoclinic
Space group	$P2_1/c$ (no. 14)	P-1 (no. 2)	$P2_12_12_1$ (no. 19)	$P2_1/c$ (no. 14)
a/Å	11.209(3)	11.387(2)	8.1798(10)	13.1670(10)
b/Å	17.931(4)	13.633(3)	15.120(3)	16.5702(15)
c/Å	26.177(5)	17.061(3)	20.506(5)	26.543(3)
α/°	90	91.285(10)	90	90
β/°	96.359(10)	93.574(10)	90	101.943(6)
γ/°	90	92.830(10)	90	90
U/Å^3	5261.4(19)	2639.4(8)	2536(8)	5665.8(9)
Z	4	2	4	4
μ/mm^{-1}	2.970	2.928	5.631	2.370
F(000)	2512.0	1292.0	1460.0	2968.0
Total no. of obsns (R_{int})	62586 (0.142)	57994 (0.175)	16310 (0.068)	73096 (0.065)
Unique obsns.	12178	12167	5726	12971
Min, max transmission	0.681, 1.000	0.586, 1.000	0.650, 1.000	0.683, 1.000
No. of parameters, restraints	633, 0	633, 0	271, 0	640, 0
Goodness-of-fit on F^2	0.92	0.97	1.09	1.07
Resid electron density /eÅ^{-3}	–1.18 to +0.99	-0.94 to +0.76	–0.91 to +0.89	–1.29 to +1.00
R1, wR2 ($I > 2\sigma(I)$)[b]	0.057, 0.101	0.066, 0.112	0.057, 0.090	0.044, 0.096
R1, wR2 (all data)	0.143, 0.128	0.162, 0.141	0.099, 0.104	0.067, 0.104

[a] Common items: temperature = 120 K; wavelength (Mo-Kα) = 0.71073 Å; θ(max) = 27.5°. [b] $R_1 = \Sigma||F_o| - |F_c||/\Sigma|F_o|$. $wR_2 = [\Sigma w(F_o^2 - F_c^2)^2/\Sigma wF_o^4]^{1/2}$.

6.7 References:

[1] L. F. Lindoy, *The Chemistry of Macrocyclic Ligand Complexes*, Cambridge University Press, **1989**.
[2] S. B. Wild, *The Chemistry of Organic Arsenic, Antimony and Bismuth Compounds*, S. Patai, Z. Rappoport (eds). Wiley N.Y., **1994**, ch. 3.
[3] C. A. McAuliffe, "*Phosphorus, arsenic, antimony and bismuth ligands*", *Comp. Coord. Chem.*, Pergamon: Oxford, **1987**, 2, ch. 14, 989-1066.
[4] W. Levason, G. Reid, *Comp. Coord. Chem. II*, J. A. McCleverty and T. A. Meyer (Eds.), Elsevier, Oxford, **2004**, 1, 475-484.
[5] E. P. Kyba, S. P. Chou, *J. Am. Chem. Soc.*, **1980**, 102, 7012-7014.
[6] E. P. Kyba, S. P. Chou, *Chem. Comm.*, **1980**, 449-450.
[7] E. P. Kyba, S. P. Chou, *J. Org. Chem.*, **1981**, 46, 860-863.
[8] T. Kauffmann, J. Ennen, *Chem. Ber*, **1985**, 118, 2692-2702.
[9] A. Tzschach, G. Pacholke, *Z. Anorg. Allg. Chem.*, **1965**, 336, 270-277.
[10] B. Bosnich, S. T. D. Lo, E. A. Sullivan, *Inorg. Chem.*, **1975**, 14, 2305-2310.
[11] R. C. Braechler, K. Mislow, J. P. Casey, R. J. Cook, G. H. Senkler Jr., *J. Am. Chem. Soc.*, **1972**, 94, 2859-2861.
[12] A. L. Rheingold, P. J. Sullivan, *Organometallics*, **1983**, 2, 327-331.
[13] I. T. Millar, H. Heaney, D.M. Heinekey, W. C. Fernelius, *Inorg. Synth.*, **1960**, 113-115.
[14] R. A. Zingaro, *Synthetic Methods of Organometallic and Inorganic Chemistry*, (Eds) H. H. Karsch, Thieme, **1996**, 3, 198-200.
[15] E. Adams, D. Jeter, A. W. Cordes, J. W. Kolis, *Inorg. Chem.*, **1990**, 29, 1500-1503.
[16] R. L. Barker, E. Booth, W. E. Jones, A. F. Millidge, F. N. Woodward, *J. Soc. Chem. Ind.*, **1949**, 68, 289-295.
[17] E. J. Cragoe, R. J. Andres, R. F. Coles, B. Elpern, J. F. Morgan, C. S. Hamilton, *J. Am. Chem. Soc.*, **1947**, 69, 925-926.
[18] K. Henrick, S. B. Wild, *J. Chem. Soc. Dalton Trans.*, **1975**, 1506-1516.
[19] V. E. Wiberg, K. Mödritzer, *Zeitschrift fur Naturforschung*, **1957**, 12B, 127-128.
[20] W. Levason, C. A. McAuliffe, *Inorg. Synth.*, **1976**, 16, 188-92.
[21] R. D. Feltham, A Kasenally, R. S. Nyholm, *J. Organomet. Chem.*, **1967**, 7, 285-288.
[22] M. Mickiewicz, S. B. Wild, *J. Chem. Soc., Dalton Trans.*, **1977**, 704-708.
[23] B. Bosnich, S. B. Wild, *J. Am. Chem. Soc.*, **1970**, 92, 459-464.
[24] T. R. Carlton, C. D. Cook, *Inorg. Chem.*, **1971**, 10, 2628-2630.
[25] G. Reid, *Ph.D Thesis, University of Edinburgh*, **1989**, 314.
[26] J. F. W. Keana, Y. Wu, G. Wu, *J. Org. Chem.*, **1987**, 52, 12, 2571-2576.
[27] L. Sacconi, I. Bertini, F. Mani, *Inorg. Chem.*, **1968**, 7, 1417–1420.
[28] M. F. Davis, M. Jura, W. Levason, G. Reid, M. Webster, *J. Organomet. Chem.*, **2007**, 692, 5589-5597.
[29] W. Levason, G. Reid, *Comp. Coord. Chem. II*, J. A. McCleverty and T. A. Meyer (Eds.), Elsevier, Oxford, **2004**, 1, 377–389.
[30] W. Levason, N. R. Champness, *Coord. Chem. Rev.*, **1994**, 133, 115–217.
[31] K. Sommer, *Z. Anorg. Allg. Chem.*, **1970**, 377, 278–286; K. Iwata, M. Kojima, J. Fujita, *Bull. Chem. Soc. Japan*, **1985**, 58, 3003–3009.
[32] P. B. Chi, F. Kober, *Z. Anorg. Allg. Chem.*, **1983**, 498, 64–74.
[33] J. R. Black, W. Levason, M. D. Spicer, M. Webster, *J. Chem. Soc., Dalton Trans.*, **1993**, 3129–3136.
[34] G. A. Bowmaker, Effendy, R. D. Hart, J. D. Kildea, E. N. de Silva, B. W. Skelton, A. H. White, *Aust. J. Chem.*, **1997**, 50, 539–552.
[35] A. M. Hill, W. Levason, M. Webster, *Inorg. Chem.*, **1996**, 35, 3428–3430.
[36] F. Cheng, A. L. Hector, W. Levason, G. Reid, M. Webster, W. Zhang, *Inorg. Chem.*, **2007**, 46, 17, 7215-7223.
[37] N. J. Hill, *Ph.D Thesis, University of Southampton*, 2002, 48.

Chapter 7

Appendix

7.1 General Experimental:

All procedures were executed in an oxygen free N_2 atmosphere, using standard Schlenk, vacuum line and glove box techniques. All solvents have been distilled prior to use unless otherwise stated. Tetrahydrofuran, Et_2O and hexane were distilled from Na-benzophenone ketyl, MeCN, CH_2Cl_2, $MeNO_2$ and CCl_4 from CaH_2 (or P_2O_5 for MeCN) and EtOH from magnesium turnings. SnF_2, $SnCl_4$, $SnBr_4$, SnI_4 and GeF_4 were obtained from Aldrich and used as received. $GeCl_4$ from Aldrich was distilled from a mixture of $CaCl_2/Na_2CO_3$. $[SnF_4\{MeCN\}_2]$ and $[GeF_4\{MeCN\}_2]$ were made as described.[1,2,3] Ligands (generally used as received) were obtained from Aldrich ($OPPh_3$, PPh_3, $AsPh_3$, PCy_3, $Me_2P(CH_2)_2PMe_2$, $Cy_2P(CH_2)_2PCy_2$), Alfa Aesar ($OPMe_3$) and was sublimed onto a cold finger before use, Fluka ($OAsPh_3$) and Strem ($AsMe_3$, $AsEt_3$, PMe_3, $Et_2P(CH_2)_2PEt_2$). Other ligands were made by literature methods: *o*-$C_6H_4(P(O)Ph_2)_2$, *o*-$C_6H_4(P(O)Me_2)_2$, Me_3AsO, $Ph_2P(O)CH_2P(O)Ph_2$, *o*-$C_6H_4(PPh_2)_2$, $Ph_2P(CH_2)_2PPh_2$, $Me_2P(O)(CH_2)_2P(O)Me_2$.[4,5,6,7,8] IR spectra were performed on a Perkin-Elmer 983G Spectrometer using Nujol mulls on CsI disks taken over a range of 4000 cm^{-1} to 200 cm^{-1}, Raman spectra using a Perkin-Elmer FT Raman 2000R with a Nd:YAG laser. ^1H NMR and $^{13}C\{^1H\}$ NMR spectra were recorded in $CDCl_3$, CD_2Cl_2 or CD_3NO_2 solutions using a Bruker AV300 spectrometer at 300 MHz and 75.47 MHz respectively, using an external reference of Me_4Si and at 298 K. $^{19}F\{^1H\}$, $^{31}P\{^1H\}$, ^{63}Cu and ^{119}Sn NMR spectra were recorded in CH_2Cl_2 with a $CDCl_3$ or CD_2Cl_2 lock, using a Bruker DPX400 Spectrometer and referenced to $CFCl_3$ at 376.44 MHz, 85% H_3PO_4 at 161.98 MHz, $[Cu(MeCN)_4]^+$ at 106.1 MHz and neat $SnMe_4$ at 149.10 MHz respectively ($Cr(acac)_3$ was also added as a relaxation agent for the ^{119}Sn NMR spectra). When quoting $^{13}C\{^1H\}$ NMR spectra of phenyl ring systems or *o*-C_6H_4 the *ipso* C is always reported first and *para* C last unless otherwise stated. Mass spectra were performed using (ESMS) Positive Ion Electrospray, in MeCN on a VG Biotech Platform or by electron impact on a VG-70-SE Normal geometry double focusing spectrometer. Elemental analyses were performed by the Microanalytical Laboratory of Strathclyde University. The single crystal X-ray diffraction data were collected on a Bruker Nonius KappaCCD diffractometer using an area detector where a CCD (charge-coupled device) is used to measure the incident X-ray photons. The crystals themselves were held on a glass fibre

using perfluoro polyether oil and placed on a goniometer head so that the crystals resided in the centre of the x-ray beam and the cryostream cooling the crystal to 120 K. Structure solution[9] and refinement[10] were routine unless otherwise stated.

7.2 Additional Ligand Synthesis:

Although a number of ligands used throughout this work are available from companies such as Aldrich and Strem, some are not or are extremely expensive and so were produced using the following literature methods.

***o*-$C_6H_4(AsMe_2)_2$ 1,2-Bis(dimethylarsino)benzene:** Iododimethylarsine is made in large quantities circa 100g by bubbling sulphur dioxide through a recently acidified ($HCl_{(aq)}$) aqueous solution of sodium cacodylate and potassium iodide. This can be stored almost indefinitely for use when needed. Reaction in THF with sodium and the subsequent addition of 1,2-dichlorobenzene gave upon work up and distillation the desired product as an air-sensitive yellow oil.[11] Me_2AsI: (81%). ^1H NMR ($CDCl_3$): 1.98 (s, Me). ^{13}C NMR ($CDCl_3$): 15.78. *o*-$C_6H_4(AsMe_2)_2$: (66%). ^1H NMR ($CDCl_3$): 1.24 (s, 12H, Me), 7.31-7.50 (m, 4H, C_6H_4).

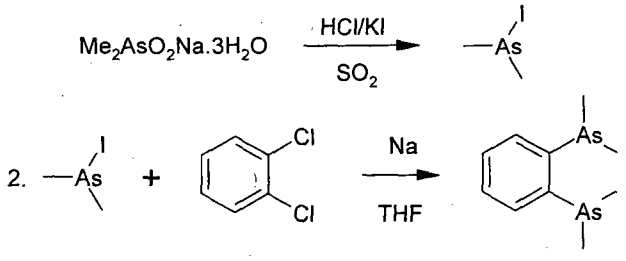

$Ph_2As(CH_2)_2AsPh_2$: $Ph_2As(CH_2)_2AsPh_2$ was produced as via literature method.[12]

[$MeC(CH_2AsMe_2)_3$]: Iododimethylarsine (48.24 g, 0.208 mol) was added drop wise to a mixture of Na (10.47 g, 0.456 mol) in THF (500 mL) under nitrogen. This was heated to reflux and stirred for 3 h, then cooled and left over night. 1,3-dichloro-2-(chloromethyl)-2-methylpropane (11.4 g, 0.065 mol) was added drop wise and refluxed over 2 h. When the solution stayed a cream colour the solution was allowed to cool and saturated aqueous sodium chloride (50 mL) was added.

The organic layer (THF & diethyl ether washings) was dried overnight in $MgSO_4$ before the solvent was removed. Distilation at 110 °C and 0.2 mbar gave the correct product, yellow oil (8.3 g, 33% yield).[11] ^1H NMR ($CDCl_3$): 0.94 (s, 18H, $AsMe_2$), 1.06 (s, 3H, MeC), 1.72 (s, 6H, CH_2As).

o-$C_6H_4(PH_2)_2$, 1,2-Bis(phosphino)benzene:

1,2-Bis(dimethoxyphosphoryl)benzene is reduced with a 1:1 mixture of $LiAlH_4$:Me_3SiCl in THF under reduced temperature to give a colourless oil.[13,14] (69 %). $^{31}P\{^1H\}$ NMR ($CDCl_3$): -125.1.

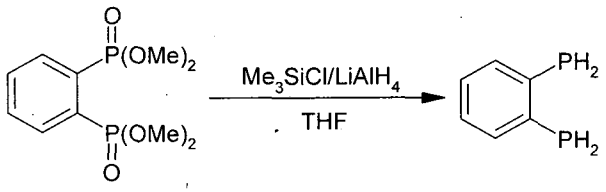

o-$C_6H_4(PMe_2)_2$, 1,2-Bis(dimethylphosphino)benzene: The diprimary phosphine in THF at reduced temperature is then reacted sequentially by MeLi, MeI and then the steps are repeated before the ligand was vacuum distilled to give a very air-sensitive colourless oil.[13] (79 %). ^1H NMR ($CDCl_3$): 1.36 (t, 12H, Me), 7.36-7.53 (m, 4H, C_6H_4). $^{31}P\{^1H\}$ NMR ($CDCl_3$): -55.

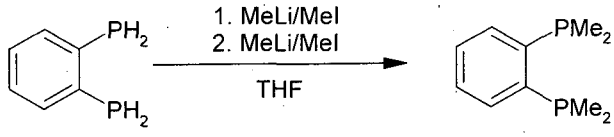

7.3 Some Possible Routes for Making Further Macrocycles Containing As Donor Atoms:

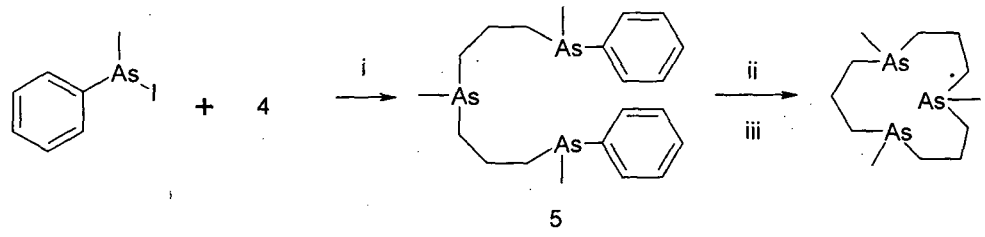

5

Scheme 3
i. Na/THF, ii. $HI_{(g)}$, iii.Na/THF/1,3-dichloropropane, v. high dilution.

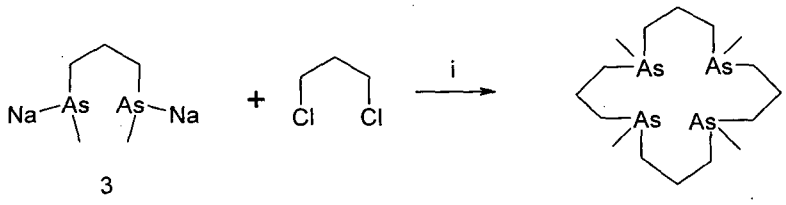

3

Scheme 4
i. High dilution

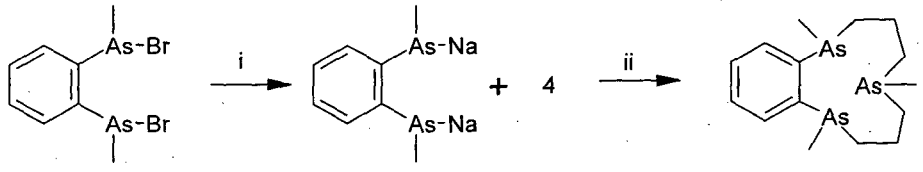

Scheme 5
i. Na/THF, ii. high dilution.
Has been made differently.[36]

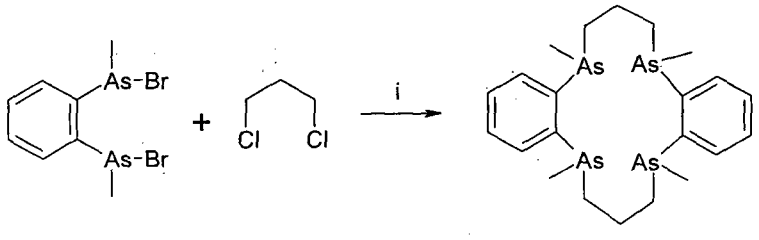

Scheme 6
i. High dilution.
Has been made differently.[36]

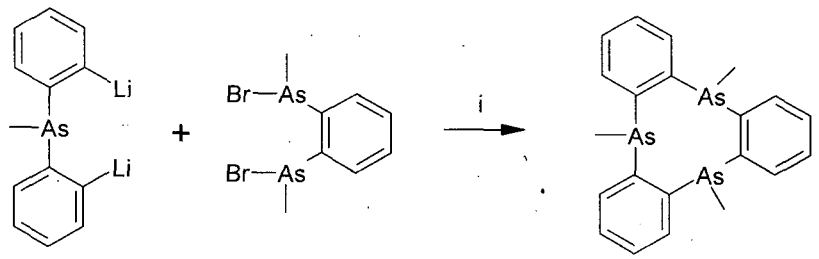

Scheme 7
i. High dilution

7.4 Bibliographic Information:

Synthesis, Structures and DFT Calculations on Alkaline-Earth Metal Azide-Crown Ether Complexes. Michael D. Brown, Martin F. Davis, John M. Dyke, Francesco Ferrante, William Levason, Steven J. Ogden, Michael Webster, *Chemistry – A European Journal*, **2008**, 14, 2615-2624.

Complexes of germanium(IV) fluoride with phosphane ligands: Structural and spectroscopic authentication of germanium(IV) phosphane complexes. Martin F. Davis, William Levason, James Paterson, Gillian Reid, Michael Webster, School of Chemistry, *Dalton Trans.*, **2008**, 2261-2269.

Complexes of Vanadium(V) Oxide Trifluoride with Nitrogen and Oxygen Donor Ligands: Coordination Chemistry and some Fluorination Reactions, Martin F. Davis, William Levason, James Paterson, Gillian Reid, Michael Webster, *European Journal of Inorganic Chemistry*, **2008**, 802-811.

The first examples of germanium tetrafluoride and tin tetrafluoride complexes with soft thioether coordination-synthesis, properties and crystal structures. Martin F. Davis, William Levason, Gillian Reid, Michael Webster, Wenjian Zhang, *Dalton Trans.*, **2008**, 533-538.

Synthesis, spectroscopic and structural systematics of complexes of germanium(IV) halides (GeX_4, X = F, Cl, Br or I) with mono-, Bi- and Tri-dentate and macrocyclic nitrogen donor ligands. Fei Cheng, Martin F. Davis,

Andrew L. Hector, William Levason, Gillian Reid, Michael Webster, Wenjian Zhang, *European Journal of Inorganic Chemistry*, **2007**, 4897-4905.

Synthesis and coordinating properties of the facultative Sb_2O- and As_2O-donor ligands $O\{(CH_2)_2ER_2\}_2$ (E=Sb or As; R=Ph or Me). Martin F. Davis, Marek Jura, William Levason, Gillian Reid, Michael Webster, *Journal of Organometallic Chemistry*, **2007**, 692, 5589-5597.

Synthesis, spectroscopic and structural systematics of complexes of germanium(IV) halides (GeX_4, X = F, Cl, Br or I) with phosphane oxides and related oxygen donor ligands. Fei Cheng, Martin F. Davis, Andrew L. Hector, William Levason, Gillian Reid, Michael Webster, Wenjian Zhang, *European Journal of Inorganic Chemistry*, **2007**, 2488-2495.

Tungsten(VI) and molybdenum(VI) complexes with soft thioether ligand coordination - synthesis, spectroscopic and structural studies. Martin F. Davis, William Levason, Mark E. Light, Raju Ratnani, Gillian Reid, Keerti Saraswat, Michael Webster, *European Journal of Inorganic Chemistry*, **2007**, 1903-1910.

Synthesis and characterisation of WVI complexes of phosphane oxide ligands, $[WO_2X_2(OPR_3)_2]$ (X = F, Cl or Br; R = Me or Ph), and of the $[MoO_2F_2(OPR_3)_2]$. Martin F. Davis, William Levason, Raju Ratnani, Gillian Reid, Tim Rose, Michael Webster, *European Journal of Inorganic Chemistry*, **2007**, 306-313.

Studies on chromium(III) and vanadium(III) complexes with crown ether and crown thioether coordination - synthesis, properties and structural systematics. Charlotte D. Beard, Loretta Carr, Martin F. Davis, John Evans, William Levason, Louise D. Norman, Gillian Reid, Michael Webster, *European Journal of Inorganic Chemistry*, **2006**, 4399-4406.

Tin(IV) fluoride complexes with tertiary phosphane ligands - a comparison of hard and soft donor ligands. Martin F. Davis, Maria Clarke, William

Levason, Gillian Reid, Michael Webster, *European Journal of Inorganic Chemistry*, **2006**, 2773-2782.

Synthesis, spectroscopic studies and structural systematics of phosphine oxide complexes with Group II metal (beryllium-barium) nitrates. Martin F. Davis, William Levason, Raju Ratnani, Gillian Reid, Michael Webster, *New Journal of Chemistry*, **2006**, 30, 782-790.

Synthesis and characterization of tin(IV) fluoride complexes of phosphine and arsine oxide ligands. Martin F. Davis, William Levason, Gillian Reid, Michael Webster, *Polyhedron*, **2006**, 25, 930-936.

7.5 References:

[1] D. Tudela, F. Rey, *Z. Anorg. Allg. Chem.*, **1989**, 575, 202-208.
[2] D. Tudela, F. Patron, *Inorg. Synth.*, **1997**, 31, 92-93.
[3] E. L. Muetterties, *J. Amer. Chem. Soc.*, **1960**, 82, 1082–1087.
[4] A. R. J. Genge, W. Levason, G. Reid., *Inorg. Chim. Acta*, **1999**, 288, 142–149.
[5] A. Merijanian, R.A. Zingaro, *Inorg. Chem.*, **1966**, 5, 187-191.
[6] W. Levason, R. Patel, G. Reid, *J. Organomet. Chem.*, **2003**, 688, 280-282.
[7] H. C. E. McFarlane, W. McFarlane, *Polyhedron*, **1983**, 2, 303-304.
[8] A. M. Aguiar, J. Beisler, *J. Org. Chem.*, **1964**, 29, 1660-1662.
[9] G.M. Sheldrick, SHELXS 97, *Program for crystal structure solution*, University of Göttingen, Germany, **1997**.
[10] G.M. Sheldrick, SHELXL 97, *Program for crystal structure refinement*, University of Göttingen, Germany, **1997**.
[11] R. D. Feltham, R. S. Nyholm, A. Kasenally, *J. Organomet. Chem.*, **1967**, 7, 285-288.
[12] W. Levason, C. A. McAuliffe, *Inorganic Syntheses*, **1976**, 16, 188-192.
[13] K. Issleib, E. Liessring, H. Meyer, *Tetrahedron Lett.*, **1981**, 22, 4475-4478.
[14] E. P. Kyba, S. T. Liu, R. L. Harris, *Organometallics*, **1983**, *2*, 1877-1879